UNIVERSITÉ DE SHERBROOKE

Faculté de génie

Département de génie chimique et de génie biotechnologique

DÉVELOPPEMENT D'UN SYSTÈME DE LIBÉRATION DE PEPTIDES DÉRIVÉS DE LA PROTÉINE MORPHOGÉNÉTIQUE OSSEUSE 9 COMME STRATÉGIE DE TRAITEMENT CONTRE LA MALADIE D'ALZHEIMER

Thèse de doctorat

Spécialité : génie chimique

Marc-Antoine LAUZON

Jury:

Prof. François BERTHOD, Ph.D (évaluateur externe)

Prof. Richard BLOUIN, Ph.D (évaluateur externe au département)

Prof. Nathalie FAUCHEUX, Ph.D (directrice)

Prof. Bernard MARCOS, ing. Ph.D (rapporteur)

Prof. Emmanuel PLANEL, Ph.D (évaluateur externe)

C'est ce que nous pensons déjà connaître qui nous empêche souvent d'apprendre
Introduction à l'étude de Médecine Expérimentale
Claude Bernard, 1813-1878, Philosophe, Médecin et Physiologiste français

REMERCIEMENTS

Dans un premier temps, j'aimerais remercier tout spécialement ma directrice de recherche, Professeure Nathalie Faucheux, qui m'a accueilli dans son laboratoire pour l'ensemble de mes études graduées. Son écoute, ses encouragements soutenus, son savoir légendaire et surtout sa passion pour la recherche m'ont guidé tout au long de ce projet. Dans un second temps, un merci spécial au Professeur Bernard Marcos qui a contribué, à de nombreuses reprises, à l'accomplissement de ce projet par ses bons conseils et sa grande expertise en modélisation mathématique. Je veux aussi remercier le CRSNG qui m'a fourni un appui financier essentiel à la réalisation de ce projet.

Je tiens également à remercier chaleureusement Olivier Drevelle qui était toujours présent pour m'aider en plus de contribuer de façon significative à mes délires. Je voulais aussi souligner la bonhomie et l'enthousiasme tant apprécié des autres membres ou ex-membres de l'équipage sans qui ces dernières années n'auraient pas été aussi divertissantes; Sabrina Beauvais, Jessica Jann, Hamid Hassanisaber, Yasaman Alinejad, Éric Bergeron, Yanick Blain, Sabrina Néron et j'en passe. Encore merci à toutes et à tous d'avoir participé à mes nombreuses élucubrations. Unis, les pirates triompheront de tout…ARRRR!

Merci également à Isabelle Arsenault, Valérie Larouche, Serge Gagnon et Stéphane Guay pour leur soutien technique exceptionnel au laboratoire et surtout pour m'avoir dépanné à de nombreuses reprises. Je tiens également à remercier Charles Bertrand et Stéphane Gutierrez du Centre de Caractérisation des Matériaux de l'Université de Sherbrooke pour leur aide lors de la caractérisation de mes échantillons.

J'ai également une pensée pour mes amis proches et ma douce moitié, Bénédicte, qui ont toujours été présents tant dans les bons moments que dans les pires. Vos encouragements soutenus et votre présence furent très appréciés!

Je ne saurais oublier mes parents qui croient toujours en moi et m'encouragent à poursuivre mes rêves. Votre soutien inconditionnel à tous les niveaux a contribué à bien des égards à l'accomplissement de ce projet.

Finalement, je tiens à remercier les membres du jury; le Professeur François Berthod, le Professeur Richard Blouin, la Professeure Nathalie Faucheux, le Professeur Bernard Marcos et le Professeur Emmanuel Planel de prendre le temps de lire cette thèse et de me faire bénéficier de leurs conseils et expertises.

RÉSUMÉ

Le vieillissement croissant de la population mondiale augmente les risques d'incidence de maladies dégénératives comme la maladie d'Alzheimer (AD). L'AD représente la forme de démence la plus commune. C'est plus de 40 millions de personnes qui sont affectés à l'échelle mondiale, créant ainsi un lourd fardeau économique annuel de plusieurs centaines de milliards de dollars. L'AD est une maladie dégénérative du cerveau qui se traduit par une perte graduelle de la mémoire et des fonctions cognitives. Cette dernière se caractérise par trois symptômes pathophysiologiques intimement reliés qui sont : (1) un système cholinergique défectueux, (2) une accumulation excessive de plaques séniles toxiques composées de peptides β–amyloïdes et (3) une hyperphosphorylation de la protéine Tau qui résulte en des enchevêtrements neurofibrillaires. Il n'existe à ce jour aucune cure contre l'AD et les traitements actuellement retrouvés sur le marché n'ont qu'un effet transitoire. En revanche, il y a de plus en plus d'indices qui suggèrent que l'utilisation de certains facteurs de croissance comme l'IGF-2, le bFGF et les neurotrophines pourraient agir à titre de traitement. Parmi ces derniers, la protéine morphogénétique osseuse 9 (BMP-9) a montré un fort potentiel thérapeutique. Cette dernière est toutefois coûteuse à produire en plus d'être volumineuse, ce qui limite fortement son acheminement au cerveau en raison de la barrière hématoencéphalique.

Dans cette optique, nous avons développé deux peptides de 23 acides aminés dérivés de l'épitope knuckle de la BMP-9, pBMP-9 et SpBMP-9, 300 fois moins chers à produire. Les travaux de ce projet de doctorat portent sur le développement d'un système de libération du SpBMP-9, le plus efficace des deux peptides, comme stratégie de traitement contre l'AD. Tout d'abord, il a été montré que le SpBMP-9 permettait d'induire la différenciation neuronale de cellules humaines SH-SY5Y de façon plus efficace que la protéine native par la présence d'une croissance plus importante des neurites et l'expression de marqueurs de différenciation neuronaux. De plus, le SpBMP-9 pouvait agir sur au moins deux symptômes de l'AD en orientant la différenciation vers le phénotype cholinergique et en inactivant la GSK3β, une Tau kinase.

Ensuite, un système de libération sous forme de nanoparticules à base de chitosane et d'alginate a été développé, puis caractérisé. Ce système de libération a permis d'encapsuler efficacement le SpBMP-9. Le suivi et la modélisation des cinétiques de libération à l'aide d'un modèle mathématique prenant en considération la distribution de taille des particules a permis d'identifier que la libération était principalement diffusive, mais qu'il existait de fortes interactions entre le peptide et l'alginate. Les tests de viabilité ont montré que les nanoparticules n'étaient pas toxiques sur des cellules SH-SY5Y. Enfin, le SpBMP-9 libéré à partir des nanoparticules était toujours bioactif et permettait une différentiation neuronale.

Finalement, une étude exploratoire a permis de mettre en évidence que le SpBMP-9 pouvait agir en synergie avec le bFGF et le NGF. La combinaison du SpBMP-9 avec le bFGF ou le NGF a montré la présence d'une différenciation neuronale accrue mise en évidence par la présence d'une croissance de neurites supérieure, par l'expression de plusieurs marqueurs de différenciation ainsi que par un niveau de calcium intracellulaire plus important.

Pour conclure, ces travaux de recherche suggèrent que le SpBMP-9 possède un fort potentiel thérapeutique dans le contexte de l'AD. Une étude plus approfondie de ses mécanismes d'action est requise ainsi que la validation de son effet *in vivo* sur modèle animal.

Mots clés : Facteurs de croissance, différenciation neuronale, SH-SY5Y, nanoparticules, modélisation mathématique

TABLE DES MATIÈRES

LISTE DES TABLEAUX

LISTE DES FIGURES

LISTE DES ACRONYMES

Ach	Acétylcholine
AchE	Acétylcholinestérase
AchR	Récepteur à acétylcholine
Alg/Chit NPs	Nanoparticules à base d'alginate/chitosane
AD	Maladie d'Alzheimer
APP	Peptide précurseur de β-amyloïde
BBB	Barrière hématoencéphalique
BDNF	Facteur neurotrophique issu du cerveau
BMP	Protéine morphogénétique osseuse
BMP-9	Protéine morphogénétique osseuse 9
βA	Peptide β-amyloïde
ChAT	Choline acétyltransférase
CNS	Système nerveux central
CSF	Liquide cérébrospinal
ECS	Espace extracellulaire
EGF	Facteur de croissance épidermique
GDNF	Facteur neurotrophique dérivé de la glie
GF	Facteur de croissance
GFDS	Système de libération de facteur de croissance
GSK3β	Glycogène synthase kinase 3 beta
IGF-1	Facteur de croissance analogue à l'insuline 1
IGF-2	Facteur de croissance analogue à l'insuline 2
ICF	Espace intracellulaire
MAPK	Protéine kinase activée par les mitogènes
MAP-2	Protéine associée aux microtubules 2
NeuN	Protéine neuronale spécifique au noyau
NGF	Facteur de croissance des nerfs
NPs	Nanoparticules
NSE	Énolase spécifique aux neurones
PI	Point isoélectrique
PI3K/Akt	Phosphatidyl inositol 3 kinase/Protéine kinase B
PP2A	Protéine phosphatase 2A
RA	Acide rétinoïque
SEM	Microscopie électronique à balayage
TGFβ	Facteur de croissance transformant beta
VAchT	Protéine transporteuse d'acétylcholine

CHAPITRE 1 : INTRODUCTION

1.1 Mise en contexte et définition du projet de recherche

Les études démographiques effectuées à l'échelle de la planète indiquent que la population mondiale vieillie de façon croissante. Selon un rapport des Nations Unies, les personnes âgées de 60 ans et plus devraient constituer plus de 56% de la population mondiale d'ici 2030, ce qui représente plus de 2 milliards de personnes (United Nation, 2015). Ce vieillissement croissant devrait augmenter l'incidence des maladies dégénératives du cerveau telles que la maladie d'Alzheimer (AD). Les études épidémiologiques les plus récentes, réalisées par l'Organisation mondiale de la Santé, estiment que plus de 46 millions de cas de AD sont répertoriés dans le monde actuellement (Alzheimer's Association, 2017). Au Canada, environ 750 000 cas ont été répertoriés en 2010 et ce nombre devrait augmenter à 1.4 million d'ici 2030 (Alzheimer's Society Canada). Il est estimé que plus de 5 millions de personnes en recevront le diagnostic aux États-Unis en 2017 (Alzheimer's Association, 2017; Alzheimer's Society Canada). Ce bilan est également accompagné d'un lourd fardeau socio-économique avec notamment des coûts de société annuels estimés à plus de 250 milliards aux États-Unis seulement (Alzheimer's Association, 2017).

L'AD représente la forme de démence la plus commune avec 60 à 80% des cas répertoriés (Alzheimer's Society Canada). C'est une maladie dégénérative du cerveau qui a une prévalence estimée de 2-10% chez les personnes âgées de 60 et plus avec un risque doublant tous les 5 ans (Alzheimer's Association, 2017). Elle se définit comme un désordre neurodégénératif progressif du cerveau sur une période généralement de 8,5 à 10 ans (Kumar *et al.*, 2005) et présente une prévalence pour les zones du cerveau associées à l'apprentissage et à la mémoire dont notamment l'hippocampe et le néocortex (Kumar *et al.*, 2005). Les symptômes observés vont des pertes de mémoire graduelles jusqu'à l'apparition d'aphasie (perte de facultés reliées au langage), d'anosognosie (perte de conscience de sa condition de santé), d'agnosie (incapacité de reconnaître des stimuli), d'apraxie (incapacité de mouvoir son corps) et d'une altération sévère de la perception (Alzheimer's Society Canada). L'évolution de l'AD va du stade léger au stade sévère en passant par le stade modéré (Alzheimer's Society Canada). Le stade léger se caractérise par l'apparition de pertes de mémoire, de changements

de comportement et de difficultés à communiquer. La détérioration de la mémoire épisodique, la confusion et les déficits cognitifs s'intensifient et affectent les tâches quotidiennes de la vie au stade modéré. Finalement, les patients au stade final de la maladie deviennent immobiles, infirmes et muets jusqu'à leur fin de vie (Alzheimer's Society Canada).

L'évolution de l'AD diffère d'un patient à l'autre et dépend des prédispositions génétiques de l'individu et de son environnement (épigénétique). Il existe deux formes principales de l'AD, la forme génétique (familiale) et la forme sporadique. La forme génétique de la maladie est observée chez des patients ayant des mutations sur des gènes codant pour les peptides β–amyloïdes qui affectent la maturation de ces peptides, dont notamment des mutations sur les gènes codant pour les présénilines 1 et 2 qui interviennent dans l'activité de la γ–sécretase responsable du clivage en C-terminal des précurseurs des peptides β-amyloïdes (Oddo *et al.*, 2003; Selkoe et Podlisny, 2002; Zhang *et al.*, 2017). En contrepartie, la forme sporadique de l'AD implique généralement la mutation de certains gènes combinés à l'environnement (épigénétique) qui augmente les prédispositions à souffrir de l'AD comme le variant ε4 du gène codant pour l'apolipoprotéine E (*ε4 –APOE*) impliquée dans le transport des lipides et jouant un rôle dans la plasticité neuronale ainsi que le gène *TREM2* codant pour le récepteur TREM2 présent dans les cellules de la microglie et étant impliqué dans le contrôle de l'inflammation du système nerveux central (CNS) (Jonsson et al., 2013; Kim et al., 2014).

Au niveau neuropathologique, l'évolution de l'AD chez un patient peut emprunter différentes avenues dépendamment de l'individu, de son environnement et de ses prédispositions génétiques. Sur le plan neuropathophysiologique, l'AD se caractérise par trois éléments : un dysfonctionnement du système cholinergique par un déclin de l'activité de l'acétylcholine transférase et de l'acétylcholine estérase (Geula *et al.*, 2008; Parent *et al.*, 2013; Teipel *et al.*, 2011), l'accumulation anormale de plaques séniles composées de peptides β–amyloïdes (Murphy et LeVine 3rd, 2010; Sinha et Lieberburg, 1999) et l'hyperphosphorylation de la protéine Tau qui résulte en des enchevêtrements neurofibrillaires (Alonso *et al.*, 1996; Augustinack *et al.*, 2002). Ces différents éléments sont inter-reliés et peuvent intervenir à différents stades de la maladie (Oddo *et al.*, 2003; Olivero *et al.*, 2014).

L'évolution de l'AD sur le plan clinique est propre à chaque patient. Trois stades sont généralement utilisés: (1) le stade asymptomatique (aucun symptôme clinique observable), (2)

le stade de démence légère (stade prodromale) et (3) le stade de démence. Ces stades diffèrent les uns des autres non seulement par rapport aux symptômes cliniques observables, mais également en fonction des biomarqueurs retrouvés dans le liquide cérébrospinal du patient (Dubois *et al.*, 2010). Chez un patient au stade de démence, l'évolution de la maladie peut emprunter différentes voies: (1) l'AD typique, l'AD atypique (développement de la maladie dans un ordre différent des stades de Braak) et l'AD mixte (AD combinée à d'autre type de démence).

L'évolution typique de l'AD peut être catégorisée par différents stades, nommés stades de Braak (Braak *et al.*, 2006; Braak et Braak, 1991, 1995, 1997). Ces stades se distinguent les uns des autres par l'ampleur et la sévérité des zones du cerveau affectées. Par exemple, dans le cas des plaques séniles, trois stades sont définis (Braak et Braak, 1997). Au premier stade, les dépôts de peptides β-amyloïdes se retrouvent au niveau du néocortex basal alors qu'au troisième stade, les plaques sont localisées au niveau de toutes les zones du néocortex incluant les zones riches en myéline. Dans le cas des enchevêtrements neurofibrillaires, l'évolution de la maladie est segmentée en six stades (Braak *et al.*, 2006). Le premier et le deuxième stade d'évolution des enchevêtrements neurofibrillaires montrent des lésions observables au niveau de la région transentorhinale pour s'étaler ensuite au niveau de l'hippocampe alors qu'au 6e stade, ce sont toutes les principales zones du néocortex qui sont affectées. À l'échelle cellulaire, les cellules neuronales montrent une signalisation intracellulaire dysfonctionnelle notamment au niveau de la voie PI3K/Akt/GSK3β ainsi que la voie des MAPK (Munoz et Ammit, 2010; O'Neill, 2013). Cette signalisation aberrante affecte notamment la survie des cellules et est impliquée à plusieurs niveaux dans l'évolution de la maladie.

Concrètement, il n'existe à l'heure actuelle aucune cure à l'AD. Les médicaments retrouvés sur le marché n'ont qu'un effet transitoire (plus efficace aux premiers stades de la maladie) en ralentissant uniquement la progression de la maladie (Giacobini et Gold, 2013; Hansen *et al.*, 2008; Tricco *et al.*, 2013; Vesey *et al.*, 2002). Ces médicaments sont principalement des inhibiteurs de la cholinestérase (rivastigmine, galantamine et donépézil), une enzyme responsable du nettoyage de l'acétylcholine (Ach) présente dans la fente synaptique ou des anti-glutamates (mémantine). Plusieurs efforts sont également mis de l'avant pour le développement de stratégies de traitement visant les deux autres symptômes

pathophysiologiques de l'AD. Il y a présentement plus d'une centaine de molécules en étude clinique visant les peptides β–amyloïdes et la protéine Tau (Bachurin *et al.*, 2017; Giacobini et Gold, 2013; Tricco *et al.*, 2013). Ces dernières sont des inhibiteurs des γ-sécrétases, impliquées dans la maturation des peptides amyloïdes, des anticorps monoclonaux visant les plaques séniles ou la protéine Tau hyperphosphorylée ou des analogues de neurotransmetteurs. Malheureusement, plusieurs de ces traitements ont échoué en phases cliniques jusqu'à maintenant en raison d'effets secondaires ou d'une absence d'efficacité par rapport au groupe contrôle (Giacobini et Gold, 2013).

En revanche, il y a un nombre croissant d'études montrant que l'utilisation de certains facteurs de croissance (GF), comme la famille des TGFβ, l'IGF-2, le bFGF, l'EGF et les neurotrophines naturellement retrouvés au niveau du cerveau de patients sains, pourrait avoir un effet thérapeutique important et pourrait restaurer la signalisation cellulaire dysfonctionnelle (Burke *et al.*, 2013; Jaeger *et al.*, 2016; Lopez-Coviella *et al.*, 2000; Marei *et al.*, 2015; Mellott *et al.*, 2014; Pascual-Lucas *et al.*, 2014; Thomas *et al.*, 2016, 2017; Yang *et al.*, 2014; Y. W. Zhang *et al.*, 2013). Parmi ces facteurs de croissance, certaines protéines morphogénétiques de l'os (BMPs) comme la BMP-9, appartenant à la famille des TGFβ, ont montré un potentiel particulièrement intéressant. Certains BMPs jouent un rôle prépondérant dans le développement du cerveau et la neurogénèse notamment par l'activation de la voie de signalisation canonique des Smad (Smad 1/5) (Hegarty *et al.*, 2013a; Mehler *et al.*, 1995, 1997). De surcroît, il a été montré que la BMP-9 pouvait agir sur plusieurs symptômes de l'AD simultanément. Par exemple, la BMP-9 permet de stimuler le système cholinergique en plus de promouvoir la différenciation neuronale sur modèle murin (Lopez-Coviella *et al.*, 2000, 2002, 2005, 2006). D'autres études ont également montré que la BMP-9 pouvait réduire l'accumulation de plaques séniles et limiter les pertes cognitives chez des souris surexprimant les peptides β–amyloïdes (Madziar *et al.*, 2008). Finalement, une étude récente a montré que la BMP-9, injectée au niveau intranasal chez la souris, permettait de réduire à la fois l'inflammation et les plaques séniles tout en restaurant le déficit cognitif chez le rat (Wang *et al.*, 2017). La BMP-9 peut également stimuler la synthèse de facteurs neurotrophiques impliqués dans le développement, la différenciation et la maintenance du CNS tels que le NGF (Schnitzler *et al.*, 2010).

Bien que le potentiel thérapeutique de la BMP-9 soit important, il faut également mentionner que d'autres BMPs, comme la BMP-2 et la BMP-4, peuvent avoir un effet contraire. Par exemple, il a été montré que l'expression de la BMP-4 augmentait au niveau du gyrus dentelé chez la souris vieillissante et que cette augmentation était associée à un déclin des fonctions cognitives (Meyers *et al.*, 2016). Une autre étude a également montré que la signalisation des BMPs pouvait réguler les comportements dépressifs (Brooker *et al.*, 2016). Il est également connu que la BMP-2 et la BMP-4 peuvent inhiber la neurogénèse tout en favorisant la maturation des astrocytes (Mercier et Douet, 2014; Xu *et al.*, 2013). Les BMPs sont divisés en sous-familles en fonction de leur homologie de séquence. Ainsi, bien que la BMP-9, la BMP-2 et la BMP-4 soient toutes des BMPs, ces dernières n'activent pas les mêmes récepteurs cellulaires de type I et, de ce fait, n'induisent pas les mêmes comportements. La BMP-9 appartient à la sous-famille BMP-9/BMP-10 alors que la BMP2 et la BMP-4 appartiennent à la même sous-famille (Senta *et al.*, 2009).

D'autres éléments comme certaines vitamines présentent également un potentiel thérapeutique non négligeable dans le contexte de l'AD. C'est notamment le cas des vitamines A (rétinols), C (acide ascorbique) et D. Par exemple, une étude récente chez le rat traité au chlorure d'aluminium pour induire un déficit cognitif a démontré que l'ajout de vitamine C pouvait rétablir les fonctions cognitives en réduisant le stress oxydatif tout en agissant comme un inhibiteur de l'acétylcholine estérase (Olajide *et al.*, 2017). D'autre part, une étude menée sur une cohorte de plus de 500 patients souffrants d'AD ou de démence vasculaire a montré que ces derniers avaient des niveaux de vitamine D inférieurs aux patients sains, faisant ainsi de la vitamine D un agent thérapeutique et un biomarqueur (Moretti *et al.*, 2017). La vitamine A, pour sa part, est connue pour son impact important sur la différenciation et la maintenance du CNS en plus d'être considérée comme une stratégie de traitement prometteuse contre l'AD (Cheung *et al.*, 2009; Sodhi et Singh, 2014). Il a été montré que l'appauvrissement en vitamine A chez des rats augmentait sensiblement leur vulnérabilité aux peptides β–amyloïde1-42 (Zeng *et al.*, 2017). L'acide rétinoïque peut également améliorer la prolifération des cellules souches neuronales murines en plus de limiter l'activation de la microglie chez des souris modèles APPswe/PS1M146V/tauP301L (3x Tg), un modèle transgénique qui accumule des peptides β-amyloïdes sous forme de plaques séniles ainsi que des enchevêtrements neurofibrilaires (Takamura *et al.*, 2017). L'acide rétinoïque est couramment employé comme agent de

différenciation neuronale, généralement en combinaison avec des facteurs de croissance comme les neurotrophines (Encinas *et al.*, 2000; Teppola *et al.*, 2016).

Bien que les facteurs de croissance comme la BMP-9 possèdent un potentiel thérapeutique intéressant, ces deniers n'en demeurent pas moins chers à produire et à purifier. De plus, la taille importante de ces protéines limite grandement leur adressage au cerveau en raison des différentes barrières naturelles du corps humain comme la barrière hématoencéphalique (BBB). Cette dernière se compose d'un tapis de cellules endothéliales liées entre elles par des jonctions serrées imperméables qui limitent grandement le passage d'éléments des capillaires sanguins vers le CNS (Alyautdin *et al.*, 2014; Haines, 2012; Lochhead et Thorne, 2012). Ces cellules font très peu de pinocytose et ne laissent généralement passer que certaines petites molécules liposolubles ou des gaz solubilisés comme le CO_2 et l'O_2 tout en limitant le passage de bactéries, virus et autres éléments indésirables. Les autres molécules comme l'insuline, le glucose et autres éléments essentiels doivent utiliser les mécanismes d'endocytose ou être acheminées via des récepteurs spécifiques (lactoferrine, lectines, LRP-1, APOE, insuline, etc.) (Haines, 2012; Marques *et al.*, 2013; Roney *et al.*, 2005). Les molécules liposolubles ou les petits peptides (<0.6 kDa) peuvent également emprunter des P-glycoprotéines (Banks, 2009). Ainsi, le principal transfert de molécules de la cavité nasale vers le CNS se fait via l'activation de récepteurs transmembranaires ou par transport actif.

Une des méthodes pour surmonter la BBB consiste dans un premier temps au développement de molécules thérapeutiques plus petites, car leur acheminement au cerveau est ainsi facilité (Lochhead et Thorne, 2012). Le laboratoire de la Professeure N. Faucheux a développé deux petits peptides dérivés de l'épitope knuckle de la BMP-9 composés de 23 acides aminés basés sur les travaux antérieurs de Saito *et al.* (2003, 2005) sur la BMP-2. Les acides aminés qui composent ces peptides correspondent à la séquence reconnue par le récepteur sérine/thréonine kinase transmembranaire des BMPs de type II (BMPRII) retrouvé en abondance dans le cerveau (Charytoniuk *et al.*, 2000). La première séquence peptidique (pBMP-9) se rapporte à la séquence native de la BMP-9 (Ac-CGGKVGKACCVPTKLSPISVLYK-NH2) alors que la deuxième (SpBMP-9) a subi une modification sur le site actif, où deux cystéines ont été remplacées par deux sérines (Ac-CGGKVGKA**SS**VPTKLSPISVLYK-NH2). Cette modification devrait augmenter l'affinité du

peptide pour le récepteur BMPRII comme cela a été montré avec les peptides dérivés de la BMP-2 (Saito *et al.*, 2003). Par ailleurs, ces peptides possèdent l'avantage d'être plus de 300 fois moins coûteux à produire sur une base massique que la protéine native, En effet, la BMP-9 utilisée pour des applications de recherche se détaille au prix de ~ 45 000US$/mg et est synthétisée *in vitro* dans des cellules issues d'ovaires de hamster chinois (CHO) alors que les peptides dérivés de cette dernière se détaillent au prix de ~110 US$/mg et sont synthétisés chimiquement. Des travaux antérieurs ont montré la bioactivité de ces peptides et leur capacité à activer les mêmes voies de signalisation que la BMP-9 en plus de promouvoir la différenciation cellulaire dans un contexte de régénération osseuse (Beauvais *et al.*, 2016; Bergeron *et al.*, 2009, 2012). Malgré tout, la BMP-9, et très certainement ses peptides dérivés, font face à une multitude de défis qui peuvent altérer leur efficacité une fois présents dans le corps humain (dénaturation, dégradation, clairance, etc.). Par exemple, le temps de demi-vie des BMPs dans le sang est de 6-7 min dans les non primates (Poynton et Lane, 2002). Le développement de stratégies pour protéger les molécules thérapeutiques le temps de les acheminer au cerveau est ainsi primordial.

Parmi les différentes stratégies de libération de facteurs de croissance ou de peptides dérivés de ces derniers, l'utilisation de systèmes de libération demeure une approche très prometteuse, car elle permet de protéger les molécules d'intérêt tout en assurant une libération soutenue dans le temps. Dans le contexte de l'acheminement au cerveau, l'utilisation d'un système de libération sous forme de nanoparticules ayant des diamètres de quelques centaines de nanomètres reste la méthode la plus efficace pour passer au travers de la BBB (Saraiva *et al.*, 2016). L'injection intranasale est généralement préconisée en raison de la proximité du tissu d'intérêt, la haute densité des capillaires sanguins et la grande capacité d'endocytose des cellules endothéliales de la paroi nasale (Dhuria *et al.*, 2010; Lochhead et Thorne, 2012). Ce site d'injection est d'ailleurs privilégié pour la libération de molécules avec des poids moléculaires variant entre 0,8 et 150 kDa (Lochhead et Thorne, 2012). Les matériaux préconisés pour la synthèse de ces nanoparticules sont généralement des polymères naturels dérivés de polysaccharides comme le chitosane, l'acide hyaluronique ou l'alginate (Ciofani *et al.*, 2008; Nagpal *et al.*, 2010). Ces matériaux possèdent l'avantage d'être biorésorbables, d'être bien tolérés par le corps humain et d'avoir de bonnes propriétés muco-adhésives qui leur assurent une meilleure interaction avec la paroi cellulaire (Aspden *et al.*, 1997; Gavini *et al.*,

2009; Nagpal *et al.*, 2010). De plus, ces matériaux ont déjà été employés pour la libération de molécules thérapeutiques au cerveau dans le contexte de l'AD. Par exemple, le groupe de Nagpal *et al.* a développé des nanoparticules à base de chitosane pour la libération de rivastigmine dans le cerveau de souris traité à la scopalamine pour induire de l'amnésie (Nagpal *et al.*, 2013). Ces chercheurs ont montré que l'encapsulation du médicament permet d'inverser les effets de la scopalamine et d'augmenter le temps de résidence au cerveau. Des nanoparticules (NPs) composites à base d'alginate et de chitosane ont également été utilisées pour l'adressage de peptides comme l'insuline ou de grosses protéines comme l'ovalbumine (Anal *et al.*, 2003; Biswas *et al.*, 2015; Borges *et al.*, 2006; Ciofani *et al.*, 2008; Goycoolea *et al.*, 2009). Ces NPs composites ont montré, par rapport aux matériaux utilisés seuls, une meilleure résistance aux environnements hostiles du corps humain, une libération soutenue dans le temps (Borges *et al.*, 2006; Maity *et al.*, 2017) ainsi qu'une meilleure incorporation intracellulaire, notamment par des cellules de l'hippocampe de souris HN9.10e (Ciofani *et al.*, 2008). De plus, Haque *et al.* (2014) ont montré que l'injection intranasale chez le rat de nanoparticles (~ 173 nm de diamètre) à base d'alginate et de chitosane pour le traitement de la dépression permettait une meilleure accumulation au cerveau par rapport au médicament seul. En outre, la combinaison de ces polymères pour transporter des peptides dérivés de facteurs de croissance au cerveau n'a pas encore été étudiée. De plus, le transport de ces molécules du passage nasal au CNS reste encore mal compris sur une base mécanistique.

En conclusion, deux problématiques majeures sont associées aux stratégies actuelles de traitement de l'AD. D'une part, ces stratégies se concentrent uniquement sur une seule des cibles thérapeutiques actuellement identifiées, ce qui pourrait expliquer les résultats transitoires observés. D'autre part, la libération des molécules thérapeutiques comme les GFs au site d'intérêt est sévèrement contrainte en raison de la BBB et fait face à une multitude de défis. La faible compréhension des mécanismes de libération et le devenir de système de libération dans le cerveau témoignent des défis à surmonter pour le développement d'une stratégie de traitement concrète et efficace.

1.2 Hypothèses de recherche

Au regard de la problématique actuelle et des nouvelles approches thérapeutiques à l'essai impliquant l'utilisation de facteurs de croissance, trois hypothèses de recherche ont été émises.

Dans un premier temps, au vu du potentiel thérapeutique de la BMP-9 dans le contexte de l'AD et, connaissant la bioactivité des peptides dérivés de cette dernière dans le contexte osseux, l'hypothèse suivante a été émise :

1) Les peptides dérivés de l'épitope knuckle de la BMP-9, pBMP-9 et SpBMP-9, sont en mesure d'induire, au même titre que la protéine native, une différenciation cellulaire neuronale et de jouer sur plusieurs cibles thérapeutiques associées à la maladie d'Alzheimer dans un modèle humain *in vitro*.

Par ailleurs, des études ont montré que des facteurs de croissance autres que la BMP-9, comme l'IGF-2, le bFGF, l'EGF ou des neurotrophines comme le NGF avaient également un effet thérapeutique important dans le contexte de la maladie d'Alzheimer (voir revue (Lauzon *et al.*, 2015a)). De plus, plusieurs études ont également mis de l'avant le fait que ces facteurs de croissance pouvaient, une fois combinés, agir en synergie. L'hypothèse suivante a donc été formulée :

2) Le pBMP-9 et/ou le SpBMP-9 peuvent agir en synergie avec d'autres facteurs de croissance et induire une différenciation neuronale supérieure dans un modèle humain *in vitro*.

Finalement, tels qu'il a été montré précédemment, l'acheminement de molécules thérapeutiques au cerveau fait face à une multitude de défis. Les barrières naturelles du corps humain telles que la BBB limitent grandement leur adressage au système nerveux central (CNS). L'utilisation d'un système de libération à l'échelle nanométrique dans l'optique d'une injection intranasale devient alors essentielle pour protéger la molécule d'intérêt et maximiser l'accumulation au tissu d'intérêt. Il a été montré que l'utilisation de polymères naturels comme l'alginate et le chitosane présentaient des caractéristiques muco-adhésives intéressantes ainsi qu'une bonne innocuité par le corps humain. En ce sens, l'hypothèse suivante a été émise :

3) Les peptides pBMP-9 et/ou SpBMP-9 peuvent être efficacement encapsulés dans un système de libération sous forme de nanoparticules composites à base d'alginate et de chitosane ayant une taille moyenne de quelques centaines de nanomètre, et ce, dans l'optique à plus long terme d'un adressage au cerveau via une injection intranasale.

1.3 Objectifs

Afin de valider ou d'infirmer les hypothèses de recherche, ce projet de doctorat reposait sur quatre objectifs principaux, eux-mêmes sous-divisés en plusieurs sous-objectifs. Le Tableau 1-1 ci-dessous présente d'ailleurs les détails de ces derniers. Tout d'abord, le premier objectif consistait à approfondir les connaissances face à l'AD et à étudier les différents acteurs liés au projet de doctorat afin d'avoir une bonne vue d'ensemble des stratégies thérapeutiques actuelles. Puis, le deuxième objectif consistait à déterminer la capacité de deux peptides dérivés de la BMP-9 à induire la différenciation neuronale de cellules dérivées de neuroblastomes humains SH-SY5Y. Cet objectif impliquait également l'évaluation de l'effet de ces deux peptides sur des cibles thérapeutiques associées à l'AD. Le troisième objectif principal s'est penché sur le développement, la caractérisation et la modélisation mathématique d'un système de libération à l'échelle nanométrique pour l'acheminement de ces mêmes peptides au cerveau.

Finalement, le quatrième objectif principal consistait à déterminer l'effet de la combinaison de peptides dérivés de la BMP-9 avec d'autres facteurs de croissance ayant un potentiel thérapeutique dans le contexte de l'AD sur le comportement de cellules SH-SY5Y.

Tableau 1-1 : Objectifs principaux et spécifiques du projet

Objectifs principaux	Objectifs spécifiques
1) Effectuer une revue de littérature sur les différents acteurs impliqués dans le projet	• Comprendre les causes et les symptômes de l'AD à l'échelle cellulaire • Rechercher les traitements actuels et leurs limitations • Déterminer les différents aspects thérapeutiques de l'utilisation de GFs dans le contexte de l'AD comme stratégie de traitement alternative • Évaluer les différentes voies d'administration et étudier l'évolution des différents systèmes de libération (matériaux, caractéristiques physiques, etc.) • Répertorier les différents phénomènes pouvant affecter l'acheminement des GFs au cerveau et comment les modéliser mathématiquement

2)	Déterminer l'effet thérapeutique *in vitro* de la BMP-9 et de ses peptides dérivés sur les cellules humaines de type SH-SY5Y	Évaluer l'effet de la BMP-9 et de ses peptides dérivés sur : • La survie cellulaire • La morphologie cellulaire et la longueur des neurites • L'expression et la localisation de marqueurs de différenciation neuronaux • La capacité à induire et maintenir le phénotype cholinergique • La capacité à inactiver la GSK3 beta
3)	Concevoir et caractériser un système de libération à base de nanoparticules d'alginate et de chitosane permettant la libération contrôlée du SpBMP-9	• Concevoir et caractériser les nanoparticules d'alginate/chitosane (distribution de taille, morphologie) • Faire le suivi et modéliser les cinétiques de libération et estimer les paramètres de transfert de masse importants • Évaluer la capacité des cellules neuronales à se différencier lorsqu'ensemencées au contact du système de libération
4)	Évaluer l'effet synergique potentiel entre les peptides dérivés de la BMP-9 et d'autres GFs (IGF-2, EGF, bFGF et NGF) ayant un potentiel thérapeutique dans le contexte de l'AD sur des cellules humaines SH-SY5Y	Évaluer l'effet de différentes combinaisons de GFs avec le pBMP-9/SpBMP-9 sur: • La morphologie et la longueur des neurites • L'expression de marqueurs de différenciation neuronale • La fonctionnalité des neurones différenciés et leur capacité à échanger de l'information (neurotransmission)

1.4 Contributions originales

1.4.1 État de l'art

Le chapitre 2 présente l'état de l'art sous forme de deux articles scientifiques publiés dans *Cellular Signaling* et *Journal of Controlled Release*.

Premier article de revue

Le premier article de revue s'est concentré sur la compréhension de l'AD et des différents acteurs impliqués dans cette maladie en plus de discuter des nouvelles stratégies thérapeutiques impliquant l'utilisation de facteurs de croissance. Les contributions originales de cet article sont les suivantes :

- Une étude des différents symptômes et des cibles thérapeutiques associés à la maladie d'Alzheimer ainsi que les différents traitements actuellement retrouvés sur le marché. Les différentes cibles thérapeutiques identifiées sont également mises en avant-plan ainsi que leurs réactions croisées.

- Une étude exhaustive des différentes voies de signalisation impliquées dans l'AD, leurs réactions croisées ainsi que leur impact sur le comportement des neurones du CNS.

- Une revue complète sur l'utilisation de facteurs de croissance comme stratégie thérapeutique alternative. L'originalité de cette section tient du fait que l'effet de ces facteurs de croissance sur l'activation de voies de signalisation cellulaire dérégulées dans le contexte de l'AD est étudié en détail.

- Une revue des nouvelles stratégies innovatrices à base de peptides dérivés de facteurs de croissance. Étant moins volumineux et moins coûteux à produire que les protéines natives, cette approche permet de faciliter le passage au travers des barrières naturelles qui limitent le transport au cerveau. Certains de nos résultats préliminaires y sont présentés et montrent, pour la première fois, l'effet de peptides dérivés de la BMP-9 (pBMP-9) sur la croissance de neurites de cellules SH-SY5Y en présence ou en absence d'acide rétinoïque, un inducteur de la différenciation neuronale.

La conclusion générale de cet article indique que l'utilisation de facteurs de croissance peut restaurer la signalisation cellulaire dysfonctionnelle observée dans l'AD. Les nouvelles stratégies thérapeutiques s'orientent vers l'utilisation de peptides dérivés de ces facteurs de croissance, moins coûteux et avec une efficacité similaire ou accrue, comme dans le cas du pBMP-9.

Deuxième article de revue

Le deuxième article de revue de la littérature s'est concentré sur les méthodes d'acheminement des facteurs de croissance au CNS. Ces travaux se sont notamment attardés sur les différents types de système de libération (GFDS) développés dans ce contexte ainsi que les phénomènes à considérer pour modéliser et ultimement optimiser l'acheminement de molécules thérapeutiques au cerveau. Les contributions spécifiques des travaux publiés dans la revue *Journal of Controlled Release* sont présentées ci-dessous :

- Les différentes méthodes d'injection ainsi que les barrières naturelles qui limitent le plus l'adressage de facteurs de croissance comme la BBB sont abordées tout comme les nouvelles stratégies pour faciliter le passage au travers de ces dernières.

- Une revue exhaustive des systèmes de libération pour l'adressage de facteurs de croissance au cerveau sous forme de NPs. Les différents matériaux employés, les méthodes de synthèse ainsi que l'effet de ces GFDS *in vitro* et *in vivo* dans le contexte de l'AD sont étudiés en détail.

- Les différents obstacles et barrières naturelles du corps humain pouvant affecter l'acheminement de GFDS sous forme de NPs suivant une injection intranasale sont présentés. Les phénomènes de transport de masse et les contraintes rencontrées du site d'injection jusqu'au CNS sont également étudiés et des pistes de solution quant à la modélisation mathématique de ces phénomènes sont abordées. Finalement, les différents phénomènes pouvant influencer la libération des molécules thérapeutiques à même les NPs et leur modélisation mathématique sont étudiés.

La contribution globale de cet article est que les GFDS favorisent l'adressage de molécules thérapeutiques afin d'assurer leur pérennité et leur accumulation au cerveau. Ces derniers sont généralement sous forme de NPs à base de polymères naturels ou synthétiques qui doivent passer outre plusieurs barrières naturelles. L'originalité de cet article tient, en autres, dans la présentation de modèles mathématiques adaptés aux contraintes de l'acheminement de molécules thérapeutiques au CNS qui peuvent fournir des pistes de solution dans la conception et l'optimisation de GFDS.

1.4.2 Étude du comportement des cellules SH-SY5Y au contact de peptides dérivés de la BMP-9

Le troisième chapitre de cette thèse présente, sous la forme d'un article scientifique publié dans la revue Scientific Reports, les résultats associés au deuxième objectif principal de la thèse. Ce travail fait la preuve de concept quant à l'utilisation de peptides dérivés de la BMP-9. Les contributions spécifiques de ces travaux sont les suivantes :

- Deux peptides dérivés de l'épitope knuckle de la BMP-9 (pBMP-9 et SpBMP-9) activent la voie canonique des Smad1/5 comme la BMP-9 et permettent leur translocation au noyau dans des cellules SH-SY5Y. Néanmoins, l'activation et la translocation des Smad1/5 semblent plus faibles avec les peptides par rapport à la BMP-9. L'effet de peptides ou de la BMP-9 sur un modèle cellulaire de neurones humains n'avait pas été démontré jusqu'à présent.
- Le pBMP-9 et le SpBMP-9 augmentent le nombre et la longueur des neurites ainsi que l'expression de marqueurs de différenciation neuronaux précoces et tardifs, et ce, de façon plus importante que le contrôle et la BMP-9. Par ailleurs, le SpBMP-9 semble

avoir un effet plus important que le pBMP-9 et cet effet est augmenté en présence d'acide rétinoïque.

- Les peptides dérivés de la BMP-9, surtout le SpBMP-9, jouent sur au moins deux cibles thérapeutiques associés à l'AD. D'une part, ils permettent d'augmenter la synthèse d'acétylcholine et l'expression d'autres marqueurs cholinergiques. D'autre part, les peptides permettent d'activer la voie PI3K/Akt et d'inactiver la GSK3beta, une Tau kinase.

La contribution globale de cet article est que le pBMP-9 et surtout le SpBMP-9 possèdent un effet thérapeutique potentiel très intéressant qui peut agir favorablement avec l'acide rétinoïque surtout au niveau du développement des neurites et l'expression de certains marqueurs. Leur faible coût de production par rapport à la protéine native et leur potentiel de différenciation plus important en font une stratégie de traitement très prometteuse.

1.4.3 Développement et caractérisation d'un système de libération de SpBMP-9

Le quatrième chapitre de la thèse porte sur le développement d'un système de libération à base de NPs pour encapsuler le SpBMP-9 et la preuve de concept que les peptides libérés restent bioactifs. Les travaux relatifs à ce chapitre ont mené à la rédaction d'un article scientifique en révision dans la revue *Carbohydrate Polymers*. Cette étude a permis d'apporter les contributions spécifiques suivantes :

- Des NPs à base d'alginate et de chitosane ont été synthétisées par méthode de gélification ionotropique. La caractérisation du système de libération a permis de montrer que les particules avaient une taille moyenne de 240 nm et une efficacité d'encapsulation de SpBMP-9 d'environ 70% avec un pourcentage massique de peptide/NPs de 3%.

- L'étude des cinétiques de libération a permis de montrer que la libération du SpBMP-9 en condition physiologique était principalement diffusive, mais qu'il existait toutefois de fortes interactions électrostatiques entre le SpBMP-9 et la matrice à base d'alginate. La nature et la force de ces interactions faisaient en sorte que la diffusion pouvait s'étendre sur plus de 72h.

- Un modèle mathématique mécanistique prenant en considération la distribution de taille des particules (basé sur les mesures expérimentales de diffraction au laser) via l'utilisation de la méthode des classes a été développé. Ce dernier a permis de confirmer la présence d'interactions entre le peptide et la matrice d'alginate ainsi que la nature diffusive du système de libération. L'estimation des paramètres par le développement d'un algorithme d'optimisation méta-heuristique stochastique a permis d'estimer la diffusivité et le coefficient global de transfert de masse. L'analyse subséquente de ces paramètres a montré que la résistance au transfert de masse se situait à l'intérieur des particules plutôt qu'à la surface, ce qui confirmait les hypothèses de présence d'interactions entre le peptide et l'alginate contenu dans les NPs.
- Des essais de survie menés sur des cellules SH-SY5Y ont montré que ces dernières pouvaient survivre sur une période de 5 jours en présence des NPs. De plus, la présence des NPs stimulait l'activité métabolique et la prolifération cellulaire. Des essais de libération de SpBMP-9 au contact des cellules ont également montré que le peptide libéré était toujours bioactif et permettait une augmentation du nombre et de la longueur des neurites ainsi que l'expression de marqueurs de différenciation neuronale.

La contribution globale de cet article est que le SpBMP-9 peut être efficacement encapsulé dans un système de libération à base de polymères naturels déjà employés pour l'acheminement de molécules thérapeutiques au cerveau. De plus, ce système est non-cytotoxique et permet d'induire la différenciation neuronale.

1.4.4 Étude de la combinaison de facteurs de croissance avec le SpBMP-9 sur la réponse des SH-SY5Y

Le cinquième chapitre de la thèse porte sur la détermination de synergie potentielle pouvant exister entre le SpBMP-9 et d'autres facteurs de croissance connus pour leur effet thérapeutique dans le contexte de l'AD. Les travaux présentés dans ce chapitre ont mené à la rédaction d'un article scientifique en révision dans la revue *Molecular and Cellular Neuroscience*. Les principales contributions découlant de ces travaux sont :

- Différentes combinaisons de facteurs de croissance (IGF-2, EGF, bFGF et NGF) avec le peptide SpBMP-9 ont été testées afin de montrer les synergies potentielles. Ceci a

permis de déterminer que le NGF et le bFGF permettait d'augmenter le nombre de neurites par rapport aux facteurs de croissance utilisés seuls sur des cellules SH-SY5Y dans des conditions de culture *in vitro* sans sérum.

- L'utilisation d'un peptide négatif, dont les acides aminés correspondant aux sites actifs ont été modifiés par des glycines, a permis de confirmer l'efficacité et la spécificité du SpBMP-9 chez les cellules humaines SH-SY5Y.

- Une étude plus approfondie a permis de mettre en évidence que le SpBMP-9, combiné avec le NGF ou le bFGF, augmente significativement la longueur des neurites ainsi que l'expression du marqueur de différenciation neuronale terminale NSE.

- Les analyses subséquentes ont montré que la combinaison entre le SpBMP-9 et le bFGF ou le NGF orientait la différenciation vers le phénotype cholinergique de façon plus importante comparativement aux facteurs de croissance utilisés seuls.

- Le SpBMP-9, utilisé en combinaison avec le bFGF ou le NGF, augmente également le niveau de calcium intracellulaire. Les niveaux de calcium intracellulaire étant notamment liés à la croissance des neurites, les résultats montrent un niveau de différenciation accru qui corrobore les observations précédentes.

En conclusion, la contribution globale de cet article est que le SpBMP-9 peut agir en synergie avec le bFGF et le NGF. Des synergies similaires impliquant le NGF ou le bFGF avec la protéine native BMP-9 avait déjà été mises en évidence par d'autres groupes de recherche. Toutefois, les travaux de ce chapitre montrent, pour la première fois, que cette synergie peut également s'étendre à un peptide dérivé de la BMP-9. Ceci est corroboré à plusieurs niveaux, notamment par l'adoption d'une morphologie cellulaire qui évolue vers un profil neuronal ou par les niveaux d'expression de marqueurs protéiques de différenciation. Connaissant le potentiel thérapeutique de ces molécules, l'utilisation d'un peptide moins coûteux témoigne encore plus du potentiel thérapeutique du SpBMP-9 dans le contexte de l'AD.

1.5 Plan du document

Cette thèse comprend 7 chapitres. Le premier chapitre est une introduction générale présentant la mise en contexte, les hypothèses de recherche ainsi que les objectifs du projet de doctorat. Un sommaire des principales contributions à la recherche des travaux réalisés est

également présenté. Le chapitre 2 de ce document présente l'état de l'art sous forme de deux articles scientifiques de revue de la littérature. Le premier article de revue, publié dans la revue *Cellular Signaling*, traite des symptômes et des cibles thérapeutiques de la maladie d'Alzheimer en plus d'aborder les nouvelles approches thérapeutiques qui mettent en jeux l'utilisation de facteurs de croissance. Le deuxième article de revue, publié dans la revue *Journal of Controlled Release* traite des systèmes de libération pour l'acheminement des facteurs de croissance au cerveau et fait une revue complète des différents matériaux et configurations employés pour passer les barrières naturelles du corps humain. Les différents phénomènes de transfert de masse et les moyens pour les modéliser dans ce contexte précis sur une base mécanistique y sont également répertoriés. Le troisième chapitre de cette thèse présente la preuve de concept quant à l'utilisation de peptides dérivés de la BMP-9 (pBMP-9 et SpBMP-9) comme nouvelle approche thérapeutique contre l'AD. Ces travaux sont présentés sous la forme d'un article scientifique de résultats publié dans la revue *Scientific Reports*. Par la suite, le chapitre 4 porte sur le développement et la caractérisation d'un système de libération de SpBMP-9 à base d'alginate et de chitosane sous la forme de NPs dans une optique d'injection intranasale à plus long terme. Ces résultats sont présentés sous la forme d'un article scientifique en révision dans la revue *Molecular Pharmaceutics*. Ensuite, le chapitre 5 présente l'effet de la combinaison entre le SpBMP-9 et d'autres facteurs de croissance tels que le bFGF et le NGF ayant déjà montré un potentiel thérapeutique dans le contexte de l'AD. Ces résultats se retrouvent sous la forme d'un article de scientifique en révision dans la revue *Molecular and Cellular Neuroscience*. Finalement, le chapitre 6 présente la conclusion générale et les perspectives.

CHAPITRE 2:   ÉTAT DE L'ART

L'état de l'art pour la réalisation de cette thèse est présenté sous forme de 2 articles de revue de la littérature qui ont été publiés en 2015.

2.1 Informations sur le 1er article de revue

Titre original: Growth factor treatment to overcome Alzheimer's dysfunctional signaling

Titre français : Traitement à base de facteurs de croissance pour surmonter la signalisation dysfonctionnelle présente dans la maladie d'Alzheimer.

Auteurs et affiliations :

- M.-A. Lauzon : Étudiant au doctorat en génie chimique, Département de génie chimique et de génie biotechnologique, Université de Sherbrooke
- A. Daviau : Ancien assistant de recherche sous la direction de Prof. N. Faucheux, Département de génie chimique et de génie biotechnologique, Université de Sherbrooke
- B. Marcos : Professeur titulaire, Département de génie chimique et de génie biotechnologique, Université de Sherbrooke
- N. Faucheux : Professeur titulaire, Département de génie chimique et de génie biotechnologique, Université de Sherbrooke

Date d'acceptation : 16 février 2015

État de l'acceptation : version finale publiée

Revue : *Cellular Signalling*

Lien d'accès : https://doi.org/10.1016/j.cellsig.2015.02.018

Contributions à la thèse :

Cet article contribue à la thèse en présentant l'état de l'art (premier objectif) concernant les principaux acteurs autour desquels s'articule le projet de doctorat. Les éléments suivant y sont présentés :

- Une revue des derniers avancements concernant les symptômes inhérents à la maladie d'Alzheimer, les traitements actuels ainsi que les nouvelles cibles thérapeutiques.
- Une revue des voies de signalisation dysfonctionnelles dans le contexte de l'AD ainsi que leurs réactions croisées.
- Une revue des différents facteurs de croissance pouvant avoir un effet thérapeutique dans le contexte de l'AD ainsi que leur effet sur les voies de signalisation cellulaire dysfonctionnelles.
- Une revue des dernières innovations dans le domaine de l'utilisation de dérivés de facteurs de croissance comme alternative aux molécules complètes. Certains de nos résultats concernant l'utilisation d'un peptide dérivé de la BMP-9 (pBMP-9) sur des cellules dérivées de neuroblastomes humains y sont également présentés.

Résumé anglais:

The number of people suffering from Alzheimer's disease (AD) will increase as the world population ages, creating a huge socio-economic burden. The three pathophysiological hallmarks of AD are the cholinergic system dysfunction, the β-amyloid peptide deposition and the Tau protein hyperphosphorylation. Current treatments have only transient effects and each tends to concentrate on a single pathophysiological aspect of AD. This review first provides an overall view of AD in terms of its pathophysiological symptoms and signaling dysfunction. We then examine the therapeutic potential of growth factors (GFs) by showing how they can overcome the dysfunctional cell signaling that occurs in AD. Finally, we discuss new alternatives to GFs that help overcome the problem of brain uptake, such as small peptides, with evidence from some of our unpublished data on human neuronal cell line.

Résumé français :

Le nombre de personnes souffrant de la maladie d'Alzheimer (AD) augmentera avec le vieillissement de la population mondiale, créant ainsi un important fardeau socio-économique. Les trois caractéristiques pathophysiologiques de l'AD sont le système cholinergique dysfonctionnel, le dépôt de peptides β–amyloïdes et l'hyperphosphorylation de la protéine Tau. Les traitements actuels possèdent uniquement un effet transitoire et tendent chacun à se concentrer sur un seul aspect pathophysiologique de l'AD. Cette revue fournit dans un premier temps une vue d'ensemble sur l'AD en termes de symptômes pathophysiologiques

et de signalisation dysfonctionnelle. Nous avons ensuite examiné le potentiel thérapeutique des facteurs de croissance (GFs) en montrant comment ils peuvent surmonter la signalisation cellulaire dysfonctionnelle qui survient dans l'AD. Finalement, nous avons discuté des nouvelles alternatives aux GFs qui aident à surmonter le problème de leur absorption au cerveau, comme des peptides de faible taille, avec des preuves provenant de certains de nos résultats non publiés sur une lignée cellulaire de neurones humains.

2.2 Introduction

Neurodegenerative diseases will become more and more common in the years to come as the world population ages. The demographic projections of the World Health Organization (WHO) estimate that there will be 2 billion people aged 60 or over by 2050 (World Health Organization, 2012), and that 2–10% of those presently aged 65 will suffer from dementia (Mota *et al.*, 2014; World Health Organization, 2012). Alzheimer's disease (AD) is the most common neurodegenerative disorder, representing 60–80% of the reported dementia cases (Alzheimer's Association, 2013; Alzheimer's Society Canada). More than 40 million people worldwide were diagnosed with AD in 2012 and this number is likely to rise further; the resulting huge socioeconomic burden will cost hundreds of billions of dollars annually (Mota *et al.*, 2014; World Health Organization, 2012).

AD patients suffer from learning impairment and changes in their spatial and temporal perception, in addition to the obvious clinical symptoms like memory loss, which get worse as the disease progresses (Kumar *et al.*, 2005; Mota *et al.*, 2014; Vesey *et al.*, 2002). There are three main pathophysiological features of AD: (1) cholinergic system dysfunction (Geula *et al.*, 2008; Gil-Bea *et al.*, 2005; Parent *et al.*, 2013; Teipel *et al.*, 2011), (2) β-amyloid peptide deposition (Murphy et LeVine 3rd, 2010; Sinha et Lieberburg, 1999) and (3) Tau protein hyperphosphorylation (Augustinack *et al.*, 2002; Giacobini et Gold, 2013; Orejana *et al.*, 2013). The current FDA-approved treatments designed to inhibit cholinesterase have only transient effects and do not stop the disease progressing (Hansen *et al.*, 2008; Molino *et al.*, 2013; Tricco *et al.*, 2013; Vesey *et al.*, 2002). Other proposed strategies such as antibodies that inhibit β-amyloid peptides or glycogen synthase kinase 3 beta (GSK3β, responsible for Tau phosphorylation (Johnson et Stoothoff, 2004; Povellato *et al.*, 2014)) target only one specific aspect; they have failed in clinical trials because they were either ineffective or produced severe

side effects (Brunden *et al.*, 2010; Do *et al.*, 2014; Giacobini et Gold, 2013; Vesey *et al.*, 2002). New insights suggest that the three main features of AD are closely interlinked and can act in synergy in disease progression. Clearly, we need to develop new therapeutic strategies to tackle this scourge.

Several recent advances in AD research suggest that growth factors (GFs) have great therapeutic potential. These GFs include the transforming growth factor β family (Burke *et al.*, 2013; Lopez-Coviella *et al.*, 2002, 2011; Schnitzler *et al.*, 2010), insulin derived GFs (insulin, insulin-like growth factor 1, IGF-1; and 2, IGF-2) (Freiherr *et al.*, 2013), fibroblast growth factor (bFGF) (Ye *et al.*, 2010) and neurotrophins (nerve growth factor, NGF; brain-derived growth factor, BDGF; glial-derived neurotrophic factor, GDNF) (Schindowski *et al.*, 2008). These GFs are found naturally in the brain and are implicated in neurodevelopment, neurogenesis and central nervous system (CNS) homeostasis (Konishi *et al.*, 1994; Schindowski *et al.*, 2008; Schmeisser *et al.*, 2012; Ueberham et Arendt, 2013; Woodbury et Ikezu, 2014). However, we need to better understand the impact of these GFs on neurons and their local environment since the signaling pathways they activate can ameliorate or worsen the pathophysiological symptoms of AD (Godoy *et al.*, 2014). The big challenge is to overcome the impaired signaling that occurs in AD.

Many hurdles must therefore overcome before GFs can be used successfully on targets within the brain. Several biological barriers prevent the accumulation of drugs and undesired proteins in the brain. The main one is the blood brain barrier (BBB) (Alyautdin *et al.*, 2014; Haines, 2012; Lochhead et Thorne, 2012), which regulates and limits the passage of molecules through active transport and specific cell receptors for molecules like insulin, transferrin and apolipoprotein related protein (Haines, 2012; Marques *et al.*, 2013; Roney *et al.*, 2005). The GFs are also susceptible to proteolytic degradation, clearance and denaturation when they are present in the blood or in the extracellular space of the brain (Di Stefano *et al.*, 2011). They also need to be specifically address to the brain since GFs can act on other cell types such as bone or endothelial cells (David *et al.*, 2007; Kang *et al.*, 2004; Suzuki *et al.*, 2010).

This review therefore examines the potential of GFs for treating AD. We first describe the current clinical and pathophysiological symptoms of AD, focusing on the cross-regulations of AD symptoms. We then look at the signaling pathways implicated in AD and how GFs can

reverse their effects when used correctly either alone or in a suitable combination. This leads on to how new peptide molecules derived from GFs can become the basis for new effective therapeutic approaches.

2.3 Symptoms and therapeutic targets of Alzheimer's disease

2.3.1 Current symptoms

There are two different forms of AD, a sporadic one that can appear without any genetic predisposition and one that results from genetically transmitted mutations (Oddo *et al.*, 2003; Selkoe et Podlisny, 2002). Three loci in the genomes of patients suffering from the dominant autosomal form of AD have been identified. These are the gene encoding β-amyloid precursor protein (βAPP), located on chromosome 21, the gene encoding presenilin 1 (PS1), located on chromosome 14, and the gene for presenilin 2 (PS2) on chromosome 1 (Oddo *et al.*, 2003; Selkoe et Podlisny, 2002). All three loci are associated with the metabolism of β-amyloid peptides (γ -secretase cleavage of β APP, β-amyloid peptide maturation for βAPP) and Ca^{2+} modulation in pre-synaptic neurons for PS1 and PS2 (Maesako *et al.*, 2011; Zhang *et al.*, 2009). Some studies also suggest that a combination of ageing and hypertension acts synergistically to increase the predisposition to AD (Csiszar *et al.*, 2013). AD can be defined as a progressive neurodegenerative disorder that can develop over 8.5 to 10 years (Kumar *et al.*, 2005; Vesey *et al.*, 2002). It affects mainly specific brain regions associated with memory and learning, such as the neocortex, the hippocampus, and the basal forebrain (Mota *et al.*, 2014; Vesey *et al.*, 2002). The symptoms of AD can be divided into two categories: (1) clinical and (2) paraclinicals (neuropathological). The clinical symptoms are the effects on the patient's cognitive capacity, whereas the paraclinical or pathophysiological symptoms describe the molecular and cellular degeneration of the brain.
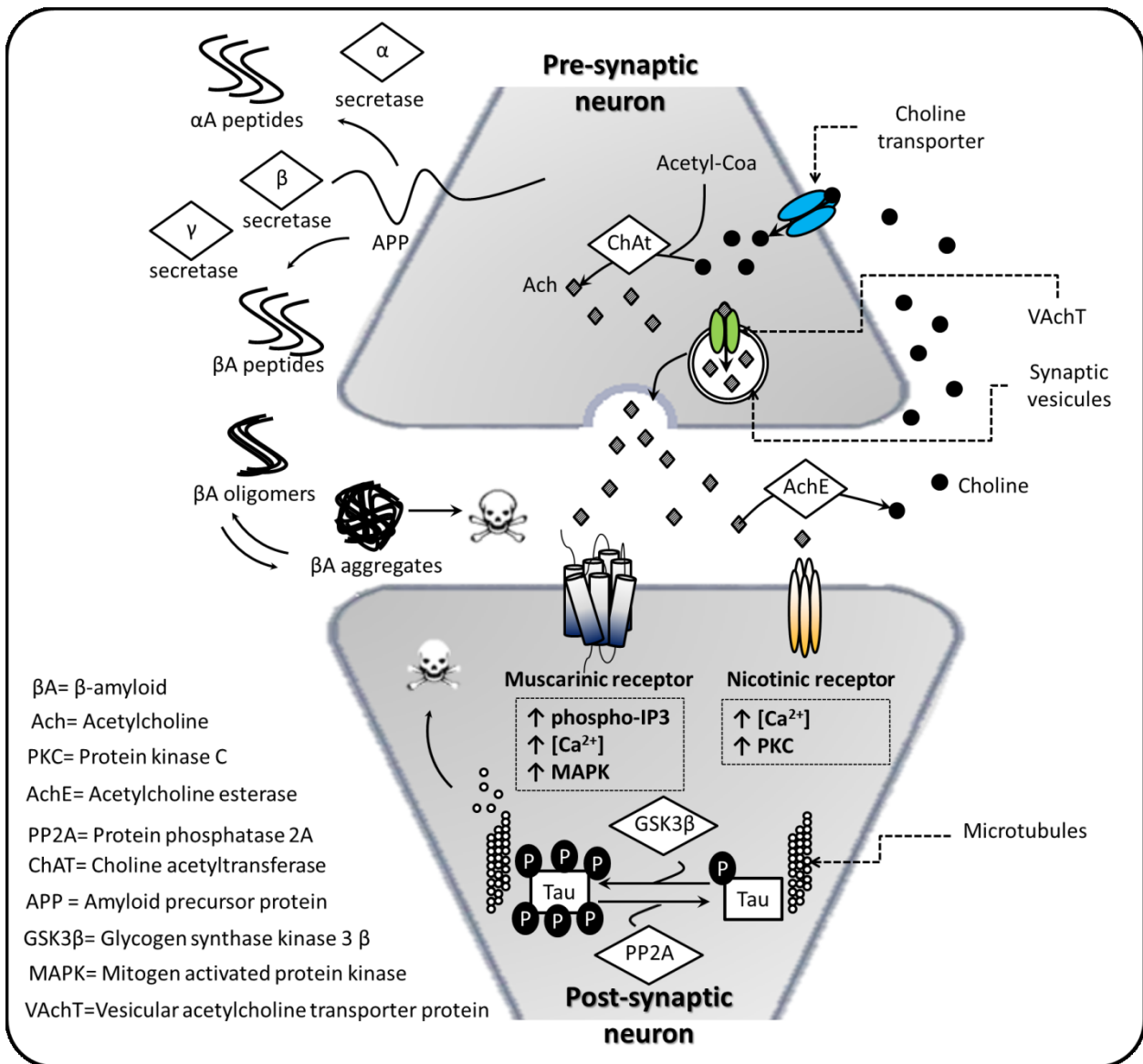
Figure 2-1 : Cholinergic transmission between pre-synaptic and post-synaptic neurons showing the main actors and the hallmarks of AD. Adapted from (Jones *et al.*, 2012) and (Grossberg, 2007)

Preclinical symptoms

Typically, AD results in the degeneration of a patient's cognitive abilities, short-term memory and learning capacity. The disease progresses in three stages: (1) mild AD, (2) moderate AD and (3) advance AD (Alzheimer's Association, 2013; Alzheimer's Society Canada). Individuals with mild AD experience cognitive impairment such as memory loss, confusion, and inability to solve problems, mood and personality changes and communication difficulties. Those with mild stage AD have difficulties with basic day-to-day tasks. Finally, in late stage

AD patients become unable to communicate, walk, eat, or move, and require full time care for the rest of their lives.

Pathophysiological symptoms and therapeutic targets

The cholinergic system

The paraclinical symptoms of AD, also known as the hallmarks of the neuropathology, are a dysfunctional cholinergic system and the formation of senile plaques and neurofibrillary tangles (Braak et Braak, 1991; Giacobini et Gold, 2013; Vesey *et al.*, 2002). Figure 2-1 shows these AD hallmarks, their interconnections and the involvement of the simplified signaling pathways in the disease.

The cholinergic system (Figure 2-1) was one of the first therapeutic targets to be studied extensively, since AD patients with mild AD and severe AD suffer from a loss of cholinergic neurons and a net decline in their choline acetyltransferase and cholinesterase activities (Geula *et al.*, 2008). Teipel *et al.* used deformation-based morphometry from magnetic resonance imaging (MRI) and diffusion tensor imaging to show a significant correlation between the changes in the cholinergic systems of patients developing AD and their cognitive impairment (Teipel *et al.*, 2011). Parent *et al.* (2013) obtained similar results using fluoroethoxybenzovesamicol [^{18}F], a ligand that binds specifically to vesicular acetylcholine transporter protein. Acetylcholine, the neurotransmitter in the cholinergic system, is released by the pre-synaptic neurons into the synaptic cleft. Here, it interacts directly with its receptor (nicotinic or muscarinic) located on the surface of the post-synaptic neurons (Figure 2-1). One way to maintain cholinergic activity in AD is to increase the availability of this neurotransmitter, by promoting acetyl-coA production, as reviewed by Szutowicz *et al.* (2013) or by increasing choline levels or using choline uptake enhancers (Kopf *et al.*, 2001; Takashina *et al.*, 2008). Another is to increase the response of the post-synaptic neuron to the neurotransmitter by stimulating the receptors on both the pre-synaptic (modulation of acetylcholine release) and post-synaptic neurons (stimulation of the post-synaptic receptors) (Vesey *et al.*, 2002). Activating the muscarinic receptors M1 and M4 could form part of a treatment for AD (Foster *et al.*, 2014; Melancon *et al.*, 2013). Jiang *et al.* (2014) found that inhibiting the muscarinic receptor M1-mACHR with scopolamine drastically decreased the cognitive abilities of rats,

particularly their task-related associative memory. This emphasizes the importance of receptor activity in cognitive impairment. The third way is to prevent the degradation of the neurotransmitter once it is released into the synaptic cleft, by inhibiting acetylcholine esterase (AchE), the enzyme responsible for cleavage of the neurotransmitter (Colovic *et al.*, 2013; Vesey *et al.*, 2002). Certain FDA-approved drugs that are delivered orally or intradermally, such as donepezil, rivastigmine and galantamine, specifically or semi-specifically target AchE (Di Stefano *et al.*, 2011). However, recent meta-analyses and reviews of the outcomes of clinical trials indicate that these treatments have only modest effects (Hansen *et al.*, 2008; Molino *et al.*, 2013; Tricco *et al.*, 2013). One of their major drawbacks is their transient effects. They slow the progression of cognitive impairment but have no effect on the disease itself.

β-Amyloid peptides and the formation of senile plaques

Senile plaques are extracellular fibrillar aggregates of β-amyloid peptides. They are derived from amyloid precursors, which are first cleaved by β- then γ-secretases within the β-amyloid sequence to induce the toxic aggregation (Sinha et Lieberburg, 1999). The review by Placido *et al.* (2014) describes 8 isoforms of the amyloid precursor protein, with the 695 amino acid isoform being the most common in the CNS. These aggregates severely impair the viability of neurons by disrupting the neuropil (brain parts composed of unmyelinated axons, dentrites and glial cells forming dense synaptic regions). This damages the cell bodies and axons (Murphy et LeVine 3rd, 2010). β-Amyloid precursors of different lengths and organizations can also be found, some are β-amyloid-derived diffusible ligands and soluble oligomers (15−20 residues). Deshpande *et al.* (2006) have shown that these organizations do not affect neurons or interact with the min the same way as the fibrillar form does. They also showed that soluble oligomers affect mitochondrial activity and cause massive, direct cytotoxicity by interacting with the synapses; the fibrillar form, in contrast, causes progressive neurocellular dystrophy and has a less toxic effect. Girao da Cruz *et al.* (2012) demonstrated that an early increase in soluble β-amyloid coincides with a decrease in acetylcholine transferase activity in the septohippocampal region of 3xTg-Ad mice. While the mechanisms by which β-amyloid peptides produce these synaptotoxic effects leading to cognitive dysfunction are still poorly understood, a recent study demonstrated that β-amyloid peptides can act like the antibiotic gramicidin. Indeed, they can move to synapses, aggregate there and form pores that puncture the cell membrane, thus causing

Ca^{2+} dysregulation (Sepulveda *et al.*, 2014). Synaptic dysfunction and loss of cholinergic neurons are due in part to Ca^{2+} dysregulation (Alkon *et al.*, 2007; Bell et Claudio Cuello, 2006; LaFerla et Oddo, 2005).

However, all the proposed treatments, most of which are based on anti-β-amyloid immunotherapy, have failed in clinical trials, as reviewed by Giacobini and Gold (2013). New findings seem to indicate that β-amyloid production and cytotoxicity are not due to the neurons alone, but mostly to their environment. Oberstein *et al.* (2015) recently showed that astrocytes and microglial cells preferentially generate truncated β-amyloid peptides, which are more likely to form senile plaques, while neurons do not. This indicates that the neuron environment is closely involved in the development of AD and should be considered in future studies. Moreover, post-mortem measurements of the concentrations of soluble β-amyloid in the brain have shown that these are better correlate with the severity of dementia than is plaque deposition itself (Naslund *et al.*, 2000).We therefore need to understand just how all these forms of β-amyloid (soluble, oligomeric, fibrillar) are implicated in AD and how the surrounding environment of neurons (astrocytes and microglial cells) is involved.

Tau hyperphosphorylation

The neurofibrillary tangles are another hallmark of AD. These tangles are the result of the hyperphosphorylation of Tau protein (Alonso *et al.*, 1996; Augustinack *et al.*, 2002). Tau is a soluble, unfolded protein that is associated with neuron microtubules and is found predominantly in axons (Buée *et al.*, 2000). The 6 known isoforms of Tau all have two functional domains. The projection domain mediates interactions between microtubules and cytoskeletal elements such as actin and spectrin filaments; the pseudo-repeat domain regulates the assembly of microtubules (Buée *et al.*, 2000). There are more than 37 mutations in Tau protein isoforms that have been shown to cause neurodegenerative disease, but no specific mutation has yet been directly linked to AD (Do *et al.*, 2014; Lai *et al.*, 2009; Wang et Liu, 2008; Wolfe, 2009). However, specific phosphorylation sites like Ser202 and Thr205 are associated with Tau protein hyperphosphorylation (Augustinack *et al.*, 2002; Orejana *et al.*, 2013). This hyperphosphorylation state is believed to be caused by an imbalance between phosphatase and kinase activities. The resulting hyperphosphorylation of Tau causes the protein to aggregate, leading to intracellular neurofilament tangles made of pairs of helical filaments,

which disrupt axonal flow (Augustinack *et al.*, 2002; Giacobini et Gold, 2013; Orejana *et al.*, 2013; Sun *et al.*, 2003). GSK3β, a proline-directed Ser/Thr kinase protein implicated in the plasticity and development of neuronal tissue (Seira et Del Río, 2014), is involved in the hyperphosphorylation of Tau and may be one of the major actors in tauopathies (Johnson et Stoothoff, 2004; Povellato *et al.*, 2014). However, no report has yet appeared on the efficiency of the therapeutic strategies used in clinical trials that target Tau protein using GSK3β inhibitors (Brunden *et al.*, 2010; Giacobini et Gold, 2013). A low phosphatase activity could also be responsible for most of the reported Tau disorders. For instance, low protein phosphatase 2A (PP2A) activity can also induce hyperphosphorylation of Tau protein in murine or rodent models, causing AD-like symptoms (Arif *et al.*, 2014; Sontag et Sontag, 2014; Sun *et al.*, 2003). PP2A accounts for about 71% of the Tau phosphatase activity in the human brain (Liu *et al.*, 2005). Zhang *et al.* recently reported that silencing inhibitor-2 of PP2A not only decreased the hyperphosphorylation of Tau, it also decreased the activity of GSK3β in murine neuroblastoma (N2A) cells (Zhang *et al.*, 2014). These results suggest that targeting the PP2A inhibitor-2 could also give rise to a treatment for AD. Other recent studies indicate that hyperphosphorylated Tau neurodegeneration could act through global chromatin relaxation, since there is a widespread loss of heterochromatin in both mouse AD and human AD (Frost *et al.*, 2014; Mookherjee et Johnson, 2001). The studies of Frost *et al.* (2014) on mice indicate that the loss of Tau induced heterochromatin is responsible for the death of neurons. However, other studies using human neuroblastoma SH-SY5Y cells have found that the heterochromatin condensation that occurs during apoptosis is associated with Tau protein hyperphosphorylation (Mookherjee et Johnson, 2001).

Crosstalk between the cholinergic system, senile plaques and Tau

There are also indications that the three hallmarks of AD (cholinergic system dysfunction, β-amyloid peptide accumulation and senile plaque formation, and Tau protein hyperphosphorylation) are closely linked. Amyloidogenesis may be related to the Tau phosphorylation state. Some studies have shown that fibrillar β-amyloid peptides can induce the phosphorylation of Tau (Ser396/Ser404) in human cortical neurons, hippocampal neurons and septal neurons (Busciglio *et al.*, 1995; Ferreira *et al.*, 1997; Zheng *et al.*, 2002), while work with H3x-TG AD mice indicates that amyloid deposition precedes tangle formation (Oddo *et al.*,

2003) and that β-amyloid immunotherapy decreases early Tau phosphorylation by sending it to the proteasome (Oddo *et al.*, 2004). Do *et al.* (2014) recently used ion-mobility experiments and theoretical modeling, to demonstrate that Tau fragments (273–284) and β-amyloid$_{25-35}$ can interact and form hetero-oligomers that may help increase the amount of neurofilament tangles by the loss of Tau function or by forming cytotoxic aggregates. Similarly, Roberson *et al.* (2007) showed that reducing endogenous Tau in transgenic mice expressing human amyloid precursor protein could prevent the development of behavioral deficits, suggesting that there is crosstalk between these hallmarks. They also showed that reducing endogenous Tau protected cells against cytotoxicity (see also review by Armstrong (2013)).

Zheng *et al.* (2002) showed that β-amyloid peptides (fragment 25–35) decrease ChAT activity in rat septal neurons, while Olivero *et al.* (2014) found that the β-amyloid$_{1-40}$ subunit inhibited the release of neurotransmitter extracellularly when the release is evoked by nicotinic receptors or intracellularly when the release is evoked by muscarinic receptor; it is thus closely linked to the cholinergic system. Another study by Noh *et al.* (2013) showed that donepezil, an FDA approved AChE inhibitor, significantly reduces β-amyloid aggregates. These authors also found that donepezil stimulated PP2A activity, which is closely link to cell survival, activated acetylcholine receptors and decreased GSK3β activity (Noh *et al.*, 2013).

Thus, future research into the treatment of AD requires a clearer understanding of these interconnections as well as new strategies that focus on several therapeutic targets simultaneously. One way to understand those cross reactions is to delineate the signaling pathways involved in AD development (Figure 2-2).

2.3.2 Signaling pathways implicated in AD

Signaling pathways are extremely important in AD because they regulate most of the behavior of cells in response to external stimuli, such as gene expression, metabolism, cell division, differentiation and survival. A major signaling pathway that seems to be concerned in AD patients is PI3K/AKT/GSK3β and PI3K/AKT/mTOR (Kitagishi *et al.*, 2014; O'Neill, 2013). This pathway mediates several cell functions, including gene expression, mRNA translation, metabolism, growth and survival (Hers *et al.*, 2011; Tang *et al.*, 2014). There is evidence that the PI3K/AKT pathway is downregulated by soluble fractions of β-amyloid

peptides (Takashima *et al.*, 1996; Tang *et al.*, 2014) (reviewed in (O'Neill, 2013)). PI3K/AKT, which normally phosphorylates GSK3β (at Ser9) and so deactivates it, is impaired in AD. This impairment can lead to an increase in Tau protein hyperphosphorylation. Studies on human neural stromal cells indicate that oligomeric β-amyloid peptides reduce cell survival and differentiation by activating GSK3β (Lee *et al.*, 2013). It is also suggested that GSK3β activation can overactivate N-methyl D-aspartate receptors (NMDAR), the cationic channels gated by glutamate that are also believed to be involved in the dysfunctional synapses found in AD (Mota *et al.*, 2014). Deng *et al.* (2014) recently used cultures of rat cortical cells to show that β-amyloid peptides impair the regulation of NMDAR by activating GSK3β. Similarly, Wang *et al.* (2006) used N2A mouse neuroblastoma cells that overproduce β-amyloid peptides to show that inactivating protein kinase C (PKC) resulted in decreased GSK3β phosphorylation on Ser9, which was correlated with an increase in the phosphorylation of Tau protein. These recent results highlight the importance of PI3K/AKT and PKC in regulating GSK3β activation in AD (Alkon *et al.*, 2007).

But the PI3K/AKT pathway is not alone. The canonical Wnt signaling pathway (Wnt/βcatenin) is known to take part in early neurodevelopment in the brain (Patthey *et al.*, 2008) and to be involved in the development and maturation of the blood brain barrier (BBB) (Liu *et al.*, 2014). The Wnt/βcatenin pathway is also important for regulating synaptic plasticity and acetylcholine receptors (Jensen *et al.*, 2012). Other studies have demonstrated that the Wnt pathway may well be implicated in AD. A net decrease in Wnt/β catenin activity is usually associated with synaptic disassembly (Chong et Maiese, 2004; Godoy *et al.*, 2014; Purro *et al.*, 2014; Wan *et al.*, 2014). β-Amyloid peptides are believed to reduce Wnt activity by activating Dickkopf-related protein 1 (DKK1), an inhibitor of the Wnt signaling pathway, which in turn increases the GSK3β activity responsible for Tau hyperphosphorylation (Boonen *et al.*, 2009; Caricasole *et al.*, 2003; De Ferrari et Inestrosa, 2000; Inestrosa *et al.*, 2002). Pinzon-Daza *et al.* (2014) recently demonstrated that P-glycoprotein, which contributes to the genesis and homeostasis of the BBB, is controlled by cooperation between the Wnt/β catenin pathway and the non-canonical Wnt signaling pathway Wnt/RhoA. Another recent study showed that restoring the BBB by stimulating P-glycoprotein production and transport activity by stimulating Wnt/β Catenin decreased the accumulation of β-amyloid in transgenic Tg2576 mice, which overproduce β-amyloid precursors (Hartz *et al.*, 2010). Thus, increasing P-

glycoprotein in the early stages of AD can help to slow progression of the disease. These results indicate that activating Wnt pathways may be a promising approach to AD therapy. Vargas *et al.* (2014) have shown that activating the Wnt signaling pathway in APP/PS1 (amyloid precursor protein/presilin 1) mice by bilateral chronic infusions of WASP-1 (Wnt-activating small protein) significantly improved episodic memory and synaptic transmission.

Yet another pathway, the mitogen activated protein kinase (MAPK) pathway has been associated with AD (for review see (Kim et Choi, 2010; Munoz et Ammit, 2010; Zhu *et al.*, 2001, 2005)). The MAPK pathway is composed of three signaling cascades, one involving JNK, the second P38 and the third ERK. Several studies point to JNK being implicated in tauopathies, which might be associated with oxidative stress. Orejana *et al.* (2013) used a senescence-accelerated mouse (Samp 8) model of AD to demonstrate that PP2A is not altered, while the JNK cascade is more active than it is in normal mice. Inhibiting JNK phosphorylation resulted in a decrease in Tau phosphorylation, suggesting that the JNK cascade is another potential target for AD treatment (Orejana *et al.*, 2013). These results agree with the conclusions of Zhu *et al.* (2001) that JNK is extremely active in Tau-positive (phosphorylated) regions of the hippocampus and cortex of AD patients. Other studies suggest that P38 is implicated in the development of AD. Zhu *et al.* (2005) used the neuroblastoma cell line M17 to show that P38 is readily activated by β-amyloid$_{1-42}$ fibrillar peptides. Their studies with the specific P38 inhibitor SB203580 also demonstrated that the neurotoxic effect of β-amyloid$_{1-42}$ is diminished when P38 activation is significantly blocked. Chen *et al.* recently used 3xTG-AD mice to show that fragments 25–35 of β-amyloid peptide, which rapidly self-aggregate, are efficient activators of P38, JNK and ERK (Chen *et al.*, 2014). The activation of ERK is mediated by PKC, which is also one of the kinases responsible for Tau phosphorylation (reviewed in (Alkon *et al.*, 2007)). The activation of ERK via PKC phosphorylation also plays a role in the activation of α-secretase. β-Amyloid$_{1-42}$ peptides, in turn, activate ERK and lead to hyperphosphorylated Tau protein (see Figure 2-2) (Alkon *et al.*, 2007). The studies of Gomez-Ramos *et al.* (2006) on human SHSY5Y neuroblastoma cells have shown that the antidiabetic drug sodium tungstate inactivates GSK3β by activating the ERK cascade. Clearly, the MAPK pathway is actively involved in the development of AD and seems to be important in the mediation and regulation of several hallmarks of AD. However, crosstalk between the signaling pathways makes it

difficult to understand the mechanism involved in AD (see review (Godoy *et al.*, 2014)). There are several published examples of multiple simultaneous pathways, such as MAPK and PI3K/AKT (Godoy *et al.*, 2014). The simplified outline of the crosstalk operating in AD and AD-like models shown in Figure 2-2 highlights some of these challenges. Vasquez de la Torre *et al.* (2013) showed that inhibiting PI3K/AKT increased P38 activity, which was linked to cell apoptosis.

However, inhibiting PI3K itself can severely impair cell Metabolism and survival since it is a central pole of signaling inside neurons (Tang *et al.*, 2014). Recent results tend to indicate that there is cross-regulation between the P38, ERK and PI3K/AKT pathways (Deng *et al.*, 2014; Leugers *et al.*, 2013; Yang et Herrup, 2007). Chen *et al.* (Chen *et al.*, 2014) showed that inhibiting the AKT pathway resulted in less activation of ERK and P38 in 3xTG-AD mice stimulated with 25–35 fragments of β-amyloid peptides. There is also cross-regulation between the PI3K/AKT and Wnt signaling pathways in AD. The studies of Mercado- Gomez *et al.* (2008) on cortical neuronal cells show that inhibiting the PI3K/AKT or the Wnt pathway results in increased GSK3β activation, which is correlated with Tau hyperphosphorylation. Also, Scali *et al.* (2006) found that inhibiting the Wnt pathway with DKK1 (linked to β-amyloid exitoxicity) decreased the phosphorylation of GSK3β on Ser9, which was associated with increased Tau hyperphosphorylation. Finally, recent results tend to indicate that Tau hyperphosphorylation in AD can lead to MAPK activation (Leugers *et al.*, 2013). These authors also stated that the crosstalk between Tau and MAPK activation needs further study, since MAPK is linked to activation of the cell cycle, which in the case of neurons leads to cell death (Yang et Herrup, 2007). For example, the studies of McShea *et al.* (2007) on AD-like ras/myc adenovirus-infected primary cortical n cells showed that cell-cycle re-entry induced Tau phosphorylation and triggered cell death.
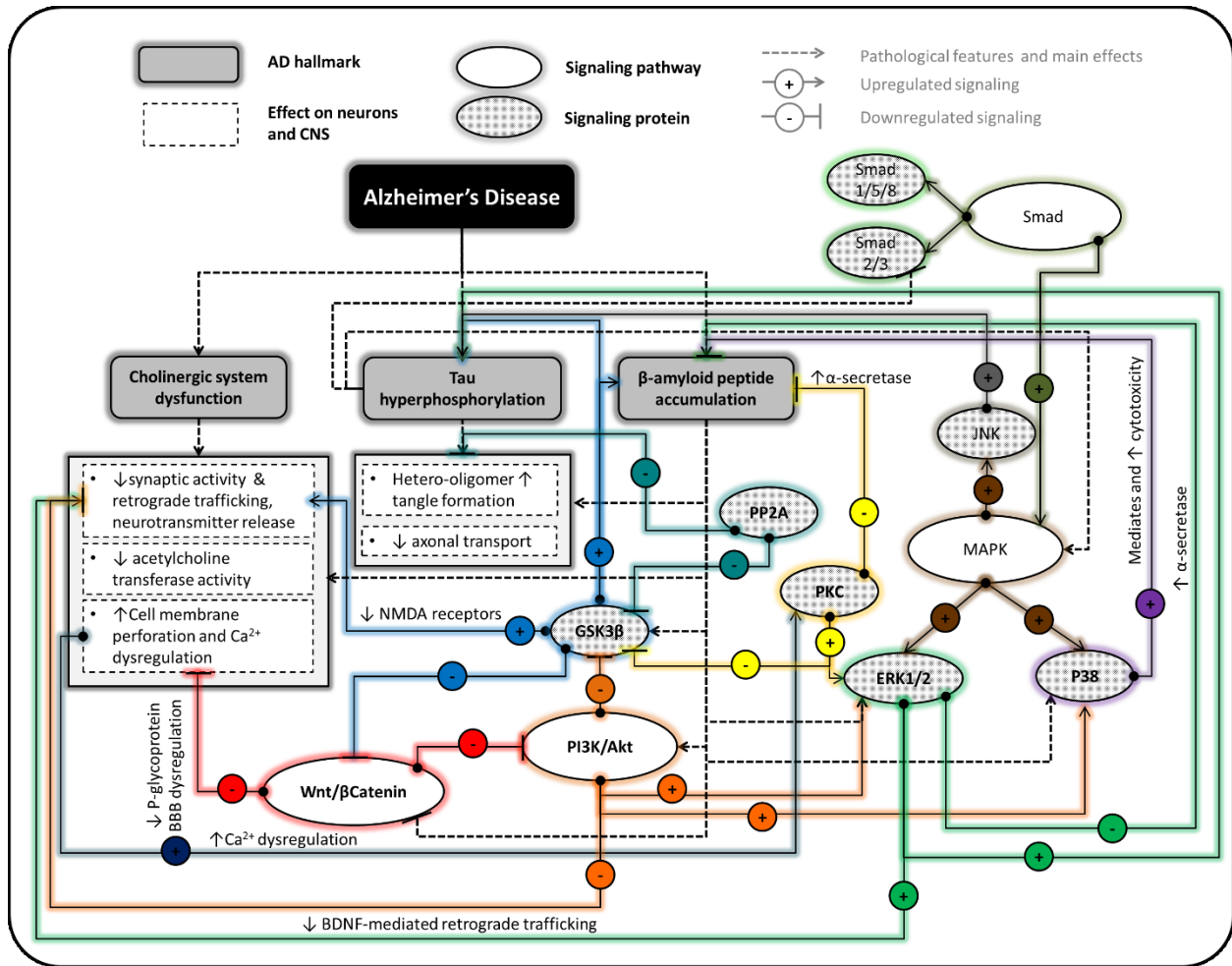
Figure 2-2 : AD pathological markers: the interactions and the implication of the simplified signaling pathways in AD-like induced cells, animals and AD patients

It therefore seems that correct regulation of the PI3K/AKT pathway, MAPK and Wnt signaling are required to prevent the development and evolution of AD. These pathways could be activated using specific GFs.

2.4 Growth factors: a new therapeutic approach

In addition to the new strategies recently proposed for treating AD, such as curcuminoid compounds, which have antioxidant properties as well as being involved in mediating the maturation of β-amyloid peptides (Agrawal *et al.*, 2010; Ahmed *et al.*, 2010; Yanagisawa *et al.*, 2011; Zhang *et al.*, 2010), there is clear evidence that GFs are promising tools for treating AD. They influence the plasticity and development of the CNS (Spillantini *et al.*, 2011). The

potentially useful GFs and their effects on brain development and plasticity are shown in Figure 2-3. The transforming growth factor (TGFβ) family members such as bone morphogenetic proteins (BMPs), glucose-metabolism-related GFs such as IGF-1, IGF-2 and neurotrophins (NGF, BDNF and BDGF) seem to be promising tools for targeting AD therapeutic hallmarks.

2.4.1 Neurotropic TGF family members and the development of the central nervous system

Transforming growth factor beta 1

There are several TGFβ subfamilies including the TGFβ/activin/nodal, BMP/growth differentiation factors (GDFs), and glial cell line-derived neurotrophic factor (GDNF) (also considered as a neurotrophin). TGFβ and BMPs act on cells by binding to specific transmembrane Ser/Thr kinase type II receptors. These then recruit Ser/Thr kinase type I receptors to form heterotetrameric complexes (Beyer *et al.*, 2013). There are 7 type I (ALKs 1–7) and 5 type II (ActR-IIA, ActR-IIB, BMPRII, AMHR-II and TbR-II) human receptors (Attisano et Wrana, 1996; Massague et Gomis, 2006). The affinities of TGFβ receptors for their ligands and their subsequent activity can be enhanced in some cells, such as endothelial cells, by a third type of co-receptor (TGFβ type III receptor) like endoglin (Ge et Butcher, 1994).

The type II receptors phosphorylate, and so activate, the type I receptors. These type I receptors in turn phosphorylate the receptor-regulated Smad (R-Smad) promoting their interaction with common partner Smad (Co-Smad) also known as Smad4. The TGFβs mainly interact with ALK5, ALK4 and ALK7 that signal through the R-Smad, Smad2 and Smad3, while the BMPs bind to ALK 1, 2, 3 or 6 to activate the R-Smads, Smad1/5 and 8. The R-Smad and Co-Smad complexes then move to the nucleus where they interact with DNA with or without additional transcription factors to regulate the expression of target genes (Docagne *et al.*, 2004).
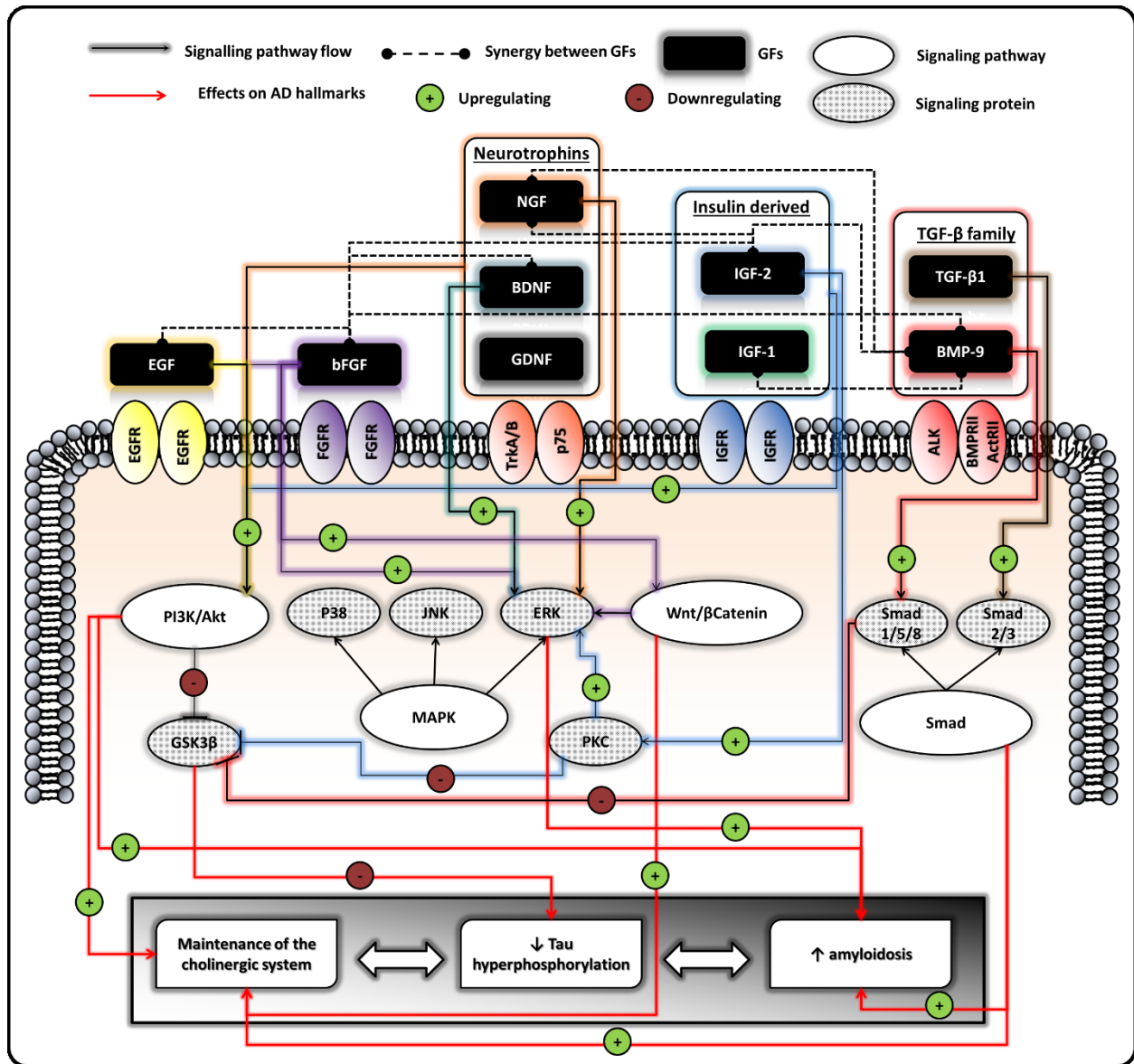
Figure 2-3 : Effects of potentially therapeutic GFs on AD hallmarks and their action on several signaling pathways

Several members of the TGFβ family also signal through the mitogen-activated protein kinase MAPK pathway composed of ERK, JNK and P38. Zhu *et al.* (2002) found that treating rat hippocampus cells with TGFβ-1 (0.1 to 10 ng/mL) for 8 h dose-dependently stimulated the phosphorylation of ERK. However, others have shown that ERK also phosphorylates several Ser–Pro and Thr–Pro residues in the linker region of R-Smad, which blocks their translocation to the nucleus (Massague et Gomis, 2006).

An injured brain produces enhanced amounts of TGFβ-1, which is synthesized by microglia and astrocytes. Its concentration is also elevated in the brains of AD patients, where it is especially abundant in neurons and astrocytes (Ueberham *et al.*, 2003). However, another study revealed that patients with moderate to severe neurofibrillary tangles had downregulated amounts of TGFβ-1 mRNA in their superior temporal gyrus (Luterman *et al.*, 2000). The transduction of the TGFβ-1 signal by Smad2/3 is also significantly impaired in the AD brain (Ueberham *et al.*, 2006). Ueberham *et al.* (2006) observed that Smad2 was mainly associated with the neurofibrillary tangles, while Smad3 was detected in the perinuclear zone of hippocampus neurons in AD patients. It was recently reported that extracts of temporal cortex proteins from AD brains contained much less (about 30 to 60%) than normal amounts of nuclear R-Smad (Smad-2, -3) and Co-Smad (Ueberham *et al.*, 2012). Baig *et al.* (2009) also showed that treating rat primary cortical cells with okadaic acid (200 nM) to increase the phosphorylation of Tau on Ser202 and Thr231 prevented the nuclear translocation of Smad2/3. Hyperphosphorylated Tau and phosphorylated Smad2/3 were also partly localized together in the cytoplasm. The same results were obtained by treating rat primary cortical cells with β-amyloid$_{1-42}$ peptides (10 μM) that induced the phosphorylation of Tau on Thr231 and Ser202, Ser396 and Ser404 (Baig *et al.*, 2009). The phosphorylated Smad2/3 can thus be sequestered by hyperphosphorylated Tau (Baig *et al.*, 2009).

The role of TGFβ-1 in AD is therefore quite complex. TGFβ-1 can reduce the deposition of amyloid peptides by activating microglia, but it can also increase their deposition by stimulating astrocytes (Wyss-Coray *et al.*, 2001). A 2006 study by Docagne *et al.* (2004) concluded that TGFβ-1 is a risk factor for developing AD since it promotes amyloidogenesis. Smad3/Smad4 complexes can bind, along with Sp-1, to the promoter of the gene encoding the amyloid precursor protein and stimulate its transcription, while Smad2/Smad4 cannot.

TGFβ-1 can also protect primary cultures of rat hippocampus neurons from β-amyloid-mediated damage (Ren et Flanders, 1996). Caraci *et al.* (2008) injected SB431542 (2.5 nmol), an inhibitor of the TGFβ-1 type I receptor ALK-5, and β-amyloid$_{1-42}$ peptides (123 nmol) simultaneously into the dorsal hippocampus of rats. This double-injection promoted the neuron degeneration induced by the β-amyloid peptides 10 days after injection (Baig *et al.*, 2009; Caraci *et al.*, 2008). The capacity of TGFβ-1 to protect neurons against β-amyloid-mediated damage

could be due to its ability to inhibit the cell cycle (Caraci *et al.*, 2008; Copani *et al.*, 2007). Ueberham *et al.* (2012) also recently reported that Smad4 decreased the transcription of the gene encoding cyclin-dependent kinase-4 (Cdk4). Cdk4 regulates the G1-to-S phase transition of the cell cycle and such reactivation of the cell cycle can lead to the death of neurons by apoptosis (Copani *et al.*, 2007; Ueberham *et al.*, 2012). Cyclin D/Cdk4, cyclin E/Cdk2 and cyclin B/Cdk1 complexes can also phosphorylate Tau (Schmetsdorf *et al.*, 2009). Another research group has also demonstrated that TGFβ-1 protects neurons against apoptosis by phosphorylating the pro-apoptotic Bad thus blocking its activity (Zhu *et al.*, 2002). TGFβ-1 can prevent the apoptosis of hippocampus neurons by stimulating the PI3K/AKT and ERK pathways, and so activating NF-kappa β (Zhu *et al.*, 2002). Caraci *et al.* (2012) has proposed using TGFβ-1 signaling to combat neurodegeneration due to AD, but we need to better understand how the signaling is impaired in AD.

Bone morphogenetic proteins

BMPs were discovered in the rat cortical bone matrix by Urist and Strates (Urist et Strates, 1971) in the early 1970s. More than 20 BMPs have been identified since then (Senta *et al.*, 2009; Wagner *et al.*, 2010) and these highly osteogenic growth factors have been extensively studied over the past few decades (see review (Senta *et al.*, 2009)). They are implicated in the recruitment and differentiation of mesenchymal stromal cells to form chondrocytes or osteoblasts (Ai-Aql *et al.*, 2008; Lauzon, Bergeron, *et al.*, 2012; Senta *et al.*, 2009). However, several recent studies have shown that they are also involved in the development and homeostasis of other tissues, including epithelial tissue (Kim *et al.*, 2012; Suzuki *et al.*, 2010), muscle (Friedrichs *et al.*, 2011; Winbanks *et al.*, 2013), and the brain (Hegarty *et al.*, 2014; Lopez-Coviella *et al.*, 2000; Ueberham et Arendt, 2013). It has been suggested that they should be called "body morphogenetic proteins" rather than bone morphogenetic proteins because of their great versatility and widespread action (Wagner *et al.*, 2010).

BMPs are involved in the early development of the CNS, particularly in gastrulation and dorsoventral patterning within the neural tube (Mehler *et al.*, 1995, 1997). BMP and Wnt signals are necessary for specifying the neural crest at the gastrula stage (Chesnutt *et al.*, 2004; Hegarty *et al.*, 2013a; Patthey *et al.*, 2008) and for the dopamine differentiation of pluripotent stromal cells (Cai *et al.*, 2013; Hegarty *et al.*, 2014). BMP-7 and GDF-7 are also required for the

extension of the axons of commissural neurons from the roof plate during spinal cord development (Butler et Dodd, 2003). *In vivo* experiments conducted on mice also showed that BMP-7 regulates the survival, proliferation and differentiation of neuron progenitors in corticogenesis while nurturing radial glia cells (Segklia *et al.*, 2012). Furthermore GDF-5 (BMP-14) plays an important role in the development and maintenance of dopaminergic systems (Clayton et Sullivan, 2007; Sullivan *et al.*, 1999). Another recent study has shown that BMP-2 is required for closure of the cephalic neural tube in murine embryos (Castranio et Mishina, 2009), while the studies of Schnitzler *et al.* (2010) on mouse embryo cells revealed that BMP-9 (100 ng/mL) acts through the type I receptor ALKI and that activating the Smad1/5/8 pathway stimulates the synthesis of nerve growth factor (NGF). NGF, in turn, acts as an autocrine/paracrine trophic factor. These authors also demonstrated that BMP-9 only stimulates NGF synthesis in developing cholinergic neurons. Likewise, Lopez-Coviella *et al.* (2002), working on murine septal cells (SN56T17), showed that BMP-9 (10 ng/mL) stimulates the synthesis of acetylcholine.

However, not all published research has shown that BMPs regulate the development of the CNS in a positive fashion. Some have shown contrary actions on the development of neurons. BMPs act more on the cellular environment surrounding neurons (glial cells) than on neurogenesis itself. Yanagisawa *et al.* (2001) used a murine model to show that BMP-2, -4 and -7 altered the fate of neuroepithelial cells in neurogenesis and directed their differentiation to astrocytogenesis by up-regulating negatively helix–loop–helix transcription factor (HLH). These results confirm the earlier work of Gross *et al.* (1996) on murine embryonic subventricular zone multipotent progenitor cells. They found that BMP-2 induced their commitment to the astroglial lineage. Shou *et al.* (2000) obtained similar results using murine embryo cells. More recently, Mercier and Douet (2014) showed that BMP-4 reduced neurogenesis in the subventricular zone. This phenomenon was modulated by fractones, which trap BMPs like BMP-7 and so modulate neurogenesis. These contradictory results underline the fact that the role of BMPs in mediating brain development is still poorly understood.

Large amounts of BMPs such as BMP-2, BMP-4, BMP-7 and BMP-8 are also present in the adult brain (Charytoniuk *et al.*, 2000; Wagner *et al.*, 2010). Lopez-Coviella *et al.* (2000) found high concentrations of BMP-9 transcripts in the spinal cord and septal area. A study of

the distribution of BMP receptors showed that type II BMP receptors (BMPRII) are widespread throughout the brain, but particularly abundant in the cortex, olfactory bulb and hippocampus (Charytoniuk *et al.*, 2000). Hegarty *et al.* (2014) recently showed that BMP-2 and BMP-14 (GDF-5) are involved in the maturation of dopaminergic neurons. Similar results were obtained by Toulouse *et al.* (2012) working with the human neuroblastoma cell line SH-SY5Y. BMP-9 also seems to be important in the development of the cholinergic system. Lopez-Coviella (2000) found that BMP-9 was the most effective of six BMPs tested (BMP-2, -4, -6, -7, -9 and -12) on embryonic CNS cells (E14 to E18); it greatly increased the concentrations of acetylcholine and increased the synthesis of specific markers such as βIII-tubulin and VAchT, indicating a change in the morphology toward the neuron phenotype.

These results clearly indicate that BMPs are crucial for the development of the brain, and also contribute to the homeostasis of mature neurons and astroglia. Several studies have shown that BMP-9 has neurotropic and neuroprotective effects on the cholinergic systems of the CNS. This could be important for the design of AD treatments (Burke *et al.*, 2013; Lopez-Coviella *et al.*, 2000, 2006, 2011; Mufson *et al.*, 2008). Lopez-Coviella *et al.* (2000) used mouse septal cultures to demonstrate that physiological concentrations (10 ng/mL) of BMP-9 induced and maintained the cholinergic phenotype. They also demonstrated that BMP-9 prevented the lesion-evoked loss of ChAT from positive medial septum neurons of CD-1 mice and increased cholinergic marker expression in the hippocampus in a dose-dependent manner (Lopez-Coviella *et al.*, 2011). As lesions of the septohippocampal cholinergic system are associated with the memory loss characteristic of AD (reviewed by Mufson *et al.* (2008)), the ability of BMP-9 to protect cholinergic neurons indicates that it is a potential treatment targeting the cholinergic system. Burke *et al.* (2013) demonstrated that BMP-9 (4 ng/h for 7 days) reduced the senile plaques in both the hippocampus and cortex of APP.PS1/CHGFP (producing β-amyloid precursor) mice while increasing the ChAT concentration. However, although BMP-9 greatly improves AD hallmarks, its mechanisms of action are still poorly understood. BMP-9 (10 ng/mL) activates the canonical Smad pathway in neurons as in other tissues (Lopez-Coviella *et al.*, 2006). However, the implication of other signaling pathways such as PI3K/AKT and MAPK in BMP-9-stimulated cells implicated in AD pathology has not yet been studied. We have used SH-SY5Y cells to evaluate the activation of Smad1/5/8 and GSK3β with and without retinoic acid (RA) (Figure 2-4). RA is an inducer of neuron differentiation that has been used extensively

to differentiate SH-SY5Y cells into cholinergic neurons (Agholme *et al.*, 2010; Jämsä *et al.*, 2004; Mookherjee et Johnson, 2001; Uberti *et al.*, 1997). We found that BMP-9 (1 nM) activated Smad1/5/8 within 30min with maximum activation after 1 h in the absence of RA (10 μM). Adding RA drastically increased the rate at which Smad1/5/8 was activated: maximum activation occurred within 15 min. Moreover, combining BMP-9 with RA maintained the phosphorylation of GSK3β (on Ser9), which was not so with BMP-9 alone. This sustained phosphorylation of GSK3β is a promising tool for attacking tauopathies and emphasizes once more the great potential of BMP-9 as the basis for an AD treatment. These results also demonstrate that more mature neurons do not seem to respond to BMP-9 in the same way as embryonic cells but require RA to be fully potent. There is also published evidence that RA potentiates the activity of BMP-2 and increases Smad1/5/8 activity in chondrocytes (Li *et al.*, 2003) and the osteogenic differentiation of mesenchymal progenitor cells (Zhang *et al.*, 2010). However, further investigation is required to fully understand the signaling mechanism by which BMP-9 acts on human neurons.

2.4.2 Other growth factors with high CNS-regenerating potential

IGF-1 and IGF-2

GFs other than the BMPs are also implicated in CNS development and neuroplasticity. Insulin-like growth factors 1 (IGF-1) and 2 (IGF-2) interact with the cell IGF receptor (IGFR), which in turn triggers an internal signaling cascade passing through the PI3K/AKT pathway (Dupraz *et al.*, 2013; Zheng et Quirion, 2004). IGF-1 and IGF-2 are also important in neurogenesis and synaptogenesis (Chen *et al.*, 2011; Dupraz *et al.*, 2013; Konishi *et al.*, 1994; O'Kusky *et al.*, 2000; O'Kusky et Ye, 2012; Schmeisser *et al.*, 2012; Zhang *et al.*, 2007). Knusel *et al.* (1990) compared the effects of several growth factors (bFGF, insulin, NGF) on rat neurons in culture and demonstrated that IGF-1 and IGF-2 are neurotropic and powerful stimulators of acetylcholine transferase activity. Hawkes *et al.* (2006) also reported that IGF-2 receptors, which are present in the CNS (Baskin *et al.*, 1988), regulate the central cholinergic function by interacting with G-coupled protein. This protein, in turn, activates the PKC-dependent signaling cascade (Heidenreich, 1993). There is also evidence that IGF-1 and IGF-2 are involved in memory retention. Thus, Chen *et al.* (2011) demonstrated that injecting IGF-2 into the hippocampus of adult Long Evans rats dramatically enhanced memory retention.

The synthesis and actions of IGF-1 and IGF-2, which are involved in maintaining the cholinergic system, are greatly disturbed in AD brains (Anitua *et al.*, 2013; de la Monte, 2012; Steen *et al.*, 2005). Rivera *et al.* (2005) used qPCR to monitor the amounts of IGF-1 mRNA in brains at different stages of AD and found that the progression of AD was associated with decreased IGF-1 synthesis and co-localization of ChAT and IGF-1 receptors. Then, Steen *et al.* showed that insulin, IGF-1 and IGF-2 signaling and their mRNAs were severely impaired in the brains of patients suffering from AD. They postulated that AD can be viewed as a type III diabetes (Steen *et al.*, 2005). More recently, Westwood *et al.* (2014) reported finding a correlation between a low concentration of IGF-1 in the serum of patients and the risk of developing dementia such as AD. These results are further support for the importance of insulin, IGF-1 and IGF-2 in brain homeostasis and neuroplasticity and their potential as targets for therapy.

Thus, increasing IGF-1 or IGF-2 expression or level in the brain using a delivery system might be a promising AD treatment since it can plan on several therapeutic targets as does BMP-9 (Freiherr *et al.*, 2013). It has been reported that IGF-1 and IGF-2 regulate Tau phosphorylation by reducing GSK3β activity through PI3K/AKT (Hong et Lee, 1997). Pascual-Lucas *et al.* (2014) recently used TG2576 transgenic mice producing IGF-2 or IGF-1 to show that IGF-2 significantly reduced the amounts of β-amyloid$_{1-42}$ and senile plaques in the hippocampus, while IGF-1 did not. Moreover, injections of IGF-2 (50 ng/h for 7 days) increased both amyloidosis and the amounts of cholinergic markers in APP.PS1 mice (Mellott *et al.*, 2014), while an intranasal injection of insulin (17.5 μL) improved the cognitive functions of 3xTG-AD mice and reduced propophol-induced Tau hyperphosphorylation (Chen *et al.*, 2014).
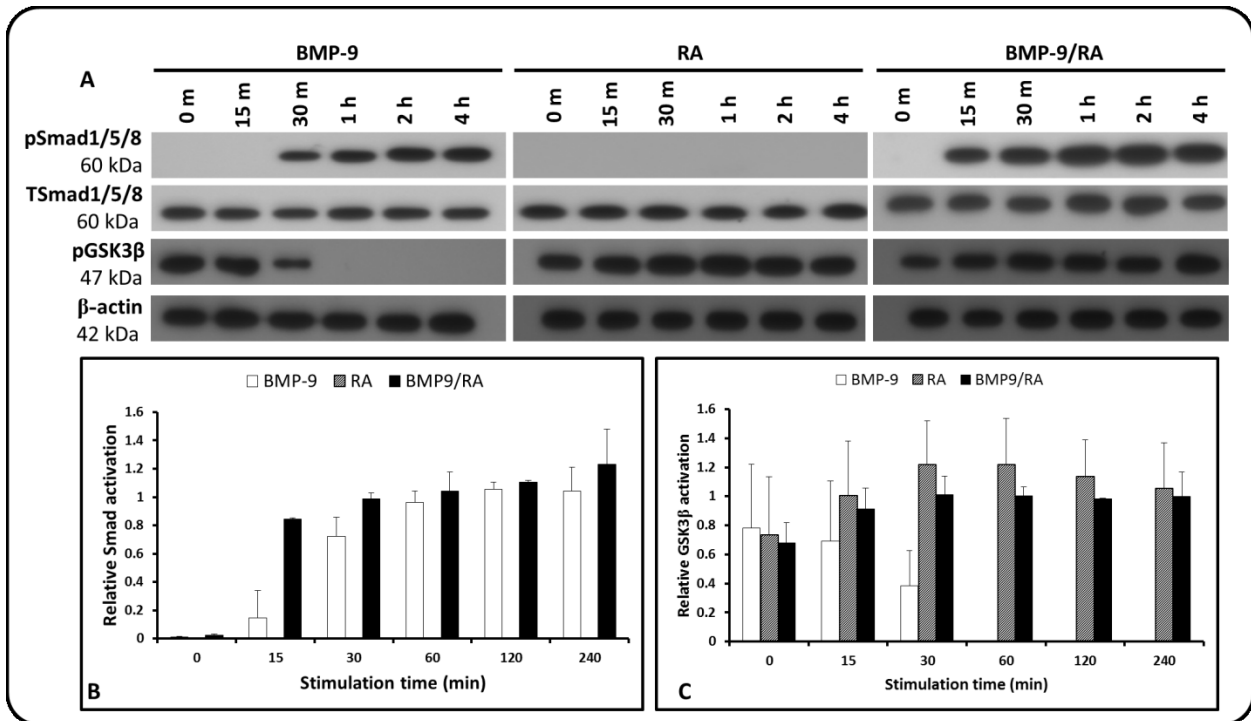
Figure 2-4 : Effect of incubating SH-SY5Y cells with BMP-9 (1nM), RA (10 µM) and BMP-9 (1nM)/RA (10 µM) for 0, 15, 30, 60, 120 and 240 min. (A) Representative results of two independent experiment showing western blots of phosphorylated Smad1/5/8 (pSmad1/5/8) and total Smad (TSmad1/5/8), phosphorylated GSK3β (Ser9) (pGSK3β) and β-actin for different stimulation times. (B) Densitometric analysis of phosphorylated Smad1/5/8 referred to total Smad band and (C) Densitometric analysis of phosphorylated GSK3β referred to β-actin band.

Basic fibroblast growth factor

A total of 22 human fibroblast growth factors have been identified to date. One of them, basic fibroblast growth factor (bFGF) is implicated in the development of the CNS and is potentially useful for treating degenerative diseases (Ford-Perriss *et al.*, 2001; Knusel *et al.*, 1990; Konishi *et al.*, 1994; Sensenbrenner, 1993; Woodbury et Ikezu, 2014). While bFGF is present in several parts of the body, it is most abundant in nervous tissues (Bikfalvi *et al.*, 1997; Noda *et al.*, 2014; Sensenbrenner, 1993). It also interacts with the FGF receptor (FGFR) and signals through the PI3K/AKT pathway (Tanabe *et al.*, 2012). Thus, bFGF is an important neurotrophic factor that promotes the survival of dopaminergic cells of the mesencephalus (Baron *et al.*, 2012).

Stevens *et al.* (2012) demonstrated that short term and long term memory required activation of the FGF receptors 2 in the hippocampus. FGF is also an important regulator of the proliferation, differentiation and maturation of the oligodendrocytes responsible for myelination

in the CNS (reviewed by Li and Yao (2013)). Woodbury and Ikezu (2014) recently reviewed the implication of bFGF in neurogenesis and neurodegeneration, highlighting the importance of this GF as a neurotrophic factor and its role in synaptic plasticity. While its major influence is on the dopaminergic systems mostly involved in disorders like Parkinson's disease, new findings indicate that this GF could be the basis for an AD therapy. A study by Knusel *et al.* (1990) in the early 1990's showed that stimulating cultures of rat septal cells with bFGF for 1 week increased ChAT more than did NGF, EGF, IGF-2, IGF-1 or insulin. Ye *et al.* (2010) demonstrated that bFGF (1μg/day for 7 days) increased and improved the memory and learning abilities of 2-VO rats (ischemic encephalopathy model). They also showed that bFGF crossed the BBB, interacted with neurons in the hippocampus and increased the number of cholinergic neurons (Ye *et al.*, 2010). Kiyota *et al.* (2011) also used the APP/PSI bigenic mouse model to demonstrate that delivering the bFGF gene to the hippocampus via an adeno-associated virus increased both amyloidosis and neurogenesis. The *in vitro* (Wistar rat embryonic E18 cells) and *in vivo* (F344/ DuCrj rats) studies of Noshita *et al.* (2012) showed that bFGF (0.3 to 3 ng/mL) decreases the cytotoxicity of β-amyloid and glutamate-induced neurotoxicity. However, bFGF also protects neurons either directly or by influencing the cells surrounding them. Cheng and Mattson (1992) worked on cultures of rat hippocampus cells and found that bFGF prevented the death of neurons in a glucose-deprived environment. Moreover, Tanabe *et al.* (2012) demonstrated that stimulating C6 cells (rat glial cell line) with bFGF (30 ng/mL) increased the synthesis of GDNF, a neurotrophin that supports neurons and mediates synaptic plasticity. A more recent study on co-cultures of neurons and glia showed that bFGF is secreted by β-amyloid-induced degenerated neurons, which could recruit glial cells (Noda *et al.*, 2014). This group also found that bFGF (100 ng/mL) increased microglial migration and the removal of neuron debris as well as protecting neurons through the ERK signaling pathway. But they did not determine whether the ERK pathway had to be activated in both the neurons and glial cells in the co-culture (Noda *et al.*, 2014). Since ERK activation in neurons is negatively implicated in AD, more investigation should be conducted. Nevertheless, these results suggest that bFGF is worth considering as a potential AD treatment: it can cross the BBB, influences the survival of neurons and increases amyloidosis.

Neutrophins

Another family of GFs that could be useful for treating AD and other dementias is the neurotrophins, which includes NGF, brain-derived neurotrophic factor (BDNF) and GDNF (Schindowski *et al.*, 2008). NGF interacts with the TrkA/p75 cell receptor, which then activates the PI3K/AKT signaling pathway (Madziar *et al.*, 2008). NGF is most abundant in the gabaergic neurons of the cerebral cortex (Biane *et al.*, 2014). It is involved in several processes of CNS development, including the innervation of cholinergic neurons, cell differentiation and the survival of the cholinergic system (Allen *et al.*, 2013; Korsching *et al.*, 1985; Lad *et al.*, 2003; Nilbratt *et al.*, 2010). It has also been shown that NGF can stimulate and reshape rapidly cholinergic dependent functional reorganization in the barrel cortex (Prakash *et al.*, 2004). Other recent studies suggest that NGF is implicated in amyloidosis (Matrone, Ciotti, *et al.*, 2008; Matrone, Di Luzio, *et al.*, 2008; Yang *et al.*, 2014). Those of Yang *et al.* (2014),on APP/PSI double transgenic mice showed that stimulation with NGF (7 μg/mL) activated amyloidosis while Matrone *et al.* studied PC12 septal cells and showed that depriving them of NGF increased their production of β-amyloid peptides, and so increased apoptosis (Matrone *et al.*, 2008). An inhibitor of the NGF receptor (TrkA) had the same effect, indicating that NGF is implicated in amyloidosis. The same authors confirmed these results in a study on rat hippocampus neurons (Matrone *et al.*, 2008b). Madziar *et al.* (2008) obtained similar results and demonstrated that NGF (50 ng/mL), signaling via the PI3K/AKT pathway, was necessary for expression of the cholinergic locus as well as the VAchT. Unless NGF signals mostly through PI3K/AKT pathway, MAPK and especially ERK might also be involved when exogenous NGF is present in basal forebrain cholinergic neurons (Lad *et al.*, 2003; Williams *et al.*, 2006). However, there is little or no evidence that NGF is implicated in AD, since neither the expression of genes encoding NGF nor the synthesis of proNGF protein is impaired, although the amount of the high affinity NGF receptor (TrkA) is significantly decreased (Counts et Mufson, 2005; Iulita et Cuello, 2014). Nevertheless, NGF seems to have a positive effect on AD. It affects Tau hyperphosphorylation. Giving rats with a traumatic brain injury NGF (5 μg/day) intranasally decreased Tau phosphorylation by more than 40%; it also maintained the phosphorylation of GSK3β (Ser9) (Lv *et al.*, 2014). NGF also improves the early signs of neurodegeneration. Capsoni *et al.* (2002) gave AD-like anti-NGF transgenic mice (AD-11) intranasal injections of NGF (1 to 10 μM) and found that Tau phosphorylation was decreased

while ChAT activity was increased. Injections of the NGF-conjugated monoclonal antibody OX-26 (50 μg/week for 2 months), which targets the transferrin receptors (Friden *et al.*, 1991), restored the NGF balance in cognitively impaired aged F344 rats (Albeck *et al.*, 2003). Thus NGF could be the basis for an AD treatment.

The main function of the neurotrophin BDNF is to promote the survival of neurons like the cholinergic and sensory neurons and to mediate the plasticity of the hippocampus (Allen *et al.*, 2013; Tapia-Arancibia *et al.*, 2008). BDNF interacts with the TrkB/p75 cell receptor and signals mainly via the PI3K/AKT pathway and ERK (Zheng et Quirion, 2004). Several BDNF-mediated functions are altered in AD and β-amyloid peptides impair the retrograde axonal trafficking of BDNF causing synaptic dysfunction (Poon *et al.*, 2011). There is also evidence that β-amyloid peptides impair the actions of BDNF by reducing the activity of its major signaling pathway (MAPK, ERK and PI3K/AKT) (Tong *et al.*, 2004). The concentration of BDNF in the plasma is also altered in disorders such as AD. Faria *et al.* (2014) recently measured the concentration of BDNF in the plasma of 50 AD patients (13 with mild cognitive impairment and 37 with severe AD) and 56 healthy elderly patients. They found that the blood plasma concentrations of BDNF of the patients with severe AD were higher than those of the healthy elderly patients, whereas the concentration in the plasma of patients with mild cognitive impairment was not significantly different from the controls. The elevated plasma BDNF concentration in AD patients is believed to be due to compensation for early neurodegeneration. Similar results were obtained in another study on patients with mild AD and mild–moderate AD (Angelucci *et al.*, 2010). Other studies indicate that the concentrations of BDNF receptors and effectors are elevated in the early stages of AD to compensate for early degeneration, but the concentration of BDNF protein does not seem to be altered (Kao *et al.*, 2012). Ferrer *et al.* (1999) showed that there was significantly more of them RNA encoding the BDNF receptor (tropomyosin-tyrosine kinase; TrkB) in the post-mortem brains of AD patients (8 patients) than in the brains of healthy individuals (6 patients), whereas the concentrations of BDNF protein remained similar. However, they also observed that BDNF protein and the BDNF neurotrophic pathway in the frontal cortex were severely depleted and that there were tangle neurons. The amounts of the mRNA encoding the capping protein β2, which is involved in actin-cytoskeleton reorganization, were also increased (Kao *et al.*, 2012). Despite disagreement about how the concentration of BDNF changes during AD, there is evidence that BDNF has a positive effect

and could be a treatment for AD. Kitiyanant *et al.* (2012) showed that BDNF treated neuron progenitor cells derived from cultures of embryonic septa blocked the neurotoxic effect of β-amyloid peptides$_{1-42}$ (10 μM) and enhanced overall cholinergic function by increasing the synthesis of ChAT. Arancibia *et al.* (2008) obtained similar results. They used rat cortical neurons that had been treated with β-amyloid$_{25-35}$ peptides and stimulated them with BDNF (50 ng/mL).

GDNF normally influences motor and dopaminergic neurons, the cells targeted in Parkinson's disease, and is important for the organization and maintenance (Allen *et al.*, 2013; Chermenina *et al.*, 2014). It also interacts with neuron via TrkB/p75 receptors, which can activate PI3K/AKT signaling or MAPK (Allen *et al.*, 2013). Intranostraglia injections of GDNF can protect the dopaminergic neurons of the substantia nigra (Chen *et al.*, 2014; Migliore *et al.*, 2014; Peng *et al.*, 2014). GDNF also seems to be indirectly involved in AD. GDNF was downregulated in the middle temporal gyrus of post-mortem AD patients, whereas the common isoform transcripts remain unchanged in comparison to normal patients (Airavaara *et al.*, 2011). The GDNF secreted by astrocytes seems to be important for maintaining the BBB (Utsumi *et al.*, 2000). Shimizu *et al.* (2012) showed that GDNF secreted by the brain or nerve pericytes was responsible for maintaining the BBB and the blood–nerve barrier by stimulating the synthesis of claudin-5, a protein involved in tight junctions. Since β-amyloid peptides seem to alter the integrity of the BBB (Hartz *et al.*, 2010) and trigger Ca^{2+} dysregulation (see above), increasing GDNF synthesis or providing exogenous GDNF might be a way of controlling the clearance of β-amyloid peptides.

2.4.3 Synergy between neurotropic GFs

Not only are individual GFs potential therapeutic agents for AD, there is now evidence that some of them act in synergy. This could greatly increase their efficiency. Fagerström *et al.* (1996) showed that bFGF (3nM) combined with IGF-1 (5nM) caused SH-SY5Y human neuroblastoma cells to differentiate, just as NGF (100 ng/mL) did, and that the differentiation was associated with activation of PKC. Lopez-Coviella *et al.* (2000) treated murine septal cells in culture (E14) with a combination of BMP-9 and bFGF, which could increase the acetylcholine production more than twice of the additive effect of each GF. BMP-9 stimulates the synthesis of NGF and IGF-1, which is associated with an increase in ChAT (Burke *et al.*, 2013; Schnitzler

et al., 2010). As BMP-9 triggers the synthesis of these GFs, which in turn enhance neuron survival, they may be acting synergistically. BMP-9 and IGF-2 can also act in synergy on cells such as bone forming cells (Chen *et al.*, 2010). We have demonstrated that IGF-2 (100 ng/mL) synergistically potentiates the response of murine preosteoblast cells to BMP-9 (1 nM) (Lauzon *et al.*, 2014). There is also evidence that IGF-2 acts in synergy with several other GFs. Konishi *et al.* (1994) showed that IGF-2 (100 ng/mL) plus NGF (100 ng/mL) or bFGF (10 ng/mL) significantly increased the synthesis of ChAT over that produced by each GF alone. Other recent results indicate that a combination of bFGF (40 ng/mL) and epidermal growth factor (EGF) (20 ng/mL) mediates the differentiation of epidermal neuron crest stem cells to neuron-like phenotype with increased concentrations of neuron markers such as βIII-tubulin, nestin and neurofilaments (Bressan *et al.*, 2014).

A combination of several GFs might positively affect AD hallmarks if the combination is based on the way they influence the activation of specific signaling pathways that are generally dysfunctional in AD. Figure 2-2 shows the positive effects of GFs targeting specific signaling pathways on AD. Other synergistic combinations and new approaches may be identified. This approach is promising but the use of several GFs simultaneously may have unexpected side-effects, such as the sequestration of signaling protein by hyperphosphorylated Tau.
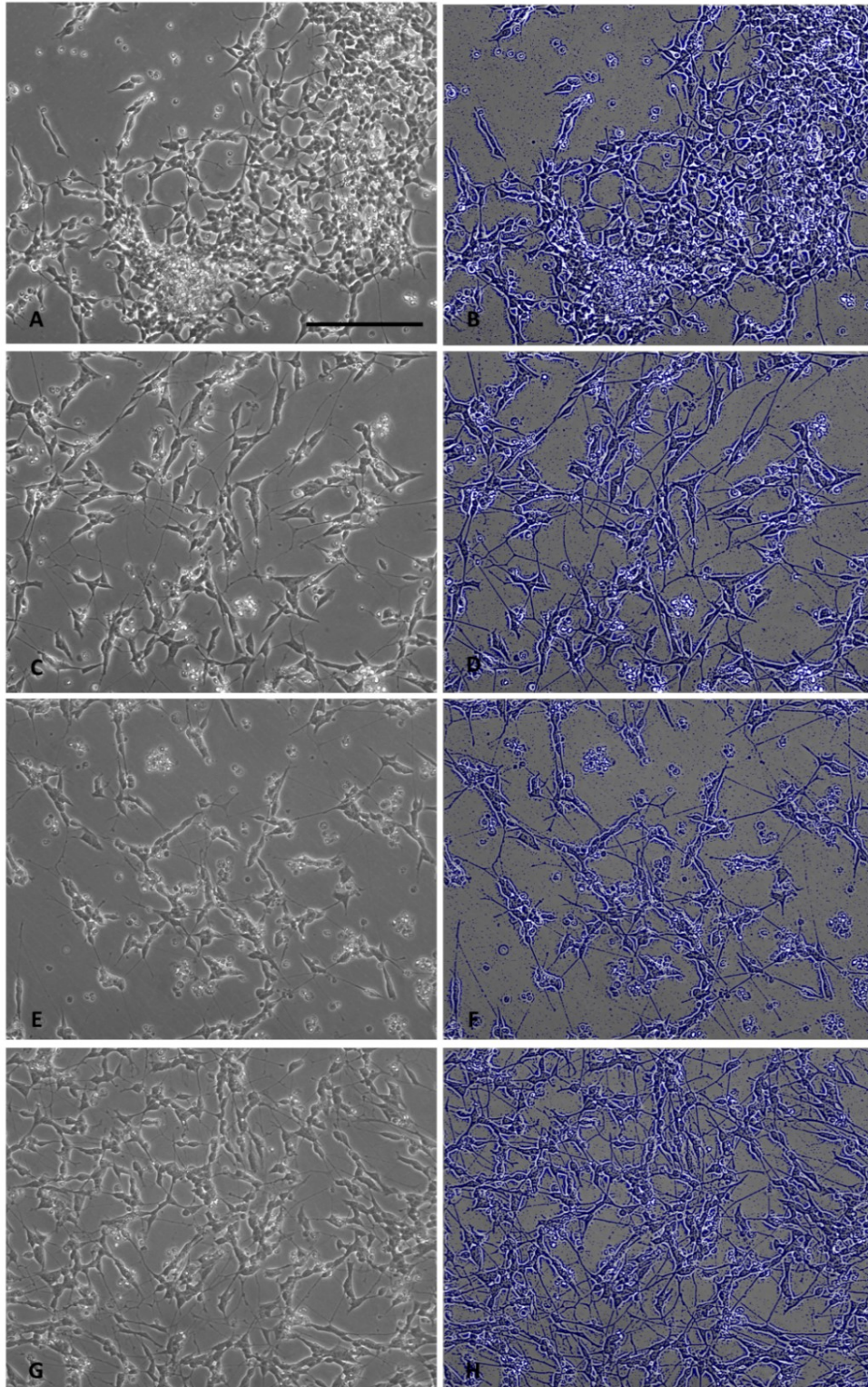
Figure 2-5 : Effects of BMP-9 and pBMP-9 on SH-SY5Y morphology after 72h of incubation (A) Control, (C) Control + AR (10 µM), (E) BMP-9 (1nM) + AR (10 µM) and (G) pBMP-9 (1nM) + AR (10 µM). Images (B), (D), (F) and (H) show images (A), (D), (E) and (G) respectively after Gaussian smoothing followed by Laplacian high pass filtering to define and enhance contours to show the neurites more clearly. Bar = 500 µm.

2.4.4 New approaches

Protein growth factors have great potential but they are rather difficult to deliver to the brain. First, there is the BBB, whose tight junctions act like a customs post regulating everything that leaves and enters the brain. Passage across the BBB is closely regulated, mostly by active transport through endocytosis and transcytosis, except for air, water and small lipid molecules (Alyautdin *et al.*, 2014; Haines, 2012; Lochhead et Thorne, 2012). One way to overcome these difficulties is to use small peptides derived from GFs since these low molecular weight molecules can cross the BBB more easily (Lochhead et Thorne, 2012; Mehdipour et Hamidi, 2009). We have developed a small peptide (pBMP-9) derived from the knuckle epitope of BMP-9 that is recognized by the type II receptor responsible for giving the first signal at the cell surface. We have already demonstrated that it can trigger a response by bone cells (preosteoblasts) that is similar to that of the whole protein both *in vitro* and *in vivo* (Bergeron *et al.*, 2009, 2012). Clearly, BMP-9 seems to be a promising GF for treating AD. Thus, the results of the effect of pBMP-9 toward bone cells could be transposed to neurons. Figure 2-5 shows the effects of pBMP-9 and BMP-9 on the differentiation of SH-SY5Y human neuroblastoma cells that had been stimulated with RA (10 μM) for 72 h. The filtered pictures (B, D, F and H) show that there is more neurite outgrowth from the pBMP-9-stimulated cells than from the controls with or without RA or from the BMP-9- stimulated cells. Although there were more, longer neurites, this may not automatically mean differentiation of the whole cell. Nevertheless, it shows that this peptide acts on neurons. There are also results showing that peptides that mimic bFGF are very promising (Enevoldsen *et al.*, 2012; Manfe *et al.*, 2010; Neiiendam *et al.*, 2004). Manfe *et al.* (2010) have developed peptides (canofins) that interact with FGFR in much the same way as bFGF. They have also shown that these peptides stimulate neurite outgrowth and protect rat cerebellum granule neurons from induced apoptosis. Enevoldsen *et al.* (2012) extended the work of Neiiendam *et al.* (2004) and created a small peptide (enreptin) that is shaped like a tetrameric dendrimer and interacts with the FGF receptor and neural cell adhesion protein (NCAM). This peptide increases neurite outgrowth from primary cultures of cerebellar granule neurons and reduces the cytotoxic effect of β-amyloid$_{25-35}$ peptides. They have also used BALB/c mice to show that enreptin crosses the BBB and decreases the memory deficit. Stimulating the NCAM receptor leads to the activation of the MAPK and PI3K/AKT pathways

favoring neurite outgrowth (Neiiendam *et al.*, 2004). Hence, this peptide might also restore the balance between these dysfunctional pathways in AD-like animal models since activating the PI3K/AKT pathway can inactivate GSK3β and so Tau protein. Finally, they have demonstrated that enreptin reduces memory loss as well as neuron death in Wistar rats injected with β-amyloid$_{25-35}$ peptides. Soumen *et al.* (2012) have also created a peptide that mimics NGF and BDNF and activates the NGF receptor (TrkB). There is evidence that other small peptides, such as the neuropeptide Y (NPY) may be promising therapeutic molecules, mostly because they can stimulate neurotrophin synthesis, regulate intracellular Ca^{2+}, and protect neurons (for review see (Angelucci *et al.*, 2014)). Finally, other small peptides have been developed to directly target specific AD hallmarks. Spencer *et al.* (2014) have developed a small (38 residues) peptide that mimics the action of the endopeptidase neprilysin. This peptide readily crosses the BBB, reduces β-amyloid peptide aggregation and significantly enhances the cognitive function of APPtg mice.

Thus, peptides derived from active regions of proteins may be able to overcome problems such as the BBB and facilitate the design of an appropriate carrier.

2.5 Conclusion

We have shown that the causes and details of AD, a degenerative disease that will afflict more and more people as the world population ages, are still not fully understood. Most FDA-approved treatments have only transient effects and many strategies targeting only one of the three hallmarks of AD at a time have failed in clinical trials. This review gathers together the latest published results showing that these hallmarks are closely interlinked. We have also shown that GFs like the TGFβs, insulin-derived peptides and neurotrophins can be beneficial for all the AD hallmarks by activating many cellular signaling pathways deregulated by the disease. This new information on the effects of GFs on the neuron signaling pathways and the *in vivo* symptoms of AD such as memory impairment and learning deficits clearly shows that using the proper combination of GFs can have measureable therapeutic effects: promoting neurogenesis, amyloidosis, reducing Tau protein phosphorylation and maintaining the cholinergic system. The GFs can also be combined so that they act in synergy. Some of the new studies quoted reveal that BMP-9 affects the Smad and GSK3β pathways. Thus, BMP-9 activates Smad1/5/8 in the presence of RA and inactivates GSK3β by maintaining the

phosphorylation on Ser9. These results confirm that GFs or derived molecules are promising for attaching the scourge of AD.

2.6 Acknowledgments

2.7 Mise à jour de la revue de littérature sur l'utilisation de facteurs de croissance pour le traitement de la maladide d'Alzheimer

Le Tableau 2-1 ci-dessous répertorie les différentes publications concernant l'utilisation de facteurs de croissance comme traitement potentiel de l'AD parues de 2016 à 2017 afin de mettre à jour certains éléments de la littérature. D'autres éléments récents sont également présentés dans les articles de résultats.

Tableau 2-1 : Mise à jour de la revue de littérature concernant l'utilisation de GFs comme stratégie thérapeutique pour le système nerveux central

	GFs	Modèle	Administration	Effets *in vitro*/*in vivo*	Ref
	TGFβ-1	Souris (Swiss)	Milieu conditionné par des astrocytes dérivés de souris ou d'humains soumis à βA_{1-42}	↑ densité synaptique ↓ interactions avec les oligomères deAβ	(Diniz *et al.*, 2017)
			Injection intra-cérébroventriculaire du milieu conditionné	↓ perte des neurones dentriques de l'hippocampe ↓ pertes cognitives	
TGFβ	BMP-9	Souris APP/PS1	Injection intranasale de BMP-9 (50 ng/g/j)	↑ fonction cognitive (apprentissage spatial et associatif) ↓ plaque βA ↓ neuroinflammation ↑ synthèse LRP1 ↓ phosphorylation Tau ↑ phosphorylation GSK3β	(Wang *et al.*, 2017)
		Rat	Injection systémique de BMP-9 (micro-vaisseaux du cerveau)	↑ activation Alk-1 ↑ expression Oatp1a4	(Abdullahi *et al.*, 2017)

Autres	bFGF	Rat (modèle blessure au cerveau)	Injection intranasale via des nano-liposomes (traitement 3j)	↑ accumulation au cerveau de nano-liposomes ↑ fonction motrice ↓ volume affecté ↑ activation PI3k/Akt dans le cerveau de rat	(Zhao *et al.*, 2016)
	EGF	Souris (E4FAD)	Injection intrapéritonéale (300 µg/kg/semaine pendant 8.5 mois)	↓ déclin cognitif ↓ microfissures cérébrales	(Thomas *et al.*, 2016)
		Souris (APOE$^{+/+}$/ 5xFAD$^{+/-}$)	Injection intrapéritonéale (300 µg/kg/semaine pendant 8.5 mois)	↓ déclin cognitif ↑ EGF dans le plasma et le cerveau ↓ fuite de fibrinogène et ↑ micro vaisseaux	(Thomas *et al.*, 2017)
	IGF-1/ IGF-2	Souris APP/PS1	Injection péri-hippocampale de cellules souches corticales humaines sur-exprimant IGF-1	↑ neuro-protection en présence de βA N'affecte pas la capacité de prolifération N'affecte pas la capacité de différenciation Survie pendant 10 semaines *in vivo*	(McGinley *et al.*, 2016)
Neurotrophines	NGF	Souris ShcCKO (tranches de cerveau) Échantillons de cerveaux humains	Tranches de cerveau cultivées dans du liquide cérébrospinal et traitées par 100 ng/mL de NGF	Contrôle le niveau de phosphorylation d'APP (T668) ↓ activité JNK ↓ interaction entre APP et récepteur TrkA ↑ circulation dans l'appareil de Golgi d'APP ↓ βA	(Triaca *et al.*, 2016)
		Humain souffrant d'AD	Implant cérébral contenant des cellules NGC-0211 exprimant du NGF (6 à 12 mois) visant le cerveau basal cholinergique (cohorte de 4 patients)	↑ relargage NGF au cerveau ↑ niveau de ChAT et d'AchE chez 2 des 4 patients corrélé avec amélioration cognitive	(Eyjolfsdottir *et al.*, 2016)
		Culture primaire de neurones cholinergiques du septum de rat (wistar)	NGF 100 ng/mL dans du milieu pauvre en sérum	↑ neurones cholinergiques ↑ compétence électrophysiologique Le retrait de NGF : - Déstabilise les microtubules - Réduit le nombre de vésicules synaptiques - Induit la mort cellulaire	(Latina *et al.*, 2017)
	BDNF	Souris C57BJ/6j subissant un stress chronique modéré	Libération de BDNF couplée aux séquences TAT et HA2 (peptides	↓ symptômes de dépression ↑ niveau de BDNF de l'hippocampe	(Ma *et al.*, 2016)

		de pénétration cellulaire) 10 µL/souris/10 jours		
	Cellules SH-SY5Y (différenciation avec 10 µM de RA pendant 2 j)	50 ng/mL + stimulation pendant 3 j	↓ désintégrine A et metalloproteinase 10 ↑ activité α-secretase ↑ croissance neurites ↓ BACE1 (clivage sAPPα)	(Nigam *et al.*, 2017)
GDNF	Rat (Sprague-Dawley)	Injection intranasale de GNDF encapsulé dans des liposomes (10 à 50 µg)	↑ rapidement niveau de GNDF dans tout le cerveau (~1h) ↑ 10x plus d'accumulation au cerveau par rapport au GNDF dans du PBS	(Bender *et al.*, 2015)
	Singe (*Macaca fascicularis*) avec une atteinte sévère dans la région nigrostratiale (modèle Parkinson)	Injection de microparticules de poly(acide lactique co-glycolique) (PLGA) dans le putamen (25 µg)	Libération soutenue de GDNF ↑ fonction motrice ↑ nombre neurones dopaminergiques stratiales (après 9 mois)	(Garbayo *et al.*, 2016)
NT-3	Cellules souches neuronales dérivées de la moelle osseuse de souris C57BL/6	Surnageant de cellules 293T transfectées par un lentivirus contenant la séquence codante de NT-3	↑ prolifération ↑ synthèse de ChAT ↑ synthèse ACh	(Yan *et al.*, 2016)

2.8 Informations sur le 2ᵉ article de revue

Titre original: Nanoparticle-mediated growth factor delivery systems: A new way to treat Alzheimer's disease

Titre français : Systèmes de libération de facteurs de croissance à base de nanoparticules : Une nouvelle façon de traiter la maladie d'Alzheimer

Auteurs et affiliations :

- M.-A. Lauzon : Étudiant au doctorat en génie chimique, Département de génie chimique et de génie biotechnologique, Université de Sherbrooke

- A. Daviau : Ancien assistant de recherche sous la direction de Prof. N. Faucheux, Département de génie chimique et de génie biotechnologique, Université de Sherbrooke

- B. Marcos : Professeur titulaire, Département de génie chimique et de génie biotechnologique, Université de Sherbrooke

- N. Faucheux : Professeur titulaire, Département de génie chimique et de génie biotechnologique, Université de Sherbrooke

Contributions à la thèse :

Cet article contribue à la thèse en présentant l'état de l'art (premier objectif) concernant les principaux acteurs autour desquels s'articule le projet de thèse. Les éléments suivant y sont présentés :

- Une brève revue de l'utilisation de facteurs de croissance comme stratégie thérapeutique contre la maladie d'Alzheimer.

- Une revue exhaustive des dernières innovations dans le développement de systèmes de libération de facteurs de croissance à l'échelle nanométrique (nanoparticules) pour acheminement au cerveau. Les effets tant au niveau *in vitro* qu'*in vivo* y sont également répertoriés tout comme les nouvelles stratégies pour augmenter la spécificité et l'abondance de ces systèmes de libération au CNS.

- Les différentes barrières naturelles du corps humain pouvant interférer avec l'acheminement des systèmes de libération sont étudiées au plan physiologique.

- Des pistes de solution quant à la modélisation mathématique du transport des nanoparticules du site d'injection jusqu'au tissu cérébral en passant par ces barrières sont présentés.

- Une revue exhaustive des modèles mathématiques décrivant les différents phénomènes de transfert de masse des molécules thérapeutiques compris dans le système de libération sont présentés.

Résumé anglais:

The number of people diagnosed with Alzheimer's disease (AD) is increasing steadily as the world population ages, thus creating a huge socio-economic burden. Current treatments

have only transient effects and concentrate on a single aspect of AD. There is much evidence suggesting that growth factors (GFs) have a great therapeutic potential and can play on all AD hallmarks. Because GFs are prone to denaturation and clearance, a delivery system is required to ensure protection and a sustainable delivery. This review provides information about the latest advances in the development of GF delivery systems (GFDS) targeting the brain in terms of *in vitro* and *in vivo* effects in the context of AD and discusses new strategies designed to increase the availability and the specificity of GFs to the brain. This paper also discusses, on a mechanistic level, the different delivery hurdles encountered by the carrier or the GF itself from its injection site up to the brain tissue. The major mass transport phenomena influencing the delivery systems targeting the brain are addressed and insights are given about how mechanistic mathematical frameworks can be developed to use and optimize them.

Résumé français:

Le nombre de personnes diagnostiquées avec la maladie d'Alzheimer (AD) augmente systématiquement avec le vieillissement de la population mondiale, créant ainsi un lourd fardeau socio-économique. Les traitements actuels possèdent uniquement un effet transitoire et se concentrent sur un seul aspect de l'AD. Il y a plusieurs éléments de preuve suggérant que les facteurs de croissance (GFs) possèdent un effet potentiel thérapeutique important et peuvent jouer sur tous les symptômes caractéristiques de l'AD. Parce que les GFs sont sujets à la dénaturation et à l'élimination, un système de libération est requis pour assurer leur protection et leur libération soutenue. Cette revue fournit des informations concernant les dernières avancées dans le développement de systèmes de libération de GFs (GFDS) visant le cerveau en termes d'effets *in vitro* et *in vivo* dans le contexte de l'AD et discute des nouvelles stratégies conçues pour augmenter l'abondance et la spécificité des GFs au cerveau. Cet article discute également, sur une base mécanistique, des différents obstacles à la libération que peut rencontrer un système de libération ou même les GFs du site d'injection jusqu'au tissu cérébral. Les principaux phénomènes de transfert de masse influençant les systèmes de libération visant le cerveau sont adressés et une discussion est initiée afin de comprendre comment des modèles mathématiques mécanistiques peuvent être développés pour les utiliser et les optimiser.

2.9 Introduction

Alzheimer's disease (AD) is the most common form of dementia (over 60–80%), targeting mostly the elderly with a prevalence of 2–10% of people aged 65 years (World Health Organization, 2012).With the aging of the world population, more and more people will be diagnosed with AD, thus creating a huge socio-economic burden (Mota *et al.*, 2014; World Health Organization, 2012).

AD is characterized by three major pathophysiological hallmarks. The first one is the dysregulation of the cholinergic systems, which has been shown to be correlated with the cognitive impairments of patients developing AD (Parent *et al.*, 2013; Teipel *et al.*, 2011). The second hallmark is the senile plaque accumulation made of β-amyloid peptide aggregates. β-amyloid peptides are derived from amyloid precursors that can undergo several cleavages by β-, γ- and α-secretase. In AD, β-amyloid peptides accumulate and lead to toxic fibrillary aggregation also known as senile plaques (Sinha et Lieberburg, 1999). Those aggregates severely impair the viability of neurons by disrupting brain parts composed of unmyelinated neurons, dendrites and glial cells also known as neuropil (Murphy et LeVine 3rd, 2010). Finally, the third hallmark of AD is the apparition of neurofibrillary tangles resulting from the hyperphosphorylation of Tau protein (Alonso *et al.*, 1996; Augustinack *et al.*, 2002). Tau is a microtubule associated protein found mostly in the axons (Buée *et al.*, 2000). Internal cell dysregulations observed in AD patients cause a hyperphosphorylation of Tau, which severely impairs the axon integrity and the neurotransmitter transport (Augustinack *et al.*, 2002; Sun *et al.*, 2003). Moreover, there is increasing evidence showing that those three hallmarks are closely interconnected, which tend to indicate that future therapeutic approaches should act simultaneously on all of them (Busciglio *et al.*, 1995; Do *et al.*, 2014; Ferreira *et al.*, 1997; Olivero *et al.*, 2014; Zheng *et al.*, 2002).

The current treatments for AD are mostly acetylcholinesterase inhibitors (Rivastigmine, Dopenezil, Galantamine) or NMDAR inhibitor (Memantine). Those inhibitors show only transient effects without stopping the progression of the disease and are principally administered orally or transdermally (Hansen *et al.*, 2008; Molino *et al.*, 2013; Tricco *et al.*, 2013). Other treatments focus on senile plaques or the hyperphosphorylation state of Tau proteins (Braak et

Braak, 1991; Giacobini et Gold, 2013; Vesey *et al.*, 2002). Treatments that focus on β-amyloid peptides have mostly failed in clinical studies due to a lack of effectiveness or the presence of severe side effects such as liver toxicity, immunogenicity and low specificity for the brain (Giacobini et Gold, 2013). Meanwhile, treatments focusing on the hyperphosphorylation of Tau, which target glycogen synthase kinase 3 beta (GSK3β) known as one of the most important Tau kinases, are currently under clinical studies (Giacobini et Gold, 2013).

Growth factors (GFs) such as bone morphogenetic proteins (BMPs) (Burke *et al.*, 2013; Lopez-Coviella *et al.*, 2000, 2002, 2011), insulin-like growth factor (IGF-1/IGF-2) (Freiherr *et al.*, 2013; Pascual-Lucas *et al.*, 2014), basic fibroblast growth factor (bFGF) (Kiyota *et al.*, 2011; Noshita *et al.*, 2012; Ye *et al.*, 2010) and neurotrophins (nerve growth factors, NGF (Allen *et al.*, 2013; Matrone, Ciotti, *et al.*, 2008; Matrone, Di Luzio, *et al.*, 2008); glial-derived neurotrophic factor, GDNF (Revilla *et al.*, 2014) and brain-derived neurotrophic factor, BDNF (Arancibia *et al.*, 2008; Kitiyanant *et al.*, 2012)) are very promising therapeutic molecules. Those GFs can normally be found in the brain and play a crucial role during the developmental stages of the central nervous system (CNS) (Dupraz *et al.*, 2013; Ford-Perriss *et al.*, 2001; Korsching *et al.*, 1985; Lad *et al.*, 2003; Lopez-Coviella *et al.*, 2006; Nilbratt *et al.*, 2010; Stevens *et al.*, 2012). There is also much evidence showing that those GFs can act simultaneously on several AD hallmarks. For example, it has been shown that BMP-9 could successfully reduce senile plaque in rodents and promote the cholinergic differentiation and maintenance (Burke *et al.*, 2013; Lopez-Coviella *et al.*, 2000, 2002). Other studies have also shown that IGF-2 and NGF can significantly reduce the senile plaques and the level of Tau hyperphosphorylation (Hong et Lee, 1997; Lv *et al.*, 2014; Matrone, Ciotti, *et al.*, 2008; Matrone, Di Luzio, *et al.*, 2008; Pascual-Lucas *et al.*, 2014).

The best administration route for GFs seems to be the intranasal injection due to a high capillary density, a large surface area, the proximity to the brain and also because of the high endocytosis activity of nasal endothelial cells (Dhuria *et al.*, 2010; Di Stefano *et al.*, 2011; Illum, 2000, 2003; Lochhead et Thorne, 2012; Thorne *et al.*, 2004; Thorne et Nicholson, 2006). However, several biological barriers can severely impair the transportation of GFs across the brain such as the blood–brain barrier (BBB), which regulates the passage of molecules from the blood to the brain through active transport and specific cell receptors (Haines, 2012; Marques *et*

al., 2013; Roney *et al.*, 2005). The GFs are also sensitive to enzymatic degradation, clearance and denaturation in the blood or in the brain (Di Stefano *et al.*, 2011). For instance, BMPs show a very small half-life of about 6–7 min in non-primate mammals (Poynton et Lane, 2002). Delivery systems that can extend the life-span of GFs and provide for their controlled, sustained and local release could overcome all these problems. However, the physical–chemical properties of the delivery carriers, such as their size, overall surface charge and chemical composition will greatly influence their capacity to specifically target brain tissue and they will need to be carefully analyzed to determine their cytotoxicity, biocompatibility and biodegradability (Giordano *et al.*, 2011; Ji *et al.*, 2014; Nagpal *et al.*, 2010).

There is also a need to understand the delivery mechanisms involved from the injection site to the brain. This knowledge can then further help to build explanatory and predictive models that enable realistic simulations. A number of mass transport phenomena govern the release of the GFs from their delivery systems; the main ones are diffusion, swelling, erosion, convection and interactions (Lauzon, Bergeron, *et al.*, 2012). These mass transport phenomena have a massive influence on the rate at which GFs are released and must be taken into account when targeting the brain, as they are involved from the site of injection to the delivery within the brain itself (Lauzon, 2014; Siepmann *et al.*, 2006; Wolak et Thorne, 2013). Research is uncovering more knowledge about the diffusion of molecules in the brain (Nicholson et Phillips, 1981; Nicholson et Tao, 1993; Salegio *et al.*, 2014; Thorne et Nicholson, 2006), but only a few mathematical frameworks have been proposed that model the mass transport of drugs in the brain (Siepmann *et al.*, 2006). Hence, our understanding of the phenomena underlying this transport is far from adequate. We need to develop and adapt mathematical models to describe these transport phenomena as they concern the delivery of GFs to the brain.

This paper first describes the particularity of the BBB affecting significantly the brain uptake of therapeutics and presents the different administration routes proposed to overcome those hurdles. Secondly, the latest advances in the development of brain-targeted GF delivery systems (GFDS) are reviewed and some of the new strategies used to address specific molecules across biological barriers into the brain are discussed. The different materials, their advantages and limitations in the context of GF delivery as well as their *in vitro* or *in vivo* effects on GF liberation are also addressed. This paper then focuses on the mass transport phenomena that can

be encountered by GFDS dealing with the release mechanisms that should be considered and the mass transport of the carrier itself across the BBB up to the brain tissue. This chapter examines how they can be modeled by adapting existing mechanistic frameworks to GFs.
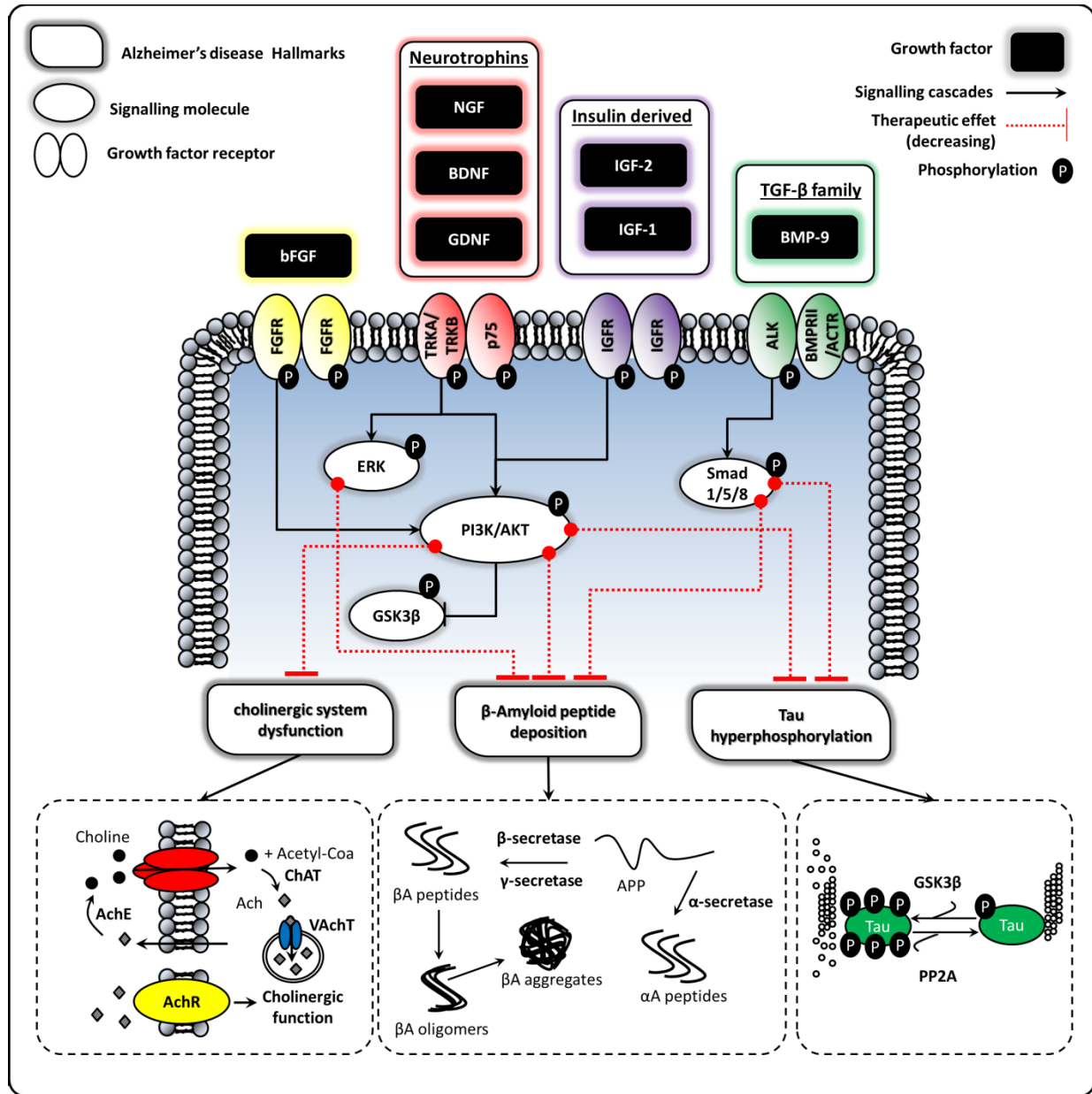
Figure 2-6 : Growth factors showing a therapeutic effect on Alzheimer's disease, their cell receptors, simplified signaling pathways and therapeutic effects on Alzheimer's disease hallmarks (APP = amyloid precursor protein, Ach = acetycholine, AchE = acetylcholine esterase, ChAT = choline acetyltransferase, AchR = acetylcholine receptor, VAchT = vesicular acetylcholine transporter protein, βA = peptide β-amyloid, GSK3β = glycogen synthase kinase 3 β, PP2A = protein phosphatase 2 A).

2.10 Growth factor to treat Alzheimer's disease and their CNS delivery

2.10.1 Overview of growth factors as therapeutic molecules

There is increasing evidence from the literature showing the promising therapeutic effects of several GFs on different AD hallmarks (Burke *et al.*, 2013; Y. Chen *et al.*, 2014; Lv *et al.*, 2014; Madziar *et al.*, 2008). GFs act as first messengers by interacting with their receptors, localized at the cell surface. This interaction can then trigger the activation of signaling pathways which in turn, modulate several cell behaviors such as survival, proliferation and differentiation (Baron *et al.*, 2012; Hawkes *et al.*, 2006; Lopez-Coviella *et al.*, 2005). It has been reported that signaling pathways such as phosphoinositide 3 kinase (PI3K)/AKT and mitogen-activated protein kinase (MAPK) composed by extracellular signal-regulated kinase ERK were dysfunctional in AD and the use of GFs could restore them (Allen *et al.*, 2013; Kitagishi *et al.*, 2014; O'Neill, 2013). Figure 2-6 and Tableau 2-2 summarize the major GFs that have shown a therapeutic potential as well as their mode of action and *in vitro* and *in vivo* effects. Those can be naturally found in the CNS and are involved both in the development of the embryonic brain and the homeostasis of the adult CNS (Allen *et al.*, 2013; Ford-Perriss *et al.*, 2001; Mehler *et al.*, 1997; O'Kusky et Ye, 2012; Zhang *et al.*, 2007). GFs also have the ability to play simultaneously on several pathophysiological symptoms of AD, which render them very attractive as an alternative therapeutic avenue. For instance, BMP-9 has been shown to decrease beta amyloid peptide deposits (senile plaque), protect cholinergic neurons of the basal forebrain and upregulate the cholinergic system by increasing the synthesis of vesicular transporter protein and acetylcholine transferase (AchT) and cholinergic fiber volume (Burke *et al.*, 2013; Lopez-Coviella *et al.*, 2000; Mellott *et al.*, 2002). Other GFs such as IGF-1 and IGF-2 can regulate the hyperphosphorylation state of Tau protein by activating the PI3K/AKT pathway and by decreasing the deposits of β-amyloid peptides (Chen *et al.*, 2014; Hong et Lee, 1997; Pascual-Lucas *et al.*, 2014). Moreover, other GFs such as bFGF can increase neurogenesis while decreasing β-amyloid deposits (Kiyota *et al.*, 2011; Noshita *et al.*, 2012).

Finally, neurotrophins (NGF, BDNF and GDNF) also show a good therapeutic effect. For instance, NGF is known to activate the PI3K/AKT pathway via its interaction with tropomyosin kinase receptors (Madziar *et al.*, 2008). It has also been shown that the presence of

NGF was necessary for the expression of acetylcholine (Ach) locus (Madziar *et al.*, 2008). Other studies have also reported that NGF can modulate the phosphorylation level of Tau protein (Capsoni *et al.*, 2002; Lv *et al.*, 2014). In addition to their effect, those GFs can sometimes have a synergistic effect. For instance, Lopez-Coviella *et al.* (2000) have shown that BMP-9 can act synergistically with bFGF on embryonic-derived murine cells from the septum and increase Ach expression. BMP-9 can also induce the expression of IGF-1 and NGF and increases choline acetyltransferase (ChAT) (Schnitzler *et al.*, 2010). Other GFs such as IGF-2 can also increase ChAT when combined with NGF and bFGF (Konishi *et al.*, 1994). However, despite the great therapeutic potential of these proteins, they need to be properly addressed to the CNS, which implies several challenges such as natural barrier, low half-life time and enzymatic degradation that can limit the therapeutics uptake.

2.10.2 CNS delivery systems

Entry sites and their limitations

One of the greatest challenges in the development of a GFDS for brain applications is the delivery of the therapeutic molecules. Only a limited amount of drugs can cross the BBB and the drugs present on the market that have been approved by the FDA do not specifically target the brain capillary endothelial cells. They are either delivered orally or transdermally. Transdermal patches are preferred since they provide better assimilation and have fewer side effects, although they are rather difficult for the patient to use (Di Stefano *et al.*, 2011). However, only a small fraction of the drug that gets into the blood stream actually enters the brain. The rest is metabolized or excreted. This non-specificity is responsible for the side effects. Many of the new treatments, such as antibody based amyloidosis or β-secretase inhibitors, have little or no clinical effect, mostly due to their delivery route, toxicity due to lack of specificity and their inability to cross the BBB (Giacobini et Gold, 2013). There are two main approaches to target therapeutic molecules to the brain. One is invasive, involving direct injection or chemical or mechanical disruption of the BBB. The second is non-invasive, using chemical, biological or intranasal delivery (Stockwell *et al.*, 2014).

There are several possible invasive strategies that target therapeutic molecules, particularly GFs, directly to the brain; these include infusion (bilateral, intraventricular,

intraparenchymal and convection-enhanced diffusion) (Barua *et al.*, 2012; Lochhead et Thorne, 2012; Motion *et al.*, 2011; Pardridge, 2007; Tam *et al.*, 2014; Yi *et al.*, 2014). However, they are extremely invasive and may cause brain edema and convulsion even if EGF and GDNF have been successfully injected with a bioactive effect on proliferation and neurogenesis in rodents (see review (Tam *et al.*, 2014)). The majority of the studies that have used intracerebroventricular and intraparenchymal injections of GFs and peptides have failed in clinical trials, mostly because they show adverse effects such as back pain and weight loss or due to rapid clearance from the cerebrospinal fluid (CSF) to the blood stream or from the ependymal lining constituting another barrier to GF diffusion (see review (Yi *et al.*, 2014)). Nonetheless, Barua *et al.* (2012) have shown that convection-enhanced delivery of virus vector-mediated neprilysin also increased the diffusion of the drug through Wistar rat brains and decreased the β-amyloid$_{1-40}$ peptide concentration. Several techniques have been used to disrupt the BBB, such as surfactants, mostly polysorbate-80 (Kreuter, 2001; Kurakhmaeva *et al.*, 2009; Rempe *et al.*, 2011; Wilson *et al.*, 2010; Kumar, *et al.*, 2008; Wohlfart *et al.*, 2012), and mechanical disruption (Burgess et Hynynen, 2013; Konofagou *et al.*, 2012). Burgess and Hynynen (2013) used focused ultrasound to create harmless acoustic cavitation that temporarily destabilized the BBB and appeared to significantly facilitate the diffusion of high molecular weight proteins (up to 40 kDa) across the BBB. Konofagou *et al.* (2012) successfully used the same method to inject BDNF into brains.

Tableau 2-2 : GF with therapeutic effects on AD hallmarks

GF	Receptors Signaling	Effects on AD symptom[1]	Dose	Ref
TGF-β family				
BMPs	<u>BMPRI/ BMPRII</u> Smad1/5/8, MAPK	• Maintain and protect cholinergic mouse neurons *	10 ng/mL	(Lopez-Coviella *et al.*, 2000)
		• ↓ β-amyloid deposits, ↑ choline acetyltransferase in mouse hippocampus and cortex **	4 ng/h for 7 days	(Burke *et al.*, 2013)
Other GFs				
IGF-1/IGF-2	<u>IGFR</u> PI3K/AKT and ERK (MAPK)	• ↓ Tau hyperphosphorylation via ↓ GSK3β activity • ↓ β-amyloid peptide deposits in hippocampus** • ↓ β-amyloid peptides, ↑ cholinergic markers** • ↑ cognitive function and ↓ Tau hyperphosphorylation **	10 ng/mL (IGF-1) Adenovirus 50 ng/h for 7 days 17.5 µL (intranasal)	(Hong et Lee, 1997) (Pascual-Lucas *et al.*, 2014) (Mellott *et al.*, 2014) (Y. Chen *et al.*, 2014)
bFGF	<u>FGFR</u> PI3K/AKT and ERK (MAPK)	• ↑ cholinergic neurons in the rat hippocampus, ↑ learning abilities** • ↑ neurogenesis, ↓ β-amyloid peptide deposits in mouse hippocampus** • ↑ expression of GDNF and ↑ neuronal plasticity in rat glial cell*	1 µg/day for 7 days ~2 pg/mg adenovirus 30 ng/mL	(Ye *et al.*, 2010) (Kiyota *et al.*, 2011) (Tanabe *et al.*, 2012)
Neurotrophins				
NGF	<u>TRKA/p75</u> PI3K/AKT and ERK (MAPK)	• ↓ Tau phosphorylation (40%) in rat, ↓ GSK3β activity** • ↓ Tau phosphorylation, ↑ choline acetyltransferase in mouse **	5 µg/day 1-10 µM	(Lv *et al.*, 2014) (Capsoni *et al.*, 2002)
BDNF	<u>TRKB/p75</u> PI3K/AKT and ERK (MAPK)	• ↓ toxicity of β-amyloid using neuronal progenitor cells* • ↓ toxicity of β-amyloid using rat cortical neurons*	10 µM 50 ng/mL	(Kitiyanant *et al.*, 2012) (Arancibia *et al.*, 2008)
GDNF	<u>TRKB/p75</u> PI3K/AKT and ERK (MAPK)	• Maintain the BBB affected by β-amyloid by ↑ claudin-5	1-10 ng/mL	(Shimizu *et al.*, 2012)

[1]* *in vitro* experiments, ** *in vivo* experiments

Non-invasive strategies for delivering therapeutic molecules across the BBB have used different sites so as to maximize the accumulation of drugs in the brain and limit the side effects. One of the most popular routes is intranasal delivery (Dhuria *et al.*, 2010; Di Stefano *et al.*, 2011; Illum, 2000, 2003; Lochhead et Thorne, 2012; Thorne *et al.*, 2004; Thorne et Nicholson, 2006). The nasal mucosa has many advantages, including a high capillary density, a large surface area, proximity to the brain (trigeminal nerves) and the endothelial cells bordering these blood vessels are highly endocytotic (Lochhead et Thorne, 2012). The intranasal route might be

the best way to deliver GFs efficiently because it is non-invasive, painless and does not require a physician (Cai *et al.*, 2014). Thorne *et al.* (1995) showed that the intranasal route is more efficient than intravenous injection for getting protein to the rat olfactory bulb. The same group confirmed their results using radio-labeled IGF-1. The concentrations that accumulated in the body and the brain were 100–1000 times higher than those produced by intravenous injection (Thorne *et al.*, 2004). Lopes *et al.* (2014) also recently showed that IGF-1 could be successfully delivered intranasally in a model of Huntington's disease. Others have reported the efficiency of nose-to-brain delivery of bFGF (Zhang *et al.*, 2014; Zhao *et al.*, 2014). NGF can also be efficiently delivered intranasally (Aloe *et al.*, 2014) and thus reduce deposits of β-amyloid peptide aggregates (Tian *et al.*, 2012). Lv *et al.* (2014) have shown that NGF delivered intranasally decreases Tau hyperphosphorylation in a traumatic brain injury model. There are also reports that BDNF can be successfully delivered to the brain by injecting it into the nasal cavity (Alcala-Barraza *et al.*, 2010; Vaka *et al.*, 2012). However, there are also natural barriers that have to be bypassed such as the moving acidic mucus layers rich in enzymes like lysozymes and lactoferrin as well as the epithelial cells bearing tight junctions limiting the transport (Casettari et Illum, 2014; Kaliner *et al.*, 1984; Mistry, Glud, *et al.*, 2009; Pardeshi et Belgamwar, 2013). Nonetheless, the intranasal route shows many advantages in terms of brain uptake capabilities and proximity to the CNS, thus suggesting that it might be the most suitable way to deliver therapeutics to the brain. Since GFs are prone to rapid clearance by enzymatic degradation or denaturation, delivery systems that can extend the life-span and ensure a controlled, sustained and local release could overcome all these problems.

The blood-brain barrier

The BBB is characterized by the tight junctions between endothelial cells and limited pinocytosis that restricts and controls the passage of molecules from the blood into the brain (Alyautdin *et al.*, 2014; Haines, 2012; Lochhead et Thorne, 2012). It is very efficient at protecting the brain from pathogens, viruses and other undesirable blood-borne compounds. Only O_2 and CO_2 diffuse freely across the BBB; all other molecules, including glucose, insulin and amino acids, must enter the brain via absorptive endocytosis or use specific receptors (insulin, transferrin, lipoprotein-related protein (LRP-1) and EGF receptors) (Haines, 2012; Marques *et al.*, 2013; Roney *et al.*, 2005). Other than receptor-mediated transport, molecules

such as lipophilic compounds and peptides with molecular weights of up to 0.6 kDa can also cross the BBB and affect the CNS by interacting with P-glycoprotein (Banks, 2009). However, the BBB of the AD or aged brain suffers from several defects, such as the downregulation of the concentrations of P-glycoprotein and low-density lipoprotein receptor-related protein (LRP-1) in the capillaries responsible for clearance of β-amyloid oligomer (Hartz *et al.*, 2010). It may well be more difficult to send therapeutic molecules across the BBB of AD patients since many of the receptors responsible for endocytosis and transcytosis are downregulated (Kang *et al.*, 2000; Steen *et al.*, 2005; Yin *et al.*, 2014; Yu *et al.*, 2014).

Approach to overcome the blood-brain barrier

A great deal of work has been done on targeting drugs to the brain and crossing physical barriers such as the BBB or the nasal mucosa but the current strategies lack specificity for the target cells; capillary endothelial cells. Recent findings indicate that using anionic surfactants and cationic stabilizers in the production of poly(butylcyanoacrylate) (PBCA) nanoparticles (NPs) can improve their ability to cross the BBB (Voigt *et al.*, 2014). Thus, non-ionic or anionic surfactants can increase or limit the delivery of drugs from a carrier to the brain. Furthermore, these new delivery systems need to be more specific for brain tissue. Surfactants such as polysorbate 80 are not very specific for brain endothelial cells despite several reports of increases in BBB crossing. Recent strategies for increasing the selective permeability of the BBB are also not specific for brain endothelial cells (Jiang *et al.*, 2014; Soliman *et al.*, 2014). Jiang *et al.* have developed NPs made of 2-deoxy-D-glucose functionalized poly(ethylene glycol)-copoly(trimethylene carbonate) for targeting brain tumors. The coated 2-deoxy-D-glucose interacts with the glucose transporter in BBB endothelial cells (Jiang *et al.*, 2014). Soliman *et al.* have also recently developed a chitosan NP conjugated to hydrocaffeic acid so as to increase its adhesion to the mucosa (Soliman *et al.*, 2014). The hydrocaffeic acid dramatically increased the permeability of the NPs and their attachment to the rabbit's small intestine mucosa, while their physico-chemical properties such as the size, bovine serum albumin (BSA) encapsulation capacity and cell viability were not affected (Soliman *et al.*, 2014).

Modern delivery systems using surface modifications to target the brain are designed to interact with specific endothelial receptors on brain capillaries and act as Trojan horses (Rempe *et al.*, 2014). There are four main receptors on BBB endothelial cells that have been used to

deliver drugs. One is the low-density lipoprotein receptor (LDLR), another is the transferrin receptor, the third is the EGF receptor and the fourth is the IGF receptor (Kreuter, 2013, 2014; Pardridge, 2007; Yi *et al.*, 2014). One of themost frequently employed strategies is the use of transferrin or transferrin-derivedmolecules (Ding *et al.*, 2014; Kamalinia *et al.*, 2013; Kuo et Chou, 2014; Pang *et al.*, 2011). For instance, Pang *et al.* (2011) prepared transferrin-coated polymersomes made of poly(ε-caprolactone), monomethoxy-polyethyleneglycol (PEG) and hydroxy-polyethyleneglycol-maleimide. They found that the transferrin coating did not affect the physical surface properties (size and zeta-potential) of NPs while it significantly increased the brain uptake. Similarly, Yu *et al.* (2013) developed a PEG-poly(lactic-co-glycolic acid) (PLGA) NP conjugated to lactoferrin and demonstrated that the lactoferrin resulted in significantly more 6-coumarin accumulating in the brain tissue than did injecting the NP alone. More recently, Kuo and Chou (2014) have developed an NGF-loaded liposome containing transferrin and RMP-7. RMP-7 is an adjuvant that increases passage across BBB cells (Boddy et Thomas, 1997). The combination of RMP-7 and transferrin significantly increased the permeability of NGF across human brain microvascular endothelial cells without any toxic effect. Ding *et al.* (2014) have produced iron oxide NPs (b10 nm) incorporated into liposomes with a transferrin shell and have shown that they are very stable over time and increase endothelial cell permeability.

Others have suggested using small transferrin-like peptides to facilitate NP production, reduce their immunogenicity and increase their stability. Li *et al.* (2013) used a phage display library to select a 12-amino acid peptide (Pep TGN) that specifically facilitated BBB crossing. This peptide was then conjugated to coumarin-loaded PEG–PLGA NPs. It targeted the coumarin to the brain significantly better than did the NPs alone. Liu *et al.* (2013) have also developed a drug delivery system made of PEG–PLA conjugated to 10-residue B6 peptides (CGHKAKGPRK) that have a strong affinity for the transferrin receptor. *In vivo* studies revealed that, as unconjugated NPs, the B6-conjugated were not cytotoxic. The B6-conjugated NPs were more widely distributed in the brain and accumulated less in other organs (kidneys, liver, heart and spleen) than did the NPs alone. Granholm *et al.* (1994) and Zhou *et al.* (2011) have proposed a strategy involving drug delivery via an antibody targeting the brain endothelial cell receptor (Albeck *et al.*, 2003; Granholm *et al.*, 1994; Zhou *et al.*, 2011), while Granholm *et al.* (1994)

used an NGF-conjugated monoclonal antibody OX-26, which targets the transferrin receptor, to increase BBB crossing. They showed that the antibody was essential for the accumulation of NGF in brain blood vessels. Albeck *et al.* (2003) obtained similar results using Fisher 344 rat basal forebrain cholinergic neurons. Zhou *et al.* (2011) have modified an anti-transferrin receptor IgG antibody by fusing an avidin protein to the C-terminus. This antibody interacts with transferrin, which then triggers transport across the BBB by endocytosis. The drug to be delivered must be biotinylated. The same group has attempted to use chimeric monoclonal antibodies targeting IGF receptor (IGFR), but this system failed to deliver the drug (Zhou *et al.*, 2012). This innovative strategy requires special consideration of IgG immunogenicity. More research is required to determine how these antibodies interact with cell receptors. However, there is published data showing the effectiveness of targeting IGFR to increase drug transport across the BBB. Kuo and Shih-Huang (2013) have produced anti-insulin monoclonal antibodies conjugated to solid lipid NPs and used them to deliver the chemotherapeutic drug Carmustin. BBB permeability was increased via insulin receptor-mediated endocytosis in a study using human brain-microvascular endothelial cells (Kuo et Shih-Huang, 2013).

LDLR is another endothelial cell receptor target used to decorate NPs. Pinzon-Daza *et al.* (2012) have developed PEGylated anionic liposomes with ApoeB100 peptides to target LDLR and transport Doxorubicin across the BBB. Zhang *et al.* (2013) have also developed PLA−PEG NPs decorated with a peptide recognized by LDLR and used them to specifically target brain endothelial cells; they observed a net increase in NP accumulation specifically in brain tissue. These new strategies are particularly interesting and could readily be used to deliver anti-AD drugs. This may well be the direction of future research on GF delivery systems.

2.10.3 Nanoparticles as growth factor delivery systems

The therapeutic molecules to be delivered intranasally need to overcome the natural clearance mechanisms such as the mucus layer, the nasal epithelium, which is rich in metabolic enzymes, the mucociliary apparatus and efflux transporters (Di Stefano *et al.*, 2011). A carrier is generally required to protect the therapeutic molecules in their journey across these natural barriers and to preserve their bioactivity. Little is known about the drug transport mechanisms involved in nose-to-brain delivery. The rate at which a non-cell membrane-like molecule traverses the nasal epithelial cells without targeting cell receptors is inversely proportional to its

molecular weight (Kissel et Werner, 1998). Thus, to increase the nose-to-brain delivery of GFs, the choice of material and the delivery enhancing strategies are both crucially important and cannot be neglected.

NPs are vehicles that can ensure the intranasal delivery of molecules to the CNS while providing adequate protection against massive clearance and denaturation (Giordano *et al.*, 2011; Nagpal *et al.*, 2013; Tam *et al.*, 2014). Nevertheless, there are reports that direct intranasal injection is more efficient than using NPs to cross the BBB. Dyer *et al.* (2002) demonstrated that a chitosan solution resulted in better insulin absorption than did chitosan NPs. A recent meta-analysis that evaluated the efficiency of the intranasal delivery of drugs targeting the brain revealed that delivery efficiency was not correlated with the physicochemical properties of the drug (Kozlovskaya *et al.*, 2014). Nevertheless, compounds attached to NPs or hydrogels and delivered intranasally appear to be transported more efficiently than did those in solution. More studies are required to clarify this point, since NPs have many advantages, including drug stability and sustained release.

Four types of NPs are commonly used and seem to have beneficial properties. Those made of natural polymers such as chitosan, those made of synthetic polymers like PLA, PLGA or PBCA, lipid-based NPs and those made of metals like iron or gold (Blasi *et al.*, 2007; Feng *et al.*, 2012; Nagpal *et al.*, 2013; Prades *et al.*, 2012; Shevtsov *et al.*, 2014; Wohlfart *et al.*, 2011). NPs have many features that ensure optimal delivery despite the fact that they may have inferior absorption and permeation properties. NPs can protect GFs against denaturation and proteases and provide a controlled, sustained delivery. GFs such as BMPs can be very sensitive to denaturation in the blood. The half-life of BMPs in the circulatory system of rodents is about 16 min, while it is 6–7 min in non-human primates (Poynton et Lane, 2002).

The NPs that are engineered to deliver molecules to the brain should be:

- Biocompatible and biodegradable (degradation metabolites should have little or no toxicity in the brain or the blood stream and should not accumulate in organs)
- Sterilizable
- Particle size of few hundred of nm
- Good encapsulating efficiency and stability during production

- Capable of encapsulating more than one GF and thus modulate releasing profiles

- Able to control and sustain the delivery of GFs and have a high brain/blood partition ratio

- Ensure the stability and bioactivity of the GFs during delivery.

The use of carriers like NPs also allows the design of simultaneous or sequential GF delivery devices. These have been used several times for other tissues such as bone (Lauzon, Bergeron, *et al.*, 2012). NPs are particularly interesting since many GFs can be used synergistically. For instance, Wang *et al.* (2013) have developed double-core NPs made of PLGA and poly(Sebacic acid) imbedded in a hyaluronan hydrogel to deliver EGF and EPO for treating strokes, thus highlighting the fact that such strategies can be applied to the brain. Viral particles can also be delivered into the brain tissue either alone or coupled with metallic NPs (Hashimoto et Hisano, 2011; Idema *et al.*, 2011). Those viral vectors can be used to deliver genes encoding for GFs (Giacca et Zacchigna, 2012). For instance, Idema *et al.* (2011) have shown that green fluorescence protein (GFP)-adenoviral particles (70–90 nm) can be injected successfully using convection-enhanced delivery and accumulate in the brain similarly as did iron NPs. Kiyota *et al.* (2011) injected stereotaxically adenovirus encoding bFGF in an AD-mouse model and have observed an increase in cognitive function and clearance of fibrillary β-amyloid peptides in the hippocampus. Another interesting strategy would be to use virus-like particles as vaccines (see review (Zhao *et al.*, 2014)). For instance, Chakerian *et al.* (2006) have applied this strategy by using human papillovirus-based particles conjugated to β-amyloid peptides in the context of AD immunotherapy and have shown a good antibody response against β-amyloid peptides without concomitant T-cell overactivation. However, even if gene therapy or virus-based vaccines are other innovative therapeutic approaches used to increase the presence of GFs or develop antibodies against therapeutic AD targets in the brain, this review will focus specifically on protein delivery.

Chitosan-based nanoparticle GFDS

One of the natural polymers most commonly used to deliver therapeutic molecules to the brain is made of chitosan. This polymer is produced by the deacetylation of chitin and has been used for tissue engineering and targeting GFDS to the brain (Nagpal *et al.*, 2010, 2013) and bone (Bergeron *et al.*, 2012; Lauzon, E. Bergeron, *et al.*, 2012). Chitosan stimulates only a

small immune response in humans, has mucoadhesive properties and interacts with the cell membrane to ensure optimal delivery (Aspden *et al.*, 1997; Fazil *et al.*, 2012; Kreuter, 2001; Nagpal *et al.*, 2010; Sarvaiya et Agrawal, 2015). Most chitosan NPs are synthesized by the ionotropic jellification process. They can be produced under normal conditions in a wet chemical environment (Aktaş *et al.*, 2005; Alam *et al.*, 2012; Nagpal *et al.*, 2013; Vila *et al.*, 2004). These reaction conditions are important since normal temperature, pressure and a wet environment all reduce the risk of GF denaturation during encapsulation. This method produces NPs, using the natural cationic properties of chitosan. A chitosan solution forms electrostatic bonds in an anionic solution, such as tripolyphosphate (TPP) under defined conditions, resulting in a precipitate of NPs. Their size depends on the degree of acetylation of the chitosan itself, the concentration of the anionic and cationic solutions and the speed of mixing (Abdel-Hafez *et al.*, 2014; Fernández-Urrusuno *et al.*, 1999; Xu et Du, 2003). The NPs usually obtained with this method are 50–400 nm in diameter, depending on the reaction conditions (Abdel-Hafez *et al.*, 2014; Agnihotri *et al.*, 2004). Chitosan NPs with a diameter of 300 nm permeate into the Madin–Darby canine kidney cell line (MDCK) most rapidly. Smaller particles (<300 nm) were more toxic on MDCK cells because they trigger massive endocytosis (Hombach et Bernkop-Schnurch, 2009). However, recent studies have shown that particles with a diameter of up to 64 nm can diffuse within the brain parenchyma once the BBB has been crossed (Salegio *et al.*, 2014; Thorne et Nicholson, 2006). NPs that are too voluminous (>300 nm) might have limitations moving along brain tissue. Perhaps the optimal size should be reconsidered to ensure optimal distribution to the region affected by the disease.

There are several reports on the efficiency of chitosan NPs for the intranasal delivery of drugs that are FDA-approved for treating AD such as Rivastigmine (Fazil *et al.*, 2012; Nagpal *et al.*, 2013). Fazil *et al.* (2012) studied the kinetics of Rivastigmine encapsulated in ~160 nm chitosan NPs into the brains of Wistar rats. The *in vitro* release kinetics indicated a diffusion-based mechanism, while *in vivo* experiment showed better drug retention in brain tissues than when the pure drug in solution was injected. Nagpal *et al.* (2013) also used chitosan NPs loaded with Rivastigmine and showed that coating them with Tween-80 reversed amnesia in Swiss albino mice more efficiently than did chitosan particles with no coating. However, using coated or uncoated NPs resulted in a biphasic release that was slower than that of Rivastigmine alone.

The biphasic profile could have occurred because a dialysis membrane was used in these release kinetic experiments and the therapeutic molecule itself diffused through this particular membrane (Nagpal *et al.*, 2013) .

Despite the great potential of GFs for treating AD, very few studies have been conducted on their entry into the brain and most of those that have been published have used chitosan solutions rather than NPs. GFs like BMP-2 (Lai *et al.*, 2013) and bFGF (Tang *et al.*, 2010) can be efficiently encapsulated into chitosan-based nanocapsules that provide a sustained, slow release. Vaka *et al.* (2012) showed that BDNF in a chitosan solution (0.25% w/v) permeated into the brains of Sprague Dawley rats about 13-times faster than did BDNF alone. Similarly, Feng *et al.* (2012) found that the intranasal delivery of bFGF in a spray solution containing chitosan was much better than the intravenous injection of bFGF; it produced dramatic increases in the brain/serum bFGF concentration ratio and acetyltransferase activity, while significantly decreasing memory impairment. Thus chitosan seems to be a promising material for carrying therapeutic GFs across the BBB. Studies are now needed to understand just how NPs facilitate GF delivery.

Synthetic polymer-based GFDS

The synthetic polymers most commonly used for delivering drugs to the brain are PLGA and PBCA (Wohlfart *et al.*, 2011). Most PLGA-based delivery systems are produced using a water/oil/water double emulsion (Fredenberg *et al.*, 2011). PLGA has been widely used to encapsulate GFs because of its high encapsulation efficiency (42% to 100%) (Kirby *et al.*, 2011). The profile of drug release from PLGA polymers is pseudo-first order, with an initial burst followed by a sustained zero order release. This profile is caused by the slow breakdown of the polyester polymer into acidic residues; creating an acid micro-environment that auto-catalyzes further hydrolysis thus driving the mass transfer (Siepmann *et al.*, 2005). The acidic micro-environment affects the surrounding tissues. The kinetics of PLGA microparticle breakdown are well documented (Fredenberg *et al.*, 2011). The shape and the ratio of lactic/glycolic monomers can be tuned to modify the degradation rate and thus provide a safe environment (Fredenberg *et al.*, 2011). PBCA NPs are also used to help drugs cross the BBB (Kreuter, 2001; Rempe *et al.*, 2011). They are mostly produced using a two-phase (aqueous/oil) micro-emulsion (Reimold *et al.*, 2008; Voigt *et al.*, 2014) or anionic polymerization (Kreuter *et al.*, 2003;

Kurakhmaeva *et al.*, 2009; Olivier, 2005; Kumar, *et al.*, 2008). PBCA is a good GF delivery carrier because it is biocompatible, biodegradable and has no toxic metabolites (Kreuter, 2001; Voigt *et al.*, 2014). PBCA NPs also temporarily disrupt the BBB, which facilitates their entry into the brain parenchyma (Rempe *et al.*, 2011), while PBCA NPs coated with polysorbate 80 undergo endocytosis and transcytosis (see review (Wohlfart *et al.*, 2012)).

These NPs are used to treat AD (Joshi *et al.*, 2010; Wilson, Samanta, Kumar, *et al.*, 2008). Joshi *et al.* (2010) used Rivastigmine encapsulated in PLGA or PBCA NPs with a diameter of about 100 nm. The *in vitro* rate of drug release from PLGA NPs (30% released after 70 h) was slower than the release from PBCA NPs (40% released after 70 h) and its drug encapsulation properties were better than those of PBCA NPs. Both types of NP have pseudo-first order release profiles indicating diffusion plus erosion-controlled delivery. However, intravenous injection experiments showed that both delivery systems produced similar increases in the learning and memory capacities of scopalamine-induced amnesic mice (Joshi *et al.*, 2010).

The synthetic polymer can also be used to encapsulate and deliver GFs to treat brain diseases like AD. Several studies have demonstrated that they efficiently encapsulate neurotrophins (NGF, BDGF and GDNF) (Aubert-Pouëssel *et al.*, 2004; Garbayo *et al.*, 2008, 2009; Joshi *et al.*, 2010; Kurakhmaeva *et al.*, 2009; Wang *et al.*, 2014). Jollivet *et al.* (2004) developed PLGA microparticles (size ~23 μm) to encapsulate GDNF. *In vitro* release experiments showed an initial burst release followed by sustained release for more than 40 days. They also showed that these microparticles increased the sprouting of doparminergic neurons in Parkinson model rats (Jollivet *et al.*, 2004). However, the first order release profile after the initial burst release was not only caused by drug adsorption, but mostly due to erosion of the polymer as stated above. Aubert-Pouëssel *et al.* (2004) obtained similar results using rat ventral mesencephalon cells. Garbayo *et al.* (2008, 2009) used the same polymer and GF and obtained similar release kinetics. They also showed that GDNF-PLGA microparticles (size ~8 μm) caused PC12 cells (neurite outgrowth) to differentiate after 7 days whereas GDNF alone did not (Garbayo *et al.*, 2009). There is also evidence that NGF can be successfully incorporated into synthetic polymers to target the brain. Kurakhmaeva *et al.* (2009) used PBCA NPs as a carrier for NGF and showed that adsorbed NGF readily passed through the BBB and significantly reduced neurotoxin-induced Parkinson's disease in mice. Finally, bFGF has been incorporated

into PLGA particles and delivered across the BBB in order to treat AD. Zhang *et al.* (2014) produced poly(ethylene-glycol) (PEG)-conjugated PLGA NPs of about 105 nm diameter to deliver bFGF to the brain via the nasal route. They showed that PEG–PLGA NPs facilitated the transport of bFGF across the BBB, decreased β–amyloid senile plaques, and increased the drug brain/blood distribution ratio as well as the learning capacity of rats. These results indicate that synthetic polymers with or without surface modifications are suitable for delivering GFs to the brain.

Lipid-based delivery systems

Lipid-based systems are more and more frequently used to deliver GFs to the brain. As reviewed by Blasi *et al.* (2007), lipid NPs are almost nontoxic and have a great drug capacity in addition to being easily scalable in terms of industrial production. However, recent studies have shown that lipid NPs accumulate in the mouse brain parenchyma (experiment for over 24 weeks), which increased neuroinflammation, caspase-1 microglia activation and neurovascular damage. These adverse effects are greatly reduced by PEG-ylation of the particles (Huang *et al.*, 2013). Thus particular attention should be paid to avoid any of these adverse effects in *in vivo* studies. Some results also indicate that AD drugs like Rivastigmine can be successfully encapsulated into liposomes and delivered to the brain. Ismail *et al.* (2013) showed that Rivastigmine encapsulated in liposomes (size ~68 nm) and injected into rats subcutaneously provided better results in terms of memory improvement and learning than did Rivastigmine injected alone.

The two main forms of lipid-based NP systems are solid lipids and liposomes. Solid lipid NPs are currently made by micro-emulsion or high pressure homogenization (Blasi *et al.*, 2007). These NPs are more stable than liposomes since they remain solid at body temperature. However, the operating temperature and the type of lipid used should be chosen carefully since they can drastically affect both the size and the stability of the NPs. Angelova *et al.* (2013) used PEG-ylated-monolein/eicosapentaenoic acid/α−tocopherol lipid NPs and cryo-transmission electron microscopic and small-angle X ray scattering images to evaluate the structural features associated with protein entrapment. They found that BDGF could be efficiently inserted into these lipid NPs without affecting the stability of their structure unlike other proteins such as chemotrypsinogen A and histone H3 which are subjected to aggregation and affect the stability

of the nanostructure. Thus the net superficial electric charge at the surface of the GF at physiological pH and the concentration needed to be pharmaceutically relevant are crucial when selecting the material for the NP. The diffusion coefficient of lipid based NPs can be significantly affected by the amount of surfactant used in the composition (Siepmann et Siepmann, 2011).

The lipid-based NPs seem to be very well tolerated by the body. Blasi *et al.* (2013) demonstrated that cetylpalminate solid-lipid NPs coated with polysorbate 80 and produced by high pressure homogenization were very stable over time, had little toxic effect on the rat brain and were effectively endocytosed/transcytosed by the BBB endothelial cells. Dhawon *et al.* (2011) also found that the kinetics of querceptin release from these solid-lipid NPs (<100 nm) *in vitro* had a diffusion controlled delivery profile. Lipid-core NPs are also promising delivery systems for drugs targeting β-amyloid peptide aggregates (Bernardi *et al.*, 2012; Frozza *et al.*, 2013). Frozza *et al.* (2013) have developed a lipid-core NP made of poly(ε-caprolactone), carpylic triglyceride and sorbitan monostearate loaded with trans-resveratrol (neuroprotective against β-amyloid-induced neurotoxicity) and showed that delivery with this system more efficiently increased the drug concentration inside rat brains (Wistar rat) than did the drug alone.

Other recent studies have shown that lipid-based NPs are suitable for encapsulating and delivering GFs for treating AD across the BBB. Hanson *et al.* (2012) encapsulated GDF-5 (BMP-14) in a lipid micro-emulsion composed of olive oil and phosphatidylserine and showed that this neutral pH micro-emulsion delivered GDF-5 more efficiently than did direct injection with an acid buffer. bFGF has also been encapsulated in a gelatin nanostructure lipid carrier (~143 nm) and injected intranasally in a hemiparkinsonian mouse model (Zhao *et al.*, 2014). This resulted in more bFGF in the olfactory bulbs than did injecting bFGF alone, and did not damage the nasal mucosa. The Parkinson symptoms of the mouse model were decreased and functional recovery enhanced. NGF encapsulated in liposomes also crosses human brain-microvascular endothelial cells and protects SK-N-MC human neuroepithelioma brain cells against β-amyloid-induced neurotoxicity (Kuo et Chou, 2014).

Metal-based nanoparticle GFDS

Metal-based NPs have recently been used to transport drugs into brain tissue. These particles seem to be promising vehicles for anti-AD drugs. Hsieh *et al.* (2013) used gold NPs coated with insulin fibrils in a β-amyloid mouse model and found that gold NPs impaired fibril formation. Prades *et al.* (2012) used a more sophisticated model; LPFFD peptides conjugated to gold NPs to treat AD. LPFFD peptides are β-sheet breakers that can disrupt β-amyloid plaques when subjected to microwave irradiation (Araya *et al.*, 2008). Grafting the transferrin-recognized sequence THRPPMWSPVWP onto the NPs also increased their ability to cross the BBB. *In vitro* survival studies on rat astrocytes and bovine brain endothelial cells showed no apparent toxicity. However, particles did accumulate in the rat brain parenchyma. The iron-based magnetic NPs (<100 nm) developed by Pilakka-Kanthikeel *et al.* (2013) can adsorb BDNF as a GFDS strategy and could be used to target specific areas of the brain using magnetic resonance imaging. The toxicity of particles for peripherical mononuclear blood cells *in vitro* is low. They cross the BBB without causing irreversible damage and can transport BDNF into SK-N-MC neuroblastoma cells. However, protein adsorption at the surface of the NP as a delivery strategy should consider the fact that this non-specific affinity between adsorbed BDNF molecules and magnetic NPs can change with the local *in vivo* micro-environment. This, in turn, could significantly impair drug delivery. Also, they conducted no *in vivo* studies to evaluate the effect of the non-specific adsorption of other proteins from the blood or the accumulation of NPs in the brain and other organs. Similarly, Shevtsov *et al.* (2014) recently developed EGF-conjugated dextran-coated super paramagnetic iron oxide NPs (size ~ 50nm) for targeting brain tumors so as to increase magnetic resonance imaging contrast. These NPs are apparently non-toxic and accumulate in the rat brain without causing any behavioral impairment. However, they were created to accumulate at a specific site and may not be a suitable delivery vehicle for AD drugs. Nevertheless, further studies should be conducted to determine the stability of GFs during delivery, how these NPs accumulate in the body and their long term toxicology. They seem to be promising potential GF carriers.

2.11 Mathematical modeling of CNS-directed drug delivery systems

Mathematical models of drug release can provide considerable information. A reliable, precise and predictive mathematical model must be firmly based on the measured kinetics and physical characteristics of the system. Knowing how the therapeutic molecules are released can help build both explanatory and predictive models that will minimize the number of experiments required and enable realistic simulations to be made. Local drug delivery can be driven by several types of transport phenomena that depend on the physical–chemical properties of the drug (charge, size, solubility, etc.) and the carrier, and also on the local environment (pH, temperature, enzyme activity, etc.) (Fu et Kao, 2010; Mehdipour et Hamidi, 2009; Wolak et Thorne, 2013).

There are not many examples of mechanistic mathematical frameworks designed to understand the delivery of GFs by NPs to the brain apart from traditional pharmaco-kinetic/pharmaco-dynamic studies (PK/PD) (Alavijeh *et al.*, 2005; de Lange, 2013; Siepmann *et al.*, 2006). However, the purpose of this section is to give insights about the mass transport phenomena that may occur during the delivery of GFs by the systems currently used and how to model them. In addition, in contrast to static delivery systems where only the release of the GFs has to be considered, the NPs can move along the body and have to face many barriers before reaching the brain, which create more challenges in the mathematical representation of delivering. The next two sections discuss the different transport phenomena that can be encountered from the injection site to the brain tissue in terms of NPs and GF concentration. The first section describes the evolution of the concentration of the NPs from the intranasal injection up to the brain tissue, whereas the second section shows the mechanisms involved for the release of the GFs from the NP itself. Those two sections are linked together as the important information to follow is the NP concentration and the GF concentration inside them along their journey to the CNS. Moreover, the mathematical representation has both time and spatial dimensions and is more mechanistic, which differs from normal PK/PD approaches even if the transport phenomena and the concept could be used in conjunction (see Tableau 2-3 for mathematical symbol definition). The modeling we propose in this paper is required to facilitate the design of a proper delivery system, whereas PK/PD analysis might be required to evaluate

the accumulation and kinetics of organ absorption since GFs can have an effect on many cell types.

2.11.1 Mass transport of nanoparticles from injection site toward the brain

Unlike body tissues such as bone, where the delivery system can probably be applied directly to the site of interest, modeling the delivery of intravenously or intranasally injected NPs to the brain has several specific challenges. The delivering carrier must pass through several biological barriers, and may be subject to enzymatic degradation throughout its journey to the brain (Grassi *et al.*, 2011; Siepmann *et al.*, 2006; Weiser et Saltzman, 2014). General mathematical frameworks have been proposed to describe the major mass transport phenomena that must be considered (see review (Weiser et Saltzman, 2014)). NPs are prone to diffusion within tissues, may interact with cells via specific receptors or become adsorbed onto cell walls, may be degraded by enzymes or eliminated from the body, or be subjected to convection (blood stream, cerebrospinal fluid). Figure 2-7 and Figure 2-8 show the mass transport features of injected NPs within the body and the phenomena that must be considered (see review (Grassi *et al.*, 2011)).

Mass transport of nanoparticles into the nasal cavity of the brain capillaries

The mechanisms of transport of NPs and therapeutic molecules inside the nasal cavities are not yet fully understood. However, it is well known that therapeutics can reach the brain via three different ways: (1) trigeminal nerves, (2) the olfactory region, and (3) through the brain capillaries (Casettari et Illum, 2014; Pardeshi et Belgamwar, 2013). Nasal cavities are estimated to be ~12 cm long with a contact area of about 150 cm^2 (Mistry, Glud, *et al.*, 2009).

The trigeminal nerve is the most important nerve in the cranial region with two entry sites in the olfactory region (cribriform plaque and the anterior foramen lacerum) which lead to the caudal and rostral zone of the brain (Pardeshi et Belgamwar, 2013). There is little information about the transport of molecules (GFs) along this entry site. However, Thorne *et al.* (2004) have shown that radio-labeled IGF-1 injected intranasally could accumulate in the trigeminal region and the olfactory bulb. However, NPs having a greater size than GFs are not likely to use this route as it is the case for the olfactory region. In fact, the olfactory region covers approximately 10% of the contact area of the nasal cavities (Casettari et Illum, 2014).

Therapeutics using the delivery route have to bypass the layer of epithelial cells via passive or active transport mediated by specific receptors (Pardeshi et Belgamwar, 2013). Molecules can then be transferred from endothelial cells to olfactory neurons via endocytosis or pinocytosis and move along the axon up to the olfactory bulb (Illum, 2000). However, since axon diameter is about 100–200 nm, the transport of NPs within the same size range might be highly limited (Pardeshi et Belgamwar, 2013). Thus, the NPs injected in the nasal cavities are more likely to reach the brain via brain capillaries, but still have to cross the epithelial cell layer and other natural barriers.

NP transport from the nose to the capillaries faces many hurdles as the body shows natural barriers. Injected NPs are first transported through air stream into the nasal cavities. The first barrier encountered is the nose mucus. The mucus is composed of 2 layers; a viscous gel-like layer (2–4 μm thick) sited on a less viscous layer (3–5 μm) (Mistry, Stolnik, *et al.*, 2009; Pardeshi et Belgamwar, 2013). The role of the mucus is to capture and filter impurities and direct them toward the stomach for further degradation. This is achieved by the presence of oscillating cilia with a commune frequency of ~1000 strokes/min resulting in a moving mucus layer at a speed of ~5 mm/min with a variation from 0.5 to 24 mm/min (Mistry, Glud, *et al.*, 2009; Pardeshi et Belgamwar, 2013). The mucus is composed of water (95%), mucin (2%), salts (1%) and proteins such as enzymes (lysozymes, lactoferrins, cytochrome p450, aldehyde dehydrogenase, peptidases and proteases) that can affect the integrity of both GFDS and GFs (Brogan, 1960; Kaliner *et al.*, 1984). The mucus is considered to be a viscoelastic fluid and shows high viscosity variations in function of its composition and shear stress (up to 2000 times more viscous than water) rendering the modeling very challenging (Lai *et al.*, 2009). The second barrier that NPs face is the epithelial cell layer itself, which has tight junctions. Some adjuvants such as chitosan have been used to temporarily destabilize the tight junction creating openings of ~15 nm insufficient for NPs to cross (Anderson, 2001). The transport of NPs across the layer is thus limited to active transport followed by transcytosis (Casettari et Illum, 2014; Johnson et Quay, 2005; Mistry *et al.*, 2009; Mistry *et al.*, 2009). NPs face many transport phenomena such as diffusion, convection and degradation via enzymatic activity and interaction with cell receptors. Figure 2-7 below shows the natural barriers crossed by the NPs in the nasal cavities and the different transport phenomena that might be encountered.

Once the NPs have been injected in the nose, they are transported by the turbulent air stream up to the nasal cavities, where they can further interact with the outer mucus layer. Hahn *et al.* (1994) have shown that the movement of therapeutics or aromatic molecules in the nasal cavities could be mathematically represented by the following equation:

$$\frac{\partial C_{NP}}{\partial t} = -K_A \sigma \left(C_{NP} - C_{NP\,sat} \right) - v_A \nabla C_{NP} \tag{2-1}$$

Where the variation of the NP concentration as a function of time depends on the air stream velocity and a pseudo-diffusion part proportional to the mass transfer coefficient (K_A), the ratio between the available exchange surface of the nasal cavity over its perimeter (σ) and the saturation concentration of NP above the boundary layer.

The transport of the NPs into the mucus layers (considered as one layer for the development of the models) has been modeled as a pure diffusion process (Kurtz *et al.*, 2004; Yang *et al.*, 2007). However, considering the particularity of the nasal tissue, other phenomena might be considered such as the convection induced by the mucus displacement and the possible enzymatic degradation. In addition, since the mucus is viscoelastic, the determination of velocity gradient required the solving of Navier–Stokes equations. The mechanistic representation of those phenomena can be described by the following set of equations:

$$\frac{\partial C_{NP}}{\partial t} = D_{NPM} \nabla \cdot (\nabla C_{NP}) - v_M \nabla C_{NP} - k_{EM} C_{NP} \tag{2-2}$$

$$-D_{NPM} \left. \frac{\partial C_{NP}}{\partial x} \right|_{x_0} = K_{AM} \left(C_{NP} - C_{NP\,sat} \right) \big|_{x0} \tag{2-3}$$

$$-D_E \left. \frac{\partial C_{NP}}{\partial x} \right|_{x_1} = k_{I\&E} C_{NP} - D_{NPM} \left. \frac{\partial C_{NP}}{\partial x} \right|_{x_1} \tag{2-4}$$

Eq. 2.2 shows that the variation of NP concentration is a function of diffusion, convection and degradation represented by k_{EM}. Eq. 2.3 shows the boundary conditions where the flux of the NPs from the air stream entering the mucus layer is proportional to the saturation concentration and a partition coefficient whereas Eq. 2.4 shows the transport of the NPs into the epithelial cell layer depending on diffusion and receptor mediated transport ($k_{I\&E}$).

NP

NP degraded

Cell receptor

Tight junctions

Nasal epithelial cell

Cilia

Ciliary movement

nasal cavity

← Gas flow direction

Gas flow direction

B

A

Lumen of nasal cavity

$x0$

x

z

← Mucus moving front (Speed ~ 5 mm/min)

C

F

E

Mucus layer #1 2-4 µm

$z1$

D

$z0$

G

Mucus layer #2 3-5 µm

$x1$

H

I

Epithelial cell layer

Basal lamina

Endothelial cell layer of the BBB

A Diffusion of NPs in the gas layer above the mucus

B Convective transport of NPs in the gas layer above the mucus

C Diffusion of NPs from the gas to the mucus layer

D Diffusion of NPs inside the mucus layer

E Convective transport of NPs caused by the ciliary movements

F Enzymatic degradation of NPs inside the mucus layer

G Interaction of NPs with the membrane receptors of the epithelial cell layer

H Endocytosis or transcytosis of NPs inside the epithelial cell layer

I Enzymatic degradation of NPs inside the epithelial cell layer

Figure 2-7 : Natural barriers crossed by NPs and the associated mass transport phenomena from the nasal cavities to the brain capillaries

Mass transport of nanoparticles from the brain capillaries to the brain parenchyma

Brain capillaries are known to be the major access route of therapeutics to the brain with a surface area of ~12 m^2 and a total length of ~650 km (Misra *et al.*, 2003). The injected NPs must reach brain capillaries, from which they may be cleared by convection ($\upsilon_B \nabla_{CNP}$) created by blood flow (Grassi *et al.*, 2011). The average blood speed in capillaries is estimated at few mm/s with a capillary diameter ~8−10 µm (Desjardins *et al.*, 2014; Fedosov *et al.*, 2014; Fedosov *et al.*, 2014). The blood itself is a viscoelastic fluid, of which the rheological properties depend strongly on the hematocrit. Figure 2-8 summarizes the major mass transport that can be encountered during the transport of NPs from the brain capillaries to the brain tissue. The transport of NPs in the blood can be described by the following equation:

$$\frac{\partial C_{NP}}{\partial t} + v_B \nabla C_{NP} = D_B \nabla^2 C_{NP} - k_{EB} C_{NP} \qquad (2\text{-}5)$$

With the given boundary condition at the surface of the capillary in the radial direction (Eq. 2.2):

$$-D_{BBB} \frac{\partial C_{NP}}{\partial r}\bigg|_{wall} = k_{ECW} C_{NP} - D_B \frac{\partial C_{NP}}{\partial r}\bigg|_{wall} \qquad (2\text{-}6)$$

Here the term $k_{ECW} C_{NP}$ describes the NPs eliminated across the blood capillary walls due to interaction with non-specific and specific membrane receptors as shown by the boundary conditions. This term must be as large as possible for NPs targeting the brain to ensure maximum accumulation, which is why it is important to target specific brain endothelial cell receptors.

The NPs then have to move within the capillary endothelial cells in order to cross the BBB by active or passive transport or via specific cell membrane receptors. They may be degraded by enzymatic degradation or metabolized inside the endothelial cells, which can be described by an equation for pure diffusion with boundary conditions similar to those of Eq. 2.2. Those NPs that reach the brain may be transported into the extracellular space (ECS), interact with their environment, be captured by cells, diffuse or be transported by movement of the cerebrospinal fluid. All these elements must be considered when building the overall model of NP distribution. Nicholson (1995) and Krewson and Saltzman (1996) have shown that drugs and GFs that enter tissues like the brain are in a multiphase environment composed of intracellular and extracellular spaces. The NPs may diffuse or be transported by convection (osmotic pressure (Buishas *et al.*, 2014) and cerebrospinal fluid movement (Saunders *et al.*, 1999)) in the ECS, interact with cells and be eliminated. The elimination of NPs can be described as a first order reaction (k_{ECS}, k_{ICS}) as shown by Eq. 2.7 (for more details see review (Weiser et Saltzman, 2014)).

NANOPARTICLES MASS TRANSPORT

Legend:
- NP
- Degraded NP
- Cell receptor
- Tight junctions
- Brain capilary epithelial cell
- Glial cell
- Astrocyte
- Neuron

Side labels: Capillary, BBB, Brain tissue

Right-side annotations:
- Diffusion **A**
- Convection **B**
- Elimination by endothelial cell surface (interaction or other transport mechanisms) **C**
- Diffusion **D**
- Convection (osmotic pressure) **E**
- Enzyme degradation and metabolism **F**
- Diffusion in the ECS **G** and ICS **H**
- Convection (cerebrospinal fluid flow) **I**
- Cell adsorption **J** and degradation **K**

Figure 2-8 : Natural barriers crossed by NPs and the associated mass transport phenomena form the capillaries to the brain tissue. (ECS = extracellular space, ICS = intracellular space). Brain cells adapted from Servier medical art (Servier.fr)

Once released into the brain tissue, several phenomena can influence NP transport within the brain itself, including diffusion, enzymatic degradation and elimination via the blood or cerebrospinal fluid, which modeling is rather difficult (Siepmann *et al.*, 2006). However, the reviews by Siepmann *et al.* (2006) and Wolak and Thorne (2013) indicate that drug transport within the brain can be represented by Fick's second law with an additional term to account for drug consumption and/or clearance. The pioneering studies of Nicholson *et al.* (1979, 1981, 1993) on diffusion inside the brain have shown that the diffusion of high molecular weight molecules or ions is hindered and have estimated the ECS tortuosity ($\tau = 1.55$) and void fraction ($\varepsilon = 0.2$), highlighting the challenges associated with drug modeling.

Any model of drug mass transport within the brain must include an accurate representation of brain morphology and porosity. The brain can be seen as a porous organ in which most diffusion occurs in the ECS since the particles and therapeutic molecules can travel within the brain via convection of the cerebrospinal fluid and interact and diffuse in the

parenchyma. Nevertheless, the ECS accounts for only 20% of the total brain volume, with an anisotropic distribution (Nicholson et Phillips, 1981; Siepmann *et al.*, 2006; Wolak et Thorne, 2013). The brain ECS fraction can change as a person ages or due to degenerative diseases, which further complicates modeling (Wolak et Thorne, 2013). Many attempts have been made to model how the ECM space available for drug convection varies across the brain, but the hydrodynamic radius of the GF is particularly important since the size of the ECS is estimated to be ~64 nm (Salegio *et al.*, 2014; Thorne et Nicholson, 2006). Other mass transport phenomena such as capillarity or osmotic force and interactions between NPs or drugs and the ECM, which might greatly affect diffusion, can occur in such small spaces (Siepmann *et al.*, 2006). It is therefore difficult to predict the brain distribution of NPs or drugs without *in vivo* experiments (Salegio *et al.*, 2014; Thorne et Nicholson, 2006). Wolak and Thorne (2013) examined the hydrodynamic radius of several GFs, including NGF (4.9 nm) and insulin (2.7 nm), and pointed out that the distance these GFs could penetrate from the cerebrospinal fluid into the brain tissue depends exponentially and inversely on their size. The mechanistic equation described by *Weiser et Saltzman* (2014) states that a drug is believed to interact with a multiphase environment (ECS, ICS and cell membrane) according to the equation that describes the mass transport of NPs in the brain (see Eq. 2.3):

$$\frac{\partial C_{NP}}{\partial t} + \frac{\delta}{\alpha^*} v_{ECS} \nabla C_{NP} = \frac{\delta}{\alpha^*} \nabla \cdot \left(\frac{D_{NP}}{\tau_{ECS}} \nabla C_{NP} \right) - \frac{\delta k_{ECS} C_{NP} + \varphi k_{ICS} P_{ECS:ICS} C_{NP}}{\alpha^*} \quad (2\text{-}7)$$

$$\tau_{ECS} = \frac{d_{NP}}{d_{ECS}} \quad (2\text{-}8)$$

where α^* is the total fraction of free NPs in all phases (ECS, intracellular space (ICS) and cell membrane), δ and φ are the volume fractions of the ECS and ICS respectively and $P_{ECS:ICS}$ is the partition coefficient of NPs between the intracellular and extracellular spaces.

The diffusion coefficient must take into account the tortuosity factor of the brain ECS (Eq. 2.7). This factor can be estimated from the ratio between the hydrodynamic radius of the NPs and the apparent radius of the ECS (~64 nm (Thorne et Nicholson, 2006)) as shown by Eq. 2.8. In addition, the last term on the right hand side of Eq. 2.7 is a global first order elimination term since it is difficult to measure experimentally either the partition coefficient or the interaction of NPs with the ICS. The convection flow in the ECS and the drug clearance can be estimated from the cerebrospinal fluid flow rate, which creates a sink effect (Saunders *et al.*,

1999). The mechanisms driving water and solute transport across the brain parenchyma, ECS and ventricles are the osmotic and transmembrane hydrostatic pressures. They can be described by the Starling oncotic hypothesis of capillaries causing convection movements (Buishas *et al.*, 2014).

Finally, we have to consider that the ECS of the brain is composed of many cell types: neurons, astrocytes and glial cells. All these cells can interact with the NPs and the therapeutic molecules diffusing from them. The total amount of NPs that interacts solely with neurons and more precisely with the neurons of interest is thus only a fraction of the NPs in the ECS. The amount of drug encapsulated within the delivery system should take these elements into account through pharmacokinetic experiments prior to *in vivo* studies. Future mathematical models of the delivery of therapeutics to the brain will involve powerful computational tools such as finite element or finite volume analysis software. New high resolution brain maps like BigBrain (Amunts *et al.*, 2013) will eventually be coupled with these programs. Their application will increase our understanding of mass transport and lead to better and more appropriate mathematical frameworks for predicting drug release.

Tableau 2-3 : Mathematical terms used

Symbol	Definition	Symbol	Definition
A_t	Surface area at a given time	γ	Kinetic rate for product formation determined empirically
α	Kinetic rate of enzymatic association from Freundlich adsorption isotherms	I	Mass transfer coefficient other than diffusion
α^*	Total fraction of free NPs in brain	K_a	Langmuir adsorption isotherm equilibrium constant
β_c	Fujita-type coefficient for solute	K_A	Partition coefficient of NPs at the interface air/nasal mucus
β_E	Fujita-type coefficient for enzyme	K_{AM}	Mass transport coefficient for NPs in the nasal cavities
β_P	Fujita-type coefficient for product of enzymatic degradation	k_2	Chemical reaction rate of product formation from enzyme degradation
β_w	Fujita-type coefficient for water	k_{ICS}	Rate of NP elimination in ICS
$C_{carrier}$	Concentration of carrier material	$k_{bulk\ erosion}$	Rate of bulk erosion
C_E	Concentration of enzyme	$k_{erosion\ 1}$	Rate of bulk erosion affecting the diffusion coefficient of solute
C_{ES}	Concentration of enzyme-substrate complex	$k_{erosion\ 2}$	Rate of surface erosion affecting the diffusion coefficient of solute
C_{GF}	Concentration of growth factor	k_p	Hydraulic permeability of polymer network

C_{GF-L}	Concentration of GF-ligand complex	k_1	Rate of enzyme/substrate reaction
C_P	Concentration of product from enzymatic degradation	k_{EB}	Rate of elimination of NPs from blood capillaries
C_S	Concentration of substrate subjected to enzyme degradation	k_{ECS}	Rate of elimination of NPs in ECS
C	Concentration of solute	k_{ECW}	Rate of elimination of NPs at the capillary wall
C_{NP}	Concentration of NPs	k_{EM}	Rate of elimination in the nasal mucus layer
$C_{NP_{sat}}$	Concentration of NPs at saturation in nose cavity	$k_{I\&E}$	Rate of elimination of NPs at the nasal epithelial cell wall
C_{Seq}	Initial Concentration of substrate	K_p	Osmotic bulk modulus
C_{Weq}	Concentration of water in completely swollen polymer matrix	M_0	Initial mass of polymer matrix
C_w	Concentration of water	M_∞	Initial mass of solute
$D_{C_{eq}}$	Diffusion coefficient of solute at equilibrium	M_a	Adsorbed mass of solute at a given time
$D_{E_{eq}}$	Diffusion coefficient of enzyme in solution	M_a^{max}	Maximum mass adsorbed of solute
D_E	Diffusion coefficient in endothelial cells	$M_{t,polymer}$	Mass of polymer at a given time
$D_{P_{eq}}$	Diffusion coefficient of product from enzyme degradation in solute	M_t	Mass of solute at a given time
$D_{W_{eq}}$	Diffusion coefficient of water in completely swollen polymer matrix	$M_{w\,polymer}$	Molecular weight of polymer at a given time
D_B	Diffusion coefficient of NPs in blood stream	η	Viscosity of the polymer network
D_{BBB}	Diffusion coefficient of NPs in the BBB	P	Product
D_C	Diffusion coefficient of solute	p	Pressure between the releasing media and the
D_P	Diffusion coefficient of product from enzyme degradation	φ	Volume fraction of the brain ICS
D_W	Diffusion coefficient of water	ρ_w	Density of water at a given temperature
D_{NPM}	Diffusion coefficient of NPs in the nasal mucus	r	Position in the radial direction
D_{C0}	Diffusion of solute in releasing media	S	Substrate
d_{ECS}	Hydrodynamic radius of the brain ECS	t	Time variable
d_{GF}	Hydrodynamic radius of GF	τ_{ECS}	Tortuosity factor of brain ECS
δ	Volume fraction of the ECS	u	Linear displacement of polymer chain
E	Enzyme	v_w	Velocity vector of water entering the polymer matrix
ES	Enzyme-substrate complex	v_A	Velocity vector of air entering nasal cavity
ε	Porosity of the polymer matrix	v_M	Velocity vector of nasal mucus
ε_{brain}	Brain porosity	x	Position in the x direction
G	Shear modulus of the polymer hydrogel	X	Edge of delivery system in the direction x

2.11.2 Modeling the delivery of growth factor from nanoparticles

The GFs carried by the NPs to the brain can be delivered from them as they evolve in the body. This delivery of GFs can be influenced by several mass transport phenomena as described by Figure 2-9 as they face different environments. We have reviewed several empirical and mechanistic mathematical models of GF delivery (Lauzon, Bergeron, *et al.*, 2012) and there are several other good reviews of drug delivery showing how it depends on the physical–chemical properties of the encapsulated drug and/or the type of mass transport phenomenon that is involved in both empirical and mechanistic mathematical models (Fu et Kao, 2010; Gures *et al.*, 2012; Siepmann *et al.*, 2005, 2006; Siepmann et Peppas, 2000; Siepmann et Siepmann, 2011). The phenomena can be mathematically addressed in order to follow the GF concentration inside NPs as they reach the brain tissue and are concomitant to the previous section. Diffusion, interactions, erosion and swelling are the main forces driving GF delivery. The development of a mechanistic model generally starts with Fick or non-Fickian diffusion, where the change in drug concentration over time depends on the concentration in space, to which additional terms can be added to account for the other important release mechanisms. For some material such as lipid-based delivery systems and especially solid–lipid NPs, pure diffusion is usually assumed (Gures *et al.*, 2012; Siepmann et Siepmann, 2011).

The preparation of NPs generally results in a distributed population of particle sizes that are mono- or poly-dispersed with ranges depending on the material and the experimental conditions, as is the case for chitosan NPs (Abdel-Hafez *et al.*, 2014; Agnihotri *et al.*, 2004). Population balance equations (PBE) could be used to understand the behavior of a whole population of NPs since the size and other characteristics might influence their mass transport. This mathematical technique has been used to model the aggregation of and changes in the size of solid–lipid NPs (Yang *et al.*, 2012) and the corona complex formation of protein on NPs (Darabi Sahneh *et al.*, 2013). These models are complex to solve and require numerical solutions such as the moment method, discretization or Monte-Carlo stimulations that are beyond the scope of this paper (for more information see (Ramkrishna, 2000)).

Another solution could be the use of a Weibull distribution to discretize in several subclasses the size distribution of NPs and solve the model for each of those subclasses. Grassi *et al.* have used this technique to model the drug release from swellable pyrrolidone

microparticles with great accuracy in respect to experimental results (Grassi *et al.*, 2000). We can, however, depict the mass transport phenomena that may be encountered in the release of drugs from NPs using a single NP with a mean size.
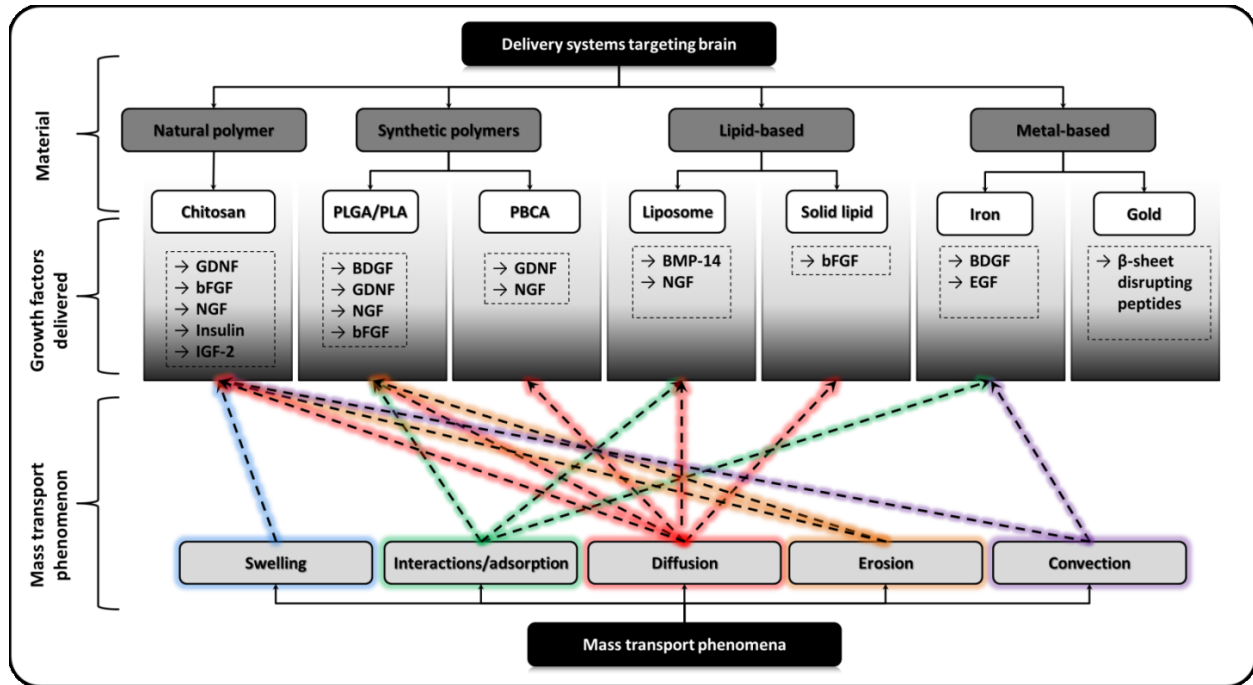
Figure 2-9 : Systems for delivering GFs to the brain and the mass transport phenomena involved

Interactions and adsorption/desorption

There are several examples of interactions between GFs and the material of the delivering system (Bergeron *et al.*, 2012; Lauzon, 2014; Tah *et al.*, 2014). GFs are proteins or peptides that have both local and overall net electric charges which can interfere with their diffusion. The spatial orientation can also dictate the importance of particular interactions that give access to more localized charges. Our work with collagen and chitosan hydrogels showed that pBMP-9 and the whole protein BMP-9 have very different release behaviors. BMP-9 (globular ~ 12 kDa) was released very quickly *in vitro*, within hours (Bergeron *et al.*, 2012), whereas the release of pBMP-9 (~2.5 kDa), which is mostly linear (Bergeron *et al.*, 2007), could last for several days (Lauzon, 2014). Bigger proteins should usually experience hindered diffusion since their size allows them to interact more with the fiber mesh of the delivering

system. However, we found the opposite, suggesting that the peptides and the material of the delivery carrier interacted (Lauzon *et al.*, 2014).

The isoelectric point of the GF is also very important as it provides information about possible attractive or repulsive interactions between the GF and its delivering carrier. BDNF (Tan *et al.*, 2012), NGF (Harper *et al.*, 1982), bFGF (Lemmon *et al.*, 1982) and the BMPs (Bergeron *et al.*, 2012) all have a PI > 9, so that they are positively charged at physiological pH, whereas IGF-2 (Honegger et Humbel, 1986) and EGF (Kim *et al.*, 2014) have a PI < 7.4. Opposite charges between the drug and the carrier might become important when a sustained or slow delivery is desired. Tan *et al.* (2012) have produced poly(glutamic acid) nanoporous microparticles to transport BDNF. They are positively charged at physiological pH (PI ~ 10) BDNF. Since the poly(glutamic acid) particles also have a net positive surface charge, they coated the particles with heparin (highly negative) so that they adsorbed BDNF. These properties are also relevant for assessing the best method of encapsulation. The GF encapsulation efficiency of NPs made of material such as chitosan (cationic), synthesized by ionotropic gellification, can be increased using such information. Other materials such as lipid-based delivery systems can also interact since they are sometimes made of cationic or anionic phospholipids (Rourke *et al.*, 1996). For instance, Tah *et al.* (2014) reported interactions between liposomes made of anionic dipalmitoylphosphatidylglycerol and insulin, while Kuo *et al.* (2011) have used catanionic solid lipid NPs to encapsulate doxorubicin and found that tuning the concentration of cationic surfactant increased the encapsulation efficiency.

Two approaches can be used to model these interactions. The first approach considers the interactions between the drug and the release system to be reversible chemical reactions in a continuous phase (Fu *et al.*, 2011):

$$C_{GF} + C_L \underset{k1}{\overset{k2}{\rightleftharpoons}} C_{GF \cdot L} \tag{2-9}$$

$$\frac{\partial C_{GF}}{\partial t} = \nabla \cdot (D_C \nabla C_{GF}) - (k_1 C_{GF} C_L - k_2 C_{GF \cdot L}) \tag{2-10}$$

Eq. 2.10 has a diffusion part and a reaction part associated with the bound drug. These reaction terms correspond to the way the drug–ligand complex changes with time.

The second approach assumes that the interactions between the drug molecule and the material of the delivery system are adsorption/desorption in a porous medium within a

multiphasic system. We have suggested that a peptide derived from BMP-9 (pBMP-9) interacts with its collagen hydrogel delivery systems (Bergeron *et al.*, 2012; Lauzon, 2014).We modeled this delivery system using Fick's second law of diffusion to which was added an adsorption/desorption term following a Langmuir adsorption kinetic to represent the interactions between the peptides and the collagen fibers. These interactions were thought to be caused by the differences in overall charges of the molecules: the PIs of collagen and pBMP-9 mean they have opposite charges at physiological pH. Our model assumes that diffusion takes place in the fiber-free spaces whereas adsorption/desorption occurs on the collagen fibers (Eq. 2.11):

$$\frac{\partial C_{GF}}{\partial t} = \left[D_c (\nabla^2 C_{GF}) + \frac{(1-\varepsilon)}{\varepsilon} C_{carrier} \frac{\partial M_a}{\partial t} \right] \tag{2-11}$$

$$M_a = \frac{M_a^{max} K_a C_{GF}}{1 + K_a C_{GF}} \tag{2-12}$$

Our studies on hydrogels with different collagen contents showed that diffusion was relatively unchanged as the collagen content of the hydrogel increased because of the high porosity of the hydrogel (~0.98), while the strength of the interactions changed due to the change in collagen fiber size as revealed by the Langmuir adsorption isotherms (Eq. 2.12) and electron microscopy (Lauzon, 2014). This model assumes that the interactions occur on the fibers of the hydrogel and not in the whole volume and might apply to other morphologies; it could easily be applied to other fibrous polymer materials.

Model considering the swelling

The swelling of the drug carrier is another important phenomenon. Some materials like chitosan can swell up to 300% in an aqueous solution (Bajpai *et al.*, 2012). Lopez-Leon *et al.* (2005) have shown that pH and ionic variation found in the body can drastically affect the size of chitosan NPs (size ~200–300 nm) with variations of up to 300%. Moreover, Gan *et al.* have shown that swelling of BSA-loaded chitosan NPs (size 200 to 580 nm) was observed in an aqueous solution and drastically affected the release of BSA, thus showing this phenomenon has to be considered (Gan et Wang, 2007). Indeed, the swelling of the drug carrier can greatly influence drug delivery since a gradual increase in the water concentration in the drug carrier can cause polymer fiber relaxation, rendering the drug more available for diffusion into the aqueous phase, thus accelerating mass transport. However, the rate of swelling must be of the same order of magnitude as the rate of drug diffusion before it becomes a major disturbance.

The time frames of carrier swelling and drug release should be carefully compared. These can be evaluated from their respective diffusion coefficients or using the dimensionless Deborah's number. Siepmann *et al.* (1999a; 1999b; 1999c) proposed a relevant mechanistic mathematical framework for drug release from swelling material; it is described by the four equations shown below (Gures *et al.*, 2012; Siepmann *et al.*, 1999; Siepmann, 1999; Siepmann *et al.*, 1999):

$$\frac{\partial C_{GF}}{\partial t} = \nabla \cdot (D_c \nabla (C_{GF})) \tag{2-13}$$

$$\frac{\partial C_w}{\partial t} = \nabla \cdot (D_W \nabla (C_w)) \tag{2-14}$$

$$D_W |_{position}^{time} = D_{W_{eq}} e^{-\beta_w \left(1 - \frac{C_w}{C_{W_{eq}}}\right)} \tag{2-15}$$

$$D_c |_{position}^{time} = D_{C_{eq}} e^{-\beta_c \left(1 - \frac{C_w}{C_{W_{eq}}}\right)} \tag{2-16}$$

This model assumes that the delivery of the therapeutic molecules (Eq. 2.13) and the entry of water into the releasing device (Eq. 2.14) are opposing diffusion processes. The water is assumed to diffuse a lot faster than the polymer fiber relaxation. The diffusion coefficients for both the drug and the water are affected because the water enters the releasing carrier. This influence can be represented as a Fujita-type relationship (Eqs. 2.15 and 2.16) (Fujita, 1961). Thus, the diffusion coefficients of both the water and the drug will change as the solvent enters, and the change is a function of the water concentration, reaching the maximal diffusion of water in the equilibrium swollen state. The parameters C_{weq} and D_{Weq} must be calculated from swelling experiments where the amount of water inside the releasing device is evaluated over time until equilibrium is reached. The diffusion coefficient of the therapeutic molecule in the completely swollen system (D_{Ceq}) must also be estimated theoretically or from experimental results.

Both Xu *et al.* (2013) and Ninawe *et al.* (2012) have proposed mathematical frameworks that take into account the swelling of a polymer matrix such as a hydrogel where water can create shear stress affecting the structure and cause small linear deformations. These models assume that the delivery carrier is a biphasic solution made of polymer fibers and water. Unlike the model proposed by Siepmann *et al.* (1999), water is assumed to diffuse more slowly than the rate at which the polymer network relaxes as water enters and creates shear stress that causes convection. The water and the polymer network are both assumed to be incompressible and the mass transfer of water is mainly driven by convection rather than diffusion. The model differs

markedly from that of Siepmann *et al.* (1999) for water transport within the matrix since the mass transfer of water is driven by the difference in pressure between the surrounding aqueous medium and the surface of the delivery device (Eq. 2.18). This pressure gradient deforms the network, causing the polymer chains to move along in the space denoted by the deformation vector "u" represented by Navier–Stokes equations. Thus, the velocity vector of water can be defined as a function of the pressure gradient, which depends on the osmotic gradient (Eq. 2.19). However, the diffusion of the drug is also assumed to follow a Fujita-type exponent, where the concentration of water at each position (C_w) is calculated from the mass fractions occupied by the polymer and the water (Eq. 2.20).

$$\frac{\partial C_{GF}}{\partial t} + v_w \nabla C_{GF} = \nabla \cdot (D_c \nabla (C_{GF})) \tag{2-17}$$

$$\left(K_p + \frac{G}{3}\right) \nabla (\nabla \cdot u) + G \nabla^2 u = \nabla p \tag{2-18}$$

$$v_w = -\left(\frac{k_p}{\eta \rho_w}\right) \nabla p \tag{2-19}$$

$$D_c|_{position}^{time} = D_{C_{eq}} e^{-\beta_w (1 - C_w)} \tag{2-20}$$

These models treat the same phenomenon (swelling) but rely on different assumptions. The assumption of mechanical distortion within the polymer matrix may be particularly relevant since the pH, temperature and other factors such as ionic strength can all affect the water taken up by a delivery system and its mechanical and physical properties (Ninawe et Parulekar, 2012; Xu *et al.*, 2013).

Model considering erosion

Some polymers can undergo erosion, which can affect the diffusion of the drug out of the delivery system by increasing drug mobility. Erosion changes the size of the releasing carrier, resulting in a moving boundary layer and changes in the exchange surface area. PLGA and other polyester polymers can be eroded by hydrolysis, resulting in alcohol and acidic residues (Fredenberg *et al.*, 2011). The hydrolysis of PLGA can produce a local acidic environment that can trigger autocatalytic hydrolysis, thus accelerating erosion (Fredenberg *et al.*, 2011; Siepmann *et al.*, 2005). Chitosan can also be degraded by lysozymes once it is inside the body (Onishi et Machida, 1999). Chitosan fragments can thus accumulate in the kidney from where they are excreted. Therefore, both *in vitro* and *in vivo* conditions can lead to degradation of the delivery system.

Siepmann *et al.* have demonstrated that the degradation of PLGA microparticles over time could be described as exponential (Eq. 2.21) (Faisant *et al.*, 2002; Siepmann *et al.*, 2005), whereas the dissolution of polymers like hydroxypropyl methylcellulose or PLA is a function of both time and available surface area (Eq. 2.22) (Siepmann, 1999c; Siepmann et Peppas, 2001). PLGA undergoes bulk erosion; water diffuses into the polymer more quickly than the rate of protolysis (Siepmann et Peppas, 2001). Bulk erosion affects mostly the inside of the releasing device, creating water, acidic residues and drug spaces, whereas surface erosion directly affects the size of the delivery device since hydrolysis, which is much more rapid than dissolution, erodes the surface. Consequently, the bigger the PLGA, particle, the greater are its chances of undergoing autocatalysis since the diffusion of both bulk solution and acidic residues are increased. However, PLGA NPs (~700 nm) may also undergo bulk erosion (Dunne *et al.*, 2000).

As a result, erosion kinetics should be measured if polymer erosion is suspected in order to evaluate its magnitude relative to that of drug release and estimate the rate of carrier degradation. A fast degradation rate will affect drug release, which in turn will directly affect the resolution of the Fick's second law model. The net radius of the NPs will also decrease over time, depending on the type of erosion, thus affecting the drug volume and concentration, whereas this will not be so at first for bulk erosion: the pores inside the releasing device will form first, followed by surface erosion. Hence, bulk erosion is very difficult to model because it is difficult to measure the pores forming inside micro- and NPs. However, a transient diffusion coefficient that varies with the decreasing polymer molecular weight can help to fit the data (Eq. 2.23) (Faisant *et al.*, 2002). This approach seems to be valid as shown by Faisant *et al.* (2003).

$$M_{t,polymer} = M_0 e^{(-k_{bulk\,erosion}t)} \tag{2-21}$$

$$M_{t,polymer} = M_0 - k_{erosion\,2} A_t t \tag{2-22}$$

$$D_C = D_{C0} - \frac{k_{erosion\,1}}{M_{w\,polymer}} \tag{2-23}$$

There are other mathematical frameworks for modeling bulk erosion. A stochastic, statistical process and Monte-Carlo simulation seems to be very efficient (Chen *et al.*, 2011; Faisant *et al.*, 2003; Perale *et al.*, 2009; Siepmann *et al.*, 2002). The polymers and pores are distributed randomly within the volume of the delivery vehicle in respect to their volume or mass fractions in these simulations. A randomly distributed life-time is normally given to each

element of volume, which will dictate when each element becomes a pore as the aqueous solution enters the delivery system and interacts with the polymer. The diffusion coefficient of the drug inside the delivery device can then be evaluated from the anisotropic pore distribution with results to be very close to experiments (Faisant *et al.*, 2003; Siepmann *et al.*, 2002).

Other mass transport phenomena such as the degradation of the delivering device by enzymes have also been described by Bause *et al.* (2006). The enzyme diffuses into the delivery carrier and interacts with it by binding to the matrix itself and degrading it to products that can diffuse out of the delivery system. It is practical to assume that the swelling caused by the enzyme entering the delivery carrier is negligible. This model is more complex and requires more experiments to estimate the decay of enzymatic activity and the enzyme kinetics, the dissolution of the product in the matrix, the rate of matrix degradation and the effect on the diffusivity. The enzyme reaction is described as a two-step chemical reaction: the enzyme is first bound to the substrate (polymer matrix) and then products are formed and the enzyme is released (Eq. 2.24). The mass transport of the enzyme is assumed to be controlled by diffusion, water transport momentum ("q") in the case of a swelling material and the reaction rate from the chemical equations (Eq. 2.25). The enzyme–substrate complex is also assumed to be immobile, following a Freundlich-type adsorption isotherm (Eq. 2.26). The product "p" diffuses out of the delivery device at the same rate as the chemical reaction (Eq. 2.28). Finally, because the matrix is lost over time, the diffusion coefficients of both enzyme and product are affected. Thus, the diffusion coefficients are assumed to vary following a Fujita dependent relation as shown by Eqs. 2.29 and 2.30 (Fujita, 1961).

$$E + S \xrightarrow{k_1} ES \xrightarrow{k_2} E + P \tag{2-24}$$

$$\frac{\partial C_E}{\partial t} = \nabla \cdot (D_E \nabla (C_E) - q C_E) + k_{act} C_E - k_1 (C_E)^\alpha C_K + k_2 C_{ES}^\gamma \tag{2-25}$$

$$\frac{\partial C_{ES}}{\partial t} = k_1 (C_E)^\alpha C_S - k_2 C_{ES}^\gamma \tag{2-26}$$

$$\frac{\partial C_S}{\partial t} = k_1 (C_E)^\alpha C_S \tag{2-27}$$

$$\frac{\partial C_P}{\partial t} = \nabla \cdot \left(D_P \nabla (C_P) \right) + k_2 C_{ES}^\gamma \tag{2-28}$$

$$D_E \big|_{position}^{time} = D_{E_{eq}} e^{-\beta_E \left(1 - \frac{c_S}{c_{S_{eq}}} \right)} \tag{2-29}$$

$$D_P|_{position}^{time} = D_{P_{eq}} e^{-\beta_P \left(1 - \frac{c_S}{c_{S_{eq}}}\right)} \tag{2-30}$$

This mathematical representation of enzymatic polymer degradation is complex because there may be many types of enzymes in the releasing environment and many experiments need to be done to estimate all the kinetic constants and the way all elements diffuse within the delivery system. Monte-Carlo or statistical simulations may be more appropriate for modeling the polymer decay or erosion as the enzyme penetrates the delivery carrier in such a complex environment.

2.12 Conclusion

In this paper, we have reviewed the latest advances in nanoparticle-mediate GF delivery systems targeting the brain and discussed their advantages and limitations. We have also presented the *in vitro* or *in vivo* effect of GF delivery from those carriers showing that GFs or GF-like molecules are promising precursors of innovative treatment for AD. Most of the latest advances in drug delivery systems targeting the brain are under the shape of NPs made of various materials from natural polymers to synthetic or metal-based materials. In addition, new materials and surface-grafted molecules that are more specific for brain endothelial cell receptors such as the transferrin receptors are also being developed to increase the selectivity of the NPs to the brain. Moreover, in order to better understand the delivery behaviors of those GFDS, we then have examined the mechanistic modeling of these systems although very few models have yet been built. We have shown that the journey of NP itself from the nasal cavities and blood capillaries to the brain tissue holds many modeling challenges. As part of this examination, we have identified the main mass transport phenomena involved in NPs as well as GFs inside them and how they can be described mechanistically, thus providing good insights about the development of predictive and explanatory mathematical frameworks. We believe that the development of GFDS addressing the BBB specifically with a proper understanding and control of the undergoing mass transport phenomena is very promising as future treatments for brain degenerative diseases.

2.13 Acknowledgments

CHAPITRE 3: EFFETS DE PEPTIDES DÉRIVÉS DE LA BMP-9 SUR DES CELLULES SH-SY5Y

3.1 Informations relatives à l'article

Auteurs et affiliations :

- M.-A. Lauzon : Étudiant au doctorat en génie chimique, Département de génie chimique et de génie biotechnologique, Université de Sherbrooke

- O. Drevelle : Étudiant Post-Doctorale, département de génie chimique, École Polytechnique de Montréal, 2900, Blvd Édouard Montpetit, Montréal, Québec, H3C 3A7, Canada

- N. Faucheux : Professeur titulaire, Département de génie chimique et de génie biotechnologique, Université de Sherbrooke. Affiliation au Centre de Recherche Clinique du Centre Hospitalier Universitaire de Sherbrooke, 12e Avenue N, Sherbrooke, Québec, J1H 5N4, Canada

Contributions à la thèse :

Cet article contribue à la thèse en présentant les résultats du deuxième objectif du projet de doctorat qui consistait à démontrer l'effet de peptides dérivés de la BMP-9 sur des cellules

neuronales humaines dans un contexte de la maladie d'Alzheimer. Les contributions majeures associées à ces travaux sont les suivantes :

- L'étude de l'effet de 2 peptides dérivés de l'épitope knuckle de la BMP-9 (pBMP-9 et SpBMP-9) sur la capacité de cellules dérivées de neuroblastome humain (SH-SY5Y) à survivre.
- La capacité des 2 peptides pBMP-9 et SpBMP-9 à induire une différenciation neuronale supérieure à la BMP-9 chez des cellules SH-SY5Y.
- La capacité des peptides pBMP-9 et SpBMP-9 à moduler au moins deux cibles thérapeutiques associées à la maladie d'Alzheimer : 1) stimulation du système cholinergique et 2) inactivation de l'enzyme intracellulaire GSK3beta, impliquée dans l'état d'hyperphosphorylation de la protéine Tau.

Résumé anglais:

The incidence of brain degenerative disorders like Alzheimer's disease (AD) will increase as the world population ages. While there is presently no known cure for AD and current treatments having only a transient effect, an increasing number of publications indicate that growth factors (GF) may be used to treat AD. GFs like the bone morphogenetic proteins (BMPs), especially BMP-9, affect many aspects of AD. However, BMP-9 is a big protein that cannot readily cross the blood-brain barrier. We have therefore studied the effects of two small peptides derived from BMP-9 (pBMP-9 and SpBMP-9). We investigated their capacity to differentiate SH-SY5Y human neuroblastoma cells into neurons with or without retinoic acid (RA). Both peptides induced Smad 1/5 phosphorylation and their nuclear translocation. They increased the number and length of neurites and the expression of neuronal markers MAP-2, NeuN and NSE better than did BMP-9. They also promoted differentiation to the cholinergic phenotype more actively than BMP-9, SpBMP-9 being the most effective as shown by increases in intracellular acetylcholine, ChAT and VAchT. Finally, both peptides activated the PI3K/Akt pathway and inhibited GSK3beta, a current AD therapeutic target. BMP-9-derived peptides, especially SpBMP-9, with or without RA, are promising molecules that warrant further investigation.

Résumé français:

L'incidence des troubles dégénératifs du cerveau telle que la maladie d'Alzheimer (AD) augmentera avec le vieillissement de la population mondiale. Bien qu'il n'y ait présentement aucune cure connue à l'AD et que les traitements actuels n'aient qu'un effet transitoire, il y a une augmentation du nombre de publications indiquant que les facteurs de croissance (GF) pourraient être utilisés pour traiter l'AD. Des GFs comme la protéine morphogénétique de l'os (BMPs), et notamment la BMP-9, affectent plusieurs aspects de l'AD. Toutefois, la BMP-9 est une protéine volumineuse qui ne peut facilement traverser la barrière hématoencéphalique. Nous avons donc étudié l'effet de deux petits peptides dérivés de la BMP-9 (pBMP-9 et SpBMP-9). Nous avons analysé leur capacité à différencier des cellules de neuroblastomes humains SH-SY5Y en neurones avec ou sans acide rétinoïque (RA). Les deux peptides ont induit la phosphorylation des Smad 1/5 et leur translocation au noyau. Ils ont augmenté le nombre et la longueur des neurites et l'expression des marqueurs neuronaux MAP-2, NeuN, NSE de manière plus importante que la BMP-9. Ils ont également favorisé la différenciation vers le phénotype cholinergique plus activement que la BMP-9, le SpBMP-9 étant le plus efficace, tel qu'il a été montré par des augmentations en acétylcholine intracellulaire, ChAT et VAchT. Finalement, les deux peptides ont activé la voie PI3K/Akt et inhibé la GSK beta, une cible thérapeutique de l'AD. Les peptides dérivés de la BMP-9, plus particulièrement le SpBMP-9, avec ou sans RA, sont des molécules prometteuses qui méritent d'être étudiées de manière plus approfondie.

3.2 Introduction

Alzheimer's disease (AD) is the most common type of dementia, accounting for about 60% of all cases, affecting over 40 million people worldwide (World Health Organization, 2012). However, there is no cure for AD and the therapies currently available or under investigation have only transient effects and slow disease progression (Giacobini et Gold, 2013; Tricco *et al.*, 2013). Most target only one of the three major hallmarks of AD at a time (cholinergic system dysfunction (Geula *et al.*, 2008), beta amyloid plaque accumulation (Murphy et LeVine 3rd, 2010) and Tau protein hyperphosphorylation (Alonso *et al.*, 1996; Augustinack *et al.*, 2002), although considerable evidence suggests that these hallmarks are all intimately linked (Lauzon *et al.*, 2015b; Roberson *et al.*, 2007; Zheng *et al.*, 2002). Growth factors (GFs) like neurotrophins (nerve growth factor and brain-derived neurotrophic factor),

bone morphogenetic proteins (BMPs) and insulin-like growth factor 2 (IGF-2), which are found in the developing and healthy mature brain, but are dysregulated in AD, seem to prevent the evolution of the disease. They could act on several AD hallmarks simultaneously and repair the dysfunctional cell signaling (Burke *et al.*, 2013; Lauzon *et al.*, 2015b; Lopez-Coviella *et al.*, 2000; Matrone, Ciotti, *et al.*, 2008; Mellott *et al.*, 2014; Pascual-Lucas *et al.*, 2014; Schnitzler *et al.*, 2010).

One subfamily of GFs, the BMPs, may have great potential as they are involved in brain development, maintenance and homeostasis (Hegarty *et al.*, 2013a; Lauzon *et al.*, 2015a; Mehler *et al.*, 1995, 1997). The BMPs, more than 20 at the last count, were discovered in bone tissue by Urist and Strates in the early 1970s (Senta *et al.*, 2009; Urist et Strates, 1971; Wagner *et al.*, 2010). BMPs signal in the brain via their type I and type II Serine/Threonine kinase receptors and activate the canonical Smad pathway (Smad 1/5/8), which is important in early brain development and neuron maturation1 (Hegarty *et al.*, 2013b, 2014; Zheng *et al.*, 2002).

One BMP, BMP-9, may be a promising candidate for therapy: it is present in the brain and seems to be linked to the function of cholinergic neurons (Lopez-Coviella *et al.*, 2002, 2005). Lopez-Coviella *et al.* (2000) found high amount of BMP-9 transcripts in the spinal cord and septal area of mice. BMP-9 also activates the transcriptome of basal forebrain cholinergic neurons, which are associated with learning and memory, and is directly implicated in their differentiation (Lopez-Coviella *et al.*, 2005). Other evidence indicates that BMP-9 has a direct therapeutic effect on AD hallmarks (Burke *et al.*, 2013; Lopez-Coviella *et al.*, 2000, 2002; Schnitzler *et al.*, 2010). Lopez-Coviella *et al.* (2000) studied mouse medial septum neurons and showed that BMP-9 increases the expression of cholinergic markers in the hippocampus and prevents the loss of choline acetyltransferase (ChAT); this loss is characteristic of AD-associated memory loss. Similarly, Burke *et al.* (2013), working on a mouse model of AD (APP.PS1, transgenic mouse overproducing β–amyloid peptides), demonstrated that intraventricular injections of BMP-9 dramatically reduced the accumulation of senile plaques in the cortex and hippocampus, and increased the ChAT levels.

But despite its interesting therapeutic features, recombinant human BMP-9 is expensive to produce and is not readily introduced into the brain by systemic or nasal injection because of its size (homodimer of 24 kDa) and the great selectivity of the blood brain barrier. Also, BMPs

have short half-lives in the circulatory system (Poynton et Lane, 2002). We have therefore developed small (23 residues) and relatively inexpensive (300-times less expensive than BMP-9) peptides derived from the knuckle epitope of BMP-9. They correspond to the sequence recognized by the BMP type II receptor (BMPRII) and are based on the work of Suzuki *et al.* (2000) and Saito *et al.* (2005) on peptides derived from BMP-2. These peptides trigger signalling and cell responses similar to those induced by the whole protein (BMP-9) in the context of bone regeneration (Beauvais *et al.*, 2016; Bergeron *et al.*, 2009, 2012) but their effects on neurons remain unknown. We therefore explored the effects of two BMP-9-derived peptides pBMP-9 (Bergeron *et al.*, 2009) and SpBMP-9 (Beauvais *et al.*, 2016) on SH-SY5Y human neuroblastoma cells, a well-known human mature neuron cell model that has been used several times in the context of AD (Agholme *et al.*, 2010; Jämsä *et al.*, 2004; Koriyama *et al.*, 2015). Recombinant human BMP-9 was used as a control in all experimental conditions. We also stimulated SH-SY5Y cells in the presence of retinoic acid (RA), a potent agent of neuron differentiation (Cheung *et al.*, 2009) that is believed to be therapeutic for AD (Sodhi et Singh, 2014).

3.3 Results

3.3.1 pBMP-9 and SpBMP-9 activate the Smad1/5 pathway

Effect of pBMP-9 and SpBMP-9 on kinetic of Smad 1/5 phosphorylation

We have recently shown that BMP-9 (1 nM) with or without RA can activate the canonical Smad1/5 pathway within 30 min in SH-SY5Y cells (Lauzon *et al.*, 2015a). We therefore verified the ability of both pBMP-9 and SpBMP-9 (1 nM) to activate the Smad 1/5 pathway (Fig. 1A). The total Smad1/5 (TSmad) was used as a control. Without RA, the phosphorylated Smad1/5 (pSmad) bands were detected after incubation for 30 min in cells stimulated with pBMP-9 or SpBMP-9. Both peptides in the presence of RA induced the phosphorylation of Smad1/5 at 15 min. The Smad1/5 remained phosphorylated within 240 min in the presence of pBMP-9 or SpBMP-9 with or without RA. Densitometric analysis of bands corresponding to pSmad1/5 and standardized to that of TSmad (Figure 3-1A) confirmed that pSmad1/5 levels reached a plateau after 1h.

Effect of pBMP-9 and SpBMP-9 on the nuclear translocation of phosphorylated Smad1/5

Since pBMP-9 and SpBMP-9 induced the phosphorylation of Smad 1/5 (pSmad1/5) in SH-SY5Y cells, we then analyzed the pSmad1/5 translocation into the nucleus after incubation for 240 min by labelling both DNA (nucleus) and pSmad1/5 (Figure 3-1B). Without RA, cells incubated with BMP-9 (1nM) had a strong pSmad1/5 staining compared to untreated cells (CTL) and the pSmad1/5 were mainly located at the nucleus. Both pBMP-9 and SpBMP-9 at 1nM induced a slight pSmad1/5 labelling compared to BMP-9. Only some cells possessed a strong nuclear translocation of the pSmad1/5. The same tendencies were observed in cells treated by BMP-9 or its derived peptides in the presence of RA

3.3.2 pBMP-9 and SpBMP-9 do not affect the number of SH-SY5Y cells

Effect of pBMP-9 and SpBMP-9 on cell metabolic activity and viability

We investigated the influence of pBMP-9 and SpBMP-9 with or without RA on the viability of SH-SY5Y cells. BMP-9 was used as a control. We measured the activity of the enzyme succinate dehydrogenase using the MTS assay (Figure 3-2A). The control (CTL) showed no alteration in the metabolic activity either with or without RA. Incubation for 3d with 0.1nM BMP-9 or 0.1nM SpBMP-9 but no RA resulted in a significant increase in metabolic activity ($p<0.05$) in comparison to the CTL. Similar results were obtained after incubation for 5d with 0.1 or 1 nM BMP-9 and with 0.1 nM SpBMP-9. Cells incubated with 0.1 or 1 nM BMP-9 and its derived peptides plus RA for 3d and 5d had significantly increased the metabolic activity

A Smad1/5 phosphorylation
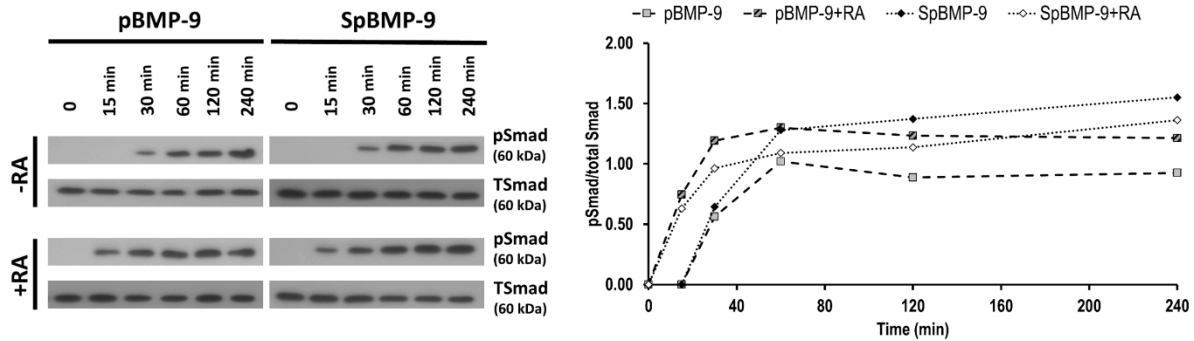
B Phosphorylated Smad1/5 translocation to the nucleus
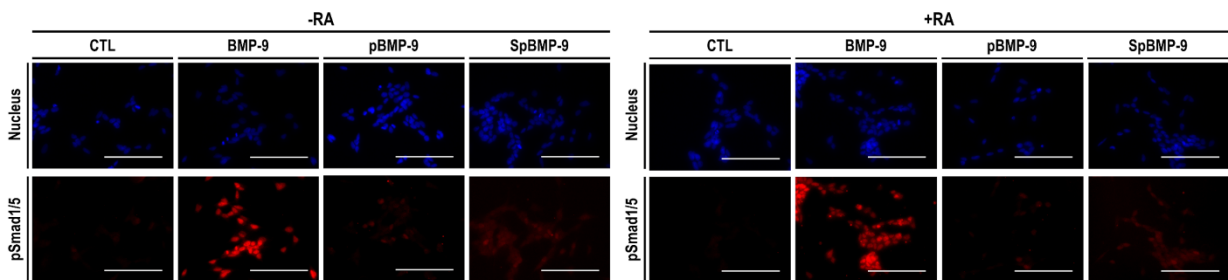
Figure 3-1 : Effect of pBMP-9 and SpBMP-9 on the activation of the canonical Smad1/5 pathway. (**A**) Western blots of phosphorylated Smad1/5 (pSmad) and densitometric analysis of pSmad1/5 as referred to total Smad (TSmad) showing the effect of 1 nM BMP-9, pBMP-9 and SpBMP-9 +/−10 μM RA in SH-SY5Y cells after incubation for 0, 15, 30, 60, 120 and 240 min. (**B**) Pictures showing the nucleus (blue) and the pSmad1/5 (red) in SH-SY5Y cells stimulated with an equimolar concentration of BMP-9, pBMP-9 or SpBMP-9 (1 nM) +/−10 μM RA after incubation for 240 min. Results are representative of 2 independent experiments performed in duplicate (Bar = 100 μm).

Effect of pBMP-9 and SpBMP-9 on cell number

Cell nucleus was stained with Hoechst 33342 to verify whether the observed increase in metabolic activity were caused by increases in cell numbers (Figure 3-2B). In the absence of RA, there was no significant difference between experimental conditions, neither in function of time. In the presence of RA, after 5d of incubation, cells stimulated with BMP-9 (1 nM), pBMP-9 (0.1nM) or SpBMP-9 (0.1nM) had a significant increased amount of nucleus relative fluorescence intensity in comparison with the control, those results being in accordance with the metabolic enzymatic assay. There was a determination coefficient of 0.7 between indirect cell counting and MTS assay results, which indicates that the metabolic activity might be related to the number of cells (Figure 3-2C).

However, since the cell number was evaluated indirectly by measuring the relative fluorescence intensity of the nucleus staining, we then looked at the cell nucleus in a higher magnification to evaluate if the increase in the cell number in experiments performed with RA could rather be explained by the presence of pyknotic cell nuclei (Figure 3-2D). There were some pyknotic nuclei for cells stimulated for 5d in the presence of BMP-9, pBMP-9 and SpBMP-9 plus RA. From those results, it appears that cells stimulated with BMP-9, pBMP-9 and SpBMP-9, especially in the presence of RA increase their metabolic activity, which is not caused by an increase in cell number.

3.3.3 pBMP-9 and SpBMP-9 affect the morphology of SH-SY5Y cells and increase their neurites outgrowth

Effect of pBMP-9 and SpBMP-9 on cell morphology

The impact of BMP-9, pBMP-9 and SpBMP-9 on neuron well-being and the differentiation of cells like SH-SY5Y require an examination of the cell morphology (Figure 3-3A). Cells incubated in serum free-medium with BMP-9, especially at 1nM, reacted more like neuroblastoma cancerous cells, forming clusters with less neuron-like morphology. Cells stimulated with pBMP-9 and SpBMP-9 show an increase amount of neurite outgrowth. RA had a dramatic effect on cell morphology under all experimental conditions: it increased neurite outgrowth and displayed more neuronal morphology. Cells stimulated with pBMP-9 or pBMP-9 plus RA had more interconnected neurites than did control plus RA.

A MTS assay

B Indirect cell count

C Correlation between MTS and indirect cell count

D Cell nucleus staining in the presence of RA
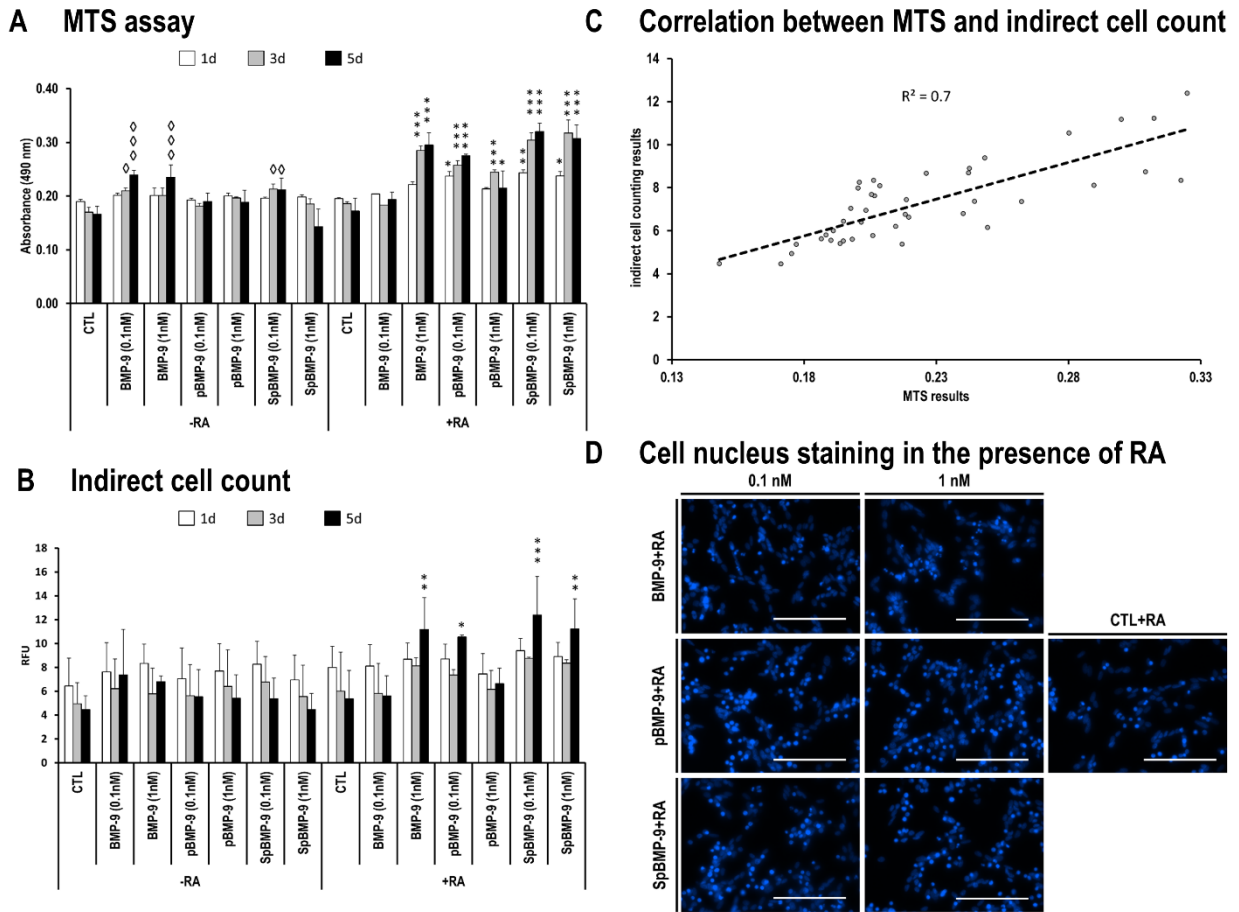
Figure 3-2 : Effect of pBMP-9 and SpBMP-9 on the metabolic enzymatic activity and indirect cell counting. (**A**) MTS assays of SH-SY5Y cells stimulated for 1d, 3d and 5d with equimolar concentrations (0.1 and 1 nM) of BMP-9, pBMP-9 and SpBMP-9 +/− 10 μM RA in serum-free culture medium (◊ $p < 0.05$ and ◊ ◊ ◊ $p < 0.001$ compared with the control without RA, *$p < 0.05$, **$p < 0.01$ and ***$p < 0.001$ compared with the control with RA). Results are the means ± SEM of at least two independent experiments performed in duplicate. (B) Indirect cell counting showing the relative fluorescence intensity of the stained nuclei in cells used to perform the MTS assays (*$p < 0.05$, ** $p < 0.01$, ***$p < 0.001$). (C) Indirect cell counting results plot in function of the MTS enzymatic assay results showing a correlation of 0.7. (D) Cell nucleus staining in SH-SY5Y cells stimulated by BMP-9, pBMP-9 or SpBMP-9 (0.1 and 1 nM) in the presence of 10 μ M RA for 5d (Bar = 100 μm).

We then measured the average length of neurites under each experimental condition (Figure 3-3B). SH-SY5Y cells stimulated with pBMP-9 (at least $p<0.01$) stimulated the formation of significantly longer neurites than did the higher concentration (1nM).

3.3.4 pBMP-9 and SpBMP-9 increase the expression of early and late neuronal differentiation markers

Effect of stimulation time on neuron markers expression

Since pBMP-9 and SpBMP-9 had an effect on the morphology of SH-SY5Y cells inducing neurite formation characteristic of the neuron phenotype, we used Western blots to evaluate the expression of MAP-2 protein, an early marker of neuron differentiation (Izant et McIntosh, 1980) (Figure 3-4A). There was significantly more of MAP-2 in cells stimulated with pBMP-9 and SpBMP-9 (0.1nM) without RA for 5d than in the CTL as shown by the densitometric analyses ($p<0.05$). There was a significant increase in MAP-2 in cells stimulated for 3d with pBMP-9 or SpBMP-9 plus RA in comparison to BMP-9 plus RA ($p<0.01$). Finally, the expression of MAP-2 decreased between 3d and 5d in the CTL ($p<0.05$) and in cells treated with SpBMP-9 ($p<0.05$), while it increased in cells stimulated with BMP-9 ($p<0.05$). The MAP-2 levels in cells stimulated with pBMP-9 for 3d and 5d were the same.

Neuron markers distribution

Knowledge of the distribution of neuron differentiation markers in cells is essential for confirming the neuron phenotype. For example, NeuN is specific to neuron cells and is restricted to the cell nucleus (Bier *et al.*, 1988; Gusel'nikova et Korzhevskiy, 2015). We used immunolabelling to determine the effect of BMP-9, pBMP-9 and SpBMP-9 on the expression and distributions of the markers of early (βIII-tubulin, MAP-2) and late neuron differentiation (NeuN and NSE) in cells incubated for 5d (Figure 3-4B).

We detected βIII-tubulin under all experimental conditions, but it was most prominent in cells stimulated with RA for all experimental conditions. BMP-9 without RA produced less intense labelling regardless of its concentration. However the cells stimulated with pBMP-9 or SpBMP-9 contained more markers than did the control or those stimulated with BMP-9 with or without RA

A Morphology analysis
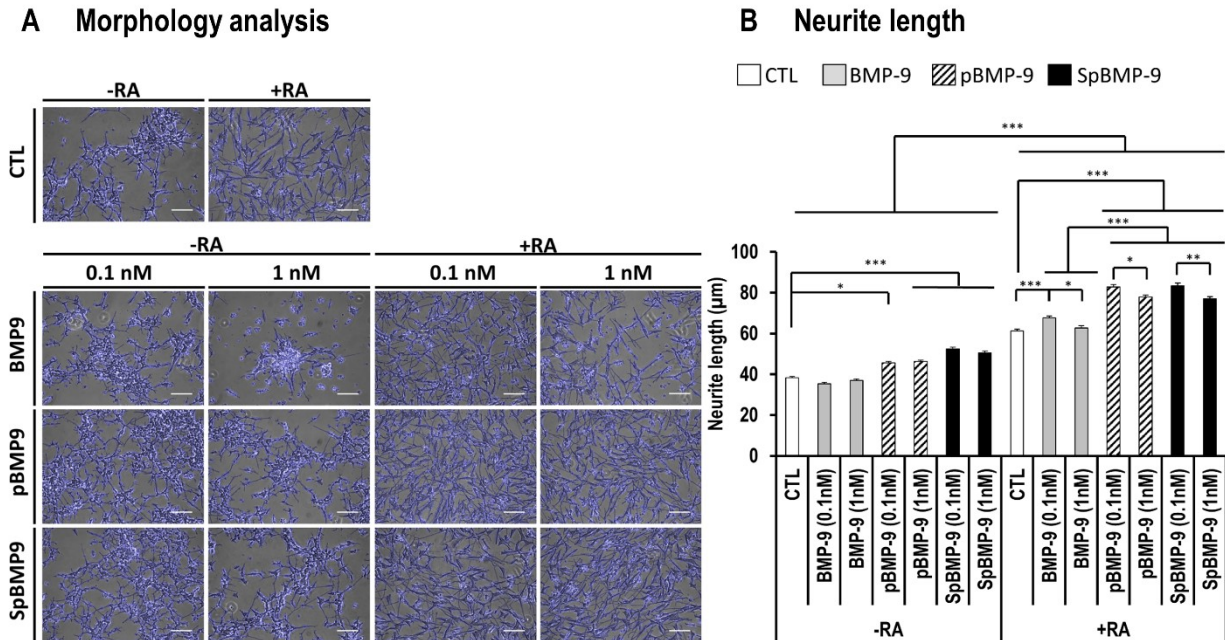
B Neurite length

Figure 3-3 : Effect of pBMP-9 and SpBMP-9 on the morphology of SH-SY5Y cells and neurite length. (A) Modified phase-contrast pictures of SH-SY5Y cells stimulated for 5d with equimolar concentrations (0, 0.1 and 1 nM) of BMP-9, pBMP-9 and SpBMP-9 +/− 10 μM RA. Pictures are representative of at least 3 independent experiments performed in duplicate. Neurites and cell bodies were highlighted with an edge-detection filter and superimposed (blue edges) on the original phase contrast image (Bar = 100 μm). (B) Average neurite length of SH-SY5Y cells stimulated for 5d with equimolar concentration of BMP-9, pBMP-9 or SpBMP-9 (0.1 and 1 nM) +/− 10 μM RA determined as the Euclidean distance between the end of neurites and the cell body. Results are the means ± SEM of at least 3 independent experiments performed in duplicate, where a total of over 300 measurements were taken per experimental condition (*p < 0.05, **p < 0.01, ***p < 0.001).

MAP-2 was most abundant in the neurites of SH-SY5Y cells stimulated with 0.1 or 1nM pBMP-9 or SpBMP-9, especially in the presence of RA. Since MAP-2 is a microtubule-associated protein, an increase in its expression and its distribution in the neurites is associated with greater neuronal differentiation (Izant et McIntosh, 1980). Staining for the marker of late differentiation, NeuN, in cell nuclei (Gusel'nikova et Korzhevskiy, 2015), was more intense in cells stimulated with pBMP-9, and especially SpBMP-9, with or without RA, than in cells stimulated with BMP-9 or the CTL (Figure 3-4B). SH-SY5Y cells stimulated with 1 nM BMP-9 were poorly stained, especially those incubated without RA. However, there was some staining in the cell body around the nucleus. This could be due to the presence of synapsin I, which is recognized by NeuN antibodies (Kim *et al.*, 2009). Finally, incubation with pBMP-9 or SpBMP-9 produced the best staining for NSE, a late marker located in the cell cytoplasm, regardless of their concentration or the presence of RA.
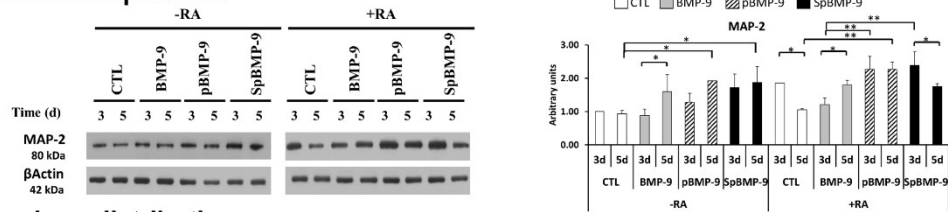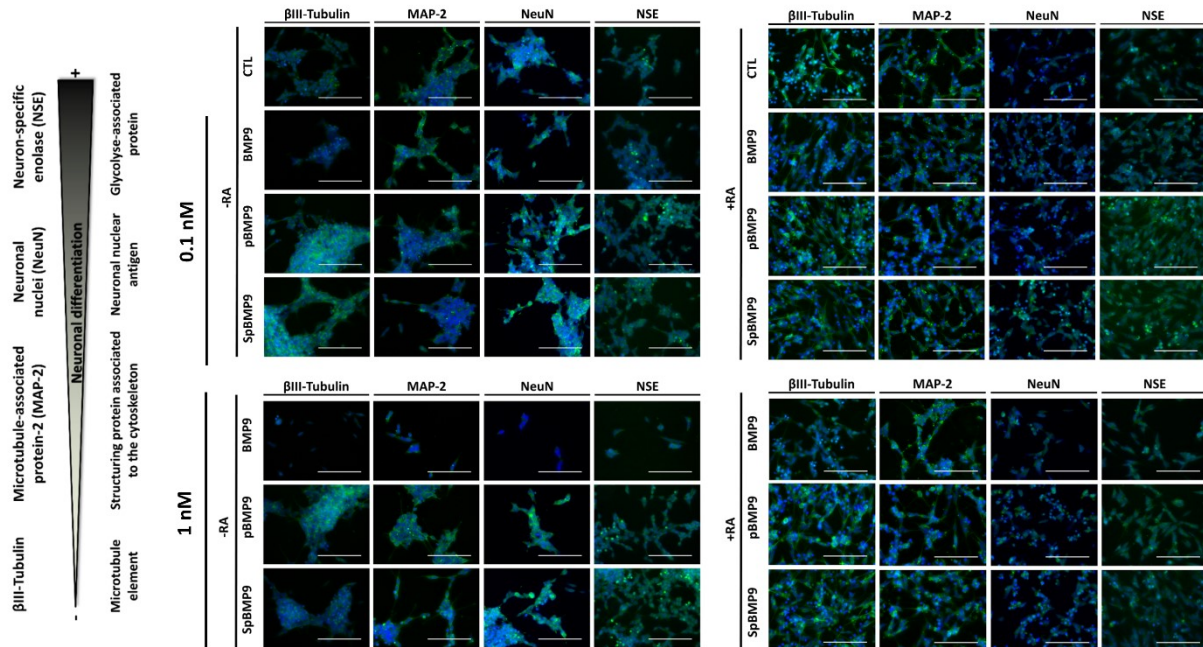
Figure 3-4 : Effect of pBMP-9 and SpBMP-9 on the differentiation of SH-SY5Y cells. (**A**) Western blots of MAP-2 and βactin (2 independent experiments) and densitometric analyses of MAP-2 bands normalized to βactin (means $\pm$ SEM) for SH-SY5Y cells stimulated with 0.1 nM BMP-9, pBMP-9 and SpBMP-9 +/− 10 µM RA for 3d and 5d (*p < 0.05, **p < 0.01). Only cropped pictures of western blots showing the 80 kDa MAP-2 isoform were presented in order to allow a better comparison between experimental conditions. Complete gel pictures are available in the supplementary data file. (**B**) Merged pictures showing immunostaining for neuronal differentiation markers βIII-tubulin (Alexa Fluor® 488, green), MAP-2 (Alexa Fluor® 488, green), NeuN (FITC, green) and NSE (FITC, green), and nuclei staining (Hoechst, blue) of SH-SY5Y cells stimulated for 5d with 0, 0.1 or 1 nM BMP-9, pBMP-9 and SpBMP-9 +/− 10 µM RA. Pictures are representative of at least two independent experiments (Bar = 100 µm).

These results indicate that pBMP-9 and SpBMP-9 induce more rapid neuron differentiation than the whole BMP-9 protein or the CTL, especially in the presence of RA. However, greater neuron differentiation does not necessarily mean that cells are moving toward the cholinergic phenotype.

3.3.5 SpBMP-9 increases the expression of choline acetyltransferase, vesicular acetylcholine transporter protein and the level of intracellular acetylcholine.

BMP-9 activates the cholinergic transcriptome of murine septal cells and basal forebrain cholinergic neurons and increase the levels of Ach and the vesicular acetylcholine transporter protein (VAchT) (Lopez-Coviella *et al.*, 2000, 2002, 2005). Ach is synthesized in the cell body by fusion of acetyl Co-A and choline catalysed by choline acetyltransferase (ChAT); it is then transported to vesicles by VAchT. The ChAT and VAchT genes are conserved at the same locus, which suggests that their expressions are coordinated (Berse et Blusztajn, 1995). We investigated the effect of pBMP-9 and SpBMP-9 on the induction and the maintenance of the cholinergic phenotype since cholinergic dysfunction is a major hallmark of AD (Figure 3-5, Figure 3-6, Figure 3-7).

Effect of pBMP-9 and SpBMP-9 on choline acetyltransferase

The ChAT enzyme responsible for converting acetyl-co-A and choline to acetylcholine in SH-SY5Y cells incubated with BMP-9 or its derived peptides with or without RA was detected by immunolabelling (Figure 3-5A and B). We found ChAT immunostaining in all cell bodies under all experimental conditions (Figure 3-5A). However, the intensity of labelling differed, especially when the cells were stimulated with SpBMP-9 without RA. The CTL without RA had the lowest ChAT staining, while cells incubated with 0.1 nM SpBMP-9 had the highest ones as confirmed by the relative fluorescence intensity analysis ($p<0.05$) (Figure 3-5B). Cells stimulated with BMP-9 and pBMP-9 had similar fluorescence intensities as the control, which were lower than that of SpBMP-9-stimulated cells. However, no difference in relative fluorescence intensities was observed when the same assays were run in the presence of RA.

Choline acetyltransferase
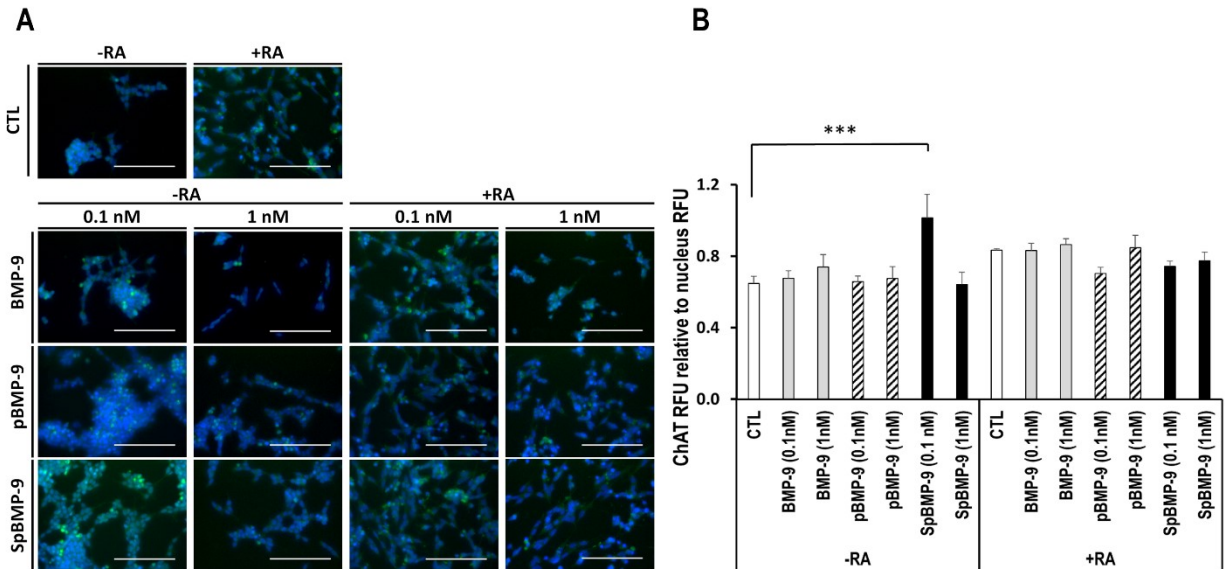
Figure 3-5 : Effect of pBMP-9 and SpBMP-9 on the expression of choline acetyltransferase. (**A**) Merged pictures showing immunostaining for ChAT (FITC, green) and nuclei labelling (Hoechst, blue) of SH-SY5Y cells stimulated for 5d with 0, 0.1, or 1 nM BMP-9, pBMP-9 and SpBMP-9 +/− 10 μM RA (Bar = 100 μm). Pictures are representative of at least 2 independent experiments. (**B**) Analysis of ChAT fluorescence intensity relative to the nucleus staining was also presented. Results are the means ± SEM (***p < 0.001).

Effect of incubation time and pBMP-9 or SpBMP-9 dose on intracellular acetylcholine concentration and VAchT expression and distributions within cells

VAchT in the axon terminals plays an important role in the accumulation of Ach prior to its release (Gilmor *et al.*, 1996). We immunolabelled VAchT to evaluate the effects of SpBMP-9 and pBMP-9 on its expression and distribution in the cells (5d, Figure 3-6). The presence of labelled VAchT in small vesicles within the neurites indicates a cholinergic differentiation. Only cells stimulated with 0.1nM or 1nM SpBMP-9 (without RA) had VAchT vesicles in their neurites, with 1 nM being more efficient. RA alone significantly stimulated VAchT accumulation in the neurites. Cells stimulated with 0.1nM BMP-9, 0.1 and 1nM pBMP-9 and SpBMP-9 plus RA all had similar amounts and distributions of VAchT vesicles in the neurites. However, cells stimulated with 1nM BMP-9 contained no vesicles.

Vesicular acetylcholine transferase distribution
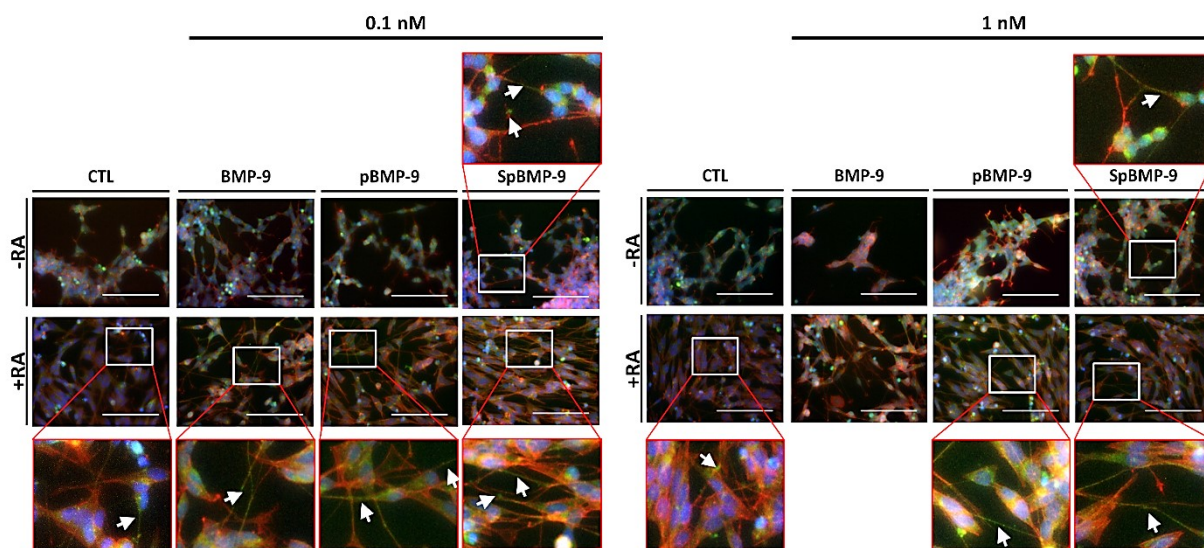
Figure 3-6 : Effect of pBMP-9 and SpBMP-9 on the expression and the distribution of VAchT. Merged pictures showing immunostaining for VAchT (FITC, green), actin cytoskeleton (rhodamine-phalloidin, red) and nuclei labelling (Hoechst, blue) of SH-SY5Y cells stimulated for 5d with 0, 0.1 or 1 nM BMP-9, pBMP-9 and SpBMP-9 +/− 10 μM RA. White squares show magnified zones, white arrows indicate VAchT vesicles in cell neurites (Bar = 100 μm). Pictures are representative of at least 2 independent experiments.

We then measured intracellular Ach to determine the abilities of BMP-9 and its derived peptides to stimulate the synthesis of Ach in SH-SY5Y cells (Figure 3-7A). Only 1 nM SpBMP-9 ($p<0.01$) and pBMP-9 ($p<0.05$) significantly stimulated Ach synthesis after incubation for 3d without RA. The concentration of Ach in SH-SY5Y cells stimulated with 1 nM SpBMP-9 for 5d was also higher than that in unstimulated cells ($p<0.05$) or cells stimulated with 0.1nM BMP-9 ($p<0.01$). Cells incubated for 3d in the presence of RA plus 1nM BMP-9, 0.1 or 1nM pBMP-9 or SpBMP-9 contained more Ach than did the CTL, while those incubated with SpBMP-9 had the highest Ach concentration ($p<0.001$). For the SH-SY5Y cells stimulated with BMP-9, pBMP-9 or SpBMP-9 for 5d in the presence of RA, intracellular Ach levels, except for cells stimulated with 1nM of BMP-9, were similar to the CTL plus RA.
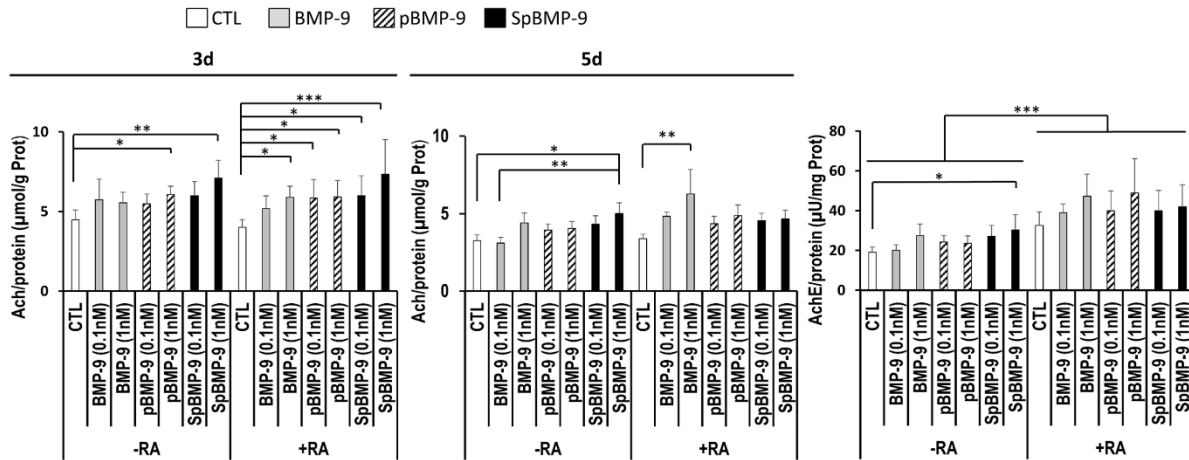
Figure 3-7 : Effect of pBMP-9 and SpBMP-9 on the intracellular Ach and AchE. (**A**) Intracellular Ach in SH-SY5Y cells stimulated with 0, 0.1 or 1 nM BMP-9, pBMP-9 and SpBMP-9 +/− 10 μM RA for 3d and 5d (**B**) AchE activity for SH-SY5Y cells stimulated with 0, 0.1 or 1 nM BMP-9, pBMP-9 and SpBMP-9 +/− 10 μM RA for 5d. Results are the means ± SEM of at least 4 independent experiments (*p ‹ 0.05, **p ‹ 0.01, ***p ‹ 0.001).

Effect of pBMP-9 and SpBMP-9 on acetylcholinesterase activity

We measured AchE activity to determine the action of SpBMP-9 on Ach breakdown (Figure 3-7B). AchE cleaves the neurotransmitter released into the synaptic clef to give choline and acetic acid; the choline is then recycled back into the cells. Only the SH-SY5Y cells incubated for 5d with SpBMP-9, but no RA, contained AchE activity that was significantly enhanced in comparison to the CTL ($p<0.05$) (Figure 3-7B). However, the presence of RA increase significantly in all experimental conditions the relative AchE activity compared to the cells without RA ($p<0.001$). In addition, cells incubated with BMP-9 or its derived peptides plus RA had AchE activities similar to the control plus RA.

3.3.6 pBMP-9 and SpBMP-9 increase the activation PI3K/Akt pathway and inactivate GSK3β

Since SpBMP-9 has been shown to induce a higher cholinergic differentiation of SH-SY5Y cells, we then evaluated the effect of SpBMP-9 on the activation state of GSK3β, a Tau kinase44. As GSK3β can be inactivated by Akt-catalysed phosphorylation of its Ser9 (Johnson et Stoothoff, 2004; Povellato *et al.*, 2014), we first analyzed the activation state of Akt in cells incubated with BMP-9, pBMP-9 or SpBMP-9 with and without RA.

Phosphorylation of Akt at Thr308

We analyzed the effect of equimolar concentration of BMP-9, pBMP-9 or SpBMP-9 (0.1nM) with or without RA on the phosphorylation of Akt at its catalytic site (Thr308) by immunostaining (Figure 3-8A). Cells stimulated with pBMP-9 or SpBMP-9 showed a higher level of fluorescence corresponding to pAkt (Thr308) compared to unstimulated cells or those incubated with BMP-9, as confirmed by relative fluorescence intensity analyses of these immunolabellings ($p < 0.001$). SpBMP-9 was also most effective than pBMP-9 ($p < 0.01$). In the presence of RA, Akt was phosphorylated at Thr308 in all experimental conditions. BMP-9 or pBMP-9 plus RA induced slightly less pAkt on Thr308 in comparison to RA alone ($p < 0.001$).

Inactivation of GSK3β by its phosphorylation at Ser9

We used Western blotting to assess phosphorylated GSK3β (pGSK3β) on Ser9 to determine whether Akt activation leads to inactivation of GSK3β (Figure 3-8B). BMP-9, without RA, had a transient effect as confirmed by densitometric analysis of bands corresponding to pGSK3β and standardized to that of β actin: pGSK3β (Ser9) increased between 0 and 60 min, plateaued and then decreased from 120 to 240min. Incubation with pBMP-9 and SpBMP-9 gave a different activation pattern. The pGSK3β (Ser9) in cells incubated with either pBMP-9 or SpBMP-9 increased from 0 to 240 min. Cells incubated with pBMP-9 or SpBMP-9 plus RA had similar time-dependent increases in pGSK3β (Ser9). pGSK3β (Ser9) was detected after 240 min in cells incubated with BMP-9, pBMP-9 or SpBMP-9 plus RA. We confirmed these observations by immunostaining for pGSK3β (Ser9) at 4 h (Figure 3-8C). pBMP-9 and SpBMP-9 induced a higher level of pGSK3β (Ser9) than BMP-9 or the CTL, as confirmed by relative fluorescence intensity analysis ($p < 0.001$ and $p < 0.01$ respectively). In addition, cells incubated with RA alone or combined with BMP-9 or its derived peptides contained more phosphorylated GSK3β on Ser9 than did cells stimulated without RA ($p < 0.001$).
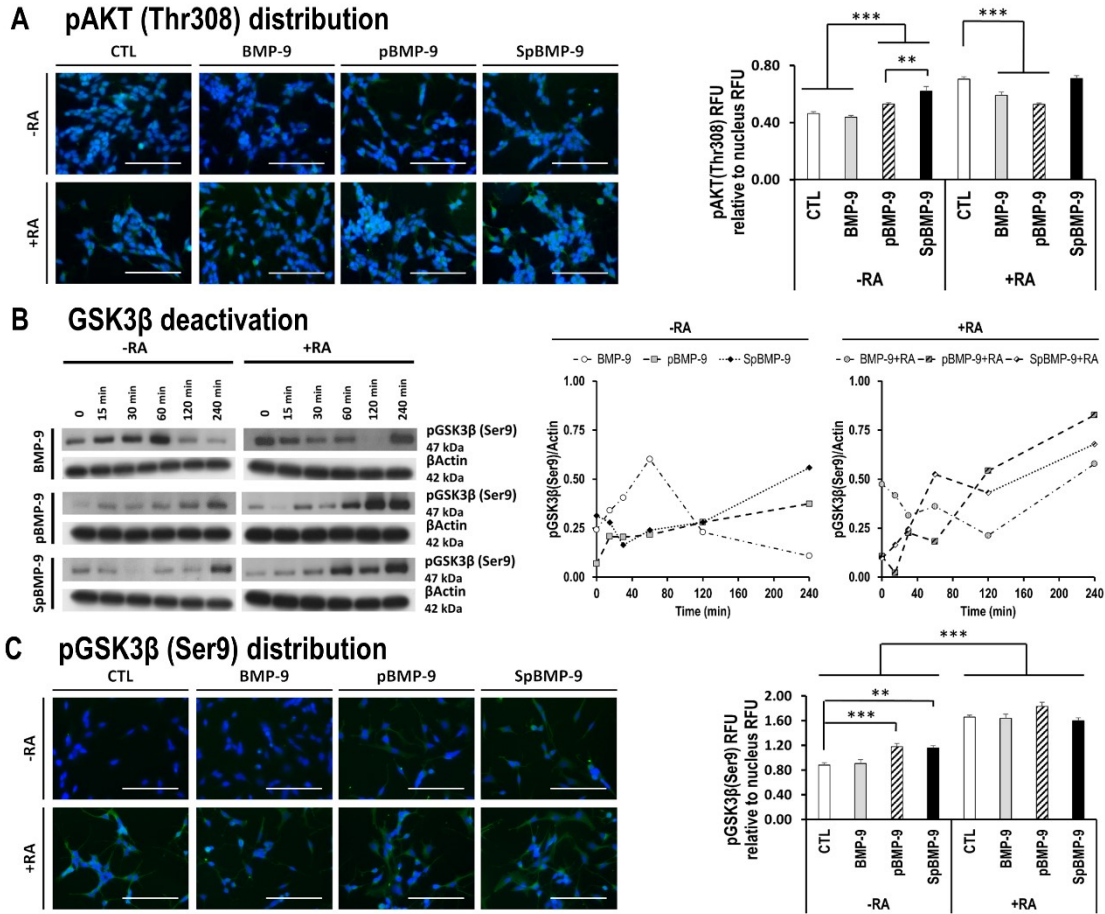
Figure 3-8 : Effect of pBMP-9 and SpBMP-9 on the PI3K/Akt/GSK3β pathway. (A) Merged pictures representative of at least 2 independent experiments showing immunostaining for pAkt (Thr308) (green) and nuclei (Hoechst, blue) of SH-SY5Y cells stimulated for 2 h with 0.1 nM BMP-9, pBMP-9 and SpBMP-9 +/− 10 μM RA (Bar = 100 μm) and pAkt(Thr308) fluorescence activity relative to the nucleus. (B) Western blots of phosphorylated GSK3β at Ser9 (pGSK3β) and densitometric analysis of pGSK3β bands standardized by actin showing the effect of 0.1 nM BMP-9, pBMP-9 and SpBMP-9 +/− 10 μM RA in SH-SY5Y cells after incubation for 0, 15, 30, 60, 120 and 240 min. Only cropped pictures of western blots were shown in order to allow a better comparison between experimental conditions. Complete gel pictures are available in the supplementary data file. (C) Merged pictures representative of at least 2 independent experiments showing immunostaining for pGSK3β (Ser9) (FITC, green) and nuclei (Hoechst, blue) in SH-SY5Y cells stimulated for 4 h with 0.1 nM BMP- 9, pBMP-9 and SpBMP-9 +/− 10 μM RA (Bar = 100 μm). Analysis of pGSK3β (Ser9) fluorescence intensity relative to the nucleus staining was also presented. Results are the means ± SEM (**p < 0.01, ***p < 0.001).

3.4 Discussion

The search for an effective treatment for AD has been, and continues to be, intense. The disease has three main hallmarks: cholinergic system dysfunction (Geula *et al.*, 2008), beta amyloid plaque accumulation (Murphy et LeVine 3rd, 2010) and protein Tau hyperphosphorylation (Alonso *et al.*, 1996; Augustinack *et al.*, 2002). Several studies have indicated that GFs may be potent therapeutic agents, particularly those of the TGF-β family, as they act on more than one hallmark simultaneously (Burke *et al.*, 2013; Lauzon *et al.*, 2015a; Lopez-Coviella *et al.*, 2000; Pascual-Lucas *et al.*, 2014; Roberson *et al.*, 2007; Schnitzler *et al.*, 2010; Zheng *et al.*, 2002). A recent study showed that the plasma of 99 AD patients had a deficient TGFβ/GDF/BMP transcriptome, proteasome and signaling (Jaeger *et al.*, 2016). This study also indicated that the TGFβ member, growth differentiation factor 3 (GDF3), could be a potent therapeutic agent against AD since it plays a role in adult neurogenesis (Jaeger *et al.*, 2016). BMPs are also part of the TGFβ family. They influence brain development and neurogenesis (Lauzon *et al.*, 2015a), (Hegarty *et al.*, 2013a; Mehler *et al.*, 1995, 1997) and so could have a great impact on brain degenerative diseases, particularly AD. A recent study found that BMP-4 expression increases in mice dentate gyrus as they age, leading to an increase of canonical Smad signalling and a decrease in BMP inhibitor Noggin which were associated with a decline in cognitive functions (Meyers *et al.*, 2016). It was also shown in mice that BMP signalling regulates the depressive behavior (Brooker *et al.*, 2016). Nonetheless, BMPs are classified into several subfamilies depending on their sequence homologies (Senta *et al.*, 2009). Other BMPs such as BMP-9, which are not part of BMP-4 subfamily, have shown promising effect in the context of AD (Burke *et al.*, 2013; Lopez-Coviella *et al.*, 2000; Schnitzler *et al.*, 2010). Lopez-Coviella *et al.* (2000) demonstrated that BMP-9 was the most efficient of the BMPs tested (BMP-2, -4, -6, -7, -9 and -12) at increasing the acetylcholine in septal neurons as well as their expression of neuron differentiation markers such as βIII-tubulin, ChAT and VAchT.

However, proteins do not readily cross the blood brain barrier, most are too big. We therefore used two small peptides (23 residues) derived from the knuckle epitope of BMP-9, corresponding to the sequence recognized by type II BMP receptor (BMPRII), to overcome the size limitation and reduce their cost, since short peptides of similar size (980Da–6.5 kDa) can

be delivered intranasally and successfully cross the blood brain barrier (Lochhead et Thorne, 2012). Our peptides sequences were based on the previous work of Saito *et al.* (2003, 2005) on BMP-2. They showed that peptides derived from the knuckle epitope of BMP-2 targeting Type II BMP receptor (BMPRII) could activate the canonical Smad signalling pathway in the context of bone repair in a similar manner as the whole protein. They have also demonstrated that the peptide could interact with both Type I and Type II BMP receptors.

We therefore show that pBMP-9 and SpBMP-9 with or without RA were able to activate the canonical Smad1/5 pathway in SH-SY5Y cells, a well-used *in vitro* model to study the effect of drugs against AD (Agholme *et al.*, 2010; Jämsä *et al.*, 2004). The SH-SY5Y cells expressed both BMPRIb and BMPRII receptors (Hegarty *et al.*, 2013a). The receptor BMPRII is also present in all the brain regions associated with memory and task learning (hippocampus and cortex) (Charytoniuk *et al.*, 2000). We have already shown in previous papers that pBMP-9 and SpBMP-9 were also able to activate the canonical Smad signalling pathway in a similar way than BMP-9 in murine mesenchymal stem cells C3H10T1/231 and murine preosteoblasts MC3T3-E1 (Beauvais *et al.*, 2016; Bergeron *et al.*, 2012). However, we found that the Smad1/5 activation and their nuclear translocation in SH-SY5Y cells in serum free medium appear lower with pBMP-9 or SpBMP-9 compared to BMP-9. Hegarty *et al.* (2013a) have shown that the Smad pathway activation in SH-SY5Y cells cultured in medium supplemented with 10% (v/v) foetal calf serum is required for BMP-2 induced neurite outgrowth. They also recently found that dynamin dependent endocytosis of BMP receptor complexes allows the maximal effect of BMP-2 (200 ng/mL) on neurite outgrowth in SH-SY5Y cells cultured in medium containing serum (Hegarty *et al.*, 2017). We confirmed that pBMP-9 and SpBMP-9 at concentrations in the physiological range of BMP-9 (~20 ng/mL) in human (Herrera et Inman, 2009) stimulate the neurite outgrowth in SH-SY5Y cells in serum free medium. However, despite a strong Smad1/5 activation and their nuclear translocation, SH-SY5Y cells stimulated by BMP-9 in serum-free medium were not able to develop significant neurite outgrowth within 5d in comparison to the control. The addition of RA is required to observe some increase in BMP-9 induced neurite outgrowth. Furthermore, BMP-9 at 1nM drastically alters the morphology of SH-SY5Y cells, making them more neuroblastoma-like. Further studies are therefore required to better understand by which signalling pathways pBMP-9 and SpBMP-9 induced neurite outgrowth in SH-SY5Y cells.

In addition, we verified that both BMP-9 derived peptides did not significantly decrease the cell number after incubation for 3d and 5d with or without RA. BMP-9 and its derived peptides with RA had also an effect on the metabolic activity of cells, which is unlikely caused by cell proliferation. However, other peptides, such as C-peptide (Li *et al.*, 2003) or other GFs like IGF-1, IGF-2 (Mattsson *et al.*, 1986) and NGF (Simpson *et al.*, 2001) have also shown to have simultaneous effects on the proliferation and neurite outgrowth of SH-SY5Y cells cultivated in serum-free or poor-serum conditions. We also found that RA alone had no significant effect on the metabolic activity of the SH-SY5Y cells. Some studies observed that RA can stop cell proliferation and promote differentiation in SH-SY5Y cells (Cheng *et al.*, 2013; Kim *et al.*, 2000; Teppola *et al.*, 2016). In contrast, it was also shown that differentiation of SH-SY5Y cells induced by sequential treatment using RA and brain-derived neurotrophic factor (BDNF) lead to an increase in ATP level and plasma membrane activity as well as an increase in metabolic need (Forster *et al.*, 2016). The impact of the increased metabolism induced by BMP-9 and its derived peptides in the presence of RA on subsequent SH-SY5Y cell behavior remains unclear.

We then confirmed that pBMP-9 and SpBMP-9 stimulate more the differentiation markers expression (MAP-2, NeuN and NSE) than the whole protein BMP-9. We also observed an increase in MAP-2 expression between 3d and 5d in cells stimulated by BMP-9 alone in serum free medium, despite no significant increase in neurite outgrowth at 5d compared to the control. Significant neurite outgrowth in the presence of BMP-9 may take longer time to occur and/or other factors may be required to promote neurite outgrowth (Dehmelt et Halpain, 2004; Huang *et al.*, 2013; Takahashi *et al.*, 2011). Other peptides derived from GFs, including neurotrophic factors such as NGF, stimulate neuronal differentiation (Colangelo *et al.*, 2008; Soumen *et al.*, 2012). Colangelo *et al.* (2008) have shown that 2 small peptides derived from functional sections of NGF can induce neuronal differentiation of PC12 cells just like the whole protein. We also found that RA alone favors neurite outgrowth and increased expression of neuronal markers. RA is known to induce SH-SY5Y differentiation (Andres *et al.*, 2013; Chakrabarti *et al.*, 2015; Cheung *et al.*, 2009; Lopes *et al.*, 2010). Lopes *et al.* (2010) showed that SH-SY5Y cells incubated for 4 and 10d in low (1% v/v) serum medium plus RA contained more terminal differentiation proteins like NSE and NeuN than did cells incubated without RA. RA also enhances the neuronal differentiation induced by pBMP-9 and SpBMP-9. The positive effect of

RA plus GFs has been observed using sequential treatment (Encinas *et al.*, 2000; Teppola *et al.*, 2016). Several studies have shown that SH-SY5Y cells stimulated with RA plus BDNF had increased neurite outgrowth and length synergistically and more early and late neuronal differentiation markers like MAP-2 and NSE (Encinas *et al.*, 2000; Teppola *et al.*, 2016).

Cholinergic system dysfunction is a major hallmark of AD and BMP-9 is known to promote the cholinergic differentiation of neuronal cells (Lopez-Coviella *et al.*, 2000). We have shown that both pBMP-9 and SpBMP-9 enhance the cholinergic phenotype of SH-SY5Y cells, with SpBMP-9 being the most efficient. The difference in the effects of SpBMP-9 and pBMP-9 might be due to small differences in their sequences. The two Cysteines in pBMP-9 are replaced by two Serines in SpBMP-9, based on the work of Saito *et al.* (2003) on BMP-2. They demonstrated that this small modification on BMP-2 derived peptide increased its affinity for type II BMP receptors, so increasing the osteogenic activity (Saito *et al.*, 2003). We find that 0.1nM SpBMP-9 stimulates the synthesis of ChAT, while SpBMP-9 at 1nM significantly increases (60%) intracellular Ach. It also enhances the production of VAchT and its distribution within the cell processes, indicating the accumulation of Ach. Adding RA to the culture system also enhances AchE activity and VAchT expression in all our experimental conditions. It is already known that RA directs SH-SY5Y cells towards the cholinergic phenotype and increases their AchE activity (Adem *et al.*, 1987; Sidell *et al.*, 1984).

We have also demonstrated that pBMP-9 and SpBMP-9 act on another AD hallmark by preventing the activation of GSK3β, a Tau kinase. pBMP-9 and SpBMP-9 (0.1nM) increase the activation of the PI3K/Akt pathway at 2h and inactivate GSK3β in a time dependent manner from time 0 to 4h. Activation of the PI3K/Akt pathway in the central nervous system regulates GSK3β and plays an important role in neuron polarity (Arimura et Kaibuchi, 2007). GSK3β is the most studied Tau kinase since it can be implicated in Tauopathies such as AD (Mookherjee et Johnson, 2001; Povellato *et al.*, 2014). Our immunolabelling studies indicate that 0.1 nM BMP-9 alone had no effect on PI3K/Akt at 2 h compared to the control, which agrees well with its transient effect on GSK3β deactivation via phosphorylation at Ser9. This observation also confirms our published results showing that the level of pGSK3β (Ser9) in SH-SY5Y cells incubated with 1nM BMP-9 alone gradually decreases from time 0 to 4h (Lauzon *et al.*, 2015a). In contrast, BMP-9 (1nM) plus RA can maintain the phosphorylation of GSK3β at Ser9 for over

4h (Lauzon *et al.*, 2015a). Indeed, the present study also revealed that RA alone or combined with BMP-9 or its derived peptides can activate the PI3K/Akt/GSK3β pathway. Cheung *et al.* (2009) found that SH-SY5Y cells incubated with RA for 7d contained more phosphorylated Akt than the control. RA also protects SH-SY5Y cells against proteasome inhibition-associated cell death via the PI3K/Akt pathway, which is common in AD (Cheng *et al.*, 2013). Since several studies have demonstrated that inhibiting GSK3β prevents Tau hyperphosphorylation at many sites (Jämsä *et al.*, 2004; Sayas *et al.*, 1999), pBMP-9 and SpBMP-9, with or without RA, might be effective anti-hyperphosphorylated-Tau agents that could also protect cells against oxidative stress programmed cell death

RA and other vitamin A derivatives have already been proposed for AD therapy, as has BMP-9. Our present results indicate that two peptides derived from the knuckle epitope of BMP-9, pBMP-9 and SpBMP-9, stimulate the differentiation of SH-SY5Y cells *in vitro* better than the whole protein. SpBMP-9 or pBMP-9 induced terminal neuron differentiation, promote cholinergic differentiation and inactivate GSK3β. Thus, BMP-9-derived peptides, especially SpBMP-9, alone or combined with RA are worth our attention since they act on several AD hallmarks simultaneously. Their small size should make them easier to deliver to the brain tissue. Further *in vitro* with neuronal stem cells and *in vivo* studies in appropriate mouse model are needed to confirm the effectiveness of these promising peptides.

3.5 Materials and methods

3.5.1 Material

Recombinant carrier-free human BMP-9 was purchased from R&D system Inc. (Minneapolis, MN, USA), pBMP-9 and SpBMP-9 were from EZBiolab (Carmel, IN, USA). Retinoic acid (RA) (Sigma Aldrich, ON, CA) was dissolved in pure ethanol, and kept frozen in the dark.

3.5.2 Cell culture

SH-SY5Y human neuroblastoma cells (ATCC® CRL-2266TM) were grown on treated polystyrene plates in DMEM/F12 (1:1) Glutamax (Gibco®, Grand Island, NY, USA) containing 1% (v/v) streptomycin (100 mg/mL) and penicillin (100U/mL) plus 10% (v/v) heat-inactivated

fetal bovine serum (FBS) (Wisent, St-Jerome, QC, CA) at 37 °C under a humidified 5% CO_2/air environment. Cells were passaged at 80% confluence using trypsin-EDTA (0.25%) (Gibco®, Grand Island, NY, USA). The trypsin was neutralized with 10% (v/v) FBS and cells were collected by centrifugation. In all experiments, cells were stimulated in serum-free culture medium with or without 10 µM retinoic acid (RA). The ethanol in which the RA was dissolved never exceeded 0.1% (v/v) of the medium volume.

3.5.3 Viability assay

SH-SY5Y cells were grown to 80% confluence on 24-well plates, washed with sterile phosphate-buffered saline (PBS) and incubated in serum-free culture medium with equimolar concentrations 0, 0.1 or 1nM of BMP-9, pBMP-9 or SpBMP-9 with or without 10µM RA for 1d, 3d and 5d. Viability was assessed using MTS CellTiter 96® Aqueous One Solution Cell Proliferation Assay kit following the manufacturer's instruction (Promega, Madison, WI, USA). Supernatants were collected after incubation with the MTS reagent and absorbance at 490nm was measured using a Biotek Synergy HT (Biotek® Instruments Inc., Winosski, VT, USA). Tests were performed in DMEM without phenol red (Gibco®, Grand Island, NY, USA) to avoid any spectrophotometric bias. Results are representative of at least two independent experiments performed in duplicate.

3.5.4 Morphology analysis

SH-SY5Y cells were grown to 80% confluence on 6-well plates, washed with sterile PBS and incubated with equimolar concentrations (0, 0.1 or 1 nM) of BMP-9, pBMP-9 and SpBMP-9 in serum-free medium with or without 10 µM RA for 5d. 5–10 representative pictures (magnification: 20X) were taken using an Eclipse TE200-S microscope coupled to a CCD camera (Zeiss AxioCam MRm, Car Zeiss, DE). Pictures were smoothed with a Gaussian filter to remove noise, with a Laplace high-pass filter and then with a median filter to detect and enhance neurites using an image analysis app (MatLab Image Processing Toolbox; MatLab 2007b, Mathworks, USA). The resulting images showing the neurite edges (blue lines) were superimposed on the original phase-contrast images. Original pictures were shrunk to fit within the figure panel. Each experiment was performed at least three times in duplicate.

3.5.5 Measurement of neurite length

Mean neurite lengths were determined from the normal size high resolution neurite-enhanced pictures taken for morphology analyses (20x magnification) using an image analysis app (Matlab Image Processing Toolbox; MatLab 2007b, Mathworks, USA). Briefly, neurite length was defined as the Euclidean distance in pixels or a combination of Euclidean distances between the cell body and the end of a neurite. The longest path was always chosen when a neurite had several branches. The length in pixels was then calibrated based on the length bar provided by the microscope image treatment software (AxioVision LE, Carl Zeiss, DE). For each experimental condition, 15 to 30 neurites were measured for each picture (4×10^{-3} cm²) and at least 5 pictures were analyzed per condition performed. Those steps were done three independent times in duplicate. The mean neurite length for each picture analyzed within a replicate was weighted by the number of measurement taken. For each independent experiment, the mean was calculated as the weighted mean (relative to the inverse of the variance) of each replicate. Finally, the overall mean was calculated as the weighted mean (relative to the inverse of the variance) of each of the three independent experiments. Overall, a total of at least 300 neurite length measurements were obtained for each experimental condition.

3.5.6 Western blotting and densitometric analysis of signaling protein and neuronal differentiation marker bands

Cells were grown to 80% confluence in 100 mm diameter tissue culture wells, washed with sterile PBS and stimulated with 0.1nM BMP-9, pBMP-9 or SpBMP-9 in serum-free medium for 3 - 5d for neuronal differentiation markers and between 0 to 240min for phosphorylated and total Smad 1/5/8 or phosphorylated GSK3β (Ser9). Treated cells were washed with cold sterile PBS containing 1mM orthovanadate (Sigma) and lysed with 50 mM Tris-HCl (pH 7.4) containing 1 mM orthovanadate (Sigma), 0.1% (v/v) SDS and a complete mini-protease inhibitor cocktail (Roche Diagnostics, Indianapolis, IN, USA). Equal amounts of protein (15 μg) were separated by SDS-PAGE and transferred to polyvinylidene fluoride (PVDF) membranes. Transferred proteins were incubated overnight at 4 °C with primary antibodies against βactin diluted 1:2,000 (Sigma), MAP-2 diluted 1:1,000 (Cell Signalling, MA, USA), phosphorylated and total Smad diluted 1:1,000 (Cell Signalling, MA, USA) or phosphorylated GSK3β (Ser9) diluted 1:1,000 (Cell Signalling, MA, USA). Membranes were

washed with PBS containing 0.1% (v/v) Tween 20 and incubated with anti-rabbit secondary antibodies (1:10,000) or anti-mouse secondary antibodies (1:10,000) coupled to horseradish peroxidase. Immunoreactive bands were visualized by chemiluminescence (ECL+Plus TM, GE Healthcare, Buckinghamshire, UK) and exposed to X-ray films (Thermo scientific, Rockford, Il, USA). Films were then digitalized using a high resolution scanner (Canon LidE 120, resolution: 600×600 DPI) and the densities of bands determined with an image analysis app (Matlab Image Processing Toolbox; MatLab 2007b, Mathworks, USA). Briefly, the intensities of all pixels in a user-defined region of interest (ROI) corresponding to a protein band were summed. The average background, the pixel intensities in an area near the ROI, was then subtracted from the ROI intensity to obtain the integrated density value (IDV). The same ROI dimensions were used for all bands in all experiments. The IDV of the bands of interest were normalized to their corresponding βactin bands, and then to the control without RA in order to account for the variability of each independent experiment. Results are representative of at least 2 independent experiments.

3.5.7 Immunolabelling of neurons differentiation markers, Smad, GSK3β and Akt

SH-SY5Y cells grown to 80% confluence on sterile microscope coverslips were washed with PBS and incubated with equimolar concentrations (0.1 or 1nM) of BMP-9, pBMP-9 or SpBMP-9 with and without 10 µM RA for 5d for neuron differentiation markers and with 0.1nM BMP-9, pBMP-9 or SpBMP-9 +/− 10µM RA for 2h (Akt) or 4h (GSK3β). Treated cells were fixed by immersion in 3% (w/v) paraformaldehyde (Sigma) for 15 min at room temperature and permeabilized by immersion in 0.5% (v/v) Triton X-100 (Sigma) for 5min. Non-specific sites were blocked by incubation with 1–3% (m/v) bovine serum albumin at 37°C for 30min. The coverslips/cells were then incubated at 37 °C for 30 min with primary antibodies: phosphorylated Smad1/5: anti-phospho-Smad 1/5 (Ser463/465) (41D10) rabbit mAb diluted 1:50 (Cell Signalling, MA, USA), βIII-tubulin: anti- βIII-tubulin IgG clone AA2+AlexaFluor 488 conjugated diluted 1:250 (EMD Millipore, Etobicoke, ON, CA), microtubule-associated protein 2 (MAP-2): anti-MAP2 monoclonal IgG clone AP20 diluted 1:120 (EMD Millipore, Etobicoke, ON, CA), neuron-specific antigen (NeuN): anti-NeuN monoclonal IgG diluted 1:50 (EMD Millipore, Etobicoke, ON, CA), NSE: anti-NSE monoclonal IgG clone 5E2 diluted 1:200

(EMD Millipore, Etobicoke, ON, CA), ChAT: goat anti-ChAT IgG diluted 1:100 (EMD Millipore, Etobicoke, ON, CA), VAchT: anti-VAchT polyclonal IgG diluted 1:100 (EMD Millipore, Etobicoke, ON, CA), Anti-phosphorylated Akt (Thr308) diluted 1:100 (Cell Signalling, MA, USA) or anti-phosphorylated GSK3β (Ser9) diluted 1:100 (Cell Signalling, MA, USA). The coverslips/cells were then washed with PBS and incubated (37 °C for 30min) with secondary antibodies: anti-mouse polyclonal IgG conjugated to AlexaFluor 488 diluted 1:400 (Life Technologies, Carlsbad, CA, USA), anti-rabbit polyclonal IgG conjugated to FITC diluted 1:100 (Sigma), anti-rabbit polyclonal IgG conjugated to Cy3 diluted 1:100 (Sigma) or anti-goat polyclonal IgG conjugated to FITC diluted 1:200 (Sigma). Cell nuclei and actin cytoskeleton were counterstained with Hoechst 33342 (5µg/mL) (Life Technologies, Carlsbad, CA, USA) and phalloidin-Alexa 594 diluted 1:100 (Life Technologies, Carlsbad, CA, USA) respectively. The coverslips/cell were mounted on microscope slides with 1:1 PBS-glycerol solution and at least 10 fluorescence pictures for each color filter per replicate were randomly taken using an Evos FL auto fluorescence microscope (Life Technologies, Carlsbad, CA, USA); magnification: 10X and 40X. Results are representative of at least 2 independent experiments. For each color channel, the same exposure time, digital gain and light intensity were used.

3.5.8 Measurements of immunofluorescence relative intensity

Immunofluorescence relative intensity quantification was assessed using a pixel-wise image analysis app (Matlab Image Processing Toolbox; MatLab 2007b, Mathworks, USA). Briefly, the relative fluorescence intensity (RFI) corresponding to the marker of interest in each picture was calculated as the cumulative sum of the value of each pixel above a pre-determined threshold. The cumulative sum of the given marker of interest of each image was then normalized in respect to the RFI of the staining corresponding to the nucleus following the same procedure. Since the pictures of every independent experiment had the same fluorescent light intensity, acquisition time and exposure for each channel, experimental condition could be compared together. At least 5 to 10 pictures with a magnification of 40X were analyzed per independent experiment for each experimental condition and at least 2 independent experiments were performed. The overall RFU mean (RFI of marker of interest/RFI of the nuclei) was determined as a weighted mean relative to the inverse of the variance of each independent experiment.

3.5.9 Intracellular acetylcholine and acetylcholinesterase assay

SH-SY5Y cells were grown to 80% confluence on 60-mm petri dishes, washed with sterile PBS and incubated for 3d and 5d with equimolar concentrations (0, 0.1 or 1 nM) of BMP-9, pBMP-9 or SpBMP-9 in serum-free medium with or without 10 µM RA. Incubated cells were washed with cold sterile PBS and lysed at 4°C with 50 mM Tris-HCl (pH 7.4) containing complete mini-protease inhibitor cocktail (Roche Diagnostics, Indianapolis, IN, USA). Supernatants were collected and protein concentrations, OD at 280 nm, were measured with Biotek Synergy HT with a Take3 micro-volume plate adaptor and Gene5 data analysis software (Biotek® Instruments Inc., Winosski, VT, USA). Acetylcholine (Ach) concentration and acetylcholinesterase (AchE) activities were assayed by fluorescence detection using Amplex® Red Acetylcholine/Acetylcholinesterase Assay Kit (Life Technologies, Carlsbad, CA, USA) following the manufacturer's instructions. Briefly, Ach was measured by mixing samples with choline oxidase, horseradish peroxidase, Amplex Red® reagent and excess AchE; AchE activity was measured with excess Ach. AchE catalyzes the hydrolysis of Ach to acetate and choline, and choline oxidase then breaks down the choline into betaine aldehyde and oxygen peroxide. The resulting oxygen peroxide is reduced by horseradish peroxidase and this reacts with Amplex Red® to give a fluorochrome. The fluorescence, measured with a spectrophotometer (Safire2, Tecan US inc., NC, USA), is a measure of the AchE activity. The Ach concentrations and AchE activities were normalized to the protein content and then to their respective controls. At least four independent experiments were performed.

3.5.10 Statistical analysis

Statistical analyses were performed with Excel (Excel 2010®). Analyses of variance (ANOVA) used confidence limits of 95% followed by a Tukey post-hoc test to determined significant differences within treatments. Only differences with a $p < 0.05$ were considered significant.

3.6 Acknowledgments

3.7 Author contributions

CHAPITRE 4: SYSTÈME DE LIBÉRATION DE SPBMP-9

4.1 Informations relatives à l'article

Titre original: Characterization of Alginate/Chitosan-based nanoparticles and mathematical modelling of their SpBMP-9 release inducing neuronal differentiation of human SH-SY5Y cells

Titre français : Caractérisation de nanoparticules à base d'Alginate/Chitosane et modélisation mathématique de leur libération de SpBMP-9 induisant la différenciation neuronale de cellules humaines SH-SY5Y

Auteurs et affiliations :

- M.-A. Lauzon : Étudiant au doctorat en génie chimique, Département de génie chimique et de génie biotechnologique, Université de Sherbrooke
- B. Marcos : Professeur titulaire, Département de génie chimique et de génie biotechnologique, Université de Sherbrooke
- N. Faucheux : Professeur titulaire, Département de génie chimique et de génie biotechnologique, Université de Sherbrooke. Affiliation au Centre de Recherche Clinique du Centre Hospitalier Universitaire de Sherbrooke, 12e Avenue N, Sherbrooke, Québec, J1H 5N4, Canada

Date d'acceptation : S/O

État de l'acceptation : Article en révision

Revue : *Carbohydrate Polymers*

Lien d'accès : S/O

Contributions à la thèse :

Cet article contribue à la thèse en présentant les résultats du troisième objectif du projet de doctorat qui consistait à faire la synthèse et la caractérisation d'un système de libération de

SpBMP-9 sous forme de nanoparticules à base d'alginate et de chitosane. Les éléments suivants sont présentés :

- La synthèse d'un système de libération de SpBMP-9 à base de nanoparticules composées d'alginate et de chitosane et leur caractérisation : distribution de taille, pourcentage d'encapsulation et masse de peptides encapsulée.
- Le suivie et la modélisation mathématique des cinétiques de libération par le développement d'un modèle mécanistique prenant en considération la distribution de taille des NPs obtenue expérimentalement. Les paramètres du modèle mathématique sont estimés à l'aide d'un algorithme méta-heuristique stochastique et les phénomènes de transfert de masse prédominant sont identifiés.
- La capacité de cellules humaines SH-SY5Y à survivre au contact des NPs d'alginate/chitosane ainsi que l'effet de la libération du peptide sur la capacité des cellules SH-SY5Y à se différencier en neurones matures.

Résumé anglais:

The incidence of brain degenerative disease such as Alzheimer's disease (AD) will increase as the world population is ageing. While current AD treatments have only a transient effect, there are many evidences indicating that some growth factors, such as BMP-9, may be used to treat AD. However, growth factors cannot readily access the brain because of their size and the presence of the blood brain barrier. We have therefore developed a small peptide derived from BMP-9, SpBMP-9, which can promote the differentiation of cholinergic neurons and inactivate GSK3beta, a Tau kinase. Here, we investigated the potential of a nanoparticle-based delivery system of SpBMP-9, made of alginate and chitosan (Alg/Chit NPs), as a new therapeutic strategy against AD. The Alg/Chit NPs size distribution revealed NPs with an average diameter of ~240 nm. The encapsulation efficiency of SpBMP-9 was ~ 70% of the initial peptide mass loading. Release kinetics of SpBMP-9 were performed in physiological conditions and modelled with a mechanistic framework that took into account the size distribution of Alg/Chit NPs. The release of SpBMP-9 revealed to be mostly diffusive, but there were interactions between the peptide and the alginate chains. The Alg/Chit NPs could also increase the viability of SH-SY5Y cells in comparison to the control. Finally, the SpBMP-9 released from Alg/Chit NPs promoted the SH-SY5Y differentiation into mature neurons as

demonstrated by a higher neurite outgrowth and an increased expression of the neuronal markers NSE and VAchT. In conclusion, the nano-scale SpBMP-9 delivery system made of Alg/Chit may be a promising therapeutic strategy against AD.

Résumé français:

L'incidence des maladies dégénératives du cerveau comme la maladie d'Alzheimer (AD) va s'accroître avec le vieillissement de la population. Alors que les traitements actuels contre l'AD possèdent seulement un effet transitoire, il y a de plus en plus de preuves qui indiquent que certains facteurs de croissance, tels que la BMP-9, pourraient être utilisés pour traiter l'AD. Toutefois, les facteurs de croissance ne peuvent pas accéder facilement au tissu cérébral en raison de leur taille et de la présence la barrière hématoencéphalique. Nous avons ainsi développé un petit peptide dérivé de la BMP-9, le SpBMP-9, qui peut favoriser la différenciation de neurones cholinergiques et inactiver la GSK3beta, une Tau kinase. Ici, nous avons étudié le potentiel d'un système de libération de SpBMP-9 à base de nanoparticules, fabriquées à partir d'alginate et de chitosane (Alg/Chit NPs), pour être utilisé comme nouvelle stratégie thérapeutique contre l'AD. La distribution de taille des Alg/Chit NPs a révélé des NPs avec un diamètre moyen de ~240 nm. L'efficacité d'encapsulation du SpBMP-9 était de ~70% de la masse initiale de peptides. Les cinétiques de libération de SpBMP-9 ont été réalisées dans des conditions physiologiques et modélisées avec un modèle mathématique qui prenait en considération la distribution de taille des Alg/Chit NPs. La libération de SpBMP-9 était majoritairement diffusive, mais il y avait des interactions entre le peptide et les chaînes d'alginate. Les NPs pouvaient également augmenter la viabilité de cellules SH-SY5Y en comparaison avec le contrôle. Finalement, le SpBMP-9 libéré à partir d'Alg/Chit NPs, a favorisé la différenciation de SH-SY5Y en neurones matures tel que démontré par une croissance plus élevée des neurites et l'augmentation de l'expression des marqueurs de différenciation neuronaux NSE et VAchT. En conclusion, le système de libération de SpBMP-9 à l'échelle nanométrique pourrait être une stratégie thérapeutique prometteuse contre l'AD.

4.2 Introduction

The World Health Organization reported that there were, as per May 2017, more than 40 million people worldwide diagnosed with dementia (World Health Organization, 2017). Alzheimer's disease (AD) is the most common type of dementia, accounting for about 60% to

80% of cases. In the USA only, it is believed that people suffering from AD will reach 16 million by 2050 (Alzheimer's Association, 2017). This number is likely to increase further in the years to come due to population ageing. Unfortunately, treatments such as rivastigmine, galantamine or memantine, or others currently under investigation, do not stop the progression of the disease and rather show a transient effect (Giacobini et Gold, 2013; Tricco *et al.*, 2013). The lack of efficient treatments thus results in a huge social and economic burden that was estimated to be around hundreds of billions US$ in 2017in USA only (Alzheimer's Association, 2017).

AD is characterized by three pathophysiological symptoms also known as therapeutic targets: 1) cholinergic system dysfunction (Geula *et al.*, 2008), 2) senile plaque accumulation composed of aggregated amyloid beta peptides (Murphy et LeVine 3rd, 2010) and 3) hyperphosphorylation of Tau protein resulting in neurofibrillar entanglements (Alonso *et al.*, 1996; Augustinack *et al.*, 2002). The use of growth factors (GFs), naturally present in the healthy brain, might restore dysregulated cell signalling observed in an AD brain and act on one or more therapeutic targets (Burke et al., 2013; Lauzon, Daviau, Marcos, & Faucheux, 2015a; Lopez-Coviella et al., 2000, 2002, 2005; Matrone, Ciotti, Mercanti, Marolda, & Calissano, 2008; Mellott, Pender, Burke, Langley, & Blusztajn, 2014; Pascual-Lucas et al., 2014; Schnitzler et al., 2010). Among those GFs, bone morphogenetic protein 9 (BMP-9) has shown interesting therapeutic properties in mouse models as it can act on several AD symptoms by decreasing senile plaque formation while promoting cholinergic system maintenance (Burke *et al.*, 2013; Lopez-Coviella *et al.*, 2000; Wang *et al.*, 2017). However, GFs like BMP-9 are large proteins (>10 kDa) that can hardly be systemically addressed to the brain tissue because of the presence of several natural barriers such as the blood brain barrier (BBB) (Alyautdin *et al.*, 2014). One way to overcome the BBB is to use intranasal injections because of the high capillary density, the large surface area, the proximity to the brain, and the high endocytosis of nasal endothelial cells (Dhuria *et al.*, 2010; Fonseca-Santos *et al.*, 2015; Illum, 2003; Lauzon *et al.*, 2015b; Lochhead & Thorne, 2012). For instance, Wang *et al.* (2017) have recently shown that BMP-9 could be assimilated, to a certain extent, to the cortex and the hippocampus of APP/PS1 mice over-expressing β-amyloid peptides when injected intranasally and thus reduced senile plaque accumulation as well as Tau hyperphosphorylation and ameliorate cognitive deficits. Nonetheless, despite its interesting therapeutic effect on AD symptoms, BMP-9 remains expensive to produce and purify (Poynton et Lane, 2002). We have therefore developed small

peptides (pBMP-9 and SpBMP-9) derived from the knuckle epitope of BMP-9, corresponding to the amino acid sequence recognized by the type II BMP receptor (Beauvais, Drevelle, Lauzon, Daviau, & Faucheux, 2016; Bergeron et al., 2009; Lauzon, Drevelle, & Faucheux, 2017). Those peptides are 300-times less expensive to produce than the native protein. We have recently shown, using human neuroblastoma SH-SY5Y cells, that those peptides, and especially SpBMP-9, could induce a neuronal differentiation to a greater extent than did the native protein (BMP-9) as shown by more and longer neurite outgrowth and increased expression of specific markers such as MAP-2, NSE and NeuN (Lauzon et al., 2017). In addition, both pBMP-9 and SpBMP-9 could increase the expression of intracellular acetylcholine and inactivate GSK3beta, a well-known Tau kinase (Lauzon et al., 2017) . However, once injected into the body, the delivery of such peptides to the brain remains a great challenge since they could be subjected to rapid clearance and a lack in brain accumulation specificity. To bypass those issues, a delivery vehicle is required. In the case of a drug released to the brain, delivery systems at the nanoscale level like nanoparticles (NPs) with an average size of a couple of hundred nanometres meant to be injected in the nasal cavity are preferred since they can more readily access the brain tissue and be diffused more easily within it (Dhuria et al., 2010; Illum, 2003; Lauzon et al., 2015b; Lochhead & Thorne, 2012).

Among the natural and synthetic materials currently under investigation for nanoscale delivery systems, polysaccharides such as chitosan and alginate display many interesting features. They are bioresorbable, well tolerated by the human body, and have good muco-adhesive properties and high encapsulation efficiency (Gavini et al., 2009; Kumar, Muzzarelli, Muzzarelli, Sashiwa, & Domb, 2004; Nagpal, Singh, & Mishra, 2010). Chitosan is a polycationic polysaccharide derived from chitin (Kumar et al., 2004; Nagpal et al., 2010). It is well known to increase absorption and cellular uptake by widening, in a transient manner, the tight junctions (Kumar *et al.*, 2004). Chitosan NPs of hundreds of nm in size have been used to deliver rivastigmine intranasally to the brain in mouse and rat models. Rivastigmine is an FDA-approved drug against AD (Fazil et al., 2012; Nagpal, Singh, & Mishra, 2013). These chitosan NPs did not induce any adverse effects and increased the brain uptake in comparison to intravenous injection. Alginate is a poly-anionic co-polymer extracted from algae composed of D-mannuronic and L-guluronic acids. L-guluronic acid subunit is responsible for intra- and inter-chain reticulation of alginate in the presence of calcium ions. The concentration of calcium

ions was shown to regulate the encapsulation and the release rate of encapsulated bovine serum albumin (BSA) (Anal *et al.*, 2003). Alginate oligosaccharides have been shown to reduce oxidative stress and apoptosis in PC-12 rat neuronal cells and promote cell survival and proliferation in the human colorectal adenocarcinoma cell line (HT-29) (Biswas *et al.*, 2015; Borges *et al.*, 2006; Guo *et al.*, 2016; Tusi *et al.*, 2011). The alginate and chitosan combination was used to form composite NPs by means of ionotropic gelation (nano-emulsion). These alginate/chitosan composite NPs (Alg/Chit NPs) showed an increase in cellular uptake in mice hippocampal cells HN9.10e and intracellular delivery of FITC-ovalbumin in rat Peyer's patches, while they induced a lower cytotoxicity in comparison to chitosan NPs alone (Anal *et al.*, 2003; Borges *et al.*, 2006; Ciofani *et al.*, 2008). Alg/Chit NPs have also been used to encapsulate molecules such as insulin, a peptide of 5.8 kDa, to target diabetes through an oral treatment (Goycoolea *et al.*, 2009; Mukhopadhyay *et al.*, 2015). Alg/Chit NPs also showed good muco-adhesive properties, higher resistance to low pH and high peptide encapsulation efficiency with no apparent cytotoxicity (Goycoolea *et al.*, 2009; Mukhopadhyay *et al.*, 2015). Such properties might be transposable for intranasal delivery of SpBMP-9, targeting the brain tissue in the context of AD.

Based on those elements, we hypothesized that a composite alginate/chitosan based nano-scale delivery system could encapsulate efficiently the small peptide derived from BMP-9, SpBMP-9, which will ensure its sustained release without affecting significantly its bioactivity. We, therefore, prepared an Alg/Chit NPs-based delivery system of SpBMP-9 using ionotropic gelation in mild aqueous conditions. After the characterization of the Alg/Chit NPs size and distribution, their capacity to encapsulate the peptide SpBMP-9 was also analyzed. We then modelled the release kinetics of SpBMP-9 mechanistically and estimated the diffusivity and the overall mass transfer coefficient. A mathematical model framework that took into account the size distribution of the Alg/Chit NPs was developed and the release kinetics were solved for each size class. Such an approach has not been widely used in the domain of nanoscale delivery system mathematical modeling. We then verified that the Alg/Chit NPs were not cytotoxic. Finally, the efficiency of the released SpBMP-9 was verified on neuronal differentiation of human SH-SY5Y cells, which is a well-known mature neuroblastoma cell line that has been used several times in the context of AD (Agholme *et al.*, 2010; Jämsä *et al.*, 2004; Koriyama *et al.*, 2015).

4.3 Experimental section

4.3.1 Materials

SpBMP-9 (2.36 kDa, with a final purity of 98%) was chemically synthesized by EZBiolab (Carmel, IN, USA) and was resuspended in milli-Q sterile water at a concentration of 10 mg/mL and stored at -80°C for further use. The SH-SY5Y cells (CRL-2266) were purchased from ATCC (Manassas, VA, USA) and were kept frozen in liquid nitrogen prior to use. Culture media (DMEM/F12 1:1), trypsin-EDTA (0.25%) and penicillin-streptomycin (10,000 U/mL) antibiotics were purchased from Gibco (ThermoFisher, Ca), whereas foetal bovine serum was purchased from Wisent Bioproduct inc. (St-Bruno, Ca). AlamarBlue cytotoxicity assay, calcium chloride and high molecular weight (HMW) chitosan with a deacetylation percentage of 85% with a molecular weight of >310 kDa were purchased from Sigma (Sigma-Aldrich, Ca). Sodium alginate with a guluronic acid to mannuronic acid ratio of 2:1 (determined by NMR) with a molecular weight of ~110 kDa (determined by GPC) was kindly offered by Kimica inc. (Tokyo, Japan). Primary antibodies against NSE and VAchT (C-terminals) produced in rabbits were purchased from Sigma (Sigma-Aldrich, Ca). Secondary antibodies against rabbits conjugated to Alexa Fluor® 488 were purchased from Cell Signalling (Cell Signalling Technology, Denver, MA, USA).

4.3.2 Nanoparticle synthesis

NPs were synthesized using an ionotropic gelation method as described in Figure 4-1 based on previous work of Haque *et al.* (2014). Briefly, sodium alginate was dissolved in ultrapure water at a concentration of 1 mg/mL. The pH was then adjusted to 5.1 using HCl at 1N. Calcium chloride was dissolved at a concentration of 18 mM (~2mg/mL) in milli-Q water. HMW chitosan was dissolved at a concentration of 1 mg/mL in 1% (v/v) acetic acid. The pH was then adjusted to 5.6 using NaOH solution at 1N. All solutions were sterile-filtered (0.22 μm) prior to use. Under aseptic conditions, calcium chloride ($CaCl_2$) solution with a final Alg:$CaCl_2$ ratio of 5:1 (w/w) was added dropwise with a 25 gauge syringe needle in a sodium alginate solution under vigorous magnetic agitation. For experiments involving SpBMP-9, different volumes of the concentrated solution of the peptide (10 mg/mL) were added to the sodium alginate solution prior to calcium chloride, and left to agitate for 5 min in order to favour

the interaction between the negatively charged alginate polymer chains and the positively charged SpBMP-9. The solution was then vigorously agitated for 30 min in order to form a pre-gel. HMW chitosan solution was then carefully added dropwise with a final Alg:Chit mass to mass ratio of 4:1 using, once again, a 25 gauge syringe needle. At this point, an opalescent solution appeared, indicative of the formation of NPs. The solution was then covered with parafilm to avoid evaporation and magnetically agitated overnight to cure the NPs and standardize their size. The NP solution was then transferred to low adhesion micro-centrifuge tubes and centrifuged at 20,000 x g (10°C) for 30 min. The supernatant was either discarded or further used to determine the peptide encapsulation efficiency using high-performance liquid chromatography (HPLC).
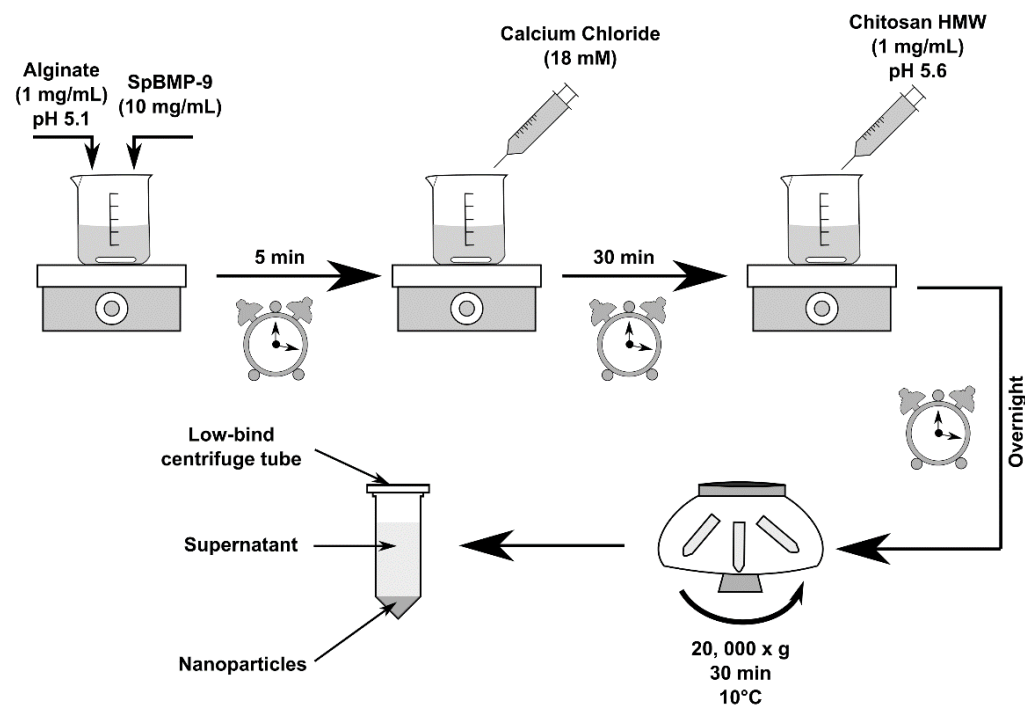
Figure 4-1 : Alg/Chit NPs synthesis

4.3.3 Size distribution and nanoparticle morphology

NP pellet following the centrifugation was re-suspended in deionized water. The solution was immediately used to measure the size distribution with laser diffraction analysis or scanning electron microscopy (SEM). For laser diffraction analysis, 20 mL of re-suspended NPs per experiment were poured into the analytic chamber (200 mL) of the laser granulometry Malvern Mastersizer 2000 (Malvern Instruments Canada, Montreal, Ca). Deionized water was added to fill the remaining volume of the analysis reservoir and an ultrasonic probe with low intensity was used to break any aggregates. For SEM observations, 20 µL of re-suspended NP solution was diluted 1:5 (v/v) and poured on a stainless-steel sample holder. The liquid was allowed to completely dry under the biologic hood for 1 h. The samples were then metallized with gold/palladium and high-resolution images were taken at 30 kV using a S4700-Hitachi field emission scanning electron microscope (Hitachi High-Technologies Canada, Toronto, Ca).

4.3.4 Percentage of peptide encapsulation

The supernatant following centrifugation of the NP solution was used to determine the remaining amount of SpBMP-9 using an HPLC. Briefly, 500 µL of supernatant were placed in a glass vial containing 1 µL trifluoroacetic acid (TFA). The SpBMP-9 concentration was determined by a ProStar analytical HPLC system (Model 335, Varian, Agilent Technology) and a Phenomenex C18 column equipped with a fluorescence detector (Model 363, Varian, Agilent Technology) ($\lambda_{excitation}$ 274 nm, $\lambda_{emission}$ 310 nm). The elution gradient was composed of an increasing fraction of (A) acetonitrile containing 0.1% (v/v) TFA over (B) water containing 0.1% (v/v) TFA with a total flow rate of 1 mL/min. Data were analyzed by using the Galaxie Chromatography Data System v 1.9.301.220. Sample concentrations were calculated by comparing the area under the eluted peak with those of a standard curve of SpBMP-9 (from 312.5 ng/mL to 20, 000 ng/mL). A 4th degree polynomial function was used to model the standard curves, because for a wide concentration range it is more accurate (Hinshaw, 2002). The linear regression used to estimate the model parameters (β) was weighted in function of the inverse of the variance to account for the high variability in the lower and higher concentrations:

$$\beta = (X^T W X)^{-1} X^T W Y \qquad\qquad (4\text{-}1)$$

Where W is a diagonal matrix and each element of the diagonal is $\frac{1}{\sigma^2}$

Since 4th degree polynomial function has more than one root, the *Regula Falsi* method, constrained within the concentration range of the standard curve, was used to estimate the concentration. The percentage of peptide encapsulation was calculated as the difference between the initial and the remaining peptide mass over the initial mass:

$$Efficiency_{encapsulation} = 100 \left[\frac{M_{initial} - M_{remaining}}{M_{initial}} \right] \qquad (4\text{-}2)$$

Where $M_{remaining}$ was the total mass remaining in the supernatant and M_{∞} was the initial loaded mass

4.3.5 Release kinetics assays

Release kinetics of SpBMP-9 were performed using Alg/Chit NPs prepared with a solution of 10 µg/mL of peptide. Following the centrifugation at 20,000 x g, 2 pellets corresponding to 1.35 mL of NP solution each were pooled together and re-suspended in 1 mL of sterile PBS tempered at 37°C in a low-protein binding microcentrifuge tube. These tubes were then incubated in a humidified cell-culture incubator (Forma Series II, water jacket CO_2 incubator, Thermo Electron Corporation, USA) set to 37°C under an atmosphere containing 5% CO_2 for different time points between 0 to 144h. After 0h, 0.5h, 1h, 2h, 3h, 4h, 8h, 24h, 72h, and 144h, the tubes were centrifuged at 20,000 x g (10°C) for 30 min. Supernatants were collected, and 500 µL were transferred to an HPLC glass vial containing 0.5 µL of TFA. Pellets were suspended with a fresh PBS solution tempered at 37°C and put back to the incubator for the next sampling. The concentration of SpBMP-9 in the supernatant was determined with the HPLC procedure following the same steps as described above. The amount of peptide released was determined as a percentage of the cumulative mass release described by the equation below.

$$\frac{M_t}{M_{\infty}} = 100 \left[\frac{\sum_{i=0}^{t} M_i}{M_{initial}} \right] \qquad (4\text{-}3)$$

Where M_t was the total mass of released SpBMP-9 and M_{∞} was the initial loaded mass.

After 144h of incubation, NPs were dissolved in NaOH 1N, centrifuged at 20, 000 x g for 30 min and the remaining SpBMP-9 concentration was determined by HPLC as described above. The SpBMP-9 recovery percentage ($M_{recovery}$) was defined as the difference between the final cumulative mass release (M_{cumul}) observed plus the mass recovery after nanoparticles dissolution over the initial loaded mass ($M_{encapsulated}$):

$$M_{recovery}(\%) = 100 \left[\frac{M_{cumul} + M_{recovered}}{M_{encapsulated}} \right] \tag{4-4}$$

Release kinetics were also evaluated according to Korsmeyer-Peppas' model in order to determine the driving mass transfer phenomena (Korsmeyer *et al.*, 1983):

$$\frac{M_t}{M_\infty} = kt^n \tag{4-5}$$

According to this model, a value of parameter $n \le 0.43$ is indicative of a Fickian diffusion.

4.3.6 Mathematical modelling

The mathematical framework was developed considering the following assumptions:

- The NPs were perfectly spherical
- The peptides molecules encapsulated were uniformly distributed along the volume of the NPs
- The peptide concentration was below the saturation, so each NP can be viewed as a delivery system having a monolithic dispersion
- Diffusion was the major mass transport phenomenon and was isotropic, i.e. happening only in the radial direction, whereas variation in the azimuthal and polar directions were both considered null over space and time dimension
- The diffusion coefficient was constant over time and space
- NPs used were already swollen, so swelling was negligible as it was already observed in similar systems (Rahaiee *et al.*, 2017)
- NPs did not undergo any erosion within the period investigated, which was observed following a similar synthesis protocol (Anal *et al.*, 2003)
- Interactions between SpBMP-9 (positively charged) and alginate chains (negatively charged) were mostly due to electrostatic interactions and drive the release at the surface of the NP

Based on those assumptions, a mathematical framework was developed using Fick's second law of diffusion for spherical coordinates:

$$\frac{\partial C_{SpBMP9}}{\partial t} = \frac{D_{eff}}{r^2} \left[\frac{\partial}{\partial r} \left(r^2 \frac{\partial C_{SpBMP9}}{\partial r} \right) \right] \tag{4-6}$$

With the following initial conditions:

$$\text{At } t = 0, \forall r \in [0, R] \rightarrow C_{SpBMP9}(0, R) = C_{initial} \tag{4-7}$$

Then, the following Newmann and Robin boundaries conditions were used:

$$\left(\frac{\partial C_{SpBMP9}}{\partial r}\right)_{r=0} = 0 \tag{4-8}$$

And

$$\left(\frac{\partial C_{SpBMP9}}{\partial r}\right)_{r=R} = k\left(C_{SpBMP9}|_R - C_{eq}\right) \tag{4-9}$$

$$\text{Where } C_{eq} = C_{initial}\left[1 - \left(\frac{M_t}{M_\infty}\right)_{eq}\right] \tag{4-10}$$

The mass flux at the centre was assumed null. In addition, since alginate and SpBMP-9 carry opposite charges at physiological pH, the release at the surface of the NP was driven by the concentration gradient between the peptide and the pseudo-equilibrium concentration. We have already observed and modelled this phenomenon in the case of a similar peptide (pBMP-9) released from a collagen hydrogel (M-A Lauzon *et al.*, 2014).

4.3.7 Mathematical model resolution

The above equations were used to model the release mechanisms and solved them for a finite difference implicit Crank-Nicolson scheme in which the first and second partial derivative can be expressed by:

$$\left(\frac{\partial f}{\partial t}\right) \approx \left(\frac{f_j^{l+1} - f_j^l}{\Delta t}\right) \tag{4-11}$$

$$\left(\frac{\partial f}{\partial x}\right) \approx \frac{1}{2}\left(\frac{f_{j+1}^{l+1} - f_{j-1}^{l+1}}{2\Delta x} + \frac{f_{j+1}^l - f_{j-1}^l}{2\Delta x}\right) \tag{4-12}$$

$$\left(\frac{\partial^2 f}{\partial x^2}\right) \approx \frac{1}{2}\left(\frac{f_{j+1}^{l+1} - 2f_j^{l+1} + f_{j-1}^{l+1}}{\Delta x^2} + \frac{f_{j+1}^l - 2f_j^l + f_{j-1}^l}{\Delta x^2}\right) \tag{4-13}$$

Where "l" stands for time steps and "j" stands for spatial steps

The Crank-Nicolson scheme is unconditionally numerically stable and, giving a small time step "l", will provide the most accurate resolution compared to other finite difference approaches. In addition, since the NPs had a given size distribution, we partitioned the size distribution into classes based on laser diffraction results and solved the model for each of those classes. To do so, the following assumptions were made:

- The amount of SpBMP-9 encapsulated was proportional to the particle volume

- Changes in NP size is negligible as a result of peptide released, so the size distribution was constant

- The number of nods (space steps "r") was proportional to the size of the class of NPs

- The NP distribution was the same in each element of volume releasing medium.

The time-space resolution process can thus be described as followed, where for each size class, a matrix system has to be solved for each time steps:

$$\forall i \in [1, n_{classes}] \text{ solve } C^{l+1}|_{classi} = A^{-1}[BC^l|_{classi} + E] \tag{4-14}$$

Where A and B were tridiagonal matrices corresponding to time equal "l+1" and time "l" respectively, whereas E was a vector containing the boundaries conditions.

At each time steps, the total amount of released SpBMP-9 (M_t) was estimated using the following discrete trapezoidal method:

$$M_t = M_\infty - \left[\frac{4N_{particles_i}\pi}{3} \sum_{i=1}^{n_{classes}} \sum_{j=0}^{R} \left(\frac{C_{j+1,i}^l + C_{j,i}^l}{2} \right) \left(r_{j+1,i}^3 - r_{j,i}^3 \right) \right] \tag{4-15}$$

$$\text{Where } N_{particlesi} = \sum_{i=1}^{n_{classes}} N_{subclassesi} \in [i, i+1[\tag{4-16}$$

Finally, the following conditions were used to solve the mathematical model:

- Number of class: 11 (from 148 nm to 2350 nm based on laser diffraction results)

- Time steps: 0.5 min

- Total time: 8640 min (144h)

- Nods number for the smallest NP size class: 10

- Nods number for the biggest NP size class: 160

4.3.8 Parameter estimation

Once the mathematical framework was set, we used an evolutionary algorithm (genetic algorithm), which is a stochastic global optimization technic. An algorithm on Matlab (MatLab 2007b, Mathworks, USA) was programmed and used to estimate the diffusion coefficient "D_{eff}" and the overall mass transfer coefficient "k" from the experimental results. An evolutionary algorithm is a global optimization method that allows the search of global minimum or

maximum either in unimodal of multimodal objective functions (Dipankar et Michalewicz, 2013; Edgar *et al.*, 2001).

Step 1: At the beginning of the algorithm sequence, a population composed of "p" individuals and having "n" genes encoded on "m" bytes was generated randomly. Each gene corresponds to a parameter to estimate. Then, the value of parameters for each individual was obtained from converting bytes to numerical values, which were further normalized to 1. So, as the number of bytes "m" increased, the precision of the parameter also increased. A wide range of possible solutions was then assigned to each parameter defined as a multiplicative factor.

Step 2: Then, for each individual "p" of the population, the mathematical framework described above was solved and the objective function for this particular individual was calculated as shown by the following equation, which corresponded to the sum of squares between experimental and model values at each experimental time point:

$$Objfc_p = \sum_{i=1}^{p_{expdata}} \left(y_{model,i} - y_{experimental,i}\right)^2 \tag{4-17}$$

Step 3: After the objective function had been evaluated for each individual, its fitness was then calculated. Since the sum of squares between the model and the experimental data has to be minimized, the fitness of each individual was determined as the difference between their objective function value and the highest value of the objective function over the sum of the total measured objective function values, so all the data were normalized and had values from 0 to 1:

$$Fitness_p = \left[\frac{\left(objfc_p - argmax(objfc)\right)}{\sum_{i=1}^{p}(objfc_i - argmax(objfc))}\right] + \alpha \tag{4-18}$$

where α was a very small number ($\sim 1 \times 10^{-10}$) to avoid having a fitness value of 0

Step 4: The next generation of individuals was selected. The next step of the algorithm consisted of randomly selecting "p" times a set of two parents from the population based on their fitness. To do so, the cumulative distribution function (CDF) of the population was determined as the cumulative sum of the fitness:

$$CDF_i = \sum_{p=1}^{i} Fitness_p \tag{4-19}$$

Where CDF_i is the ith element of the vector containing all the CDF values:

$$CDF = [CDF_1 \quad CDF_2 \quad ... \quad CDF_p] \tag{4-20}$$

And

$$\sum_{i=1}^{p} CDF_i = 1 \tag{4-21}$$

Since the fitness values were normalized, the CDF varied from 0 to 1. Hence, an individual having a higher fitness had a greater chance to be selected from the population.

Step 5: Then, based on a defined crossing-over probability (based on a uniform distribution), both parents could be mixed together to form a child by mixing their genes randomly. If the probability of the crossing-over was not achieved, one of the two parents was randomly selected as a member of the next generation.

Step 6: Once the new generation had been determined, each byte of genes of all new individuals underwent, or not, a mutation process based on a user-defined probability of mutation in order to increase the population variability and to avoid the convergence of the algorithm to a local minimum. In this process, if, for a given byte of an individual, the random value was lower than the obtained probability of mutation, the value was switched from 0 to 1 or inversely from 1 to 0, and so forth.

Steps 2 to 6 were repeated for several generations until the convergence criterion was met. For each generation, the best parameters (the ones having the lowest objective function values) were compared with the ones from the previous generation. If the value of the new set of parameters was lower than previous ones, they were stored, so was the average value of the objective function of each generation. The algorithm converged when the variation of the average fitness value became negligible. The best parameters stored so far were considered the optimal parameters.

In this case, the parameters of the mathematical model were found with the following:

- Genes: 2
- Population size: 40
- Number of bytes: 8
- Probability of crossing-over: 60%
- Probability of mutation: 0.5%
- Number of generation: 200

4.3.9 Parameter evaluation

Parameter and their physical meaning was assessed using the mass transfer Biot dimensionless number (Bi_m), which corresponds to the ratio between the resistance of mass transfer inside (diffusion) and at the surface (natural or forced convection) of the NP as described by the following equation:

$$Bi_m = \frac{kL_c}{D_{eff}} \tag{4-22}$$

Where L_c corresponds to the characteristic length being defined as the ratio between the volume and the surface area in contact with the surrounding releasing media. The value of Bi_m gives much information about which phenomena limits the mass transfer.

4.3.10 Cell culture

The human SH-SY5Y neuroblastoma cells (ATCC, CRL-2266) were cultured in a T75 cell-treated flask (Corning, USA) following the manufacturer's instructions. Briefly, cells were cultured in DMEM/F12 culture media supplemented with 1% (v/v) penicillin-streptomycin (10,000 U/mL) and 10% (v/v) foetal bovine serum (FBS). When cells reached 80% confluence, they were trypsinized using trypsin-EDTA (0.25%), centrifuged and seeded into new T75 cell culture-treated flasks or 24-well plates or 6-well plates (Corning, USA).

4.3.11 Cell survival and indirect cell count in the presence of Alg/Chit nanoparticles

The human SH-SY5Y cells were cultured in 24-well plates until they reached 80% confluence. Cells were then washed with a sterile phosphate buffer saline (PBS) and stimulated for 24h, 72h and 120h with or without various concentrations of NPs (¼ diluted, ½ diluted and non-diluted) suspended in a serum-free medium. After each incubation time, the cells were washed with sterile PBS, and AlamarBlue® dye was added according to the manufacturer's instructions. After 2 h of incubation, supernatant was collected for fluorescence measurements. The cells were fixed for 15 min with 3% (w/v) paraformaldehyde and kept at 4°C in sterile PBS. Supernatant fluorescence was measured with a spectrophotometer (Safire2, Tecan US inc., NC, USA) with $\lambda_{excitation} = 555 \pm 15$ nm and $\lambda_{emission} = 595 \pm 15$ nm.

For indirect cell counting measurements, fixed cells were incubated with Hoechst 33342 solution (5 μg/mL) for 20 min at room temperature in order to stain the DNA (nucleus). The cells were washed twice with PBS and kept away from light in fresh PBS solution. 25 stitched-pictures per well with a magnification of 10X were taken using Evos FL-Auto epifluorescence microscope (Life Technologies, Thermo Fisher, USA). An image analysis application developed in Matlab (Matlab Image Processing Toolbox; MatLab 2007b, Mathworks, USA) was then used to quantify, pixel-wise, the total fluorescent intensity in the blue channel. Since the same acquisition parameters (light intensity, digital gain, exposure time, etc.) were used for each experiment, results could be compared between each other.

4.3.12 Cell morphology and neurite length measurements

The human SH-SY5Y cells were seeded into 6-well plates containing a microscope glass coverslip and allowed to grow until they reached 80% confluence. They were then washed with sterile PBS, and stimulated for 120h with NPs containing SpBMP-9 at a dilution ¼ into serum-free culture media. NPs without SpBMP-9 were used as negative control. 10 pictures per well were taken at a magnification of 20X using a phase-contrast microscope (Nikon, Eclipse TE2000, Nikon Instruments inc., Japan) coupled with a CCD camera (Moticam Pro CCD 285C, Motic, Hong Kong). Each picture then underwent multiple numerical filtering treatments to highlight the neurites using an image analysis app developed under Python environment (Python 2.7.3) and OpenCV library (OpenCV 3.2). Briefly, pictures were smoothed with a Gaussian filter to remove noise. Pictures were then filtered with a Laplace high-pass filter following a median filter to detect and enhance neurites while reducing the background features. The resulting images showing the neurite edges (blue lines) and cell bodies (yellow) were superimposed to the original phase-contrast images.

The mean neurite lengths were further determined from the high-resolution neurite-enhanced pictures. The neurite length was defined as the Euclidean distance in pixels or a combination of Euclidean distances between the cell body and the end of a neurite. The longest path was always chosen when a neurite had several branches. The length in pixels was then calibrated based on the length bar provided by the microscope image treatment software (Motic Image Advanced 3.2). For each experimental condition, 10 to 20 neurites were measured for each picture ($4x10^{-3}$ cm^2) and at least 10 pictures were analyzed per condition per replicate.

Those steps were performed for at least two independent times in quadruplicate. The mean neurite length for each picture analyzed within a replicate was weighted by the number of measurements taken. For each independent experiment, the mean was calculated as the weighted mean (relative to the inverse of the variance) of each replicate. Finally, the overall mean was calculated as the weighted mean (relative to the inverse of the variance) of each of the three independent experiments.

4.3.13 Immunostaining

The SH-SY5Y cells were seeded into 6-well plates containing a microscope glass coverslip and allowed to grow until they reached 80% confluence. They were then washed with sterile PBS, and stimulated for 120h with a NP solution diluted ¼ into serum-free culture media with or without SpBMP-9. Cells were washed with sterile PBS, then fixed for 15 min with paraformaldehyde 3% (w/v) at room temperature. Coverslips were then washed with PBS and cells were permeabilized with a Triton X-100 solution (0.5% v/v) for 5 min at room temperature. Non-specific sites were then blocked using a skimmed milk solution (3% w/v) for 30 min at 37°C under 5% CO_2 atmosphere. Coverslips were then incubated for 30 min at 37 °C (5% CO_2) with primary antibodies: rabbit C-terminal anti-NSE diluted at 1:100 (Sigma-Aldrich, Ca) or rabbit C-terminal anti-VAchT diluted at 1:500 (Sigma-Aldrich, Ca) followed by an incubation in the presence of anti-rabbit IgGs fragments conjugated to Alexa Fluor® 488 diluted at 1:250 (Cell Signalling, precision, MA, USA) for 30 min at 37°C (5% CO_2). Nucleus and actin cytoskeleton were counterstained using Hoechst 33342 (Life Technologies, ThermoFisher, USA) with a final concentration of 5µg/mL and rhodamine-phalloidin diluted at 1:200 (Life Technologies, ThermoFisher, USA). Coverslips were mounted on microscope glass slide and visualized with an Evos FL-Auto epifluorescence microscope with a magnification of 40X.

4.3.14 Statistical analysis

Statistical analyses were conducted with an Excel 2010® data analyses package. Data were analysed with ANOVA followed by the Tukey post-hoc pair-wise comparison test. Only differences with $p \leq 0.05$ were considered statistically significant.

4.4 Results

4.4.1 Characterization of alginate/chitosan nanoparticles

The size distribution of the Alg/Chit NPs in deionized water without entrapped SpBMP-9 was first characterized using laser diffraction (Figure 4-2A). The results, given as size distribution in function of the volume fraction, showed that the Alg/Chit NPs were monodispersed with an average size of about 240 nm. Moreover, the distribution was not bell-shaped since larger particles with diameters between 0.5 and 10 μm could be observed on the right tail of the (Figure 4-2A). In order to verify whether those large particles accounted for a great number, the volume fraction was then converted to particle density (Figure 4-2B). The results showed that the distribution is narrow (from 100 to 500 nm) and monodispersed with an average size similar to that determined by volume fraction (~240 nm). However, no particles with diameters varying from 0.5 to 10 μm were detected. The discrepancy between the values of the size distribution obtained in function of volume fraction compared to those gained with particle density can be explained by the presence of large particle aggregates that could not be dispersed using the ultrasound probe. Those aggregates influenced greatly the total volume, even at a small number, thus creating the appearance of a wider size range. However, their contribution to the particles' density was negligible as depicted by the particle density function.

SEM observations were then used to confirm the laser diffraction results (Figure 4-2, C et D). SEM pictures showed Alg/Chit NPs with diameters varying from 50 nm to several hundreds of nm. Some large aggregates composed of smaller particles were also observed (Figure 4-2C), which agree well with the laser diffraction data. The most abundant NPs had a diameter of ~ 50 nm. We also confirmed that the encapsulated SpBMP-9 did not affect the average size of Alg/Chit NPs using SEM, thus confirming the hypothesis that the size distribution was not affected by the presence.

We then evaluated the capacity of those Alg/Chit NPs to encapsulate SpBMP-9. The peptide was premixed with alginate solution since they carried opposite charges, which may increase the encapsulation efficiency. Several initial SpBMP-9 mass loadings were used in order to determine the mass encapsulation efficiency (

Tableau 4-1). Using initial mass loadings of SpBMP-9 varying from 50 ng per µg of Alg/Chit NPs to 200 ng per µg of Alg/Chit NPs, we found that the encapsulation efficiency significantly decreased between 100 and 200 ng SpBMP-9 per µg of Alg/Chit NPs (p<0.001), while it was similar with 50 and 100 ng SpBMP-9 per µg of Alg/Chit NPs, reaching almost 70%. However, increasing the initial mass loading from 50 ng to 200 ng SpBMP-9 per µg of NPs significantly enhanced of about 3.3-fold the total encapsulated mass (p<0.001).
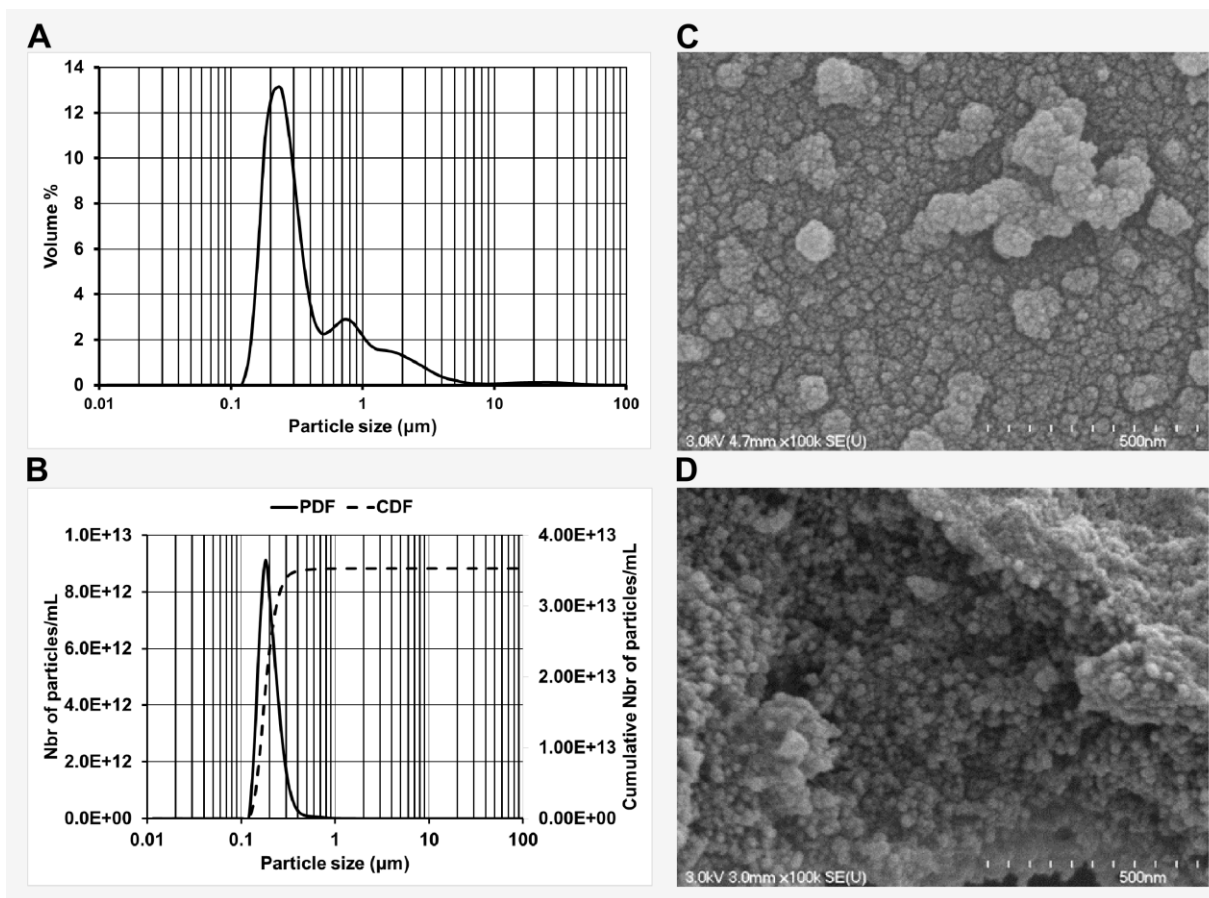
Figure 4-2 : A) Alg/Chit NPs size distribution (volume) from laser diffraction analyses. 5 to 10 measurements were taken per experiment and results are representative of three independent experiments. B) NP density in function of size and NP cumulative density function. C) Representative SEM pictures showing non-purified Alg/Chit NPs forming big aggregates. D) Representative SEM pictures showing Alg/Chit NPs. Results are representative of at least three independent experiments.

Initial SpBMP-9 mass loading ng SpBMP-9/µg NPs	Total SpBMP-9 mass encapsulated ng SpBMP-9/µg NPs	Encapsulation efficiency %
50	$34 \pm 4^{b,c}$	69 ± 8^{c}
100	$66 \pm 7^{a,c}$	66 ± 7^{c}
200	$111 \pm 4^{a,b}$	55 ± 2

a statistically different with 50 ng/ SpBMP-9/µg NPs ($p<0.001$), **b** statistically different with 100 ng/ SpBMP-9/µg NPs ($p<0.001$), **c** statistically different with 200 ng/ SpBMP-9/µg NPs ($p<0.001$)

4.4.2 Release kinetics of SpBMP-9 from alginate/chitosan nanoparticles and its Korsmeyer-Peppas representation

For SpBMP-9 release kinetics experiments (Figure 4-3A), an initial loading mass ratio of 100 ng peptides per µg of Alg/Chit NPs was selected, since its percentage of encapsulation was similar to that of 50 ng SpBMP-9 per µg of Alg/Chit Nps (~66 %), with a greater absolute encapsulated mass. Furthermore, there was no substantial loss of SpBMP-9 in the NP fabrication process using 100 ng peptides per µg of Alg/Chit NPs in comparison to the 200 ng SpBMP-9 per µg of Alg/Chit NPs. The release of SpBMP-9 from the Alg/Chit NPs was quantified within 144h, using a SpBMP-9 standard curve obtained by HPLC measurements (Figure 4-3B). The results (Figure 4-3C) showed a characteristic rapid burst release of the peptide within the first 2h followed by a sustained release for up to 24h, at which the cumulative mass release of SpBMP-9 reached a pseudo-plateau at almost 80 % of the encapsulated SpBMP-9 mass. In order to confirm that ~ 20% of SpBMP-9 mass were still entrapped in the delivery system at 144h, Alg/Chit NPs were dissolved and the remaining SpBMP-9 was quantified using HPLC measurements. We found that the cumulative mass release plus the remaining SpBMP-9 in NPs at 144h account for 95.0 ± 3.5 % of the encapsulated SpBMP-9 mass, thus confirming that SpBMP-9 peptides were still entrapped inside the Alg/Chit NPs.

We then used the experimental results to model the release kinetics and extract the mechanistic parameters. We first modelled the release kinetics data representing the first 8h of release (cumulative mass release at almost 70% of the encapsulated SpBMP-9 mass) using the Kormeyer-Peppas representation to evaluate the driving mass transport phenomenon (Figure 4-3D) . The results showed that the model could fit well the experimental data with a coefficient

of determination (R^2) of 0.98. In addition, the value of the parameter "n" of Korsmeyer-Peppas representation can give insights on the governing mass transport phenomena occurring. The "n" value obtained from the data was 0.3, which for a spherical geometry, is indicative of diffusive phenomenon (Korsmeyer *et al.*, 1983).
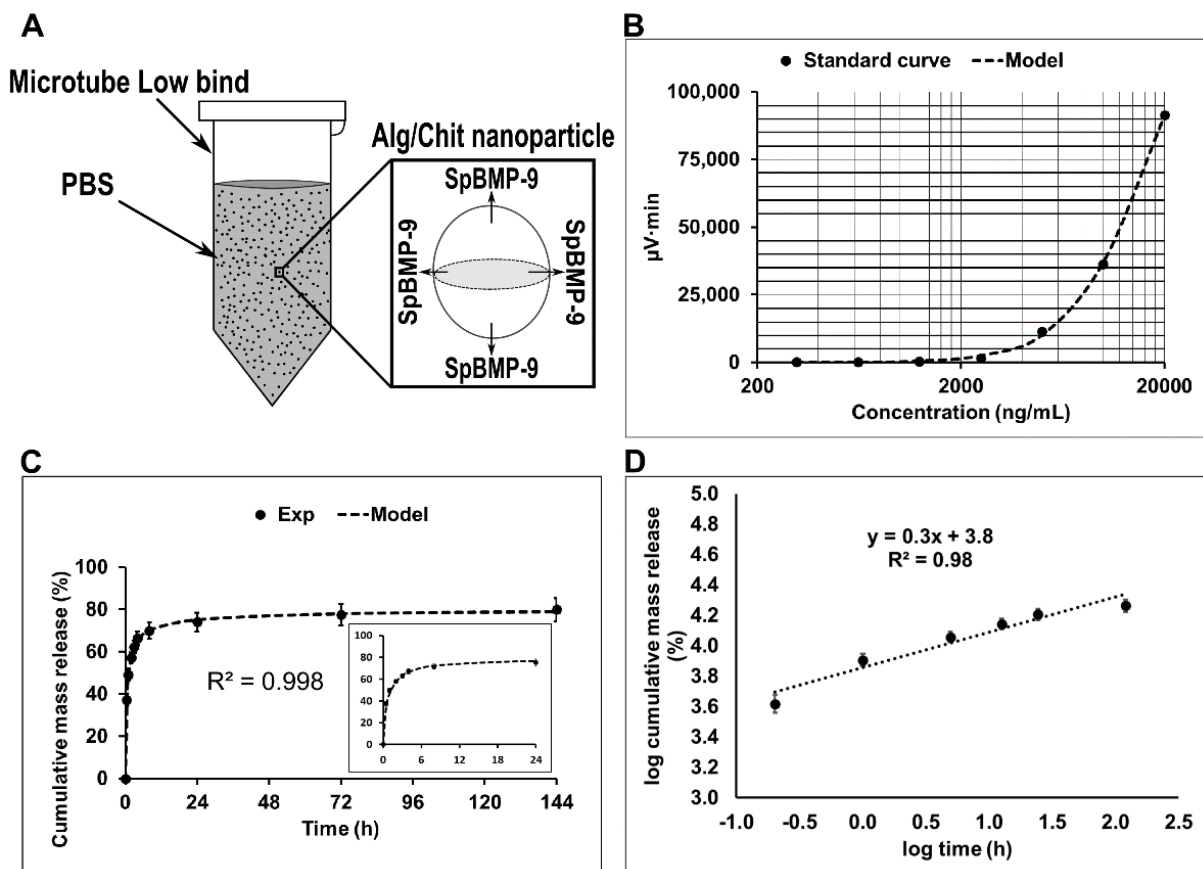
Figure 4-3 : **A)** Schematic showing the release kinetics experiments. **B)** Standard HPLC curve for SpBMP-9. Curve was modeled with a forth degree polynomial weighted regression (dashed curve). **C)** Mean cumulative mass release ± SEM and model data (Model, dashed curve) for Alg/Chit NPs containing SpBMP-9 for 4 experiments performed in duplicate. **D)** Korsmeyer-Peppas representation of the first 8h of SpBMP-9 release on a log-log scale showing a linear profile (R^2 = 0.98) with a value of "n" of 0.3.

4.4.3 Influence of size distribution on release kinetics of SpBMP-9

Since the main mass transport phenomenon driving the release of SpBMP-9 was shown to be mostly diffusive, we then used Fick's second law applied to spherical geometry to model, on a mechanistic basis, the release kinetics with boundary conditions that considered the interactions between SpBMP-9 and the NPs alginate chains. Moreover, we also used the size distribution to model the release more faithfully, since smaller particles, for instance, contained less encapsulated peptides relative to their volume and had a smaller surface in contact with the

surrounding media. The Alg/Chit NPs size distribution was separated in several classes based on laser diffraction results (Figure 4-4A) and the mathematical framework was solved for each of those classes (Figure 4-4B). We then used an evolutionary algorithm in order to estimate the model parameters (Tableau 4-2). The diffusion coefficient was estimated at 3.5 E-17 $m^2 \cdot s^{-1}$ whereas the overall mass transfer coefficient was of about 3E-08 m/s. The evolutionary algorithm reached a plateau after 15 generations, thus confirming the ability of the optimization algorithm to converge toward the solution (Figure 4-4C). To verify whether the parameters were identifiable and the combinations of parameters were unique in this case, a sensitivity study was performed, where both parameters were varied over 4 orders of magnitude higher and lower and we determined the sum of square of residuals (Figure 4-4D). The system displayed many local minima and one global minimum, thus suggesting that the parameters are identifiable. In addition, the fact that this system has many local minima justified the use of an evolutionary algorithm, which was particularly efficient in this situation.

The model parameters as well as the mathematical framework was a good fit to the experimental data with a determination coefficient (R^2) of 0.998 as represented by the dotted line on (Figure 4-3C). In addition, the model was highly statistically significant with a $p<0.001$ and a non-significant lack of fit of 0.87, which indicated whether a proposed model is able to represent the data. In addition, we studied the effect of each NP size class on the release kinetics patterns (Figure 4-4E) and their contribution to the total mass release at a given point in time (Figure 4-4B). As the diameter of the NP increased, the cumulative mass release was slowing down due to an increase in the path that each SpBMP-9 molecule needed to cross to diffuse out of the particle. However, since there were more small Alg/Chit NPs in comparison with the larger ones as shown by the size distribution data, their overall contribution to the total mass release was more important. When the equilibrium was reached for the smaller particles, the bigger ones then started to contribute more, but with a very small absolute mass release since the solution contained few of them. We then studied the physical implication of the estimated parameters by calculating the mass transfer Biot dimensionless number (Bi_m) for each NP size class (Figure 4-4F). The Bi_m number gave a ratio between the mass transfer resistance within the Alg/Chit NPs and the resistance to the mass transfer at their surface. When increasing the size of the NP, the Bi_m raised from 6.5E01 to 2.5E03. $Bi_m \gg 1$ indicated that the resistance to the mass transfer was rather predominant within the NP in comparison to their surface. This

resistance to the mass transfer enhanced as the particle size did, since the characteristic length was greater. In this case, the Bi_m values obtained indicated that the mass transfer was highly limited by the diffusion inside the sphere and might be explained by the electrostatic interactions between the negatively charged alginate and the positively charged peptides.

Tableau 4-2 : Model parameters estimated values

Model parameter	Symbol	Units	Value
Diffusion coefficient	D_{eff}	$m^2 \cdot s^{-1}$	3.3E-17 ± 0.8E-17
Overall mass transfer coefficient	k	$m \cdot s^{-1}$	2.8E-08 ± 1.0E-08
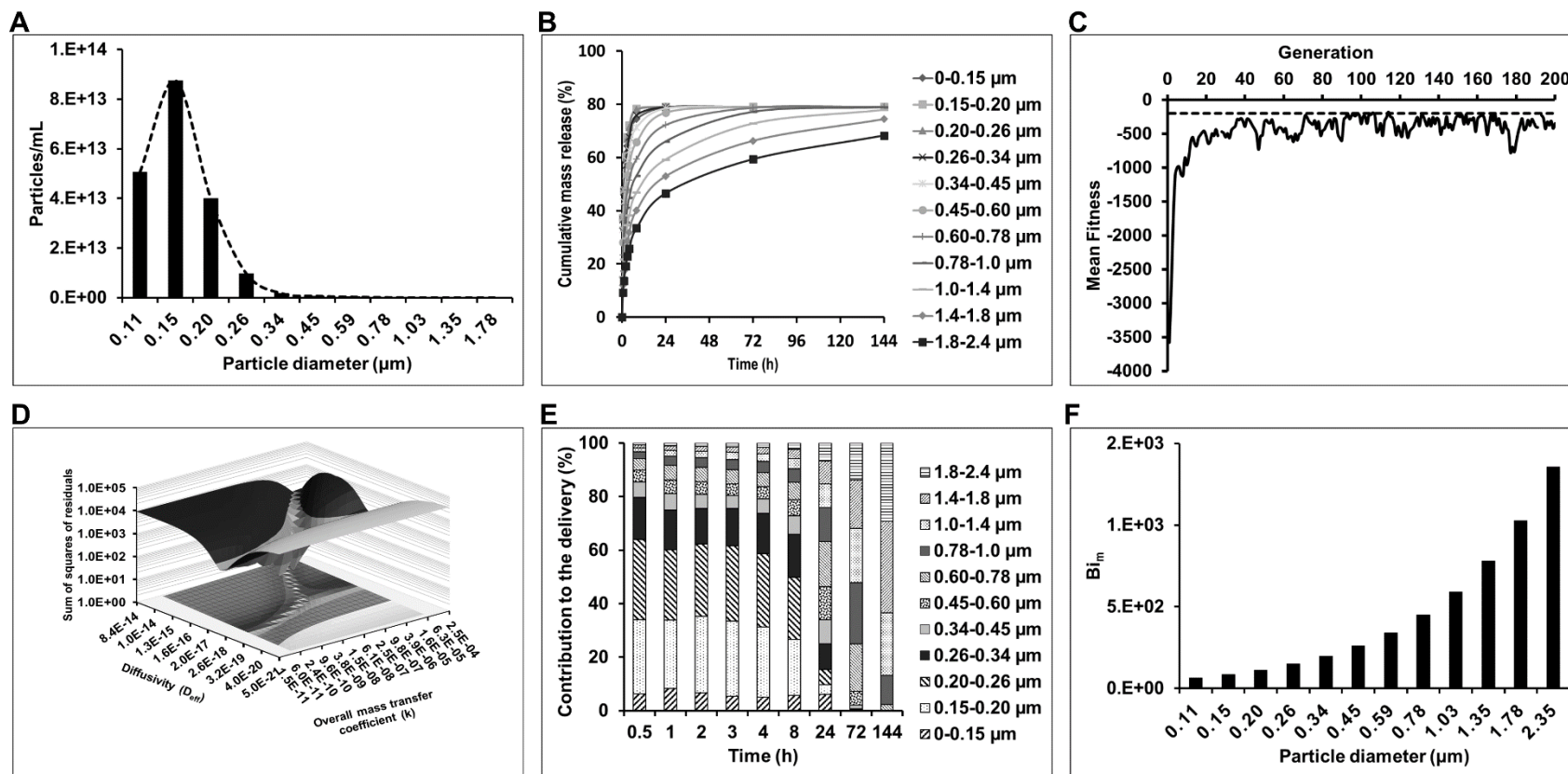
Figure 4-4 : **A)** Particle volume concentration as a function of size class used for mathematical modeling. **B)** Cumulative mass release curves for each NP size class as per calculated from the mathematical model. **C)** Mean fitness for each generation of the genetic algorithm showing the convergence of the algorithm. **D)** Sensibility analysis where the model parameters "D_{eff}" and "k" were varied over 8 orders of magnitude. **E)** Contribution to the release for NP size class for each time point. **F)** Bi_m number for each size NP class determined from the estimated model parameters.

4.4.4 SH-SY5Y cell survival in contact to nanoparticles

Once the Alg/Chit NPs were characterized, their effects were assessed with or without dilution on the metabolic activity of SH-SY5Y human neuroblastoma cells after incubation for 24, 72 and 120h using AlamarBlue enzymatic activity assay (Figure 4-5A). There was a decrease in cell metabolic activity between 24h and 72h for each experimental condition (at least $p<0.01$). However, this decrease was less important for cells incubated with ¼ and ½ diluted Alg/Chit NPs in comparison to the CTL (no Alg/Chit NPs, $p<0.001$). Indirect cell counting was also performed (Figure 4-5B). The results showed that there were more cells after 24h, 72h and 120h for those stimulated with Alg/Chit NPs with or without dilution in comparison to the CTL ($p<0.001$). Alg/Chit NPs with or without dilution were not cytotoxic and appeared to have a protective effect over time on SH-SY5Y cells cultured in a serum-free medium.
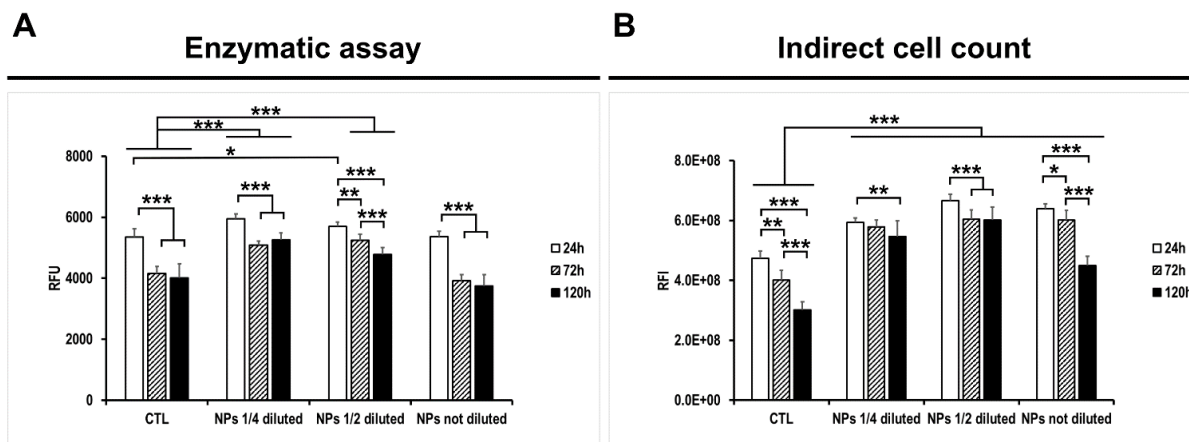
Figure 4-5 : **A)** AlamarBlue assays and **B)** indirect cell counting for SH-SY5Y cells stimulated for 24h, 72h and 120h in a serum-free medium with Alg/Chit NPs (diluted ¼, ½ or not diluted) or without (CTL). Not diluted Alg/chit NPs solution contained ~ 3.5E+13 particles/mL. Results are the mean ± SD of three independent experiments performed in triplicate. * $p<0.05$, ** $p<0.01$ and *** $p<0.001$.

4.4.5 Neuronal differentiation of SH-SY5Y cells in contact to nanoparticles

Since the Alg/Chit NPs did affect the number of cells, the efficacy of released SpBMP-9 to induce neuronal differentiation of SH-SY5Y cells was then studied. We used ¼ diluted NPs (~ 100 nM) solutions since we have previously demonstrated that SH-SY5Y cells responded to SpBMP-9 concentration as low as 0.1 nM (Lauzon *et al.*, 2017). The effect of

released SpBMP-9 from Alg/Chit NPs was first assessed on the capacity of SH-SY5Y cells to develop and extend neurites, which is indicative of neuronal differentiation. To do so, cells were stimulated with Alg/Chit NPs +/- SpBMP-9 for 120h. Phase contrast pictures were taken, then treated with several image filter routines in order to highlight the cell body (yellow) and the neurites (blue) (Figure 4-6A). Alg/Chit NPs alone had no significant impact on cell morphology. However, SH-SY5Y cells treated with Alg/Chit NPs + SpBMP-9 had more and longer neurite outgrowth in comparison to both control (CTL) and Alg/Chit NPs. The neurite length was also quantified as previously shown (Figure 4-6B) (Lauzon *et al.*, 2017). Cells stimulated with Alg/Chit NPs + SpBMP-9 had significantly longer neurites (p<0.001) in comparison to both CTL and Alg/Chit NPs alone. Those results showed that SpBMP-9 released from NPs can induce morphological changes associated with neuronal differentiation.

To confirm whether Alg/Chit NPs + SpBMP-9 could induce SH-SY5Y neuronal differentiation, the expression of specific neuronal markers was further studied in SH-SY5Y cells incubated for 120h with or without Alg/Chit NPs +/- SpBMP-9 by immunostaining (Figure 4-6C et D). Firstly, neuron specific enolase-2 (NSE), which is a terminal differentiation marker (Marangos *et al.*, 1978; Odelstad *et al.*, 1981) was immunostained (Fig. 6C). Cells stimulated with Alg/Chit NPs plus SpBMP-9 showed more fluorescence intensity associated with NSE expression (green) in comparison with both CTL and Alg/Chit NPs alone, which was indicative of a higher level of differentiation.

We then evaluated the capacity of Alg/Chit NPs containing SpBMP-9 to induce the expression of markers related to the cholinergic phenotype. Fixed SH-SY5Y cells incubated with or without Alg/Chit NPs +/- SpBMP-9 were immunostained for a vesicular acetylcholine transport protein (VAchT), which is a protein essential in the storage and liberation of the neurotransmitter acetylcholine (Figure 4-6D). SH-SY5Y cells stimulated with Alg/Chit NPs plus SpBMP-9 had a more intense fluorescence associated with the expression of VAchT (green) in comparison to both CTL and Alg/Chit NPs alone. More importantly, several vesicles located in the neurites were also observed in cells incubated with Alg/Chit NPs plus SpBMP-9. Those vesicles were indicative of encapsulation of acetylcholine and its transport along the neurites. Overall, Alg/Chit NPs plus SpBMP-9 could induce morphological changes associated with neuronal differentiation as well as a greater expression of NSE and VAchT, thus

confirming that its bioactivity was conserved when encapsulated inside a nanoscale delivery system.
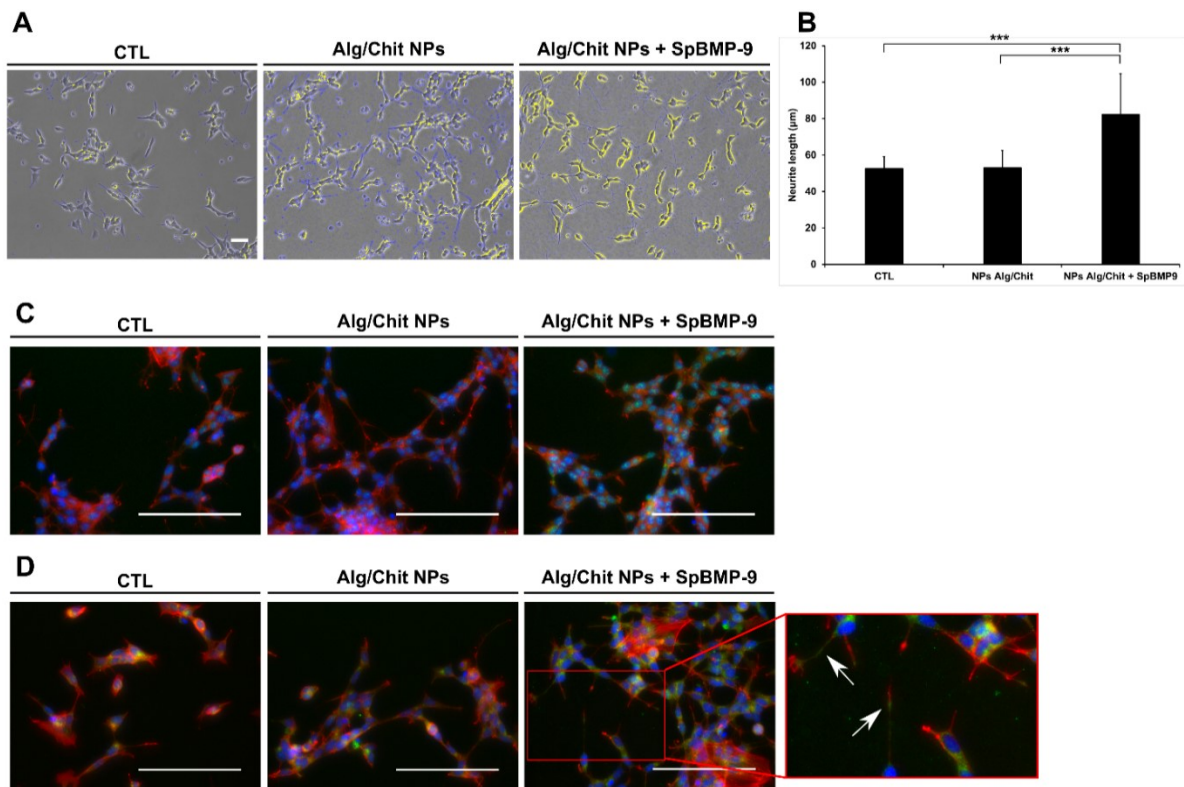
Figure 4-6 : **A)** Representative phase contrast pictures that were filtered in order to enhance the neurites (blue) and the cell body (yellow) for SH-SY5Y cells stimulated for 120h in a serum-free medium alone (CTL) or in a serum-free medium supplemented with ¼ diluted Alg/Chit NPs or ¼ diluted Alg/Chit NPs plus SpBMP-9. Bar = 100 μm. Results are representative of 3 independent experiments performed in quadruplicate. **B)** Mean neurite length ± SD for SH-SY5Y cells stimulated for 120h in a serum-free medium alone (CTL) or in a serum-free medium supplemented with ¼ diluted Alg/Chit NPs or ¼ diluted Alg/Chit NPs plus SpBMP-9. Results are representative of 2 independent experiments performed in quadruplicate. Overall, a total of at least 1200 neurite length measurements were obtained for each experimental condition. **C)** Representative immunostaining pictures showing NSE (green), Actin (red) and nucleus (blue) for SH-SY5Y cells incubated for 120h with or without of ¼ diluted Alg/Chit NPs ± SpBMP-9. **D)** Representative immunostaining pictures showing VAchT (green), Actin cytoskeleton (red) and nucleus (blue) for SH-SY5Y cells stimulated for 120h with or without Alg/Chit ± SpBMP-9. Results are representative of three independent experiments. Bar = 100 μm.

4.5 Discussion

In the context of new therapeutic strategies against AD, BMP-9 was found in mouse models to be an interesting candidate as it plays a role in many AD hallmarks (Burke *et al.*, 2013; Lopez-Coviella *et al.*, 2000; Wang *et al.*, 2017). However, to overcome the production and purification cost of BMP-9 in addition to its low BBB permeation, we have developed small peptides (23-residues long, 2.36 kDa), derived from the knuckle epitope of BMP-9 (pBMP-9

and SpBMP-9), based on previous work of Saito *et al.* (2003, 2005) on BMP-2. SpBMP-9 could increase the differentiation of SH-SY5Y cells toward the neuronal phenotype and acted on more than one therapeutic target of AD to a greater extent than BMP-9 did (Lauzon *et al.*, 2017). However, SpBMP-9 is not specific to the brain and is still subjected to rapid clearance once injected in the body. In this study, we have therefore prepared Alg/Chit NPs as a brain-targeting SpBMP-9 delivery system to overcome those issues.

The size distribution of the NPs was first characterized with a laser diffraction method and SEM. Laser diffraction gave a monodisperse distribution of NPs with an average size (diameter) of ~ 240 nm, which is similar to what was recently observed by Rahaiee *et al.* (2017, 2015) using SEM, atomic force microscopy and laser spectroscopy. However, the comparison of the volume percentages versus the particle density suggested the presence of aggregates having size values up to several microns, which was further confirmed by SEM observations. This has already been observed for various alginate-based nano-aggregate systems (Paques *et al.*, 2014). Moreover, SEM pictures also showed that NPs had mainly a diameter ranging from 20 to 50 nm. Nonetheless, the difference between the NP size determined from the laser diffraction and SEM can be explained by the fact that SEM imaging requires the particles to be dried out and Alg/Chit NPs are nanoscale hydrogels that are known to swell. Indeed, this phenomenon has already been observed with Alg/Chit NPs, where alginate is known to swell at a pH near neutrality with an observed swelling ratio of ~ 400-600% (Mi *et al.*, 2002; Mukhopadhyay *et al.*, 2015; Rahaiee *et al.*, 2017). Similar SEM results with Alg/Chit NPs were observed in several studies with encapsulation of peptides or smaller molecules (Emami *et al.*, 2014; Goycoolea *et al.*, 2009; Haque *et al.*, 2014; Li *et al.*, 2008). For instance, Emami *et al.* (2014) synthesized Alg/Chit NPs to encapsulate an anti-diabetes drug called Glipizide, member of the sulfonylurea class (Emami *et al.*, 2014). They conducted a parametric study and showed that the ratio of alginate/chitosan/calcium, using low molecular weight chitosan with a deacetylation percentage of 60%, could greatly impact the NP size with values ranging from ~170 to 4500 nm using laser diffraction technics. In the present study, HMW chitosan with a deacetylation percentage of ~ 85% was used. The molecular weight and the degree of deacetylation of chitosan could explain the difference in NPs size. Li *et al.* (2008) have synthesized Alg/Chit NPs using HWM chitosan with a degree of deacetylation > 80% with a similar alginate to chitosan mass ratio to what we used in order to encapsulate Nefidipine, a

member of the dihydropyridine family of calcium channel blockers against angina and hypertension. They observed NPs with of 20-50 nm in diameter as well as some aggregates using transmission electron microscopy, which is in accordance with our results. Furthermore, it has been reported that Alg/Chit NPs, dependent on the composition and the ratio of the reactants, can have different size distributions (Paques *et al.*, 2014).

We then studied the capacity of SpBMP-9 (2.36 kDa) to be encapsulated in the Alg/Chit NPs. Using initial SpBMP-9 mass loadings of 50 ng up to 200 ng per µg of Alg/Chit NPs, we observed a percentage of encapsulation varying between 55 and 70 % with a peptide loading to NPs mass ratio between 3% and 11% respectively. Similar encapsulation efficiency has been observed for soluble molecules such as insulin (5.8 kDa, isoelectric point of 5.3) (Goycoolea *et al.*, 2009; Hecq *et al.*, 2015; Mukhopadhyay *et al.*, 2015) or ovalbumin (45 kDa, isoelectric point of ~4.6) (Borges *et al.*, 2006) entrapped in Alg/Chit NPs or alginate-coated chitosan NPs. For instance, Goycoolea *et al.* (2009) used alginate-coated chitosan NPs to encapsulate insulin and observed a percentage encapsulation of 47% with a peptide loading to NPs mass ratio between 20-30%. Borges *et al.* (2006) used alginate-coated NPs to adsorb ovalbumin and obtained an encapsulation efficiency of 57 % with protein loading to NPs mass ratio of 34%. Haque *et al.* (2014) used a similar Alg/Chit NPs formulation to what we used (composition and mass ratio) to encapsulate Venlafaxine (~0.3 kDa, pKa ~9), a water-soluble anti-depression drug, and observed a percentage of encapsulation higher than 85.6% with a drug loading to NPs mass ratio of 26.74%. The variation in encapsulation efficiency and mass to mass loading ratio might be explained by both the composition of the NPs and the properties (size, charge, etc.) of the therapeutic molecules loaded. Good encapsulation efficiency can be obtained when the charges of the entrapped molecules versus the carrier is considered in the process. The synthesis process can also play an important role. For instance, Borges *et al.* (2006) and Goycoolea *et al.* (2009) developed chitosan nanoparticles coated with alginate, which is basically the opposite of what we did. Chitosan was put into contact with ovalbumin, which carries negative charges at physiological pH, followed by the addition of alginate. On the contrary, SpBMP-9 or Venlaxafine are positively charged in an acidic environment, which explains why they are mixed with the sodium alginate solution prior to NPs synthesis. Since SpBMP-9 is highly positively charged in acidic pH compared to insulin which is slightly negatively charged in the synthesis conditions (pH ~5.6), the electrostatic interactions with alginate sodium or chitosan

can influence the encapsulation efficiency and might explain why we obtained a higher percentage. For instance, Anal *et al*. (2003) showed that the addition of HMW chitosan (degree of acetylation of 85%) to calcium-induced alginate NPs could increase the entrapment efficiency of BSA (66 kDa, PI ~ 4.7) from 16-35% to 60-89% compared to alginate alone as it provided more favorable ionic interactions. In addition, SpBMP-9 is mostly linear, which more easily gives access to locally charged amino acid residues (Bergeron *et al.*, 2009). The size of the protein being encapsulated may also play an important role on the encapsulation efficiency on a molar basis rather than on a mass basis. If we compared our results of encapsulation efficiency on a molar basis, there are a lot more molecules of SpBMP-9 in comparison to ovalbumin and insulin. Also, comparing our results with a similar synthesis process, Venlaxafine encapsulation efficiency was higher to what we observed with SpBMP-9, which can be explained by the difference in size of the drug (~ 0.3 kDa vs 2.36 kDa) (Haque *et al.*, 2014). In addition, they used alginate with a guluronic to a mannuronic ratio of 2:3, whereas we used sodium alginate with a 2:1 ratio. Since guluronic residues are the ones that form the egg-box complex with calcium ions, the available negatively charged domains might, for a similar alginate to calcium mass ratio, influence the interactions between the drug and the NPs (Paques *et al.*, 2014).

We then studied the release kinetics of SpBMP-9 from the Alg/Chit NPs in PBS at physiological pH and body temperature (37°C). The release kinetics profile, showing a burst release followed by a slow release until a plateau was reached, was similar to what was observed in the literature (Lauzon et al., 2014). The plateau, reached before all the peptides were released could be explained by the presence of electrostatic interactions between SpBMP-9 and the alginate matrix, which carries opposite charges at physiological pH. We observed the same tendency in a previous study where we studied the release kinetics of pBMP-9 (a peptide similar to SpBMP-9 in terms of the number of amino acids and the isoelectric point) from a type I collagen hydrogel (Bergeron *et al.*, 2012; Lauzon *et al.*, 2014). The presence of an electrostatic interaction was also observed for other molecules such as ovalbumin or insulin (Borges *et al.*, 2006; Hecq *et al.*, 2015; Mukhopadhyay *et al.*, 2015). For instance, Borges *et al.* (2006) observed a similar release kinetics pattern for ovalbumin released from alginate-coated chitosan NPs, which was attributed to the presence of electrostatic interactions. In the present study, the mass transfer Biot number (Bi_m) with a value >>1 also suggested that the resistance to the transfer lies within the particle rather than at its surface, thus confirming this statement.

We then modelled the release kinetics, first using the Korsmeyer-Peppas' empiric model, which gives insight about the driving release mechanism. Modeling the first 70% of release, we obtained a value of "n" below 0.45 (~0.3), which is distinctive of a diffusion-controlled mechanism for a spherical geometry (Korsmeyer *et al.*, 1983). Indeed, since Alg/Chit NPs are hydrogels, the driving release mechanism is usually diffusion-based as observed with similar delivery systems (Emami *et al.*, 2014; Goycoolea *et al.*, 2009; Lauzon *et al.*, 2014; Li *et al.*, 2008; Rahaiee *et al.*, 2017). However, other mass transport phenomena have also been observed in the literature such as case II and super case II mass transport (Emami *et al.*, 2014; Shi *et al.*, 2008), but might depend on pH and physical state (dried, swollen, molecular weight, etc.) of the Alg/Chit NPs as well as the molecular weight of each component. The fact that the value of "n" is below 0.45 can be explained by the presence of interactions as stated above. For instance, we observed that increasing the concentration of collagen in a hydrogel reduced the "n" as the interactions between pBMP-9 and the collagen fibres increased (Lauzon et al., 2014).

Since the driving mass transport phenomenon observed was diffusion, we developed a mechanistic mathematical framework based on Fick's second law of diffusion, to which we considered the electrostatic interactions between SpBMP-9 and the alginate chains using modified Robin boundary conditions at the surface of the NPs. This approach was already developed in a previous study (Lauzon et al., 2014). We also considered the size distribution in order to get a more precise modeling and applied the class method directly based on laser diffraction results. A similar approach has already been used in a drug delivery system to consider the size distribution of swellable microparticles based on a Weibull distribution and showed great accuracy in respect to experimental results (Grassi *et al.*, 2000). However, it is the first time that this method is used to model the release of therapeutics from NPs based on size distribution from common laser diffraction techniques. The model could be a good fit for the experimental data, thus confirming the proposed hypothesis. In addition, the fact that we considered the size distribution and the number of particles doing the mathematical modeling could represent more faithfully the system being investigated, since Alg/Chit NPs aggregates were present in the preparation as shown with laser diffraction and SEM results. We hypothesized that the encapsulation of SpBMP-9 would not affect the size of NPs, which was further confirmed with SEM analyses (data not shown). Those results were also consistent with those obtained by Goycoolea *et al.* (2009) with insulin. In addition, we also hypothesized that

the particle size would not change within the time-frame of the release kinetics experiments because of erosion. Goycoolea *et al.* (2009) have shown that alginate-coated chitosan NPs in which insulin was encapsulated kept their size during the release kinetics experiments for over 2h at physiological pH. In addition, Anal *et al.* (2003) showed that coating alginate NPs with HMW chitosan could drastically reduce the erosion caused by the ionic strength of sodium ions present in PBS and keep the integrity of the particles for over 24h.

The challenge in brain-targeting delivery systems is the available space for those NPs to circulate freely once in the brain tissue. Brain extracellular space having a void fraction of 0.2 is very tortuous with an estimated hydraulic extracellular space radius of ~ 64 nm, which limits the size of NPs (Salegio *et al.*, 2014; Thorne et Nicholson, 2006). Salegio *et al.* (2014) showed that the distribution and the speed of diffusion of small particles (~10-20 nm) infused inside the brain depended on the size of the particles. They also showed that the cerebrospinal fluid movement plays an important role in distributing those NPs. Haque *et al.* (2014) synthesized Alg/NPs with a similar protocol compared to what we used (composition, Alg/Chit/calcium mass ratio) and having an average size of ~173 nm (in aqueous solution). They showed that Alg/Chit NPs injected intranasally could be successfully delivered to the brain tissue (cerebellum and left, right and frontal encephalon) of Wistar rats. Conversely, too small NPs carrying hydrophilic drugs would too rapidly deliver their content in contrast to larger ones (Arifin *et al.*, 2006). For instance, mathematical modeling of SpBMP-9 released for each size class showed that NPs with diameters from 150 nm to 500 nm would have completely delivered their SpBMP-9 within 8h whereas bigger NPs (from 500 to 2400 nm) could sustain the delivery for at least 72h. There is obviously a middle point that has to be reached in order to optimize the size of NPs. Since it was shown that Alg/Chit NPs can be successfully injected intranasally even with size > 60 nm, Alg/Chit NPs as a SpBMP-9 delivery system remain a very interesting therapeutic approach in the context of Alzheimer's disease.

We also estimated the mechanistic parameters using an evolutionary algorithm. We first confirmed that the parameters were identifiable doing a systematic sensibility analysis. The presence of a multimodal function having many local minima and one global minimum supported the use of such a stochastic metaheuristic algorithm, which explores more globally the possible range of solutions. We estimated the effective diffusivity and the overall mass

transfer coefficient. The diffusivity estimated had quite a low value (3.3E-17 m²/sec), which is more commonly seen with hydrophobic drugs (Arifin *et al.*, 2006). Indeed, hydrophilic drugs released from NPs are expected to have an even higher effective diffusivity and a more rapid release since the available specific surface is higher (Arifin *et al.*, 2006). Hecq *et al.* (2015) have studied and modelled the release of insulin from chitosan NPs and have also observed a very low effective diffusivity (3.8E-16 m²/sec), which was less than one order of magnitude lower than expected for a hydrogel filled with hydrophilic drugs. The presence of interactions might explain this phenomenon as they also concluded. As for the overall mass transfer coefficient "k", we obtained a similar value in a previous study with a macroscopic delivery systems using a similar peptide (pBMP-9) (Lauzon *et al.*, 2014). The fact that the apparent diffusivity that we estimated in this study is lower than expected supports the fact that strong electrostatic interactions between SpBMP-9 and the alginate polymer chains might regulate the delivery.

Finally, once the Alg/Chit NPs were fully characterized, we investigated whether the encapsulated SpBMP-9 were still bioactive and could induce neuronal differentiation of human SH-SY5Y neuroblastoma cells. We first evaluated the impact of Alg/Chit NPs on the ability of SH-SY5Y cells to survive. Surprisingly, we found that the presence of NPs alone in a serum-free medium could increase the number of viable cells in comparison with the control as shown by the AlamarBlue enzymatic assay and confirmed with indirect cell counting. Borges *et al.* (2006) studied the cytotoxicity of alginate-coated chitosan NPs in the context of mucosal vaccination on splenocytes and found, using several different technics, that the presence of chitosan increased the cell viability in comparison to the control after 20h of incubation. Biswas *et al.* (2015) used alginate-coated chitosan NPs and found that the presence of alginate increased the cell viability on HT-29 cells. Huang *et al.* (2004) showed that chitosan NPs cytotoxicity using A549 cells depends on the percentage of deacetylation rather than molecular weight and that chitosan NPs were not more cytotoxic than soluble chitosan. In addition, at a concentration lower than ~0.7 mg/mL of chitosan in solution, no apparent cytotoxic effect could be observed. We found that SpBMP-9 released from Alg/Chit NPs was still bioactive as it could increase the neurite outgrowth, the neurite length, the expression of NSE, a terminal differentiation marker as well as the expression of VAchT and its localization within the neurites. Those results were in accordance with our previous study using the peptide directly in solution (Lauzon *et al.*, 2017). SpBMP-9, encapsulated in Alg/Chit NPs, still had its neuroinductive effect.

4.6 Conclusion

To conclude, we have demonstrated that SpBMP-9, a neuroinductive peptide derived from BMP-9, can successfully be encapsulated into Alg/Chit NPs having an average size of ~240 nm. We have also modelled the release kinetics using a new mechanistic approach and shown that there were electrostatic interactions between the peptide and the alginate chains, which mostly influenced the diffusivity. We based the mathematical modeling on the size distribution of the Alg/Chit NPs in order to take into account the size range and the presence of aggregates. This modeling approach is very interesting since it allows us to study the impact of the size on the contribution of delivery and might be helpful in determining the size range appropriate for brain targeting delivery systems having to cross the BBB. We finally demonstrated that, even when encapsulated, SpBMP-9 was still bioactive as it increased the levels of neuronal differentiation markers. The next step would be to evaluate the effect of this delivery system as an intranasal treatment and assess its efficacy *in vivo* using an AD mouse model.

4.7 Acknowledgments

CHAPITRE 5: COMBINAISON DE FACTEURS DE CROISSANCE

5.1 Informations relatives à l'article

Titre original: A small peptide derived from BMP-9 can increase the effect of bFGF and NGF on neuronaldifferentiation of SH-SY5Y cells.

Titre français : Un petit peptide dérivé de la BMP-9 peut augmenter l'effet du bFGF et du NGF sur la différenciation neuronale des cellules SH-SY5Y.

Auteurs et affiliations :

- M.-A. Lauzon : Étudiant au doctorat en génie chimique, Département de génie chimique et de génie biotechnologique, Université de Sherbrooke
- N. Faucheux : Professeur titulaire, Département de génie chimique et de génie biotechnologique, Université de Sherbrooke. Affiliation au Centre de Recherche Clinique du Centre Hospitalier Universitaire de Sherbrooke, 12e Avenue N, Sherbrooke, Québec, J1H 5N4, Canada

Date d'acceptation : S/O

État de l'acceptation : article en révision

Revue : *Molecular and Cellular Neuroscience*

Lien d'accès : S/O

Contributions à la thèse :

Cet article contribue à la thèse en présentant les résultats du quatrième objectif du projet de doctorat qui consistait à déterminer la présence de synergies entre les peptides dérivés de la BMP-9 et d'autres facteurs de croissance ayant montré un effet thérapeutique dans le contexte de l'AD. Les éléments suivants sont présentés :

- L'étude de la combinaison de différents de facteurs de croissance (IGF-2, EGF, bFGF et NGF) sur leur capacité à induire un effet synergique avec le SpBMP-9 en termes de morphologie

- L'effet de la combinaison du bFGF ou du NGF avec le SpBMP-9 sur la croissance et la taille des neurites ainsi que sur l'expression de marqueurs de différenciation neuronale et les niveaux de calcium intracellulaire.

Résumé anglais:

The current aging of the world population will increase the amount of people suffering from brain degenerative diseases such as Alzheimer's disease (AD). There are much evidence showing that the use of growth factors such as BMP-9 could restored cognitive function as it plays on many AD hallmarks at the same time. However, BMP-9 is a big protein expensive to produce that can hardly access the central nervous system. We have therefore developed a small peptide, SpBMP-9, derived from the knuckle epitope of BMP-9 and showed its therapeutic potential in a previous study. Since it is known that the native protein, BMP-9, can act in synergy with other growth factors in the context of AD, here we study the potential synergistic effect of various combinations of SpBMP-9 with bFGF, EGF, IGF-2 or NGF on the cholinergic differentiation of human neuroblastoma cells SH-SY5Y. We found that, in opposition to IGF-2 or EGF, the combination of SpBMP-9 with bFGF or NGF can stimulate to a greater extent the neurite outgrowth and neuronal differentiation toward the cholinergic phenotype as shown by expression of the neuronal markers NSE and VAchT and the levels of intracellular calcium. Those results strongly suggest that SpBMP-9 plus NGF or bFGF are promising therapeutic combinations against AD that required further attention.

Résumé français

Le vieillissement actuel de la population mondiale augmentera le nombre de personnes souffrant de maladies dégénératives comme la maladie d'Alzheimer (AD). Il existe de nombreuses preuves montrant que l'utilisation de facteurs de croissance telle que la BMP-9 pourrait restaurer les fonctions cognitives, car ces facteurs jouent sur plusieurs symptômes pathophysiologiques de l'AD en même temps. Cependant, la BMP-9 est une grosse protéine coûteuse à produire qui peut difficilement accéder au système nerveux central. Nous avons ainsi développé un petit peptide, SpBMP-9, dérivé de l'épitope Knuckle de la BMP-9 et nous avons

montré son potentiel thérapeutique dans une étude antérieure. Sachant qu'il est connu que la protéine native, BMP-9, peut agir en synergie avec d'autres facteurs de croissance dans le contexte de l'AD, nous avons ici étudié les effets synergiques potentiels de plusieurs combinaisons de SpBMP-9 avec le bFGF, l'EGF, l'IGF-2 ou le NGF sur la différenciation cholinergique de neuroblastomes humains SH-SY5Y. Nous avons montré que, contrairement à l'IGF-2 ou l'EGF, la combinaison du SpBMP-9 avec le bFGF ou le NGF peut stimuler dans une plus grande mesure la croissance des neurites et la différenciation neuronale vers le phénotype cholinergique mise en évidence par les marqueurs neuronaux NSE et VAchT et le niveau de calcium intracellulaire. Ces résultats suggèrent fortement que le SpBMP-9 plus le NGF ou le bFGF sont des combinaisons prometteuses contre l'AD qui requièrent une attention future.

5.2 Introduction

The current aging of the world population will increase the incidence of neurodegenerative disorders such as Alzheimer's disease (AD), thus creating a huge socio-economic burden estimated to be over several hundreds of billions of US dollars (Alzheimer's Association, 2017; World Health Organization, 2017). AD is characterized by three major hallmarks: (1) dysfunctional cholinergic system (Geula *et al.*, 2008), (2) senile plaque accumulation made of toxic β–amyloid peptide aggregates (Murphy et LeVine 3rd, 2010) and (3) the hyperphosphorylation of Tau protein, resulting in neurofibrillar entanglements (Alonso *et al.*, 1996; Augustinack *et al.*, 2002).The current treatments found on the market such as rivastigmine, galantamine, donepezil, or memantine cannot stop the evolution of the disease (Giacobini et Gold, 2013; Hansen *et al.*, 2008; Tricco *et al.*, 2013). Yet, there is no known cure of AD.

It has been shown that the use of growth factors, normally found in the healthy brain, but dysregulated in AD patients, could have a promising therapeutic potential (Lauzon *et al.*, 2015a). Among the growth factors, Bone Morphogenetic Protein-9 (BMP-9), a member of the TGF-β superfamily, was shown to act simultaneously on several hallmarks of the disease (Burke *et al.*, 2013; Lopez-Coviella *et al.*, 2000, 2002; Schnitzler *et al.*, 2010). For instance, it has been shown that BMP-9 could reduce the accumulation of senile plaque within the mouse brain and restore the cholinergic function (Burke *et al.*, 2013). It was also demonstrated that BMP-9 can induce the neuronal differentiation toward the cholinergic phenotype of mouse septal neurons

(Lopez-Coviella *et al.*, 2000). However, BMP-9 is a large (24 kDa) and expensive protein to produce that cannot access readily the brain tissue because of the naturel barriers such as the blood-brain barrier (Alyautdin *et al.*, 2014). However, a recent study has shown that BMP-9, injected intranasally into APP/PSI mice could access the brain to a certain extent (0.1 ng BMP-9/100 mg of protein in the cortex or hippocampus) and reduce senile plaque accumulation and restore cognitive function, but required important dosage (50 ng/g/d for 30 days) (Wang *et al.*, 2017). To overcome this issue, we have developed a small peptide derived from the knuckle epitope of BMP-9 (SpBMP-9) based on the previous work of Saito *et al.* (Saito *et al.*, 2003, 2005) on BMP-2. This peptide is 300-times less expensive than the native protein and we have recently demonstrated its capacity to induce the cholinergic differentiation of human neuroblastoma cells SH-SY5Y (Lauzon *et al.*, 2017). We have also showed that this peptide could act on at least two of the three major hallmarks of AD as it could deactivate GSK3beta, a Tau kinase, and increase the cholinergic activity with or without retinoic acid (Lauzon *et al.*, 2017).

Other growth factors have also showed promising effects in terms of their capacity to overcome the cell signaling dysregulation observed in AD patients and their ability to restore cognitive function (Gaviglio *et al.*, 2017; Lauzon *et al.*, 2015a; Pascual-Lucas *et al.*, 2014; Thomas *et al.*, 2017; Xu *et al.*, 2016). For instance, insulin-like growth factor-2 (IGF-2) was shown to reverse cognitive deficit, promote dendritic spine formation and restore hippocampal excitatory synaptic transmission in Tg256 mice, which is an AD mouse model overexpressing β–amyloid peptides (Pascual-Lucas *et al.*, 2014). Basic fibroblast growth factor (bFGF) encapsulated in lectin-PEG-PLGA nanoparticles, which were further injected intranasally into Sprague Dawley rats treated with β-amyloid peptides, was also shown to improve spatial and learning ability (Zhang *et al.*, 2014). In addition, it was recently shown that epidermal growth factors (EGF) could prevent the cognitive and cerebrovascular deficits of E4FAD mice bearing ε4-APOE alleles and overexpressing β–amyloid peptides (Thomas *et al.*, 2016, 2017). Another recent study also suggest that heparin-binding EGF like growth factors can promote the differentiation of neuroblastoma cells such as SH-SY5Y (Gaviglio *et al.*, 2017). Neurotrophins, which are neuronal differentiation factors implicated in the neural development and maintenance, can have also a therapeutic effect (Allen *et al.*, 2013; Xu *et al.*, 2016). Among them, nerve growth factor (NGF) was shown to decrease the accumulation of β–amyloid plaque

when injected intranasally in APP/PSE mice (Yang *et al.*, 2014). More recently, Marei *et al.* (2015) demonstrated, using Wistar rats with AD-like symptoms induced by ibotenic acid, that human olfactory bulb neural stem cells overexpressing human NGF that were transplanted into the hippocampus could restored the cognitive deficit.There are also multiple evidences showing that those growth factors can act in synergy (Lauzon *et al.*, 2015a; Lopez-Coviella *et al.*, 2000; Mellott *et al.*, 2014; Schnitzler *et al.*, 2010). For instance, Lopez-Coviella *et al.* (2000) demonstrated that bFGF could increase signficantly the cholinergic differentiation effect of BMP-9 on mouse septal neuron cultures. Schnitzler *et al.* (2010) showed that BMP-9 could increase the synthesis of NGF as an autocrine and paracrine cholinergic trophic factor. Burke *et al.* (2013) also showed that BMP-9, infused in APP/PS1 Alzheimer mouse model could increase the expression of NGF and IGF-1. Mellott *et al.* (2014) also showed that IGF-2 could increase, in APP/PS1 mice, the expression of BMP-9 and neurotrophin such as NGF which decreased the β–amyloid peptide accumulation and stimulated the expression of cholinergic markers. However, the synergistic effect between SpBMP-9 and other growth factors in the context of neuronal differentiation has not been shown yet.

This study surveys potential synergistic effect between SpBMP-9 and other growth factors that are known to have a therapeutic potential in the context of AD on SH-SY5Y cells, which is a well-known mature neuroblastoma cell line that has been used several times in the context of AD (Agholme *et al.*, 2010; Hegarty *et al.*, 2013b; Jämsä *et al.*, 2004; Koriyama *et al.*, 2015). We therefore stimulated SH-SY5Y cells with SpBMP-9 in combination with bFGF, EGF, IGF-2 or NGF and investigated their capacity to differentiate into mature neurons based on morphology and neuronal markers expression.

5.3 Materials and methods

5.3.1 Materials

SpBMP-9 (2.36 kDa, with a final purity of 98%) was chemically synthesized by EZBiolab (Carmel, IN, USA) and was resuspended in milli-Q sterile water at a concentration of 10 mg/mL and stored at -80°C for further use. IGF-2, bFGF, NGF and EGF (with a final purity >98%) were purchased from PeproTech (PeproTech Canada, Ca) and were resuspended to a final concentration of 100 μg/mL following the manufacturer's instructions and stored at -80°C

for further use. SH-SY5Y human neuroblastoma cells (CRL-2266) were purchased from ATCC (Manassas, VA, USA) and were kept frozen in liquid nitrogen prior to use. Culture media (DMEM/F12 1:1), trypsin-EDTA (0.25%) and penicillin-streptomycin (10,000 U/mL) antibiotics from Gibco® were purchased from ThermoFisher (ThermoFisher Scientific, Ca). Foetal bovine serum (FBS) was purchased from Wisent Bioproduct inc. (St-Bruno, Ca). Primary antibodies against VAchT (C-terminal polyclonal Rabbit IgG) and NSE (C-terminal polyclonal rabbit IgGs) were purchased from Sigma (Sigma Canada, ON, CA). Anti-rabbit secondary antibody conjugated to AlexaFluor® 488 was purchased from Cell Signal (New England Biolabs, ON, Ca). Calcium flux assay kit *Fluo-4 Direct™ Calcium Assay Kit* from Invitrogen was purchased from ThermoFisher (ThermoFisher Scientific, Ca).

5.3.2 Cell culture

SH-SY5Y cells were cultivated in T75 cell culture flasks containing DMEM/F12 supplemented with 10% (v/v) FBS in a water jacket humidified controlled environment (5% (v/v) CO_2) incubator (ThermoScientific, ThermoFisher, Ca). When cells reached 80% of confluency, they were trypsinized (Trypsin-EDTA 0.25%), centrifuged (100 x g, 5 min) and seeded either in 6-well plates containing sterile microscope coverslips, 96-well plates (Corning, USA).

5.3.3 Morphology analysis

SH-SY5Y cells were seeded on microscope coverslips. When cells reached 80% of confluency, culture medium was withdrawn and cells were washed with sterile phosphate buffered saline (PBS). Cells were then stimulated for 5 days in serum-free culture media supplemented with either IGF-2 (100 ng/mL), bFGF (20 ng/mL), EGF (100 ng/mL) or NGF (100 ng/mL) with or without SpBMP-9 (0.1 nM). After 5 days of incubation, 10 microscopic pictures per well were taken at a magnification of 10X for the GFs survey experiment and at 20X for the thorough analyzes with bFGF and NGF using a phase-contrast microscope (Nikon, Eclipse TE2000, Nikon Instruments inc., Japan) coupled with a CCD camera (Moticam Pro CCD 285C, Motic, Hong Kong). Each picture then underwent multiple numerical filtering treatments to highlight the neurites and cell body using an image analysis application developed under Python environment (Python 2.7.3) and OpenCV library (OpenCV 3.2). Briefly, pictures

were first smoothed with a Gaussian filter to remove noise. Pictures were then filtered with a Laplace high-pass filter following a median filter to detect and enhance neurites and cell bodies while reducing the background features. The resulting images showing the neurite edges (blue lines) and cell bodies (yellow) were superimposed to the original phase-contrast images.

5.3.4 Neurite length measurements

The mean neurites lengths were assessed using the 20X magnification high-resolution phase-contrast pictures previously described. The neurites were measured using an application programmed in a MatLab environment using the Image Analysis Toolbox (MatLab 2015, MathWorks, USA). The neurite length was defined as the Euclidean distance in pixel or a combination of Euclidean distances between the cell body and the end of the cell extension. Whenever there was multiple branching, the longest path was always chosen. The length in pixel was then converted to actual distance from the length bar provided by the microscope image acquisition software (Motic Image Advanced 3.2). Briefly, around 10 to 20 neurites were measured for each picture ($4x10^{-3}$ cm²/picture) and 10 pictures per experimental condition and per replicate were analyzed. The mean neurite length for each picture analyzed within a replicate was defined as the weighted mean based on the number of neurites measured. For each independent experiment, the average neurite length was weighted relative to the inverse of the variance of each replicate. The overall mean was calculated as the weighted mean of each independent experiment.

5.3.5 Immunostainings

SH-SY5Y cells cultivated on microscope coverslips and stimulated for 5 days in serum-free culture media containing bFGF (20 ng/mL) or NGF (100 ng/mL) with or without SpBMP-9 (0.1 nM) or the negative peptide NSpBMP-9 (0.1 nM) were fixed with paraformaldehyde 3% (w/v) for 15 min at room temperature. Cells were then permeabilized with 0.5 % (v/v) Triton-X100 (Sigma, Ca) for 5 min and then incubated with skim milk dissolved in PBS (3% w/w) for 30 min at 37°C. Coverslips were then incubated with primary antibodies against VAchT (diluted 1:500, Sigma) or NSE (diluted 1:100, Sigma) for 30 min at 37°C. Thereafter, samples were incubated with anti-Rabbit AlexaFluor® 488 conjugate antibodies (diluted 1:250, Cell Signalling) for 30 min at 37°C. Nucleus and actin cytoskeleton were also counter stained with

Hoechst 33342 (5µg/mL, Life Technologies, ThermoFisher Scientific, USA) and Rhodamin-Phalloidin (diluted 1:200, Sigma) respectively. Coverslips were mounted on microscope glass slide and visualized at a magnification of 40X with an Evos FL Auto epifluorescence microscope (LifeTechnologies, ThermoFisher Scientific, USA).

5.3.6 Intracellular calcium assay

SH-SY5Y cells were seeded on a cell culture-treated 96-well plate. When cells reached 80% of confluency, they were stimulated for 5 days in serum-free media containing either bFGF (20 ng/mL) or NGF (100 ng/mL) with or without SpBMP-9 (0.1 nM) or NSpBMP-9 (0.1 nM). After 5 days of incubation, levels of intracellular calcium were assessed using *Fluo-4 Direct™ Calcium Assay Kit* following the manufacturer's instructions. Briefly, culture media was removed and cells were washed with sterile PBS. 50 µL/well of serum-free culture media and 50 µL/well of 2X Fluo-4 Direct™ calcium reagent loading solution containing probenecid with a final concentration of 5 mM were added and allowed to react for 30 min at 37°C (5% CO_2) followed by an incubation of 30 min at room temperature covered from light. Cells were then observed at a magnification of 20X using an Eclipse TE2000 epifluorescence microscope (Nikon, Nikon Instruments inc., Japan) coupled with a CCD camera (Moticam Pro CCD 285C, Motic, Hong Kong). All the pictures were taken using the same light intensity and exposure time.

5.3.7 Statistics

Statistical analyzes were performed with an Excel 2010® data analyzes package. Data were analyzed with ANOVA followed by the Tukey post-hoc pair-wise comparison test. Only differences with $p \leq 0.05$ were considered statistically significant.

5.4 Results

5.4.1 Preliminary growth factor combinations survey

To determine whether a growth factor with a known therapeutic potential in the context of AD could act in synergy with SpBMP-9, SH-SY5Y cells were stimulated for 5 days in the presence of IGF-2 (100 ng/mL), EGF (100 ng/mL), bFGF (20 ng/mL) or NGF (100 ng/mL) with or without SpBMP-9 (0.1 nM). Phase-contrast pictures were then taken and filtered to highlight

the cell body (yellow) and the neurite (blue) and the morphology and neurite outgrowth were studied (Figure 5-1). SpBMP-9 alone induced an increase in neurite outgrowth in comparison to the control (CTL). In addition, cells stimulated with IGF-2, bFGF and EGF promoted the proliferation of the cells in comparison with the control as shown by a greater cell density depicted with more yellow in the picture. Only cells stimulated with bFGF and NGF induced neurite outgrowth when combined with SpBMP-9 as it was highlighted with the magnified pictures (Figure 5-1).
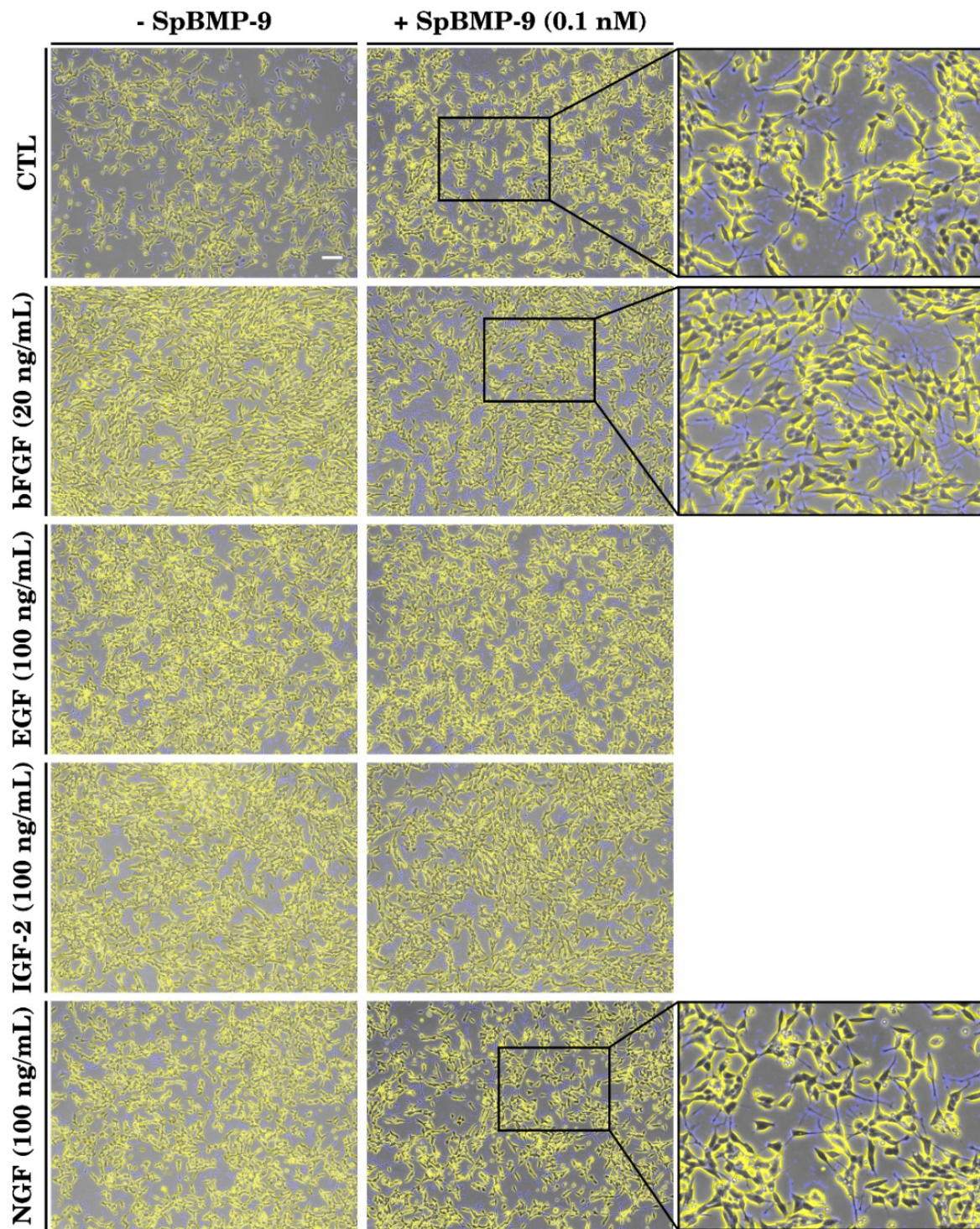
Figure 5-1 : Representative phase contrast pictures that were filtered in order to enhance the neurites (blue) and the cell body (yellow) for SH-SY5Y cells stimulated for 5 days in serum-free culture medium alone or serum-free culture medium containing bFGF (20 ng/mL), EGF (100 ng/mL), IGF-2 (100 ng/mL) or NGF (100 ng/mL) with or without SpBMP-9 (0.1 nM). Results are representative of 3 independent experiments performed in duplicate. Bar = 100 μm

5.4.2 Morphology analyzes and neurite lengths

The combination of SpBMP-9 with bFGF and NGF was then studied more thoroughly in terms of morphology and neurite outgrowth. Phase contrast pictures were taken at a higher magnification (Figure 5-2A and B). Cells stimulated with SpBMP-9 showed more and longer neurites compared with both the control (CTL) and the negative peptide NSpBMP-9 (0.1 nM). In the case of SH-SY5Y cells stimulated with bFGF (20 ng/mL), SpBMP-9 alone induced more and longer neurites in comparison with both the control and the negative peptide NSpBMP-9 (Figure 5-2A). bFGF alone induced even more and longer neurites. However, the presence of SpBMP-9 increased the length of the neurites when combined with bFGF. The same observations could be made for cells stimulated in the presence of NGF (Figure 5-2B) with neurite length similar to what was observed in cells stimulated with bFGF.

Since the neurites appeared to be longer in the presence of bFGF or NGF for cells stimulated with SpBMP-9, the neurites were measured as previously described (Lauzon *et al.*, 2017). Results confirmed the qualitative observations made on the phase contrast pictures. Cells stimulated in the presence of SpBMP-9 had longer neurites in comparison to both the control (CTL) and the negative peptide NSpBMP-9 ($p<0.001$). Cells stimulated with bFGF (Figure 5-2C) or NGF (Figure 5-2D) alone also induced longer neurites compared with SpBMP-9 ($p<0.001$). Finally, the combination of SpBMP-9 with bFGF (Figure 5-2C) or NGF (Figure 5-2D) induced the longest neurites with length higher than bFGF or NGF alone. In addition, bFGF or NGF gave similar lengths with or without SpBMP-9. Those results indicate that combining SpBMP-9 with bFGF or NGF can increase the SH-SY5Y neuronal differentiation to a similar extent based on morphological analyzes.

5.4.3 Neuronal marker expression and localization

Since the morphology analyzes indicated that SpBMP-9 combined with bFGF or NGF could increase the neuronal differentiation in terms of neurite outgrowth, the next step was to confirm whether those growth factors could increase the expression of the late terminal neuronal marker NSE, located within the cell body (Figure 5-3). Results agreed well with the morphology analysis. Indeed, cells stimulated with SpBMP-9, bFGF or NGF alone increased the level of NSE in comparison with the control or the negative peptide NSpBMP-9 as the level of green

fluorescence where higher. bFGF or NGF combined with SpBMP-9 showed an increased level of NSE expression as seen by a more pronounced fluorescence intensity in the green channel.
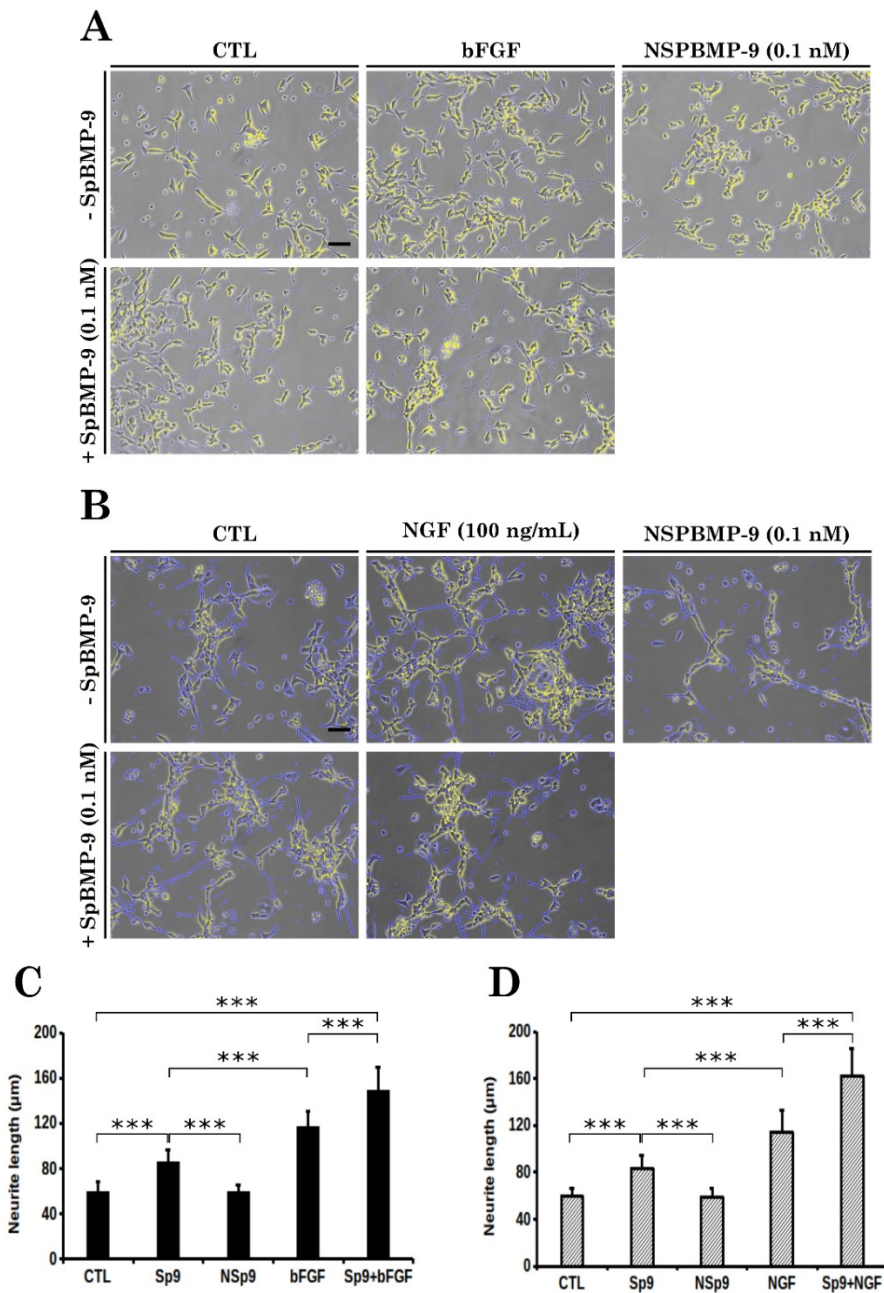
Figure 5-2 : Representative phase contrast pictures with a magnification of 20X that were filtered in order to enhance the neurites (blue) and the cell body (yellow) for SH-SY5Y cells stimulated for 5 days in serum-culture medium containing A) bFGF (20 ng/mL) or B) NGF (100 ng/mL) with or without SpBMP-9 (0.1 nM) or the negative peptide NSpBMP-9 (0.1 nM). Results are representative of at 3 independent experiments performed in duplicate. Bar = 100 μm. Average neurite lengths ± SD for SH-SY5Y cells stimulated for 5 days in serum-free culture medium containing C) bFGF (20 ng/mL) or D) NGF (100 ng/mL) with or without SpBMP-9 (Sp9, 0.1 nM) or NSpBMP-9 (NSp9, 0.1nM). Results are representative of at least 2 independent experiments performed in duplicate. Over 500 measurements were made for each experimental condition. (*** p<0.001).
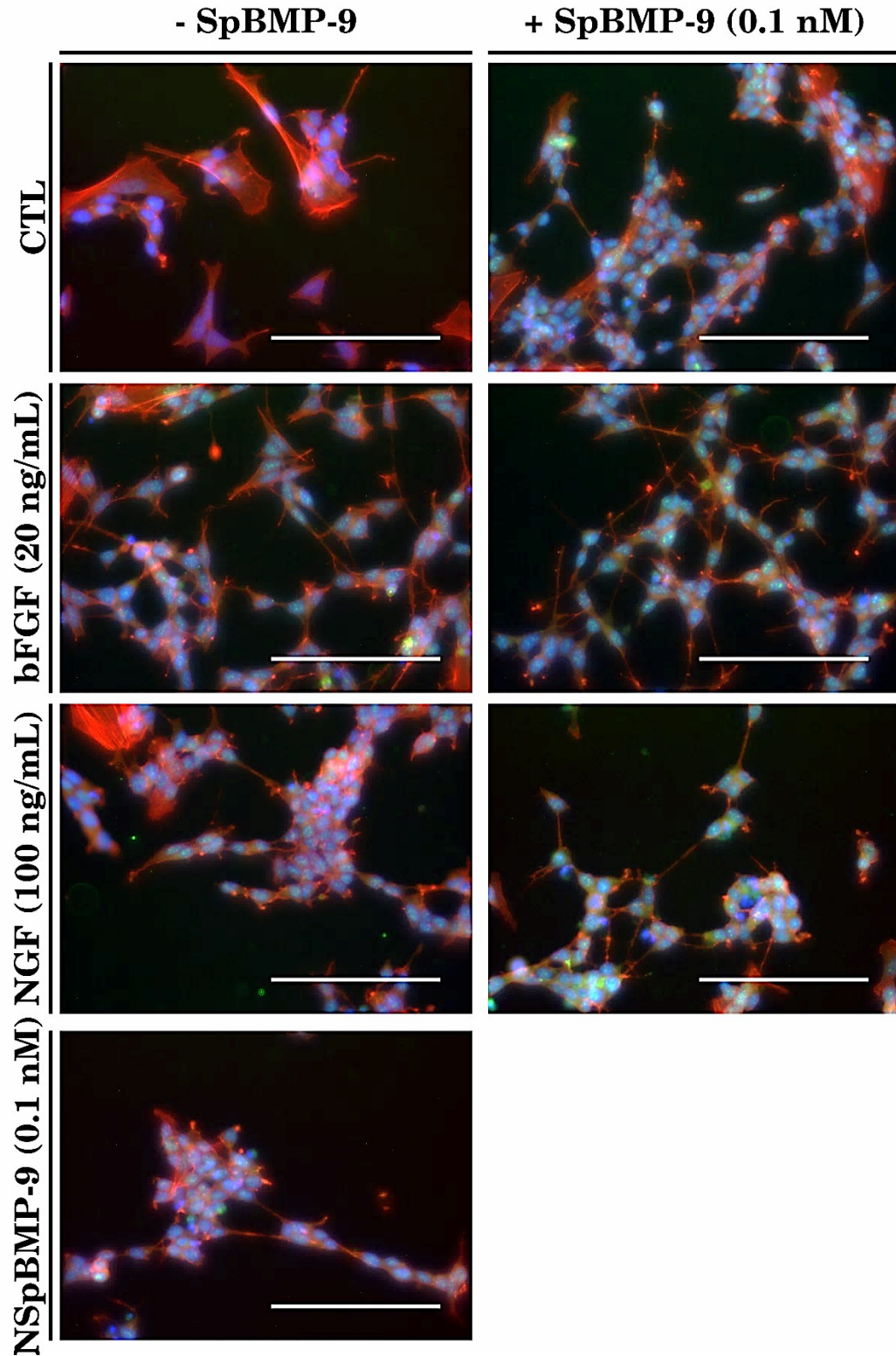
Figure 5-3 : Representative immunostaining pictures of NSE (green), nucleus (blue) and actin cytoskeleton (red) of SH-SY5Y cells stimulated for 5 days in serum-free culture medium alone or supplemented with bFGF (20 ng/mL) or NGF (100 ng/mL) with or without SpBMP-9 (0.1 nM) or containing NSpBMP-9 (0.1 nM). Bar = 100 μm. Results are representative of at least 2 independent experiments.

The expression and the localization VAchT, a protein responsible for the storage of intracellular acetylcholine within the cell neurites, was then studied in order to determine whether bFGF or NGF combined with SpBMP-9 could promote the cholinergic differentiation as SpBMP-9 alone (Lauzon *et al.*, 2017). Cells stimulated with SpBMP-9 showed an increase of VAchT staining within the cell neurites in comparison with both the control and the negative peptide NSpBMP-9 (Figure 5-4). An increase in the fluorescence intensity could also be observed for cells stimulated with NGF alone. However, bFGF alone appeared to induce an important accumulation of VAchT under the shape of large vesicles located along neurites. The intensity of the staining was even more important when cells were stimulated with bFGF or NGF in the presence of SpBMP-9, especially with bFGF where large vesicles could be observed along the neurites as pointed out by the white arrows (Figure 5-4). Those results confirmed that NGF and especially bFGF can increase the differentiation toward the cholinergic phenotype.
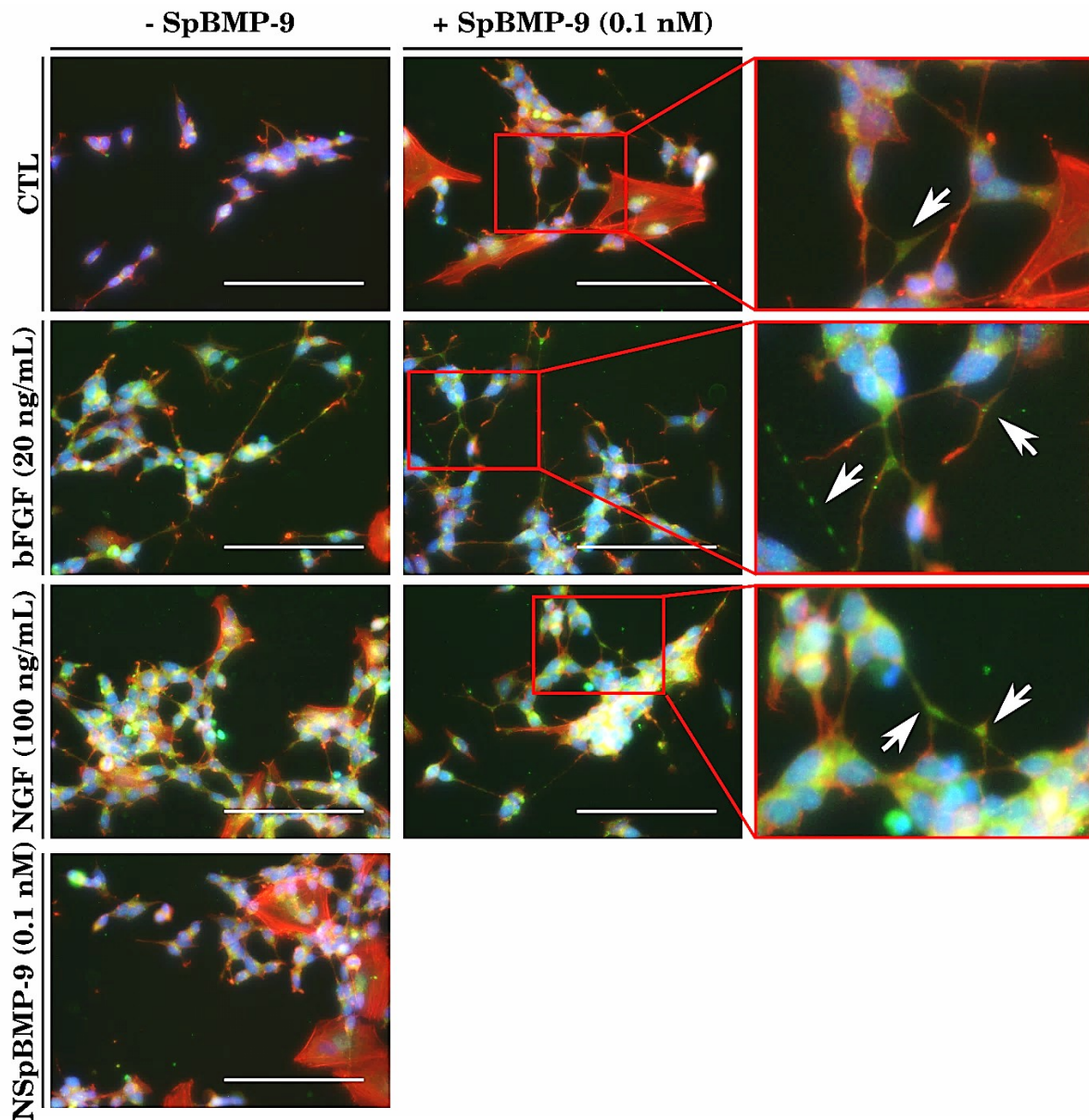
Figure 5-4 : Representative immunostaining pictures of VAchT (green), nucleus (blue) and actin cytoskeleton (red) of SH-SY5Y cells stimulated for 5 days in serum-free culture medium alone or supplemented with bFGF (20 ng/mL) or NGF (100 ng/mL) with or without SpBMP-9 (0.1 nM) or containing NSpBMP-9 (0.1 nM). White arrows show the presence of VAchT vesicles located in the neurites of the cells on magnified pictures. Bar = 100 μm. Results are representative of at least 2 independent experiments.

5.4.4 Intracellular levels of calcium

To verify whether cells were functional, calcium exchange was studied using cell-permeable calcium dye Fluo-4. Intracellular calcium is known to be implicated in neurite outgrowth as it contribute to neurite growth cone elongation and important levels of intracellular calcium can be associated with neuronal differentiation (Streit et Stern, 1999). Stained cells

where visualized under an epifluorescence microscope with the green filter (Figure 5-5). Cells stimulated with SpBMP-9 showed a higher staining intensity in comparison to the control and the negative peptide NSpBMP-9. However, the negative peptide induced itself a fluorescence staining slightly more intense than the control. Both bFGF and NGF-stimulated cells also showed an increase in calcium staining compared with the control. Combining SpBMP-9 with bFGF or NGF resulted in an increase in fluorescence intensity compared to the growth factors alone and an accumulation within the neurites. Those results indicate that SpBMP-9 could increase the level of intracellular calcium within SH-SY5Y cells, whereas the combination of SpBMP-9 with bFGF or NGF appeared to increase slightly this calcium exchange.
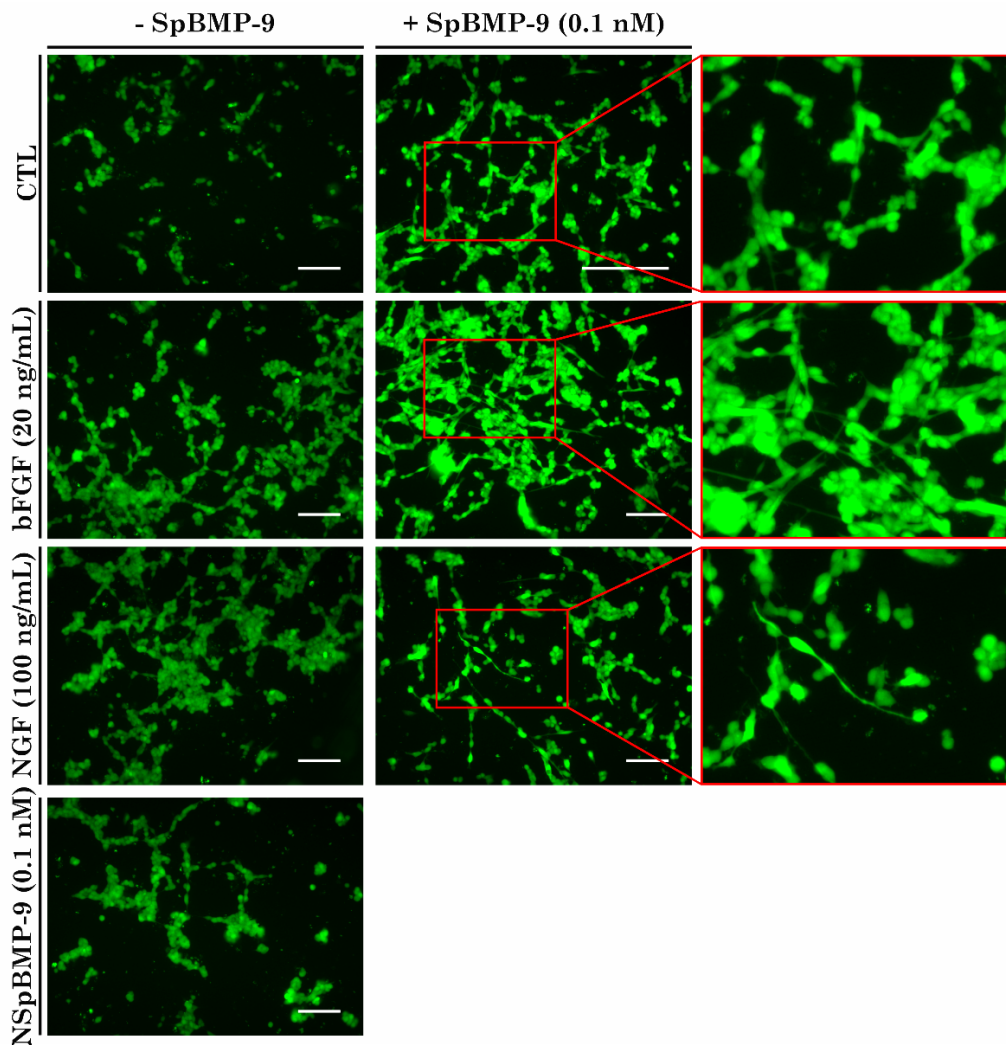
Figure 5-5 : Representative pictures of calcium staining (calcium Fluo-4 staining) of SH-SY5Y cells stimulated for 5 days in serum-free culture medium alone or supplemented with bFGF (20 ng/mL) or NGF (100 ng/mL) with or without SpBMP-9 (0.1 nM) or containing NSpBMP-9 (0.1 nM). Bar = 100 µm. Results are representative of at least 2 independent experiments performed in sixtiplicate.

5.5 Discussion

In this study, the effect of various combinations of SpBMP-9 with growth factors known to have a therapeutic effect in the context of AD was investigated. We have recently demonstrated that SpBMP-9 alone could increase the number and the length of neurites in SH-SY5Y cells in addition to increase MAP-2, NSE and VAchT expression (Lauzon *et al.*, 2017). SpBMP-9 alone was used as the base-line in this study and we obtained similar results in comparison to our previous work for cell morphology and neuronal marker expression and localization. In addition, we compared the peptide SpBMP-9 with a negative peptide, to which, the active site residues were changed for Glycine. We observed that NSpBMP-9 failed to increase the neurite length and the level of neuronal markers nor the calcium exchanges compared to the control. Thus, those results confirm the bioactivity of SpBMP-9 and the specificity of its active site. Previous work of Saito *et al.* (2003) on a similar peptide derived from BMP-2 (P4/P24) also showed its specificity compared to a scramble peptide in the context of bone repair.

In the first GFs survey, we investigated the combination of SpBMP-9 with various GFs such as IGF-2, EGF, bFGF and NGF. There was no strong synergistic effect in terms of morphology changes and neurite outgrowth for cells stimulated with SpBMP-9 combined with IGF-2 nor EGF using various concentrations (see supplementary data). This was unexpected in the case of IGF-2, since it was shown that IGF-2 can stimulate the expression of protein mRNA of BMP-9 and neurotrophins in PSI/APP mice as well as increasing the level of cholinergic marker (Mellott *et al.*, 2014). We have also demonstrated in a previous study a synergistic effect between BMP-9 and IGF-2 in the context of bone regeneration (Lauzon *et al.*, 2014). However, the fact that IGF-2 stimulates mRNA expression does not necessarily imply the presence of a synergistic effect afterwards. We also observed higher cell density for cells stimulated with IGF-2 either alone or with SpBMP-9 compared with the control, which indicated a dual effect of differentiation/proliferation since the cells were incubated in serum-free culture media. The high proliferating effect of IGF-2 already reported in SH-SY5Y cells cultivated in low serum condition (0.1% v/v) may explain its low effect in terms of neuronal differentiation (Leventhal *et al.*, 1995). As of EGF, our morphology results showed that EGF (100 ng/mL) alone induced

more neurite outgrowth compared to the control, but there was no significant synergistic effect observed when combined with SpBMP-9. A recent study showed that a heparin-binding EGF-like growth factor at low concentrations (0.5 and 1 ng/mL) can promote the neuronal differentiation and increase neurite outgrowth of SH-SY5Y cells (Gaviglio *et al.*, 2017). The effect of this growth-factor-like molecule was also greater than that of EGF. However, there have been no report yet about synergistic interactions between BMP-9 and EGF in the context of brain cells. In murine mesenchymal stem cell line C3H10T1/2, a synergistic effect between BMP-9 and EGF was observed in osteogenic differentiation (Liu *et al.*, 2013). Since cell type and experimental condition are different, that may explain the absence of effect we observed in this study.

Contrary to EGF and IGF-2, bFGF and NGF appeared to act in synergy with SpBMP-9. We observed that bFGF alone with a concentration of 20 ng/mL induced high cell density in comparison with the control in serum-free medium after 5 days of cultures. Similar effect were observed in the literature since it was shown that bFGF can promote cell proliferation of SH-SY5Y in a dose-dependent manner in B-27 supplemented proliferation culture medium (Boku *et al.*, 2013). However, we also observed more and longer neurites in comparison with the control at the same time. Mie *et al*. (2014) used bFGF-tethered extracellular matrix-like coating to cultivate PC12 cells and also observed neurite outgrowth. bFGF also promoted the neuronal differentiation as observed by an increased expression of the neuronal markers NSE and VAchT. Similar tendencies were also shown in literature using neuronal stem cells. For instance, neuronal mouse stem cells stimulated with 100 ng/mL of bFGF also expressed more NSE in comparison with the control (Chen *et al.*, 2014). The combination of bFGF (100 ng/mL) and NGF (100 ng/mL) increased even more the level of neuronal markers. From those results, even if bFGF seems to promote the proliferation of SH-SY5Y, the presence of neurite outgrowth at the same time is also possible. Levinius *et al*. (1994) demonstrated that bFGF-induced differentiation of SH-SY5Y cells was not associated with growth arrest as cells increased their neurites while proliferating. There is also evidence of interactions between bFGF and BMPs. However, the synergistic effect observed between bFGF and BMPs appear to be BMPs-type dependent. For instance, Mabie *et al*. (1999) observed that high concentration of BMP-2 (100 ng/mL or 3.84 nM) negatively regulated the cell viability of cortical E13 murine cells and reversed the proliferation effect induced by bFGF. They also showed that BMP-2 alone

promoted, within a concentration range of 1-10 ng/mL, the astroglial and neuronal differentiation. The involvement of BMP and bFGF signalling in neuronal development have already been shown many times in the last decades where positive effects were also observed. For instance, Streit and Stern (1999) demonstrated that BMP-4 and bFGF signalling were important cues in the establishment and maintenance of the border of the neural plate in avian model. In addition, Lopez-Coviella *et al.* (2000) showed that bFGF could increase in a dose dependant manner the BMP-9-induced synthesis of acetylcholine of E14 murine cells from septal culture with a maximum concentration obtained at 20 ng/mL. Our results also showed an increase in cholinergic differentiation for SH-SY5Y cells stimulated with SpBMP-9 in combination with bFGF (20 ng/mL) where more VAChT was expressed and located into the neurites. Morphology analysis also indicate that combining bFGF and SpBMP-9 resulted in more and longer neurites. BMP-9 belongs to another BMP subfamily than do BMP-2 and BMP-4 and therefore does not activate the same cell receptors (Senta *et al.*, 2009). This difference in sequence might explain why neuronal and neuronal progenitor cells react differently in function of the BMP used.

Cells stimulated with NGF alone also induced neurite outgrowth to a greater extent in comparison with the control as well as an increase in the expression of neuronal differentiation markers as shown by immunostainings against NSE and VAChT. Similar results in terms of neurite length and growth were observed for SH-SY5Y cells stimulated for 10 days in the presence of 50 ng/mL of NGF (Simpson *et al.*, 2001). However, the authors of this study noticed that NGF could also increase the cell number of SH-SY5Y cells. However, we did not observe a proliferation effect of NGF in serum-free medium. NGF also increased the level of NSE, which is in agreement with the literature as it was shown that NGF can increase the expression of NSE in PC12 rat cells (Vinores *et al.*, 1981). We also observed an increase in VAChT expression as well as the presence of vesicle within the neurites. It was demonstrated in PC12 cells that NGF can regulate the cholinergic locus via the activation of PI3K/Akt pathway (Madziar *et al.*, 2008). It was also shown that mouse neuronal stem cells stimulated with NGF (100 ng/mL) express more NSE in comparison to the control (Chen *et al.*, 2014). There are also evidences showing that NGF can act in synergy with BMP-9. Schnitzler *et al.* (2010) demonstrated that BMP-9 can induce the expression of NGF in mouse septal neurons, which, in return, can act as an autocrine or paracrine cholinergic trophic factor. Burke *et al.* (2013) also demonstrated that

intracerebroventricular infusion of BMP-9 into APP/PS1 Alzheimer mouse model increased the level of NGF protein expression measured in the basal forebrain cholinergic neurons. We have also recently demonstrated that SpBMP-9 can activate the PI3K/Akt pathway in SH-SY5Y (Lauzon *et al.*, 2017). Since NGF requires the activation of this signalling pathway to promote the cholinergic differentiation, this might explain why SpBMP-9 and NGF can act in synergy. We have also showed that NGF combined with SpBMP-9 could increase the neurite outgrowth as well as the level of NSE to a greater extent than NGF nor SpBMP-9 alone did.

Finally, we measured the amount of calcium inside the cytosol of SH-SY5Y cells. We observed for SpBMP-9 induced an increase in intracellular calcium in comparison with the control or the negative peptide. bFGF and NGF alone also increase the level of intracellular calcium. However, the combination of SpBMP-9 plus bFGF or NGF increased even more the fluorescence intensity observed. Increased in intracellular calcium has been shown to play an important role in neurite outgrowth (Streit et Stern, 1999). For instance, Pieri *et al*. (1997) showed that differentiation of SH-SY5Y cells induced by retinoic acid resulted in an accumulation of intracellular calcium. Ronn *et al.* (2002) showed that an increase in intracellular calcium was required in NCAM-derived peptide PC12-E2 cells differentiation. In addition, Cohen *et al.* (2015) also showed that PC12 differentiated with NGF had a higher level of intracellular calcium, which was associated with neurite and axonal growth. Similar results were also obtained using cervical gaglia cells (Howard *et al.*, 2013). Zatkova *et al.* (2017) demonstrated that oxytocin required an increase in intracellular calcium to promote the differentiation of SH-SY5Y and the neurite outgrowth. Therefore, since higher level of intracellular calcium is associated with neuronal differentiation, those results suggest that SpBMP-9, bFGF and NGF either alone or combined increase the neuronal differentiation and are thus in accordance with neurite outgrowth and neuronal marker expression.

Taken together, those results suggest that SpBMP-9 can act in synergy with both bFGF and NGF and direct the differentiation of human neuroblastoma cells toward the cholinergic phenotype. The results of this study also suggest that the known synergistic effect between the native protein BMP-9 and NGF or bFGF can be extended to one of its derived peptide.

5.6 Conclusion

To conclude, we have shown in this study that SpBMP-9 combined with bFGF or NGF can increase significantly the neurite length of SH-SY5Y cells, promote their differentiation toward the cholinergic phenotype and increase their intracellular calcium. Those results strongly suggest that these growth factor combinations feature a great therapeutic potential in the context of Alzheimer's disease that will required further analysis to understand the underlying mechanisms.

5.7 Acknowledgments

5.8 Declaration of interest

All authors have no conflict of interests to disclose.

CONCLUSION ET PERSPECTIVES

5.9 Conclusion générale

L'AD est une maladie dégénérative du cerveau qui induit un lourd fardeau socio-économique de plusieurs centaines de milliard de dollars annuellement. Le vieillissement croissant de la population mondiale, notre faible connaissance des causes exactes de cette maladie ainsi que l'inefficacité des traitements actuellement retrouvés sur le marché font de l'AD un fléau à prendre très au sérieux.

La revue de littérature a permis de mettre en évidence que l'utilisation de certains facteurs de croissance naturellement présents chez le cerveau de patients sains pourrait être une alternative thérapeutique prometteuse face aux traitements actuels. Parmi ces derniers, le potentiel thérapeutique de la BMP-9 a été abondamment étudié dans ce contexte. Toutefois, ces mêmes facteurs de croissance sont généralement volumineux et coûteux à produire en plus d'avoir un faible pouvoir de pénétration au cerveau en raison des barrières naturelles du corps humain. Il subsiste ainsi une multitude d'inconnues quant aux stratégies d'acheminement de facteurs de croissance au cerveau et la compréhension des phénomènes qui sont impliqués.

À cet effet, les travaux réalisés dans le cadre de ce projet de doctorat ont permis de mettre en évidence que l'utilisation d'un peptide dérivé de la BMP-9, le SpBMP-9, pouvait surmonter plusieurs problèmes que rencontrent les facteurs de croissance dans leur adressage au CNS. Ce peptide, 300 fois moins couteux à produire que la protéine native, possède un potentiel thérapeutique qui a été montré à plusieurs niveaux tout au long de ce document. Dans un premier temps, il a été montré que le SpBMP-9 pouvait stimuler la croissance de neurites et induire la différenciation neuronale plus efficacement que la protéine native, et ce, en présence ou non d'acide rétinoïque. Par ailleurs, les travaux réalisés ont également montré que le SpBMP-9 était en mesure d'intervenir sur au moins deux symptômes pathophysiologiques associés à l'AD, soit en stimulant l'orientation de la différenciation vers le phénotype cholinergique et en désactivant la GSK3β.

Ensuite, il a été montré que le SpBMP-9 pouvait être encapsulé dans un système de libération à l'échelle nanométrique. L'utilisation d'un tel système de libération est nécessaire afin de protéger le peptide tout au long de son acheminement au cerveau, mais permet également

de favoriser le passage au travers de la barrière hématoencéphalique. L'utilisation d'un système de libération composite à base d'alginate et de chitosane permet de bénéficier des qualités et avantages propres à chacun de ces matériaux en limitant notamment l'inflammation tout en favorisant l'adhésion aux muqueuses. Les résultats ont montré que, non seulement le SpBMP-9 pouvait être encapsulé dans les nanoparticules de quelques centaines de nanomètre de diamètre, mais que ces dernières pouvaient créer des interactions électrostatiques avec le peptide, permettant ainsi une libération plus soutenue dans le temps. Le développement d'un modèle mathématique mécanistique a également permis de mieux cerner les phénomènes de transfert de masse présents dans le système en plus de fournir une plateforme mathématique permettant l'optimisation d'un système de libération à base de nanoparticules. De plus, les essais *in vitro* ont montré à plusieurs niveaux que le système de libération était non toxique et que le peptide libéré restait bioactif.

Les travaux subséquents ont permis de montrer que les synergies observées entre la BMP-9 et d'autres facteurs de croissance comme le bFGF et le NGF étaient transposables au peptide SpBMP-9. En effet, le SpBMP-9 combiné au bFGF ou au NGF pouvait stimuler plus efficacement que les molécules utilisées séparément la différenciation neuronale et l'orientation des cellules vers un phénotype cholinergique.

En conclusion, les travaux réalisés dans cette thèse confirment les hypothèses qu'un peptide dérivé de la BMP-9 : (1) possède, tout comme la protéine native, un fort potentiel thérapeutique dans un contexte de l'AD, (2) peut être encapsulé dans un système de libération et (3) peut agir en synergie avec d'autres facteurs de croissance ayant eux-mêmes un potentiel thérapeutique démontré. Des études plus approfondies sur le mode de fonctionnement du SpBMP-9 sont maintenant requises ainsi que la mise à l'épreuve du système de libération en conditions *in vivo* afin d'avancer vers le développement d'une stratégie de traitement concrète.

5.10 Perspectives

Bien que les travaux réalisés dans cette thèse répondent à plusieurs interrogations quant à l'utilisation de peptides dérivés de facteurs de croissance comme stratégie de traitement contre l'AD, plusieurs perspectives en découlent.

5.10.1 Comprendre la signalisation induite par le SpBMP-9 versus la protéine native

Les résultats obtenus dans cette thèse montrent que les peptides dérivés de la BMP-9, le pBMP-9 et le SpBMP-9, sont en mesure d'activer la voie des Smad1/5 et de permettre leur translocation au noyau. Cette activation est toutefois moins importante que la celle de la BMP-9.

En outre, la littérature semble mitigée sur l'importance des réactions croisées entre la voie canonique des Smad et celle des MAPK dans la différenciation neuronale. Par exemple, les travaux d'Hegarty *et al.* (2013b) ont montré que la différenciation des cellules SH-SY5Y induite par la BMP-2 et la BMP-14 (GDF-5) passait principalement par la voie des Smad1/5 alors que la voie des MAPK était plutôt dérégulée. Les travaux récents de Wang *et al.* (2017) ont montré que l'injection intranasale de BMP-9 chez des souris APP/PSI activait la voie des Smad, mais non celle des MAPK (ERK1/2 et P38) dans un contexte d'AD. En contrepartie, les travaux de Guan *et al.* (2016) ont mis en évidence que l'effet protecteur de la BMP-7 sur des cellules SH-SY5Y mis en pré-conditionnement ischémique dans un contexte d'accident vasculo-cérébral passait par l'activation des Smad1/5, d'ERK et de P38. Les travaux récents de Gomita *et al.* (2017) ont également montré que le plasma de rat ayant subi une auto-stimulation intra crâniale augmentait la croissance des neurites chez des cellules de rat PC12. Cette augmentation était également associée à l'activation de P38. Chen *et al.* (2016) ont pour leur part montré que la croissance des neurites induites par des séquences non codantes d'ARN de Malat1 nécessitait l'activation d'ERK chez des neuroblastes de souris N2A.

Les résultats de cette thèse montrent également que le pBMP-9 et surtout le SpBMP-9, activent la voie PI3K/Akt de façon plus importante que la BMP-9, résultant en la désactivation de la GSK3β. La voie PI3K/Akt semble également très importante pour la différenciation neuronale. En effet, il a été montré que la croissance de neurite induite par la BMP-7 dans des neurones sympathétiques nécessitait l'activation du récepteur à NGF (p75) (Courter *et al.*, 2016), connu pour activer à son tour la voie PI3K/Akt. Cette voie de signalisation est d'ailleurs très importante pour la différenciation cholinergique. En effet, Madziar *et al.* (2008) ont mis en évidence que l'activation de la voie PI3K/Akt était nécessaire pour l'expression des gènes présents sur le locus associé à la synthèse, le stockage et le traitement de l'acétylcholine. Nous

avons également montré que le SpBMP-9 pouvait agir en synergie avec le bFGF et le NGF, connus pour activer cette même voie de signalisation comme nous l'avons abordé dans la revue de la littérature (section 2.1). L'activation de la voie des Smad et de la voie PI3K/Akt expliquerait peut-être pourquoi un tel effet combiné est observable. Toutefois, il a été également montré que la protéine Tau hyperphosphorylée pouvait séquestrer les Smad 2/3 activés par TGFβ, limitant par le fait même leur capacité de transloquer au noyau (Baig *et al.*, 2009). Ainsi, dans un contexte pathologique, l'effet thérapeutique de la BMPs ou du SpBMP-9 n'est peut-être pas uniquement Smad-dépendante comme le mentionnent des travaux réalisés sur la BMP-2 (Hegarty *et al.*, 2013b, 2014), ce qui nécessiterait une étude plus approfondie.

Finalement, les résultats présentés au 3 ont mis en évidence que les peptides dérivés de la BMP-9 étaient en mesure d'inactiver la GSK3β en induisant sa phosphorylation sur la Ser9 via l'activation de la voie de signalisation PI3K/Akt. Bien que la GSK3β semble jouer un rôle important dans le contexte de l'AD, l'inhibition de cette dernière jouerait également un rôle important dans la maladie de Parkinson en limitant à la fois la phosphorylation de Tau et l'expression d'α-synucléine (Kozikowski *et al.*, 2006). D'ailleurs, une étude récente a montré que l'activation de la voie PI3K/Akt/GSK3β par l'isoflurane chez le rat (Wistar) ayant subi une lésion unilatérale induite par la 6-hydroxydopamine afin de mimer la maladie de Parkinson améliorait drastiquement le déficit moteur (Leikas *et al.*, 2017).

Les différences observées en termes de signalisation cellulaire entre les peptides dérivés de la BMP-9 et la protéine native soulèvent plusieurs questionnements quant aux mécanismes d'action du pBMP-9 et du SpBMP-9. Au regard de la complexité et de la spécificité des mécanismes de signalisation cellulaire et des réactions croisées présentes, il serait alors important d'approfondir notre compréhension des voies de signalisation impliquées ici. De plus, une meilleure compréhension de certaines de ces voies de signalisation permettrait d'évaluer l'application de ces peptides dans d'autres pathologies d'intérêt touchant le système nerveux central.

5.10.2 Améliorer la spécifié du système de libération pour le système nerveux central

Comme discuté précédemment, le chitosane et l'alginate sont des matériaux de choix pour le développement d'un système de libération, notamment en raison de leurs bonnes propriétés muco-adhésive. Toutefois, il existe maintenant des stratégies d'adressage plus évoluées qui ciblent spécifiquement des récepteurs présents à la surface des cellules endothéliales formant la barrière hématoencéphalique. Ces stratégies impliquent le greffage ou l'adsorption de molécules dirigées contre ces récepteurs présents chez les cellules endothéliales de la BBB afin de permettre le passage des particules du sang vers le CNS, adoptant ainsi une stratégie de Cheval de Troie comme discuté dans la revue de la littérature (section 0).

L'une des stratégies employées est l'utilisation de l'apolipoprotéine E (APOE) (Dal Magro *et al.*, 2017; Kuo et Rajesh, 2017; Neves *et al.*, 2017). Par exemple, Kuo et Rajesh (2017) ont développé un système de libération à base de nanoparticules composées de polyéthylène glycol (PEG), chitosane et de polyacrylamide fonctionnalisé avec l'APOE et le facteur CRM197. Ces derniers ont montré que la présence de l'APOE et le facteur CRM197 favorisait le passage au travers d'une couche de cellules endothéliales microvasculaires du cerveau humain (HBMEC). Dans le même ordre d'idées, Dal Magro *et al.* (2017) ont fonctionnalisé des nanoparticules à base de lipides solides avec un peptide dérivé de l'APOE et ont montré *in vitro* qu'elles pouvaient passer au travers d'une couche de cellules endothéliales microvasculaires du cerveau humain (hCMEC/D3). Ces derniers ont ensuite montré *in vivo* que les particules s'accumulaient plus spécifiquement au cerveau par rapport au contrôle après une administration via les poumons chez des souris balb/c.

D'autres stratégies récentes visent également les récepteurs à lactoferrine pour faciliter le transport au travers la BBB. Par exemple, Xu *et al.* (2017) ont développé des nanoparticules à base de polysaccharides (hydrochlorure de chitosane/acide hyaluronique/PEG) encapsulant des curcuminoïdes sur lesquelles a été adsorbée de la lactoferrine pour le traitement de gliomes. La présence de lactoferrine a augmenté significativement l'accumulation au cerveau de ces particules chez des souris ICR après une injection systémique. Song *et al.* (2017) ont pour leur part greffé chimiquement (avec EDC/NHS) de la lactoferrine couplée au PEG sur des nanoparticules à base de silicate. Ces chercheurs ont montré que les nanoparticules avaient une

plus grande capacité à passer à travers une couche de cellules endothéliales extraites de capillaires cérébraux de rat par rapport aux particules non fonctionnalisées. Finalement, Yemisci *et al.* (2015) ont développé des nanoparticules à base de chitosane co-encapsulant du bFGF et un inhibiteur de la caspase-3 sur lesquelles des anticorps visant les récepteurs de transferrine ont été couplés via un système biotine-streptavidine. L'injection systémique de ces nanoparticules a montré une accumulation dans le tissu cérébral après seulement 1h d'injection dans des souris Swiss albino.

Ainsi, au regard des dernières tendances dans la littérature au sujet des techniques d'amélioration et de complexification des systèmes de libération visant le cerveau, il serait intéressant d'évaluer la possibilité d'adsorber ou de greffer chimiquement des molécules (peptide ou protéines) favorisant le passage au travers la BBB sur le système de libération développé dans cette thèse. Cette amélioration permettrait de favoriser la spécificité du système de libération pour le tissu ciblé. Par ailleurs, les travaux de Yemisci *et al.* (2015) permettent également de confirmer que la co-encapsulation de bFGF et d'un peptide dans des nanoparticules à base de chitosane est possible. Sachant que les résultats de la thèse démontrent un effet bénéfique entre le SpBMP-9 et le bFGF, un tel système de libération complexifié semble ainsi envisageable.

5.10.3 Étude l'effet du SpBMP-9 *in vivo* sur modèle murin

La preuve de concept quant au potentiel thérapeutique du SpBMP-9 a été réalisée sur une lignée cellulaire humaine *in vitro*. Or, la plupart des travaux témoignant de l'effet thérapeutique de la BMP-9 dans un contexte de l'AD ont été réalisé *in vivo* sur modèle murin. Par exemple, les travaux de Burke *et al.* (2013), ont montré que la BMP-9 administrée par injection intraventriculaire permettait de diminuer le nombre de plaques séniles chez des souris transgéniques (APP/PS1) surexprimant le peptide β–amyloïde en plus de restaurer les fonctions cognitives. Une étude plus récente a également montrée que l'injection intranasale de BMP-9 chez les mêmes souris transgéniques améliorait l'apprentissage spatial et associatif ainsi que la mémoire en plus d'inhiber l'hyperphosphorylation de Tau et limiter la neuroinflammation (Wang *et al.*, 2017). Les travaux de Lopez-Coviella *et al.* (2011) ont également mis en évidence la capacité du BMP-9 à assurer la maintenance et la protection du système cholinergique chez des souris mâles CD-1.

Sachant que le SpBMP-9 est en mesure d'induire la différenciation neuronale et qu'il peut agir sur au moins deux cibles thérapeutiques associées à l'AD, il serait intéressant de valider son efficacité *in vivo* sur un modèle murin, et ce, non seulement au niveau histologique, mais également au niveau comportemental. Cette étape permettrait de conclure la preuve de concept de l'utilisation du SpBMP-9 comme analogue à la BMP-9 comme stratégie de traitement contre l'AD. Dans un premier temps, une dose analogue à celle utilisée dans les travaux de Wang *et al.* (2017) (50 ng BMP-9/g/jour) permettrait une comparaison pour une injection intranasalle chez la souris APP/PS1. Sur une base molaire équivalente, une dose de ~ 5 ng SpBMP-9/g/jour en solution ou encapsulée dans le système de libération pourrait être utilisée. Des essais préliminaires *in vitro* sur des neuroblastomes murins N2A ont d'ailleurs montré que le pBMP-9 et le SpBMP-9 était en mesure de stimuler la croissance des neurites comme en témoigne la Figure C- 1 en Annexe C.

Par ailleurs, l'utilisation de nouveaux modèles murins plus représentatifs de la neuropathologie de l'AD pour les essais *in vivo* serait également à envisager. En effet, les souris transgéniques de type APP/PS1 ou 3xTg surexpriment des précurseurs de peptides β-amyloïdes qui sont des protéines transmembranaires. Cette surexpression résulte en une accumulation importante de protéines au niveau de la membrane plasmique qui affecte notamment la fluidité de la paroi cellulaire. Or, il existe maintenant des modèles transgéniques alternatifs de type « knock-in » qui permettent d'éviter une surproduction de précurseurs amyloïdes par l'introduction de mutations spécifiques. Ces souris présentent des caractéristiques similaires voir même plus représentative au niveau neuropathologique et comportemental en comparaison aux souris typiquement utilisées comme modèle AD (Masuda *et al.*, 2016; Saito *et al.*, 2014).

5.10.4 Étude de l'effet du SpBMP-9 chez des cellules souches neuronales

Les BMPs sont fortement impliqués dans le développement du CNS comme nous l'avons rapporté dans la revue de la littérature (section 2.4.1). Voyant l'effet des peptides sur la différenciation de cellules humaines neuroblastomes, ces derniers pourraient également être appliqués pour résoudre d'autres problématiques reliées au CNS, comme le comblement et la recolonisation par les cellules souches lors de pertes cérébrales.

Il est connu que la signalisation induite par les BMPs régule fortement la neurogénèse. Par exemple, il a été montré que la signalisation induite par les BMPs via l'activation des récepteurs

BMPR-1a chez des cellules souches d'hippocampe de souris était requise pour balancer leur proliféraiton et leur quiescence (Mira *et al.*, 2010; Xu *et al.*, 2013). Cette signalisation serait d'autant plus importante pour assurer un support continuel et ainsi réguler la neurogénèse au niveau de l'hipoccampe mature. Des travaux récents ont également montré que l'activation de Smad4, impliquée dans la cascade de signalisation des Smad canoniques (Smad1/5), en régulant notamment la prolifération et en orientant la différenciation, serait essentielle pour assurer le contrôle et l'orientation des cellules souches de la zone sub-ventriculaire du cerveau vers le phénotype neuronal (Kawaguchi-Niida *et al.*, 2017). Par ailleurs, nous avons montré au chapitre 3 que les peptides pBMP-9 et SpBMP-9 étaient en mesure, via l'activation de la voie PI3K/Akt, d'inactiver la GSK3β en induisant sa phosphorylation sur la Ser9. Or, des études ont démontré que l'inactivation de la GSK3β, contribuant à l'accumulation de β-caténine dans le cytosol, jouerait un rôle important sur la prolifération de cellules souches neuronales plutôt que sur leur différenciation (Chao *et al.*, 2014; Pei *et al.*, 2012).

D'autres travaux ont également mis en évidence que les BMPs pouvaient orienter la différenciation des cellules souches neuronales. Par exemple, la combinaison entre plusieurs facteurs dont la BMP-7 et l'aFGF permettait la différenciation de cellules souches neuronales humaines en neurones dopaminergiques compétents (Yang *et al.*, 2016). La BMP-2 et la BMP-4 peuvent également orienter préférentiellement la différenciation des cellules souches du CNS vers le phénotype astrogliale en limitant par le fait même la différenciation neuronale et oligodendrogliale (Gomes *et al.*, 2003; Kohyama *et al.*, 2010; Okano-Uchida *et al.*, 2013). Connaissant le rôle important des BMPs dans le contrôle de la neurogénèse, une étude plus approfondie de l'effet des peptides dérivés de la BMP-9 sur le maintien, la prolifération et l'orientation de la différenciation de cellules souches du CNS serait à envisager.

ANNEXE A: DONNÉES SUPPLÉMENTAIRES ARTICLE SCIENTIFIC REPORTS
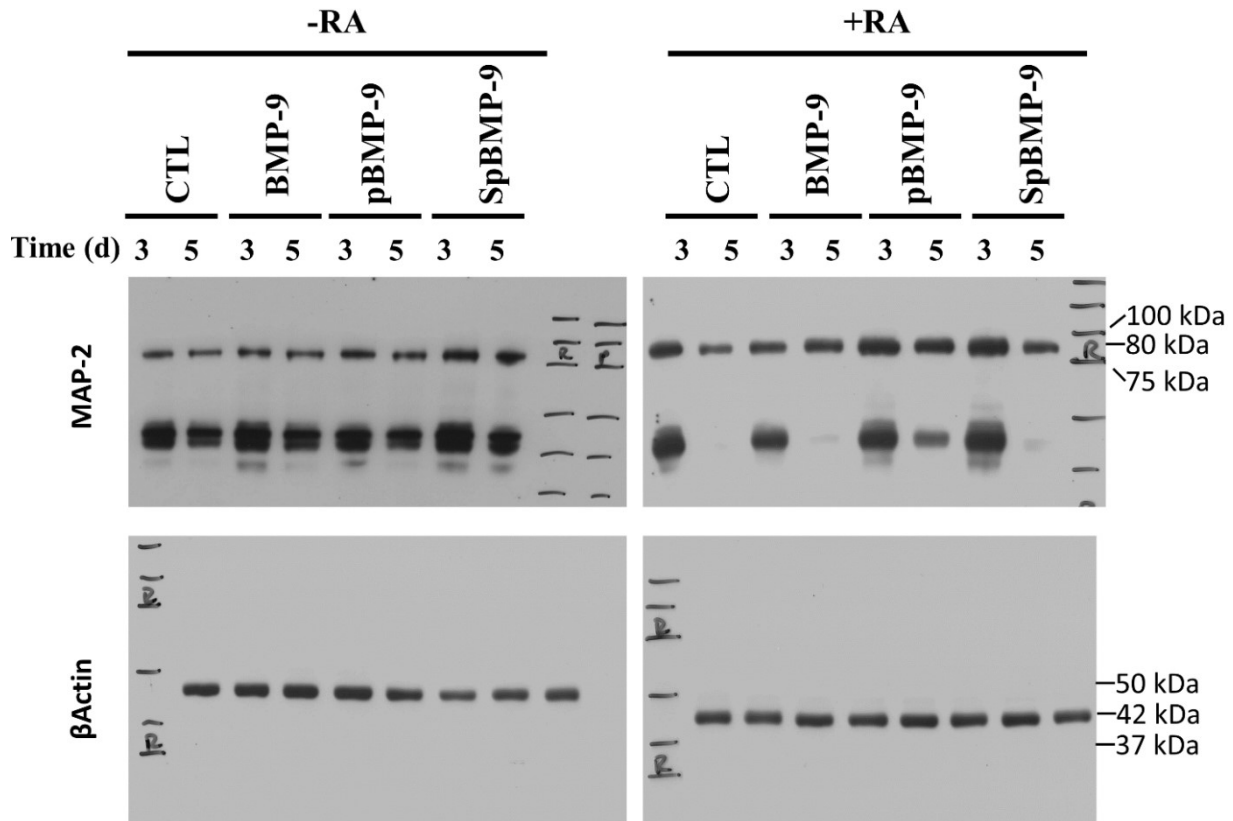
Figure A- 1 : Western blots of MAP-2 and βactin for SH-SY5Y cells stimulated with 0.1 nM BMP-9, pBMP-9 and SpBMP-9 +/- 10 μM RA for 3d and 5d. The 80 kDa band was used since it corresponds to MAP-2 low molecular weight isoform. βActin band, with a MW of 42 kDa was used as a control. Those are the original (non-cropped) blots presented in Figure 4A of the article.
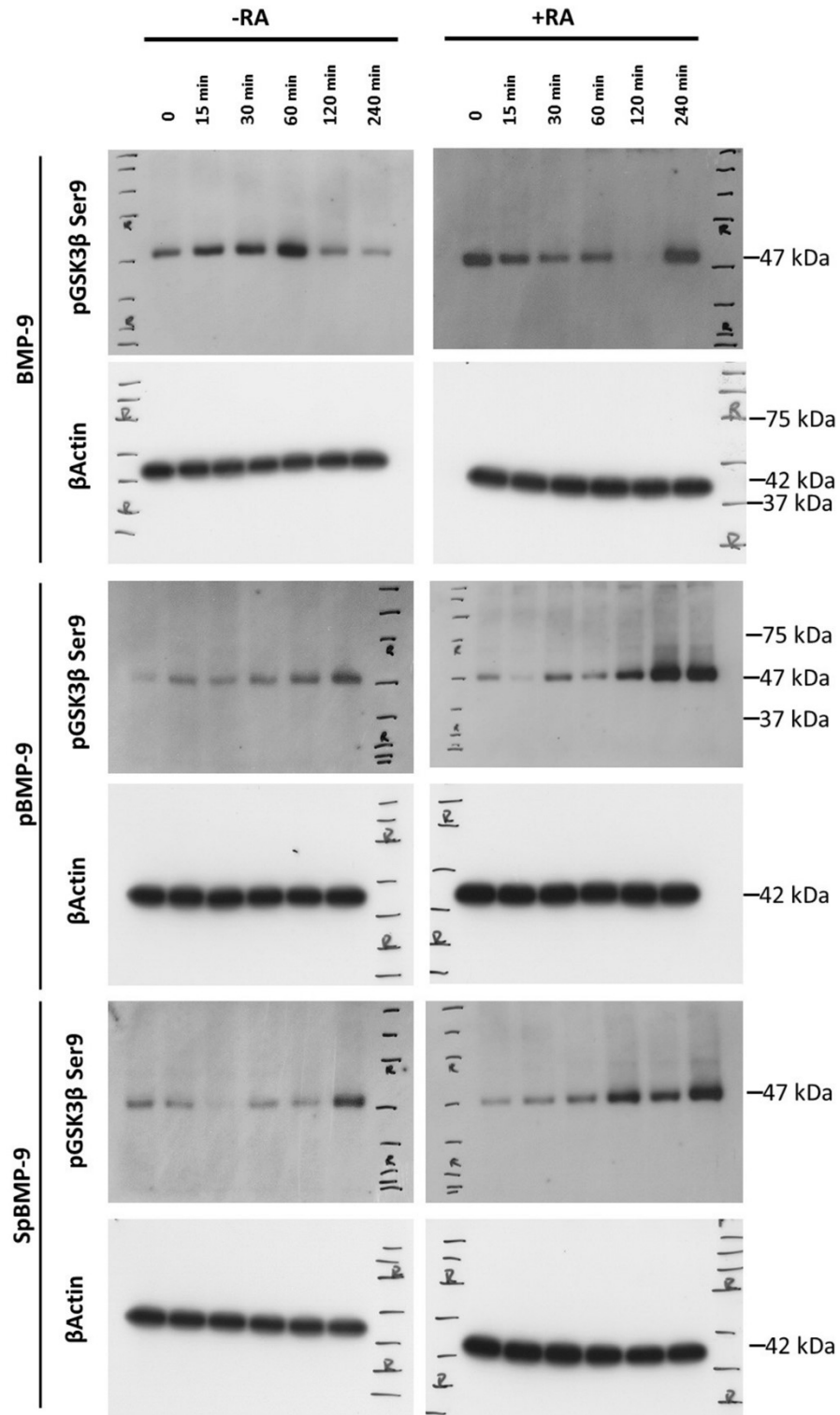
Figure A- 2 : Western blots showing the effect of 0.1 nM BMP-9, pBMP-9 and SpBMP-9 +/- 10 μM RA on the phosphorylation of GSK3β at Ser9 (MW 47 kDa) in SH-SY5Y cells after incubation for 0, 15, 30, 60, 120 and 240 min. βActin (MW of 42 kDa) was used as a control. These pictures are the original (non-cropped) blots presented in Figure 8B of the article.
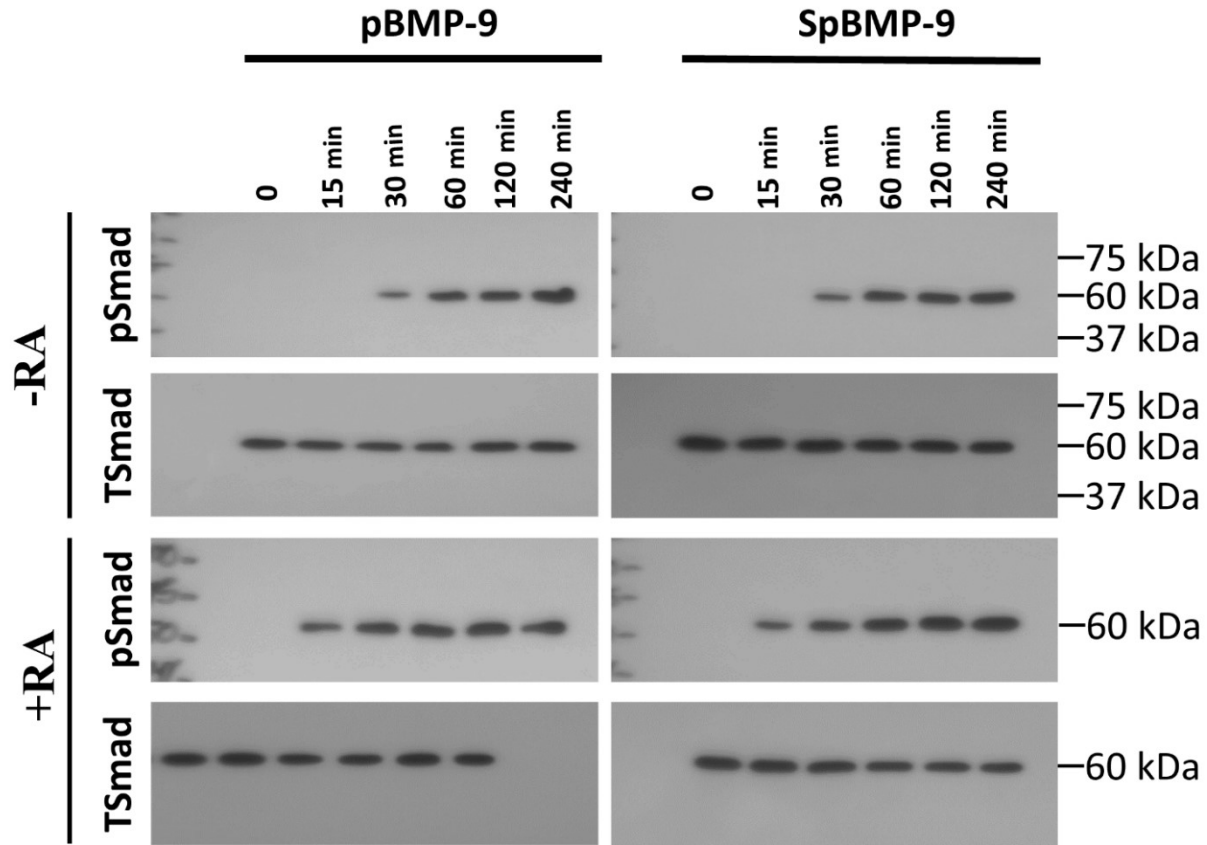
Figure A- 3 : Western blots showing the effect of 1 nM of pBMP-9 or SpBMP-9 +/- 10 μM RA on the phosphorylation of Smad1/5 (pSmad, MW 60 kDa) in SH-SY5Y cells after incubation for 0, 15, 30, 60, 120 and 240 min. Total Smad1/5/8 (TSmad, MW 60 kDa) was used as a control. These pictures are the original (non-cropped) blots presented in Figure 1A of the article.

ANNEXE B: DONNÉES SUPPLÉMENTAIRES ARTICLE MOLECULAR AND CELLULAR NEUROSCIENCE
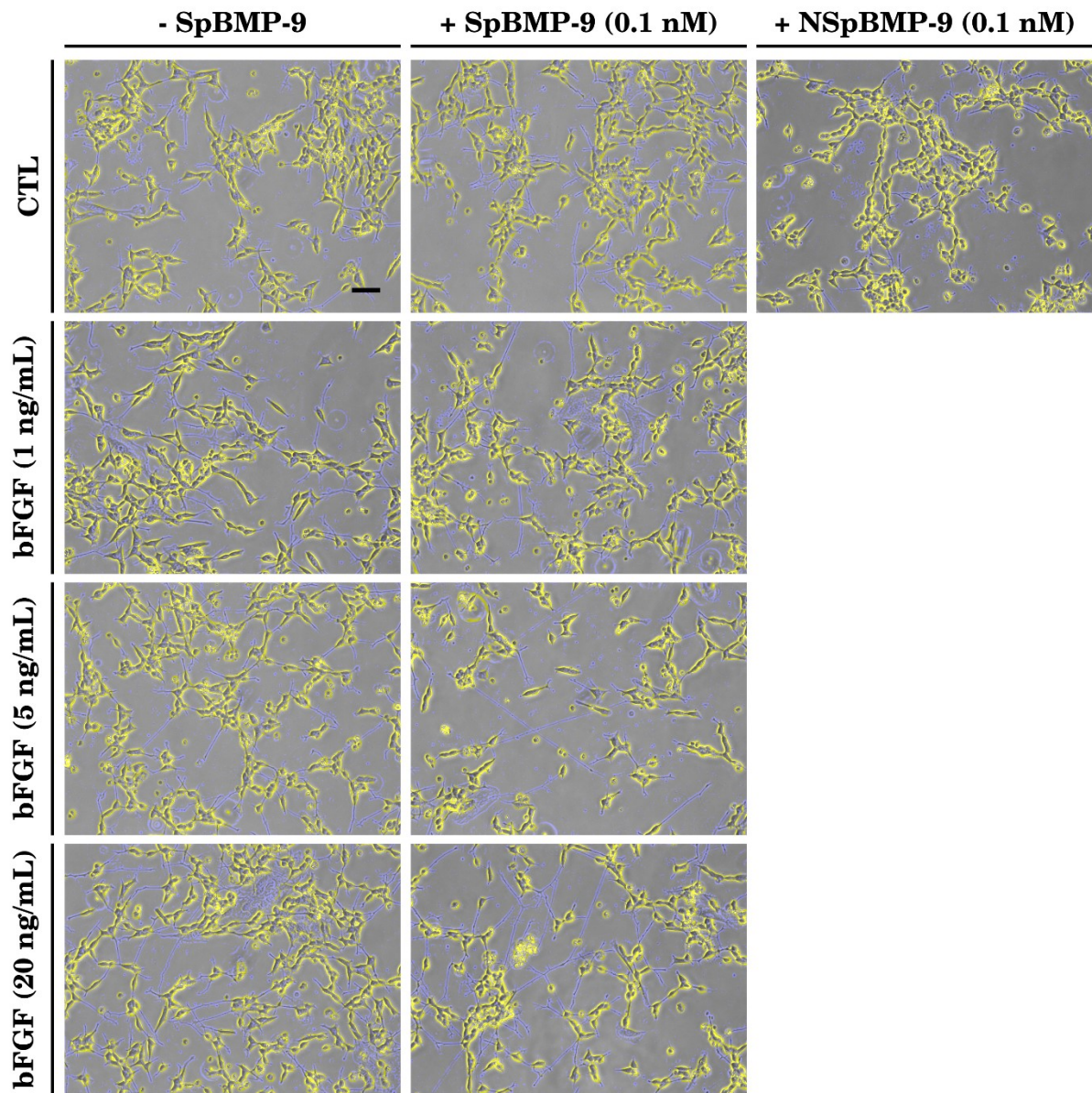
Figure B- 1 : Representative phase contrast pictures that were filtered to enhance the neurites (blue) and the cell body (yellow) for SH-SY5Y cells stimulated for 5 days in serum-free culture medium alone or serum-free culture medium containing bFGF (1, 5 or 20 ng/mL) or with or without SpBMP-9 (0.1 nM). Results are representative of 3 independent experiments performed in duplicate. Bar = 100 µm.
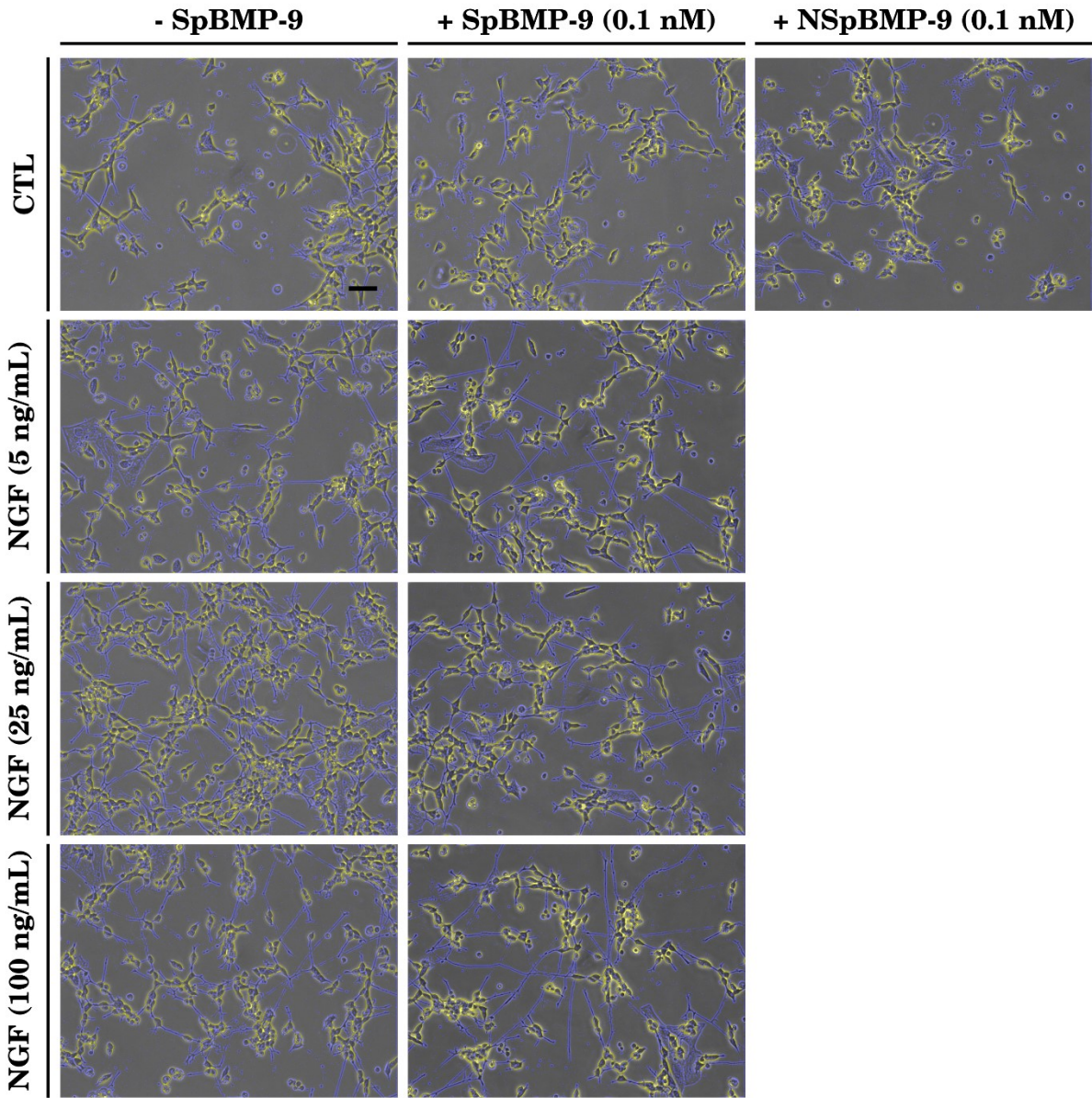
Figure B- 2 : Representative phase contrast pictures that were filtered to enhance the neurites (blue) and the cell body (yellow) for SH-SY5Y cells stimulated for 5 days in serum-free culture medium alone or serum-free culture medium containing NGF (5, 25 or 100 ng/mL) or with or without SpBMP-9 (0.1 nM). Results are representative of 3 independent experiments performed in duplicate. Bar = 100 μm.
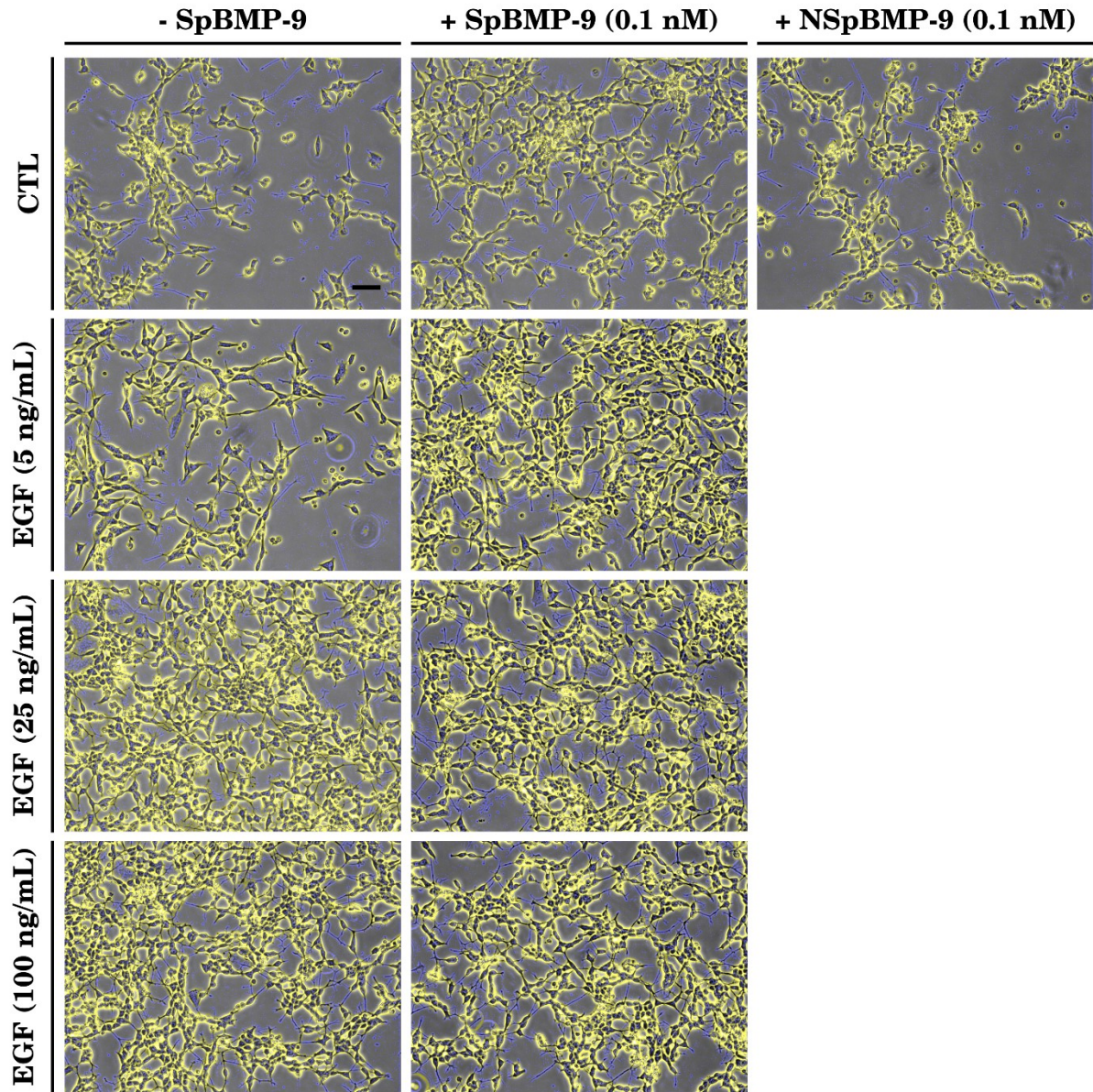
Figure B- 3 : Representative phase contrast pictures that were filtered to enhance the neurites (blue) and the cell body (yellow) for SH-SY5Y cells stimulated for 5 days in serum-free culture medium alone or serum-free culture medium containing EGF (5, 25 or 100 ng/mL) or with or without SpBMP-9 (0.1 nM). Results are representative of 3 independent experiments performed in duplicate. Bar = 100 μm.
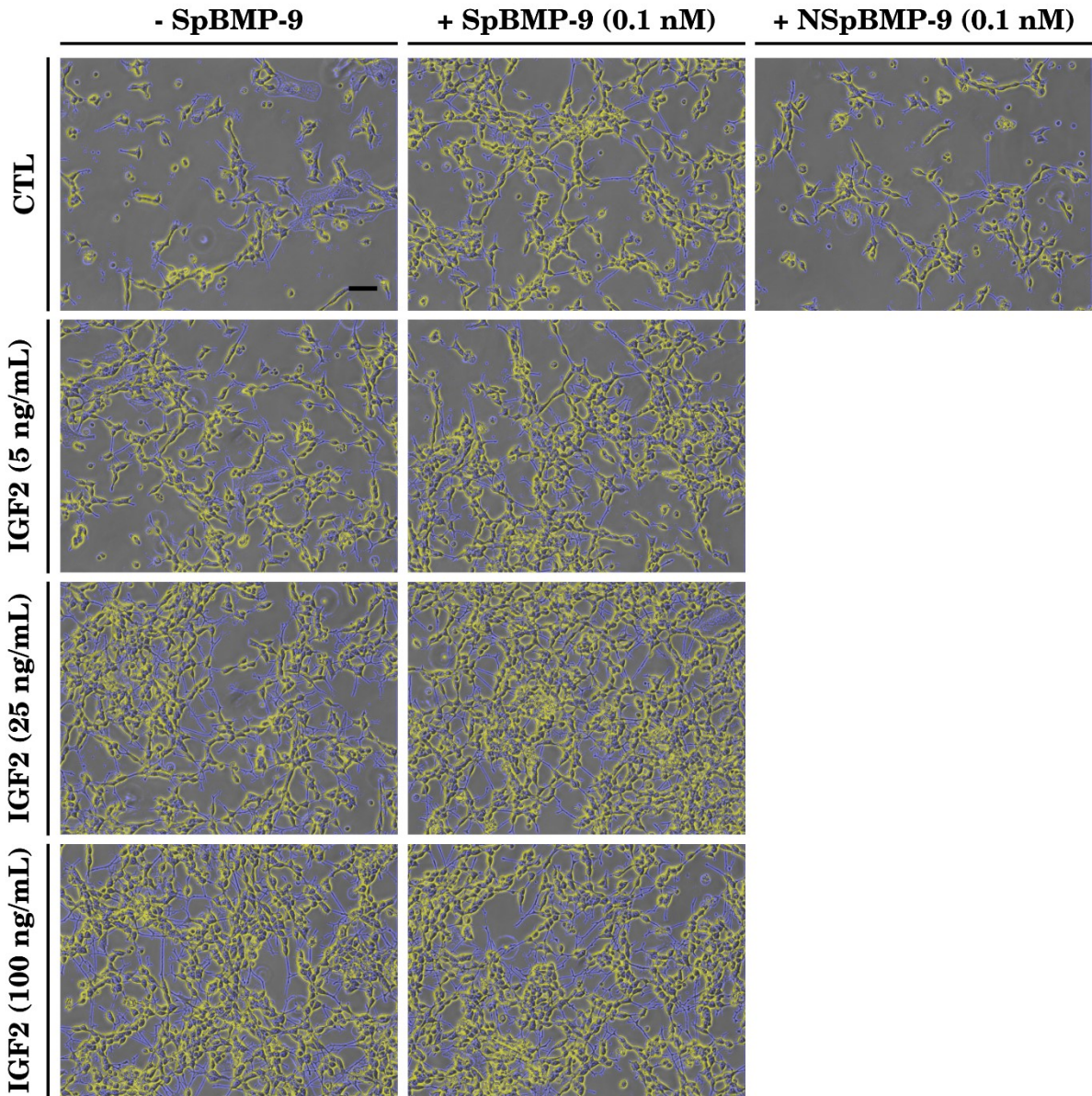
Figure B- 4 : Representative phase contrast pictures that were filtered to enhance the neurites (blue) and the cell body (yellow) for SH-SY5Y cells stimulated for 5 days in serum-free culture medium alone or serum-free culture medium containing IGF2 (5, 25 or 100 ng/mL) or with or without SpBMP-9 (0.1 nM). Results are representative of 3 independent experiments performed in duplicate. Bar = 100 μm.

ANNEXE C: ESSAIS PBMP-9 ET SPBMP-9 SUR N2A
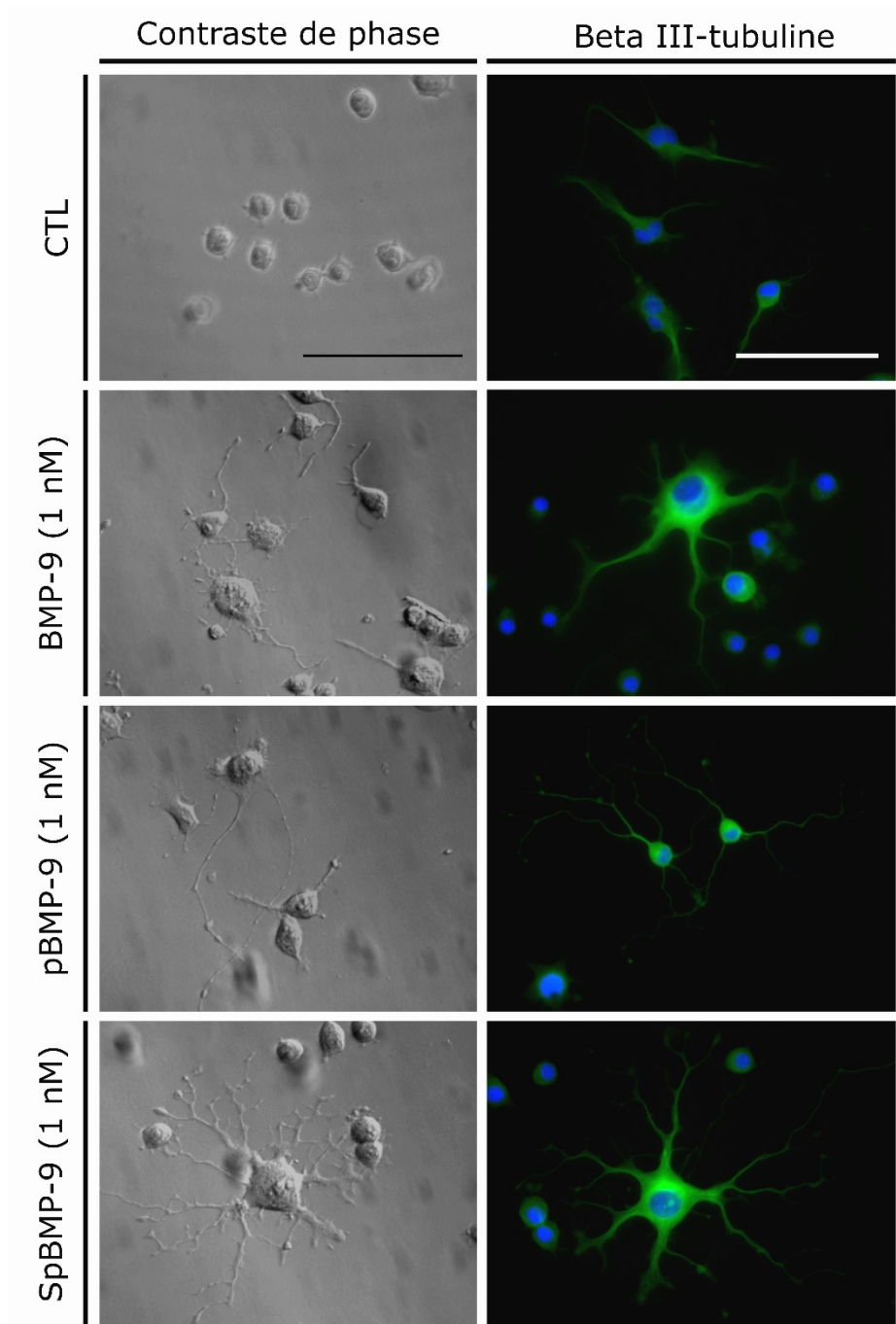
Figure C- 1 : Images représentatives en contraste de phase et immunomarquages dirigés contre la βIII-tubuline (Hoechst en bleu, βIII-tubuline en vert) de cellules N2A stimulées pendant 3 jours sans sérum par BMP-9 (1nM), pBMP-9 (1nM) ou SpBMP-9 (1 nM). Barre 100 μm. Ces résultats sont représentatifs de 2 expériences indépendantes.

LISTE DES RÉFÉRENCES

Abdel-Hafez, S. M., Hathout, R. M. et Sammour, O. A. (2014) Towards better modeling of chitosan nanoparticles production: Screening different factors and comparing two experimental designs. International journal of biological macromolecules, vol. 64, n°0, p. 334-340.

Abdullahi, W., Brzica, H., Ibbotson, K., Davis, T. P. et Ronaldson, P. T. (2017) Bone morphogenetic protein-9 increases the functional expression of organic anion transporting polypeptide 1a4 at the blood-brain barrier via the activin receptor-like kinase-1 receptor. Journal of cerebral blood flow and metabolism : official journal of the International Society of Cerebral Blood Flow and Metabolism, vol. 37, n°7, p. 2340-2345.

Adem, A., Mattsson, M. E., Nordberg, A. et Pahlman, S. (1987) Muscarinic receptors in human SH-SY5Y neuroblastoma cell line: regulation by phorbol ester and retinoic acid-induced differentiation. Brain research, vol. 430, n°2, p. 235-242.

Agholme, L., Lindström, T., Kgedal, K., Marcusson, J. et Hallbeck, M. (2010) An in vitro model for neuroscience: Differentiation of SH-SY5Y cells into cells with morphological and biochemical characteristics of mature neurons. Journal of Alzheimer's Disease, vol. 20, n°4, p. 1069-1082.

Agnihotri, S. A., Mallikarjuna, N. N. et Aminabhavi, T. M. (2004) Recent advances on chitosan-based micro- and nanoparticles in drug delivery. Journal of Controlled Release, vol. 100, n°1, p. 5-28.

Agrawal, R., Mishra, B., Tyagi, E., Nath, C. et Shukla, R. (2010) Effect of curcumin on brain insulin receptors and memory functions in STZ (ICV) induced dementia model of rat. Nutraceuticals and Functional Foods, vol. 61, n°3, p. 247-252.

Ahmed, T., Enam, S. A. et Gilani, A. H. (2010) Curcuminoids enhance memory in an amyloid-infused rat model of Alzheimer's disease. Neuroscience, vol. 169, n°3, p. 1296-1306.

Ai-Aql, Z. S., Alagl, A. S., Graves, D. T., Gerstenfeld, L. C. et Einhorn, T. A. (2008) Molecular mechanisms controlling bone formation during fracture healing and distraction osteogenesis. Journal of dental research, vol. 87, n°2, p. 107-118.

Airavaara, M., Pletnikova, O., Doyle, M. E., Zhang, Y. E., Troncoso, J. C. et Liu, Q. R. (2011)

Identification of novel GDNF isoforms and cis-antisense GDNFOS gene and their regulation in human middle temporal gyrus of Alzheimer disease. The Journal of biological chemistry, vol. 286, n°52, p. 45093-45102.

Aktaş, Y., Andrieux, K., Alonso, M. J., Calvo, P., Gürsoy, R. N., Couvreur, P., Çapan, Y., Aktas, Y., Andrieux, K., Alonso, M. J., Calvo, P., Gursoy, R. N., Couvreur, P. et Capan, Y. (2005) Preparation and in vitro evaluation of chitosan nanoparticles containing a caspase inhibitor. International journal of pharmaceutics, vol. 298, n°2, p. 378-383.

Alam, S., Khan, Z. I., Mustafa, G., Kumar, M., Islam, F., Bhatnagar, A. et Ahmad, F. J. (2012) Development and evaluation of thymoquinone-encapsulated chitosan nanoparticles for nose-to-brain targeting: A pharmacoscintigraphic study. International Journal of Nanomedicine, vol. 7, p. 5705-5718.

Alavijeh, M. S., Chishty, M., Qaiser, M. Z. et Palmer, A. M. (2005) Drug metabolism and pharmacokinetics, the blood-brain barrier, and central nervous system drug discovery. NeuroRx : the journal of the American Society for Experimental NeuroTherapeutics, vol. 2, n°4, p. 554-571.

Albeck, D., Mesches, M. H., Juthberg, S., Browning, M., Bickford, P. C., Rose, G. M. et Granholm, A.-C. (2003) Exogenous NGF restores endogenous NGF distribution in the brain of the cognitively impaired aged rat. Brain research, vol. 967, n°1–2, p. 306-310.

Alcala-Barraza, S. R., Lee, M. S., Hanson, L. R., McDonald, A. A., Frey 2nd, W. H. et McLoon, L. K. (2010) Intranasal delivery of neurotrophic factors BDNF, CNTF, EPO, and NT-4 to the CNS. Journal of drug targeting, vol. 18, n°3, p. 179-190.

Alkon, D. L., Sun, M.-K. et Nelson, T. J. (2007) PKC signaling deficits: a mechanistic hypothesis for the origins of Alzheimer's disease. Trends in pharmacological sciences, vol. 28, n°2, p. 51-60.

Allen, S. J., Watson, J. J., Shoemark, D. K., Barua, N. U. et Patel, N. K. (2013) GDNF, NGF and BDNF as therapeutic options for neurodegeneration. Pharmacology and Therapeutics, vol. 138, n°2, p. 155-175.

Aloe, L., Bianchi, P., De Bellis, A., Soligo, M. et Rocco, M. L. (2014) Intranasal nerve growth factor bypasses the blood-brain barrier and affects spinal cord neurons in spinal cord injury. Neural

regeneration research, vol. 9, n°10, p. 1025-1030.

Alonso, A. C., Grundke-Iqbal, I. et Iqbal, K. (1996) Alzheimer's disease hyperphosphorylated tau sequesters normal tau into tangles of filaments and disassembles microtubules. Nature medicine, vol. 2, n°7, p. 783-787.

Alyautdin, R., Khalin, I., Nafeeza, M. I., Haron, M. H. et Kuznetsov, D. (2014) Nanoscale drug delivery systems and the blood-brain barrier. International Journal of Nanomedicine, vol. 9, n°1, p. 795-811.

Alzheimer's Association (2013) 2013 Alzheimer's disease facts and figures. Alzheimer's & Dementia, vol. 9, n°2, p. 208-245.

Alzheimer's Association (2017) Alzheimer's disease facts and figures, www.alz.org/facts, (consulté juin 2017).

Alzheimer's Society Canada, www.alzheimer.ca, (consulté décembre 2014 et juin 2017).

Amunts, K., Lepage, C., Borgeat, L., Mohlberg, H., Dickscheid, T., Rousseau, M. E., Bludau, S., Bazin, P. L., Lewis, L. B., Oros-Peusquens, A. M., Shah, N. J., Lippert, T., Zilles, K. et Evans, A. C. (2013) BigBrain: an ultrahigh-resolution 3D human brain model. Science (New York, N.Y.), vol. 340, n°6139, p. 1472-1475.

Anal, A. K., Bhopatkar, D., Tokura, S., Tamura, H. et Stevens, W. F. (2003) Chitosan-alginate multilayer beads for gastric passage and controlled intestinal release of protein. Drug development and industrial pharmacy, vol. 29, n°6, p. 713-724.

Anderson, J. M. (2001) Molecular structure of tight junctions and their role in epithelial transport. News in physiological sciences : an international journal of physiology produced jointly by the International Union of Physiological Sciences and the American Physiological Society, vol. 16, p. 126-130.

Andres, D., Keyser, B. M., Petrali, J., Benton, B., Hubbard, K. S., McNutt, P. M. et Ray, R. (2013) Morphological and functional differentiation in BE(2)-M17 human neuroblastoma cells by treatment with Trans-retinoic acid. BMC neuroscience, vol. 14, p. 49.

Angelova, A., Angelov, B., Drechsler, M., Garamus, V. M. et Lesieur, S. (2013) Protein entrapment in PEGylated lipid nanoparticles. Targeted Drug Delivery, vol. 454, n°2, p. 625-632.

Angelucci, F., Gelfo, F., Fiore, M., Croce, N., Mathe, A. A., Bernardini, S. et Caltagirone, C. (2014) The effect of neuropeptide Y on cell survival and neurotrophin expression in in-vitro models of Alzheimer's disease. Canadian journal of physiology and pharmacology, vol. 92, n°8, p. 621-630.

Angelucci, F., Spalletta, G., di Iulio, F., Ciaramella, A., Salani, F., Colantoni, L., Varsi, A. E., Gianni, W., Sancesario, G., Caltagirone, C. et Bossu, P. (2010) Alzheimer's disease (AD) and Mild Cognitive Impairment (MCI) patients are characterized by increased BDNF serum levels. Current Alzheimer research, vol. 7, n°1, p. 15-20.

Anitua, E., Pascual, C., Perez-Gonzalez, R., Antequera, D., Padilla, S., Orive, G. et Carro, E. (2013) Intranasal delivery of plasma and platelet growth factors using PRGF-Endoret system enhances neurogenesis in a mouse model of Alzheimer's disease. PloS one, vol. 8, n°9, p. e73118.

Arancibia, S., Silhol, M., Mouliere, F., Meffre, J., Hollinger, I., Maurice, T. et Tapia-Arancibia, L. (2008) Protective effect of BDNF against beta-amyloid induced neurotoxicity in vitro and in vivo in rats. Neurobiology of disease, vol. 31, n°3, p. 316-326.

Araya, E., Olmedo, Y., Bastus, N. G., Guerrero, S., Puntes, V. F., Giralt, E. et Kogan, M. J. (2008) Gold Nanoparticles and Microwave irradiation inhibit beta-amyloid amyloidogenesis . Nanoscale Research Letter, n°3, p. 461-467.

Arif, M., Wei, J., Zhang, Q., Liu, F., Basurto-Islas, G., Grundke-Iqbal, I. et Iqbal, K. (2014) Cytoplasmic Retention of Protein Phosphatase 2A-Inhibitor 2 (I2PP2A) Induces Alzheimer-like Abnormal Hyperphosphorylation of Tau. The Journal of biological chemistry.

Arifin, D. Y., Lee, L. Y. et Wang, C.-H. (2006) Mathematical modeling and simulation of drug release from microspheres: Implications to drug delivery systems. Computational Drug Delivery, vol. 58, n°12–13, p. 1274-1325.

Arimura, N. et Kaibuchi, K. (2007) Neuronal polarity: from extracellular signals to intracellular mechanisms. Nature reviews. Neuroscience, vol. 8, n°3, p. 194-205.

Armstrong, R. A. (2013) What causes Alzheimer's disease? Folia Neuropathologica, vol. 51, n°3, p. 169-188.

Aspden, T. J., Mason, J. D. T., Jones, N. S., Lowe, J., Skaugrud, Ø. et Illum, L. (1997) Chitosan as a nasal delivery system: The effect of chitosan solutions on in vitro and in vivo mucociliary

transport rates in human turbinates and volunteers. Journal of pharmaceutical sciences, vol. 86, n°4, p. 509-513.

Attisano, L. et Wrana, J. L. (1996) Signal transduction by members of the transforming growth factor-β superfamily. Cytokine & growth factor reviews, vol. 7, n°4, p. 327-339.

Aubert-Pouëssel, A., Venier-Julienne, M.-C., Clavreul, A., Sergent, M., Jollivet, C., Montero-Menei, C. N., Garcion, E., Bibby, D. C., Menei, P. et Benoit, J.-P. (2004) In vitro study of GDNF release from biodegradable PLGA microspheres. Journal of Controlled Release, vol. 95, n°3, p. 463-475.

Augustinack, J. C., Schneider, A., Mandelkow, E. M. et Hyman, B. T. (2002) Specific tau phosphorylation sites correlate with severity of neuronal cytopathology in Alzheimer's disease. Acta Neuropathologica, vol. 103, n°1, p. 26-35.

Bachurin, S. O., Bovina, E. V et Ustyugov, A. A. (2017) Drugs in Clinical Trials for Alzheimer's Disease: The Major Trends. Medicinal research reviews, vol. 37, n°5, p. 1186-1225.

Baig, S., van Helmond, Z. et Love, S. (2009) Tau hyperphosphorylation affects Smad 2/3 translocation. Neuroscience, vol. 163, n°2, p. 561-570.

Bajpai, J., Kaur Maan, G. et Bajpai, A. K. (2012) Preparation, Characterization and Water Uptake Behavior of Polysaccharide Based Nanoparticles. Progress in Nanote chnology and Nanomaterials, vol. 1, n°1, p. 9-17.

Banks, W. A. (2009) Characteristics of compounds that cross the blood-brain barrier. BMC neurology, vol. 9 Suppl 1, p. S3-2377-9-S1-S3.

Baron, O., Ratzka, A. et Grothe, C. (2012) Fibroblast growth factor 2 regulates adequate nigrostriatal pathway formation in mice. The Journal of comparative neurology, vol. 520, n°17, p. 3949-3961.

Barua, N. U., Miners, J. S., Bienemann, A. S., Wyatt, M. J., Welser, K., Tabor, A. B., Hailes, H. C., Love, S. et Gill, S. S. (2012) Convection-enhanced delivery of neprilysin: a novel amyloid-beta-degrading therapeutic strategy. Journal of Alzheimer's disease : JAD, vol. 32, n°1, p. 43-56.

Baskin, D. G., Wilcox, B. J., Figlewicz, D. P. et Dorsa, D. M. (1988) Insulin and insulin-like growth factors in the CNS. Trends in neurosciences, vol. 11, n°3, p. 107-111.

Bause, M., Friess, W., Knabner, P. et Radu, F. A. (2006) A comprehensive mathematical model describing drug release from collagen matrices. Proceedings of the Fifth Workshop on Mathematical Modelling of Environmental and Life Sciences Problems, p. 27-34.

Beauvais, S., Drevelle, O., Lauzon, M.-A., Daviau, A. et Faucheux, N. (2016) Modulation of MAPK signalling by immobilized adhesive peptides: Effect on stem cell response to BMP-9-derived peptides. Acta biomaterialia, vol. 31, p. 241-251.

Bell, K. F. S. et Claudio Cuello, A. (2006) Altered synaptic function in Alzheimer's disease. Neurodegenerative disorders From novel pathogenic mechanisms towards a better treatment, vol. 545, n°1, p. 11-21.

Bender, T. S., Migliore, M. M., Campbell, R. B., John Gatley, S. et Waszczak, B. L. (2015) Intranasal administration of glial-derived neurotrophic factor (GDNF) rapidly and significantly increases whole-brain GDNF level in rats. Neuroscience, vol. 303, p. 569-576.

Bergeron, E., Leblanc, E., Drevelle, O., Giguere, R., Beauvais, S., Grenier, G. et Faucheux, N. (2012) The evaluation of ectopic bone formation induced by delivery systems for bone morphogenetic protein-9 or its derived Peptide. Tissue engineering.Part A, vol. 18, n°3-4, p. 342-352.

Bergeron, E., Marquis, M. E., Chretien, I. et Faucheux, N. (2007) Differentiation of preosteoblasts using a delivery system with BMPs and bioactive glass microspheres. Journal of materials science.Materials in medicine, vol. 18, n°2, p. 255-263.

Bergeron, E., Senta, H., Mailloux, A., Park, H., Lord, E. et Faucheux, N. (2009) Murine preosteoblast differentiation induced by a peptide derived from bone morphogenetic proteins-9. Tissue engineering.Part A, vol. 15, n°11, p. 3341-3349.

Bernardi, A., Frozza, R. L., Meneghetti, A., Hoppe, J. B., Battastini, A. M., Pohlmann, A. R., Guterres, S. S. et Salbego, C. G. (2012) Indomethacin-loaded lipid-core nanocapsules reduce the damage triggered by Abeta1-42 in Alzheimer's disease models. International journal of nanomedicine, vol. 7, p. 4927-4942.

Berse, B. et Blusztajn, J. K. (1995) Coordinated up-regulation of choline acetyltransferase and vesicular acetylcholine transporter gene expression by the retinoic acid receptor alpha, cAMP, and leukemia inhibitory factor/ciliary neurotrophic factor signaling pathways in a murine septal

cell. The Journal of biological chemistry, vol. 270, n°38, p. 22101-22104.

Beyer, T. A., Narimatsu, M., Weiss, A., David, L. et Wrana, J. L. (2013) The TGFβ superfamily in stem cell biology and early mammalian embryonic development. Biochemistry of Stem Cells, vol. 1830, n°2, p. 2268-2279.

Biane, J., Conner, J. M. et Tuszynski, M. H. (2014) Nerve growth factor is primarily produced by GABAergic neurons of the adult rat cortex. Frontiers in cellular neuroscience, vol. 8, p. 220.

Bier, E., Ackerman, L., Barbel, S., Jan, L. et Jan, Y. N. (1988) Identification and characterization of a neuron-specific nuclear antigen in Drosophila. Science (New York, N.Y.), vol. 240, n°4854, p. 913-916.

Bikfalvi, A., Klein, S., Pintucci, G. et Rifkin, D. B. (1997) Biological roles of fibroblast growth factor-2. Endocrine Reviews. Affiliation: Department of Cell Biology, Kaplan Cancer Center, New York University Medical Center, New York, NY 10016, United States; Affiliation: Raymond Beverly Sackler Found. Lab., Kaplan Cancer Center, New York University Medical Center, New York, NY .

Biswas, S., Chattopadhyay, M., Sen, K. K. et Saha, M. K. (2015) Development and characterization of alginate coated low molecular weight chitosan nanoparticles as new carriers for oral vaccine delivery in mice. Carbohydrate polymers, vol. 121, p. 403-410.

Blasi, P., Giovagnoli, S., Schoubben, A., Ricci, M. et Rossi, C. (2007) Solid lipid nanoparticles for targeted brain drug delivery. Advanced Drug Delivery Reviews, vol. 59, n°6, p. 454-477.

Blasi, P., Schoubben, A., Traina, G., Manfroni, G., Barberini, L., Alberti, P. F., Cirotto, C. et Ricci, M. (2013) Lipid nanoparticles for brain targeting III. Long-term stability and in vivo toxicity. A Position Paper and Commentaries on More effective advanced drug delivery systems, vol. 454, n°1, p. 316-323.

Boddy, A. V et Thomas, H. D. (1997) RMP-7, Potential as an adjuvant to the Drug Treatment of Brain Tumours. CNS Drugs, vol. 7, n°4, p. 257-263.

Boku, S., Nakagawa, S., Toda, H., Kato, A., Takamura, N., Omiya, Y., Inoue, T. et Koyama, T. (2013) ROCK2 regulates bFGF-induced proliferation of SH-SY5Y cells through GSK-3beta and beta-catenin pathway. Brain research, vol. 1492, p. 7-17.

Boonen, R. A. C. M., van Tijn, P. et Zivkovic, D. (2009) Wnt signaling in Alzheimer's disease: Up

or down, that is the question. Ageing Research Reviews, vol. 8, n°2, p. 71-82.

Borges, O., Cordeiro-da-Silva, A., Romeijn, S. G., Amidi, M., de Sousa, A., Borchard, G. et Junginger, H. E. (2006) Uptake studies in rat Peyer's patches, cytotoxicity and release studies of alginate coated chitosan nanoparticles for mucosal vaccination. Journal of controlled release : official journal of the Controlled Release Society, vol. 114, n°3, p. 348-358.

Braak, H., Alafuzoff, I., Arzberger, T., Kretzschmar, H. et Del Tredici, K. (2006) Staging of Alzheimer disease-associated neurofibrillary pathology using paraffin sections and immunocytochemistry. Acta Neuropathologica, vol. 112, n°4, p. 389-404.

Braak, H. et Braak, E. (1991) Neuropathological stageing of Alzheimer-related changes. Acta Neuropathologica, vol. 82, n°4, p. 239-259.

Braak, H. et Braak, E. (1995) Staging of Alzheimer's disease-related neurofibrillary changes. Neurobiology of aging, vol. 16, n°3, p. 271-284.

Braak, H. et Braak, E. (1997) Frequency of stages of Alzheimer-related lesions in different age categories. Neurobiology of aging, vol. 18, n°4, p. 351-357.

Bressan, R. B., Melo, F. R., Almeida, P. A., Bittencourt, D. A., Visoni, S., Jeremias, T. S., Costa, A. P., Leal, R. B. et Trentin, A. G. (2014) EGF–FGF2 stimulates the proliferation and improves the neuronal commitment of mouse epidermal neural crest stem cells (EPI-NCSCs). Experimental cell research, vol. 327, n°1, p. 37-47.

BROGAN, T. D. (1960) The high molecular weight components of sputum. British journal of experimental pathology, vol. 41, p. 288-297.

Brooker, S. M., Gobeske, K. T., Chen, J., Peng, C.-Y. et Kessler, J. A. (2016) Hippocampal bone morphogenetic protein signaling mediates behavioral effects of antidepressant treatment. Molecular psychiatry.

Brunden, K. R., Ballatore, C., Crowe, A., Smith, A. B., Lee, V. M. Y. et Trojanowski, J. Q. (2010) Tau-Directed Drug Discovery for Alzheimer's Disease and Related Tauopathies: A Focus on Tau Assembly Inhibitors. Experimental neurology, vol. 223, n°2, p. 304-310.

Buée, L., Bussière, T., Buée-Scherrer, V., Delacourte, A. et Hof, P. R. (2000) Tau protein isoforms, phosphorylation and role in neurodegenerative disorders. Brain Research Reviews, vol. 33, n°1, p. 95-130.

Buishas, J., Gould, I. G. et Linninger, A. A. (2014) A computational model of cerebrospinal fluid production and reabsorption driven by Starling forces. Croatian medical journal, vol. 55, n°5, p. 481-497.

Burgess, A. et Hynynen, K. (2013) Noninvasive and targeted drug delivery to the brain using focused ultrasound. ACS chemical neuroscience, vol. 4, n°4, p. 519-526.

Burke, R. M., Norman, T. A., Haydar, T. F., Slack, B. E., Leeman, S. E., Blusztajn, J. K. et Mellott, T. J. (2013) BMP9 ameliorates amyloidosis and the cholinergic defect in a mouse model of Alzheimer's disease. Proceedings of the National Academy of Sciences of the United States of America. Affiliation: Department of Pathology and Laboratory Medicine, Boston University School of Medicine, Boston, MA 02118, United States; Affiliation: Department of Anatomy and Neurobiology, Boston University School of Medicine, Boston, MA 02118, United States.

Busciglio, J., Lorenzo, A., Yeh, J. et Yankner, B. A. (1995) β-Amyloid fibrils induce tau phosphorylation and loss of microtubule binding. Neuron, vol. 14, n°4, p. 879-888.

Butler, S. J. et Dodd, J. (2003) A role for BMP heterodimers in roof plate-mediated repulsion of commissural axons. Neuron, vol. 38, n°3, p. 389-401.

Cai, J., Schleidt, S., Pelta-Heller, J., Hutchings, D., Cannarsa, G. et Iacovitti, L. (2013) BMP and TGF-beta pathway mediators are critical upstream regulators of Wnt signaling during midbrain dopamine differentiation in human pluripotent stem cells. Developmental biology, vol. 376, n°1, p. 62-73.

Cai, Y., Xu, M., Yuan, M., Liu, Z. et Yuan, W. (2014) Developments in human growth hormone preparations: sustained-release, prolonged half-life, novel injection devices, and alternative delivery routes. International journal of nanomedicine, vol. 9, p. 3527-3538.

Capsoni, S., Giannotta, S. et Cattaneo, A. (2002) Nerve growth factor and galantamine ameliorate early signs of neurodegeneration in anti-nerve growth factor mice. Proceedings of the National Academy of Sciences of the United States of America, vol. 99, n°19, p. 12432-12437.

Caraci, F., Battaglia, G., Busceti, C., Biagioni, F., Mastroiacovo, F., Bosco, P., Drago, F., Nicoletti, F., Sortino, M. A. et Copani, A. (2008) TGF-β1 protects against Aβ-neurotoxicity via the phosphatidylinositol-3-kinase pathway. Neurobiology of disease, vol. 30, n°2, p. 234-242.

Caraci, F., Spampinato, S., Sortino, M. A., Bosco, P., Battaglia, G., Bruno, V., Drago, F., Nicoletti,

F. et Copani, A. (2012) Dysfunction of TGF-beta1 signaling in Alzheimer's disease: perspectives for neuroprotection. Cell and tissue research, vol. 347, n°1, p. 291-301.

Caricasole, A., Copani, A., Caruso, A., Caraci, F., Iacovelli, L., Sortino, M. A., Terstappen, G. C. et Nicoletti, F. (2003) The Wnt pathway, cell-cycle activation and beta-amyloid: novel therapeutic strategies in Alzheimer's disease? Trends in pharmacological sciences, vol. 24, n°5, p. 233-238.

Casettari, L. et Illum, L. (2014) Chitosan in nasal delivery systems for therapeutic drugs. 30th Anniversary Special Issue, vol. 190, n°0, p. 189-200.

Castranio, T. et Mishina, Y. (2009) BMP2 is required for cephalic neural tube closure in the mouse. Developmental Dynamics, vol. 238, n°1, p. 110-122.

Chackerian, B., Rangel, M., Hunter, Z. et Peabody, D. S. (2006) Virus and virus-like particle-based immunogens for Alzheimer's disease induce antibody responses against amyloid-β without concomitant T cell responses. Vaccine, vol. 24, n°37–39, p. 6321-6331.

Chakrabarti, M., McDonald, A. J., Will Reed, J., Moss, M. A., Das, B. C. et Ray, S. K. (2015) Molecular Signaling Mechanisms of Natural and Synthetic Retinoids for Inhibition of Pathogenesis in Alzheimer's Disease. Journal of Alzheimer's disease : JAD, vol. 50, n°2, p. 335-352.

Chao, J., Yang, L., Yao, H. et Buch, S. (2014) Platelet-Derived Growth Factor-BB Restores HIV Tat-Mediated Impairment of Neurogenesis: Role of GSK-3β/β-Catenin. Journal of neuroimmune pharmacology : the official journal of the Society on NeuroImmune Pharmacology, vol. 9, n°2, p. 259-268.

Charytoniuk, D. A., Traiffort, E., Pinard, E., Issertial, O., Seylaz, J. et Ruat, M. (2000) Distribution of bone morphogenetic protein and bone morphogenetic protein receptor transcripts in the rodent nervous system and up-regulation of bone morphogenetic protein receptor type II in hippocampal dentate gyrus in a rat model of global cerebral isc. Neuroscience, vol. 100, n°1, p. 33-43.

Chen, D. Y., Stern, S. A., Garcia-Osta, A., Saunier-Rebori, B., Pollonini, G., Bambah-Mukku, D., Blitzer, R. D. et Alberini, C. M. (2011) A critical role for IGF-II in memory consolidation and enhancement. Nature, vol. 469, n°7331, p. 491-497.

Chen, L., Feng, P., Zhu, X., He, S., Duan, J. et Zhou, D. (2016) Long non-coding RNA Malat1 promotes neurite outgrowth through activation of ERK/MAPK signalling pathway in N2a cells. Journal of cellular and molecular medicine, vol. 20, n°11, p. 2102-2110.

Chen, L., Jiang, W., Huang, J., He, B. C., Zuo, G. W., Zhang, W., Luo, Q., Shi, Q., Zhang, B. Q., Wagner, E. R., Luo, J., Tang, M., Wietholt, C., Luo, X., Bi, Y., Su, Y., Liu, B., Kim, S. H., He, C. J., Hu, Y., Shen, J., Rastegar, F., Huang, E., Gao, Y., Gao, J. L., Zhou, J. Z., Reid, R. R., Luu, H. H., Haydon, R. C., He, T. C. et Deng, Z. L. (2010) Insulin-like growth factor 2 (IGF-2) potentiates BMP-9-induced osteogenic differentiation and bone formation. Journal of bone and mineral research : the official journal of the American Society for Bone and Mineral Research, vol. 25, n°11, p. 2447-2459.

Chen, S.-S., Yang, C., Hao, F., Li, C., Lu, T., Zhao, L.-R. et Duan, W.-M. (2014) Intrastriatal GDNF gene transfer by inducible lentivirus vectors protects dopaminergic neurons in a rat model of parkinsonism. Experimental neurology, vol. 261, n°0, p. 87-96.

Chen, S. Q., Cai, Q., Shen, Y. Y., Cai, X. Y. et Lei, H. Y. (2014) Combined use of NGF/BDNF/bFGF promotes proliferation and differentiation of neural stem cells in vitro. International journal of developmental neuroscience : the official journal of the International Society for Developmental Neuroscience, vol. 38, p. 74-78.

Chen, Y., Run, X., Liang, Z., Zhao, Y., Dai, C. L., Iqbal, K., Liu, F. et Gong, C. X. (2014) Intranasal insulin prevents anesthesia-induced hyperphosphorylation of tau in 3xTg-AD mice. Frontiers in aging neuroscience, vol. 6, p. 100.

Chen, Y., Zhou, S. et Li, Q. (2011) Mathematical modeling of degradation for bulk-erosive polymers: applications in tissue engineering scaffolds and drug delivery systems. Acta biomaterialia, vol. 7, n°3, p. 1140-1149.

Cheng, B., Martinez, A. A., Morado, J., Scofield, V., Roberts, J. L. et Maffi, S. K. (2013) Retinoic acid protects against proteasome inhibition associated cell death in SH-SY5Y cells via the AKT pathway. Neurochemistry International, vol. 62, n°1, p. 31-42.

Cheng, B. et Mattson, M. P. (1992) Glucose deprivation elicits neurofibrillary tangle-like antigenic changes in hippocampal neurons: Prevention by NGF and bFGF. Experimental neurology, vol. 117, n°2, p. 114-123.

Chermenina, M., Schouten, P., Nevalainen, N., Johansson, F., Orädd, G. et Strömberg, I. (2014) GDNF is important for striatal organization and maintenance of dopamine neurons grown in the presence of the striatum. Neuroscience, vol. 270, n°0, p. 1-11.

Chesnutt, C., Burrus, L. W., Brown, A. M. et Niswander, L. (2004) Coordinate regulation of neural tube patterning and proliferation by TGFbeta and WNT activity. Developmental biology, vol. 274, n°2, p. 334-347.

Cheung, Y.-T., Lau, W. K.-W., Yu, M.-S., Lai, C. S.-W., Yeung, S.-C., So, K.-F. et Chang, R. C.-C. (2009) Effects of all-trans-retinoic acid on human SH-SY5Y neuroblastoma as in vitro model in neurotoxicity research. Neurotoxicology, vol. 30, n°1, p. 127-135.

Chong, Z. Z. et Maiese, K. (2004) Targeting WNT, protein kinase B, and mitochondrial membrane integrity to foster cellular survival in the nervous system. Histology and histopathology, vol. 19, n°2, p. 495-504.

Ciofani, G., Raffa, V., Menciassi, A. et Dario, P. (2008) Alginate and chitosan particles as drug delivery system for cell therapy. Biomedical microdevices, vol. 10, n°2, p. 131-140.

Clayton, K. B. et Sullivan, A. M. (2007) Differential effects of GDF5 on the medial and lateral rat ventral mesencephalon. Neuroscience letters, vol. 427, n°3, p. 132-137.

Cohen, M. R., Johnson, W. M., Pilat, J. M., Kiselar, J., DeFrancesco-Lisowitz, A., Zigmond, R. E. et Moiseenkova-Bell, V. Y. (2015) Nerve Growth Factor Regulates Transient Receptor Potential Vanilloid 2 via Extracellular Signal-Regulated Kinase Signaling To Enhance Neurite Outgrowth in Developing Neurons. Molecular and cellular biology, vol. 35, n°24, p. 4238-4252.

Colangelo, A. M., Bianco, M. R., Vitagliano, L., Cavaliere, C., Cirillo, G., De Gioia, L., Diana, D., Colombo, D., Redaelli, C., Zaccaro, L., Morelli, G., Papa, M., Sarmientos, P., Alberghina, L. et Martegani, E. (2008) A new nerve growth factor-mimetic peptide active on neuropathic pain in rats. The Journal of neuroscience : the official journal of the Society for Neuroscience, vol. 28, n°11, p. 2698-2709.

Colovic, M. B., Krstic, D. Z., Lazarevic-Pasti, T. D., Bondzic, A. M. et Vasic, V. M. (2013) Acetylcholinesterase inhibitors: pharmacology and toxicology. Current neuropharmacology, vol. 11, n°3, p. 315-335.

Copani, A., Caraci, F., Hoozemans, J. J. M., Calafiore, M., Angela Sortino, M. et Nicoletti, F. (2007) The nature of the cell cycle in neurons: Focus on a « non-canonical » pathway of DNA replication causally related to death. Cell Cycle Dysregulation and Neurodegenerative Diseases, vol. 1772, n°4, p. 409-412.

Counts, S. E. et Mufson, E. J. (2005) The role of nerve growth factor receptors in cholinergic basal forebrain degeneration in prodromal Alzheimer disease. Journal of neuropathology and experimental neurology, vol. 64, n°4, p. 263-272.

Courter, L. A., Shaffo, F. C., Ghogha, A., Parrish, D. J., Lorentz, C. U., Habecker, B. A. et Lein, P. J. (2016) BMP7-induced dendritic growth in sympathetic neurons requires p75(NTR) signaling. Developmental neurobiology, vol. 76, n°9, p. 1003-1013.

Csiszar, A., Tucsek, Z., Toth, P., Sosnowska, D., Gautam, T., Koller, A., Deak, F., Sonntag, W. E. et Ungvari, Z. (2013) Synergistic effects of hypertension and aging on cognitive function and hippocampal expression of genes involved in beta-amyloid generation and Alzheimer's disease. American journal of physiology.Heart and circulatory physiology, vol. 305, n°8, p. H1120-30.

Dal Magro, R., Ornaghi, F., Cambianica, I., Beretta, S., Re, F., Musicanti, C., Rigolio, R., Donzelli, E., Canta, A., Ballarini, E., Cavaletti, G., Gasco, P. et Sancini, G. (2017) ApoE-modified solid lipid nanoparticles: A feasible strategy to cross the blood-brain barrier. Journal of controlled release : official journal of the Controlled Release Society, vol. 249, p. 103-110.

Darabi Sahneh, F., Scoglio, C. et Riviere, J. (2013) Dynamics of Nanoparticle-Protein Corona Complex Formation: Analytical Results from Population Balance Equations. PLoS ONE, vol. 8, n°5.

David, L., Mallet, C., Mazerbourg, S., Feige, J. J. et Bailly, S. (2007) Identification of BMP9 and BMP10 as functional activators of the orphan activin receptor-like kinase 1 (ALK1) in endothelial cells. Blood, vol. 109, n°5, p. 1953-1961.

De Ferrari, G. V et Inestrosa, N. C. (2000) Wnt signaling function in Alzheimer's disease. Brain research. Brain research reviews, vol. 33, n°1, p. 1-12.

de la Monte, S. M. (2012) Brain Insulin Resistance and Deficiency as Therapeutic Targets in Alzheimer's Disease. Current Alzheimer Research, vol. 9, n°1, p. 35-66.

de Lange, E. C. (2013) The mastermind approach to CNS drug therapy: translational prediction of human brain distribution, target site kinetics, and therapeutic effects. Fluids and barriers of the CNS, vol. 10, n°1, p. 12.

Dehmelt, L. et Halpain, S. (2004) Actin and microtubules in neurite initiation: are MAPs the missing link? Journal of neurobiology, vol. 58, n°1, p. 18-33.

Deng, Y., Xiong, Z., Chen, P., Wei, J., Chen, S. et Yan, Z. (2014) β-Amyloid impairs the regulation of N-methyl-D-aspartate receptors by glycogen synthase kinase 3. Neurobiology of aging, vol. 35, n°3, p. 449-459.

Deshpande, A., Mina, E., Glabe, C. et Busciglio, J. (2006) Different conformations of amyloid beta induce neurotoxicity by distinct mechanisms in human cortical neurons. The Journal of neuroscience : the official journal of the Society for Neuroscience, vol. 26, n°22, p. 6011-6018.

Desjardins, M., Berti, R., Lefebvre, J., Dubeau, S. et Lesage, F. (2014) Aging-related differences in cerebral capillary blood flow in anesthetized rats. Neurobiology of aging, vol. 35, n°8, p. 1947-1955.

Dhawan, S., Kapil, R. et Singh, B. (2011) Formulation development and systematic optimization of solid lipid nanoparticles of quercetin for improved brain delivery. The Journal of pharmacy and pharmacology, vol. 63, n°3, p. 342-351.

Dhuria, S. V, Hanson, L. R. et Frey 2nd, W. H. (2010) Intranasal delivery to the central nervous system: mechanisms and experimental considerations. Journal of pharmaceutical sciences, vol. 99, n°4, p. 1654-1673.

Di Stefano, A., Iannitelli, A., Laserra, S. et Sozio, P. (2011) Drug delivery strategies for Alzheimer's disease treatment. Expert opinion on drug delivery, vol. 8, n°5, p. 581-603.

Ding, H., Sagar, V., Agudelo, M., Pilakka-Kanthikeel, S., Atluri, V. S., Raymond, A., Samikkannu, T. et Nair, M. P. (2014) Enhanced blood-brain barrier transmigration using a novel transferrin embedded fluorescent magneto-liposome nanoformulation. Nanotechnology, vol. 25, n°5, p. 055101-4484/25/5/055101. Epub 2014 Jan 9.

Diniz, L. P., Tortelli, V., Matias, I., Morgado, J., Bergamo Araujo, A. P., Melo, H. M., Seixas da Silva, G. S., Alves-Leon, S. V, de Souza, J. M., Ferreira, S. T., De Felice, F. G. et Gomes, F. C. A. (2017) Astrocyte Transforming Growth Factor Beta 1 Protects Synapses against Abeta

Oligomers in Alzheimer's Disease Model. The Journal of neuroscience : the official journal of the Society for Neuroscience, vol. 37, n°28, p. 6797-6809.

Dipankar, D. et Michalewicz, Z. (dir.) (2013) Evolutionary Algorithms in Engineering Applications (1st éd.). Springer-Verlag Berlin Heidelberg.

Do, T. D., Economou, N. J., Chamas, A., Buratto, S. K., Shea, J. E. et Bowers, M. T. (2014) Interactions between Amyloid-beta and Tau Fragments Promote Aberrant Aggregates: Implications for Amyloid Toxicity. The journal of physical chemistry.B.

Docagne, F., Gabriel, C., Lebeurrier, N., Lesne, S., Hommet, Y., Plawinski, L., Mackenzie, E. T. et Vivien, D. (2004) Sp1 and Smad transcription factors co-operate to mediate TGF-beta-dependent activation of amyloid-beta precursor protein gene transcription. The Biochemical journal, vol. 383, n°Pt 2, p. 393-399.

Dubois, B., Feldman, H. H., Jacova, C., Cummings, J. L., Dekosky, S. T., Barberger-Gateau, P., Delacourte, A., Frisoni, G., Fox, N. C., Galasko, D., Gauthier, S., Hampel, H., Jicha, G. A., Meguro, K., O'Brien, J., Pasquier, F., Robert, P., Rossor, M., Salloway, S., Sarazin, M., de Souza, L. C., Stern, Y., Visser, P. J. et Scheltens, P. (2010) Revising the definition of Alzheimer's disease: a new lexicon. The Lancet.Neurology, vol. 9, n°11, p. 1118-1127.

Dunne, M., Corrigan, I. et Ramtoola, Z. (2000) Influence of particle size and dissolution conditions on the degradation properties of polylactide-co-glycolide particles. Biomaterials, vol. 21, n°16, p. 1659-1668.

Dupraz, S., Grassi, D., Karnas, D., Nieto Guil, A. F., Hicks, D. et Quiroga, S. (2013) The insulin-like growth factor 1 receptor is essential for axonal regeneration in adult central nervous system neurons. PloS one, vol. 8, n°1, p. e54462.

Dyer, A. M., Hinchcliffe, M., Watts, P., Castile, J., Jabbal-Gill, I., Nankervis, R., Smith, A. et Illum, L. (2002) Nasal delivery of insulin using novel chitosan based formulations: a comparative study in two animal models between simple chitosan formulations and chitosan nanoparticles. Pharmaceutical research, vol. 19, n°7, p. 998-1008.

Edgar, T. F., Himmelblau, D. M. et Lasdon, L. S. (2001) Optimization of chemical processes. (McGraw-Hill International Chemical Engineering, Dir.) (2nd éd.). Thomas E. Casson.

Emami, J., Boushehri, M. S. S. et Varshosaz, J. (2014) Preparation, characterization and

optimization of glipizide controlled release nanoparticles. Research in pharmaceutical sciences, vol. 9, n°5, p. 301-314.

Encinas, M., Iglesias, M., Liu, Y., Wang, H., Muhaisen, A., Cena, V., Gallego, C. et Comella, J. X. (2000) Sequential treatment of SH-SY5Y cells with retinoic acid and brain-derived neurotrophic factor gives rise to fully differentiated, neurotrophic factor-dependent, human neuron-like cells. Journal of neurochemistry, vol. 75, n°3, p. 991-1003.

Enevoldsen, M. N., Kochoyan, A., Jurgenson, M., Jaako, K., Dmytriyeva, O., Walmod, P. S., Nielsen, J. D., Nielsen, J., Li, S., Korshunova, I., Klementiev, B., Novikova, T., Zharkovsky, A., Berezin, V. et Bock, E. (2012) Neuroprotective and memory enhancing properties of a dual agonist of the FGF receptor and NCAM. Neurobiology of disease, vol. 48, n°3, p. 533-545.

Eyjolfsdottir, H., Eriksdotter, M., Linderoth, B., Lind, G., Juliusson, B., Kusk, P., Almkvist, O., Andreasen, N., Blennow, K., Ferreira, D., Westman, E., Nennesmo, I., Karami, A., Darreh-Shori, T., Kadir, A., Nordberg, A., Sundstrom, E., Wahlund, L.-O., Wall, A., Wiberg, M., Winblad, B., Seiger, A., Wahlberg, L. et Almqvist, P. (2016) Targeted delivery of nerve growth factor to the cholinergic basal forebrain of Alzheimer's disease patients: application of a second-generation encapsulated cell biodelivery device. Alzheimer's research & therapy, vol. 8, n°1, p. 30.

Fagerstrom, S., Pahlman, S., Gestblom, C. et Nanberg, E. (1996) Protein kinase C-epsilon is implicated in neurite outgrowth in differentiating human neuroblastoma cells. Cell growth & differentiation : the molecular biology journal of the American Association for Cancer Research, vol. 7, n°6, p. 775-785.

Faisant, N., Siepmann, J. et Benoit, J. P. (2002) PLGA-based microparticles: elucidation of mechanisms and a new, simple mathematical model quantifying drug release. European Journal of Pharmaceutical Sciences, vol. 15, n°4, p. 355-366.

Faisant, N., Siepmann, J., Richard, J. et Benoit, J. P. (2003) Mathematical modeling of drug release from bioerodible microparticles: effect of gamma-irradiation. European Journal of Pharmaceutics and Biopharmaceutics, vol. 56, n°2, p. 271-279.

Faria, M. C., Gonçalves, G. S., Rocha, N. P., Moraes, E. N., Bicalho, M. A., Gualberto Cintra, M. T., Jardim de Paula, J., José Ravic de Miranda, L. F., Clayton de Souza Ferreira, A., Teixeira, A. L., Gomes, K. B., Carvalho, M. das G. et Sousa, L. P. (2014) Increased plasma levels of

BDNF and inflammatory markers in Alzheimer's disease. Journal of psychiatric research, vol. 53, n°0, p. 166-172.

Fazil, M., Md, S., Haque, S., Kumar, M., Baboota, S., Sahni, J. K. et Ali, J. (2012) Development and evaluation of rivastigmine loaded chitosan nanoparticles for brain targeting. European Journal of Pharmaceutical Sciences, vol. 47, n°1, p. 6-15.

Fedosov, D. A., Dao, M., Karniadakis, G. E. et Suresh, S. (2014) Computational biorheology of human blood flow in health and disease. Annals of Biomedical Engineering, vol. 42, n°2, p. 368-387.

Fedosov, D. A., Noguchi, H. et Gompper, G. (2014) Multiscale modeling of blood flow: from single cells to blood rheology. Biomechanics and modeling in mechanobiology, vol. 13, n°2, p. 239-258.

Feng, C., Zhang, C., Shao, X., Liu, Q., Qian, Y., Feng, L., Chen, J., Zha, Y., Zhang, Q. et Jiang, X. (2012) Enhancement of nose-to-brain delivery of basic fibroblast growth factor for improving rat memory impairments induced by co-injection of β-amyloid and ibotenic acid into the bilateral hippocampus. International journal of pharmaceutics, vol. 423, n°2, p. 226-234.

Fernández-Urrusuno, R., Calvo, P., Remuñán-López, C., Vila-Jato, J. L. et Alonso, M. J. (1999) Enhancement of nasal absorption of insulin using chitosan nanoparticles. Pharmaceutical research, vol. 16, n°10, p. 1576-1581.

Ferreira, A., Lu, Q., Orecchio, L. et Kosik, K. S. (1997) Selective Phosphorylation of Adult Tau Isoforms in Mature Hippocampal Neurons Exposed to Fibrillar Aβ. Molecular and Cellular Neuroscience, vol. 9, n°3, p. 220-234.

Ferrer, I., Marin, C., Rey, M. J., Ribalta, T., Goutan, E., Blanco, R., Tolosa, E. et Marti, E. (1999) BDNF and full-length and truncated TrkB expression in Alzheimer disease. Implications in therapeutic strategies. Journal of neuropathology and experimental neurology, vol. 58, n°7, p. 729-739.

Fonseca-Santos, B., Gremiao, M. P. D. et Chorilli, M. (2015) Nanotechnology-based drug delivery systems for the treatment of Alzheimer's disease. International journal of nanomedicine, vol. 10, p. 4981-5003.

Ford-Perriss, M., Abud, H. et Murphy, M. (2001) Fibroblast growth factors in the developing central

nervous system. Clinical and experimental pharmacology & physiology, vol. 28, n°7, p. 493-503.

Forster, J. I., Koglsberger, S., Trefois, C., Boyd, O., Baumuratov, A. S., Buck, L., Balling, R. et Antony, P. M. A. (2016) Characterization of Differentiated SH-SY5Y as Neuronal Screening Model Reveals Increased Oxidative Vulnerability. Journal of biomolecular screening, vol. 21, n°5, p. 496-509.

Foster, D. J., Choi, D. L., Conn, P. J. et Rook, J. M. (2014) Activation of M1 and M4 muscarinic receptors as potential treatments for Alzheimer's disease and schizophrenia. Neuropsychiatric disease and treatment, vol. 10, p. 183-191.

Fredenberg, S., Wahlgren, M., Reslow, M. et Axelsson, A. (2011) The mechanisms of drug release in poly(lactic-co-glycolic acid)-based drug delivery systems--a review. International journal of pharmaceutics, vol. 415, n°1-2, p. 34-52.

Freiherr, J., Hallschmid, M., Frey 2nd, W. H., Brunner, Y. F., Chapman, C. D., Holscher, C., Craft, S., De Felice, F. G. et Benedict, C. (2013) Intranasal insulin as a treatment for Alzheimer's disease: a review of basic research and clinical evidence. CNS drugs, vol. 27, n°7, p. 505-514.

Friden, P. M., Walus, L. R., Musso, G. F., Taylor, M. A., Malfroy, B. et Starzyk, R. M. (1991) Anti-transferrin receptor antibody and antibody-drug conjugates cross the blood-brain barrier. Proceedings of the National Academy of Sciences of the United States of America, vol. 88, n°11, p. 4771-4775.

Friedrichs, M., Wirsdoerfer, F., Flohe, S. B., Schneider, S., Wuelling, M. et Vortkamp, A. (2011) BMP signaling balances proliferation and differentiation of muscle satellite cell descendants. BMC cell biology, vol. 12, p. 26.

Frost, B., Hemberg, M., Lewis, J. et Feany, M. B. (2014) Tau promotes neurodegeneration through global chromatin relaxation. Nature neuroscience, vol. 17, n°3, p. 357-366.

Frozza, R. L., Bernardi, A., Hoppe, J. B., Meneghetti, A. B., Matte, A., Battastini, A. M., Pohlmann, A. R., Guterres, S. S. et Salbego, C. (2013) Neuroprotective effects of resveratrol against Abeta administration in rats are improved by lipid-core nanocapsules. Molecular neurobiology, vol. 47, n°3, p. 1066-1080.

Fu, A. S., Thatiparti, T. R., Saidel, G. M. et Von Recum, H. A. (2011) Experimental studies and

modeling of drug release from a tunable affinity-based drug delivery platform. Annals of Biomedical Engineering, vol. 39, n°9, p. 2466-2475.

Fu, Y. et Kao, W. J. (2010) Drug release kinetics and transport mechanisms of non-degradable and degradable polymeric delivery systems. Expert opinion on drug delivery, vol. 7, n°4, p. 429-444.

Fujita, H. (1961) Diffusion in polymer-diluent systems. Fortschritte der Hochpolymeren-Forschung, vol. 3, n°1, p. 1-47.

Gan, Q. et Wang, T. (2007) Chitosan nanoparticle as protein delivery carrier—Systematic examination of fabrication conditions for efficient loading and release. Colloids and Surfaces B: Biointerfaces, vol. 59, n°1, p. 24-34.

Garbayo, E., Ansorena, E., Lana, H., Carmona-Abellan, M. D. M., Marcilla, I., Lanciego, J. L., Luquin, M. R. et Blanco-Prieto, M. J. (2016) Brain delivery of microencapsulated GDNF induces functional and structural recovery in parkinsonian monkeys. Biomaterials, vol. 110, p. 11-23.

Garbayo, E., Ansorena, E., Lanciego, J. L., Aymerich, M. S. et Blanco-Prieto, M. J. (2008) Sustained release of bioactive glycosylated glial cell-line derived neurotrophic factor from biodegradable polymeric microspheres. European Journal of Pharmaceutics and Biopharmaceutics, vol. 69, n°3, p. 844-851.

Garbayo, E., Montero-Menei, C. N., Ansorena, E., Lanciego, J. L., Aymerich, M. S. et Blanco-Prieto, M. J. (2009) Effective GDNF brain delivery using microspheres--a promising strategy for Parkinson's disease. Journal of controlled release : official journal of the Controlled Release Society, vol. 135, n°2, p. 119-126.

Gaviglio, A. L., Knelson, E. H. et Blobe, G. C. (2017) Heparin-binding epidermal growth factor-like growth factor promotes neuroblastoma differentiation. FASEB journal : official publication of the Federation of American Societies for Experimental Biology, vol. 31, n°5, p. 1903-1915.

Gavini, E., Rassu, G., Haukvik, T., Lanni, C., Racchi, M. et Giunchedi, P. (2009) Mucoadhesive microspheres for nasal administration of cyclodextrins. Journal of drug targeting, vol. 17, n°2, p. 168-179.

Ge, A. Z. et Butcher, E. C. (1994) Cloning and expression of a cDNA encoding mouse endoglin, an endothelial cell TGF-beta ligand. Gene, vol. 138, n°1-2, p. 201-206.

Geula, C., Nagykery, N., Nicholas, A. et Wu, C. K. (2008) Cholinergic neuronal and axonal abnormalities are present early in aging and in Alzheimer disease. Journal of neuropathology and experimental neurology, vol. 67, n°4, p. 309-318.

Giacca, M. et Zacchigna, S. (2012) Virus-mediated gene delivery for human gene therapy. Drug Delivery Research in Europe, vol. 161, n°2, p. 377-388.

Giacobini, E. et Gold, G. (2013) Alzheimer disease therapy - Moving from amyloid-ß to tau. Nature Reviews Neurology, vol. 9, n°12, p. 677-686.

Gil-Bea, F. J., García-Alloza, M., Domínguez, J., Marcos, B. et Ramírez, M. J. (2005) Evaluation of cholinergic markers in Alzheimer's disease and in a model of cholinergic deficit. Neuroscience letters, vol. 375, n°1, p. 37-41.

Gilmor, M. L., Nash, N. R., Roghani, A., Edwards, R. H., Yi, H., Hersch, S. M. et Levey, A. I. (1996) Expression of the putative vesicular acetylcholine transporter in rat brain and localization in cholinergic synaptic vesicles. The Journal of neuroscience : the official journal of the Society for Neuroscience, vol. 16, n°7, p. 2179-2190.

Giordano, C., Albani, D., Gloria, A., Tunesi, M., Rodilossi, S., Russo, T., Forloni, G., Ambrosio, L. et Cigada, A. (2011) Nanocomposites for neurodegenerative diseases: hydrogel-nanoparticle combinations for a challenging drug delivery. The International journal of artificial organs, vol. 34, n°12, p. 1115-1127.

Girao da Cruz, M. T., Jordao, J., Dasilva, K. A., Ayala-Grosso, C. A., Ypsilanti, A., Weng, Y. Q., Laferla, F. M., McLaurin, J. et Aubert, I. (2012) Early increases in soluble amyloid-beta levels coincide with cholinergic degeneration in 3xTg-AD mice. Journal of Alzheimer's disease : JAD, vol. 32, n°2, p. 267-272.

Godoy, J. A., Rios, J. A., Zolezzi, J. M., Braidy, N. et Inestrosa, N. C. (2014) Signaling pathway cross talk in Alzheimer's disease. Cell communication and signaling : CCS, vol. 12, p. 23.

Gomes, W. A., Mehler, M. F. et Kessler, J. A. (2003) Transgenic overexpression of BMP4 increases astroglial and decreases oligodendroglial lineage commitment. Developmental biology, vol. 255, n°1, p. 164-177.

Gomez-Ramos, A., Dominguez, J., Zafra, D., Corominola, H., Gomis, R., Guinovart, J. J. et Avila, J. (2006) Sodium tungstate decreases the phosphorylation of tau through GSK3 inactivation. Journal of neuroscience research, vol. 83, n°2, p. 264-273.

Gomita, Y., Esumi, S., Sugiyama, N., Kitamura, Y., Koike, Y., Motoda, H., Sendo, T. et Kano, Y. (2017) Intracranial self-stimulation-reward induces neurite extension in PC12m3 cells and activation of the p38 MAPK pathway. Neuroscience letters, vol. 649, p. 78-84.

Goycoolea, F. M., Lollo, G., Remunan-Lopez, C., Quaglia, F. et Alonso, M. J. (2009) Chitosan-alginate blended nanoparticles as carriers for the transmucosal delivery of macromolecules. Biomacromolecules, vol. 10, n°7, p. 1736-1743.

Granholm, A. C., Backman, C., Bloom, F., Ebendal, T., Gerhardt, G. A., Hoffer, B., Mackerlova, L., Olson, L., Soderstrom, S. et Walus, L. R. (1994) NGF and anti-transferrin receptor antibody conjugate: short and long-term effects on survival of cholinergic neurons in intraocular septal transplants. The Journal of pharmacology and experimental therapeutics, vol. 268, n°1, p. 448-459.

Grassi, M., Colombo, I. et Lapasin, R. (2000) Drug release from an ensemble of swellable crosslinked polymer particles. Journal of Controlled Release, vol. 68, n°1, p. 97-113.

Grassi, M., Lamberti, G., Cascone, S. et Grassi, G. (2011) Mathematical modeling of simultaneous drug release and in vivo absorption. Mathematical modeling of drug delivery systems: Fifty years after Takeru Higuchi's models, vol. 418, n°1, p. 130-141.

Gross, R. E., Mehler, M. F., Mabie, P. C., Zang, Z., Santschi, L. et Kessler, J. A. (1996) Bone morphogenetic proteins promote astroglial lineage commitment by mammalian subventricular zone progenitor cells. Neuron, vol. 17, n°4, p. 595-606.

Grossberg, G. T. (2007) Current Strategies for the Treatment and Prevention of Alzheimer's Disease. Primary Psychiatry.

Guan, J., Du, S., Lv, T., Qu, S., Fu, Q. et Yuan, Y. (2016) Oxygen-glucose deprivation preconditioning protects neurons against oxygen-glucose deprivation/reperfusion induced injury via bone morphogenetic protein-7 mediated ERK, p38 and Smad signalling pathways. Clinical and experimental pharmacology & physiology, vol. 43, n°1, p. 125-134.

Guo, J.-J., Ma, L.-L., Shi, H.-T., Zhu, J.-B., Wu, J., Ding, Z.-W., An, Y., Zou, Y.-Z. et Ge, J.-B.

(2016) Alginate Oligosaccharide Prevents Acute Doxorubicin Cardiotoxicity by Suppressing Oxidative Stress and Endoplasmic Reticulum-Mediated Apoptosis. Marine drugs, vol. 14, n°12.

Gures, S., Siepmann, F., Siepmann, J., Kleinebudde, P., Güres, S., Siepmann, F., Siepmann, J. et Kleinebudde, P. (2012) Drug release from extruded solid lipid matrices: Theoretical predictions and independent experiments. European Journal of Pharmaceutics and Biopharmaceutics, vol. 80, n°1, p. 122-129.

Gusel'nikova, V. V et Korzhevskiy, D. E. (2015) NeuN As a Neuronal Nuclear Antigen and Neuron Differentiation Marker. Acta naturae, vol. 7, n°2, p. 42-47.

Hahn, I., Scherer, P. W. et Mozell, M. M. (1994) A mass transport model of olfaction. Journal of theoretical biology, vol. 167, n°2, p. 115-128.

Haines, D. E. (2012) Fundamental Neuroscience for Basic and Clinical Applications , For basic and clnical application. Philadelphia, PA, USA : Elsevier, Saunders.

Hansen, R. A., Gartlehner, G., Webb, A. P., Morgan, L. C., Moore, C. G. et Jonas, D. E. (2008) Efficacy and safety of donepezil, galantamine, and rivastigmine for the treatment of Alzheimer's disease: A systematic review and meta-analysis. Clinical Interventions in Aging, vol. 3, n°2, p. 211-225.

Hanson, L. R., Fine, J. M., Hoekman, J. D., Nguyen, T. M., Burns, R. B., Martinez, P. M., Pohl, J. et Frey 2nd, W. H. (2012) Intranasal delivery of growth differentiation factor 5 to the central nervous system. Drug delivery, vol. 19, n°3, p. 149-154.

Haque, S., Md, S., Sahni, J. K., Ali, J. et Baboota, S. (2014) Development and evaluation of brain targeted intranasal alginate nanoparticles for treatment of depression. Journal of psychiatric research, vol. 48, n°1, p. 1-12.

Harper, G. P., Glanville, R. W. et Thoenen, H. (1982) The purification of nerve growth factor from bovine seminal plasma. Biochemical characterization and partial amino acid sequence. The Journal of biological chemistry, vol. 257, n°14, p. 8541-8548.

Hartz, A. M., Miller, D. S. et Bauer, B. (2010) Restoring blood-brain barrier P-glycoprotein reduces brain amyloid-beta in a mouse model of Alzheimer's disease. Molecular pharmacology, vol. 77, n°5, p. 715-723.

Hashimoto, M. et Hisano, Y. (2011) Directional gene-transfer into the brain by an adenoviral vector tagged with magnetic nanoparticles. Journal of neuroscience methods, vol. 194, n°2, p. 316-320.

Hawkes, C., Jhamandas, J. H., Harris, K. H., Fu, W., MacDonald, R. G. et Kar, S. (2006) Single transmembrane domain insulin-like growth factor-II/mannose-6-phosphate receptor regulates central cholinergic function by activating a G-protein-sensitive, protein kinase C-dependent pathway. The Journal of neuroscience : the official journal of the Society for Neuroscience, vol. 26, n°2, p. 585-596.

Hecq, J., Siepmann, F., Siepmann, J., Amighi, K. et Goole, J. (2015) Development and evaluation of chitosan and chitosan derivative nanoparticles containing insulin for oral administration. Drug development and industrial pharmacy, vol. 41, n°12, p. 2037-2044.

Hegarty, S. V, Collins, L. M., Gavin, A. M., Roche, S. L., Wyatt, S. L., Sullivan, A. M. et O'Keeffe, G. W. (2014) Canonical BMP-Smad signalling promotes neurite growth in rat midbrain dopaminergic neurons. Neuromolecular medicine, vol. 16, n°2, p. 473-489.

Hegarty, S. V, Sullivan, A. M. et O'Keeffe, G. W. (2013a) BMP-Smad 1/5/8 signalling in the development of the nervous system. Progress in neurobiology, vol. 109, p. 28-41.

Hegarty, S. V, Sullivan, A. M. et O'Keeffe, G. W. (2013b) BMP2 and GDF5 induce neuronal differentiation through a Smad dependant pathway in a model of human midbrain dopaminergic neurons. Molecular and cellular neurosciences, vol. 56, p. 263-271.

Hegarty, S. V, Sullivan, A. M. et O'Keeffe, G. W. (2017) Endocytosis contributes to BMP2-induced Smad signalling and neuronal growth. Neuroscience letters, vol. 643, p. 32-37.

Heidenreich, K. A. (1993) Insulin and IGF-I receptor signaling in cultured neurons. Annals of the New York Academy of Sciences, vol. 692, p. 72-88.

Herrera, B. et Inman, G. J. (2009) A rapid and sensitive bioassay for the simultaneous measurement of multiple bone morphogenetic proteins. Identification and quantification of BMP4, BMP6 and BMP9 in bovine and human serum. BMC cell biology, vol. 10, n°20, p. 1-11.

Hers, I., Vincent, E. E. et Tavaré, J. M. (2011) Akt signalling in health and disease. Cellular signalling, vol. 23, n°10, p. 1515-1527.

Hinshaw, J. V. (2002) Non-linear calibration. LC-GC Europe, vol. 15, n°7, p. 406-409.

Hombach, J. et Bernkop-Schnurch, A. (2009) Chitosan solutions and particles: evaluation of their permeation enhancing potential on MDCK cells used as blood brain barrier model. International journal of pharmaceutics, vol. 376, n°1-2, p. 104-109.

Honegger, A. et Humbel, R. E. (1986) Insulin-like growth factors I and II in fetal and adult bovine serum. Purification, primary structures, and immunological cross-reactivities. The Journal of biological chemistry, vol. 261, n°2, p. 569-575.

Hong, M. et Lee, V. M.-Y. (1997) Insulin and insulin-like growth factor-1 regulate tau phosphorylation in cultured human neurons. Journal of Biological Chemistry, vol. 272, n°31, p. 19547-19553.

Howard, L., Wyatt, S., Nagappan, G. et Davies, A. M. (2013) ProNGF promotes neurite growth from a subset of NGF-dependent neurons by a p75NTR-dependent mechanism. Development (Cambridge, England), vol. 140, n°10, p. 2108-2117.

Hsieh, S., Chang, C. et Chou, H. (2013) Gold nanoparticles as amyloid-like fibrillogenesis inhibitors. Colloids and Surfaces B: Biointerfaces, vol. 112, n°0, p. 525-529.

Huang, J., Lu, Y., Wang, H., Liu, J., Liao, M., Hong, L., Tao, R., Ahmed, M. M., Liu, P., Liu, S., Fukunaga, K., Du, Y. et Han, F. (2013) The effect of lipid nanoparticle PEGylation on neuroinflammatory response in mouse brain. Biomaterials, vol. 34, n°32, p. 7960-7970.

Huang, M., Khor, E. et Lim, L.-Y. (2004) Uptake and cytotoxicity of chitosan molecules and nanoparticles: effects of molecular weight and degree of deacetylation. Pharmaceutical research, vol. 21, n°2, p. 344-353.

Huang, Y.-A., Kao, J.-W., Tseng, D. T.-H., Chen, W.-S., Chiang, M.-H. et Hwang, E. (2013) Microtubule-associated type II protein kinase A is important for neurite elongation. PloS one, vol. 8, n°8, p. e73890.

Idema, S., Caretti, V., Lamfers, M. L., van Beusechem, V. W., Noske, D. P., Vandertop, W. P. et Dirven, C. M. (2011) Anatomical differences determine distribution of adenovirus after convection-enhanced delivery to the rat brain. PloS one, vol. 6, n°10, p. e24396.

Illum, L. (2000) Transport of drugs from the nasal cavity to the central nervous system. European Journal of Pharmaceutical Sciences, vol. 11, n°1, p. 1-18.

Illum, L. (2003) Nasal drug delivery—possibilities, problems and solutions. Proceeding of the

Seventh European Symposium on Controlled Drug Delivery, vol. 87, n°1–3, p. 187-198.

Inestrosa, N. C., De Ferrari, G. V, Garrido, J. L., Alvarez, A., Olivares, G. H., Barría, M. I., Bronfman, M. et Chacón, M. A. (2002) Wnt signaling involvement in β-amyloid-dependent neurodegeneration. Neurochemistry international, vol. 41, n°5, p. 341-344.

Ismail, M. F., Elmeshad, A. N. et Salem, N. A. (2013) Potential therapeutic effect of nanobased formulation of rivastigmine on rat model of Alzheimer's disease. International journal of nanomedicine, vol. 8, p. 393-406.

Iulita, M. F. et Cuello, A. C. (2014) Nerve growth factor metabolic dysfunction in Alzheimer's disease and Down syndrome. Trends in pharmacological sciences, vol. 35, n°7, p. 338-348.

Izant, J. G. et McIntosh, J. R. (1980) Microtubule-associated proteins: a monoclonal antibody to MAP2 binds to differentiated neurons. Proceedings of the National Academy of Sciences of the United States of America, vol. 77, n°8, p. 4741-4745.

Jaeger, P. A., Lucin, K. M., Britschgi, M., Vardarajan, B., Huang, R.-P., Kirby, E. D., Abbey, R., Boeve, B. F., Boxer, A. L., Farrer, L. A., Finch, N., Graff-Radford, N. R., Head, E., Hofree, M., Huang, R., Johns, H., Karydas, A., Knopman, D. S., Loboda, A., Masliah, E., Narasimhan, R., Petersen, R. C., Podtelezhnikov, A., Pradhan, S., Rademakers, R., Sun, C.-H., Younkin, S. G., Miller, B. L., Ideker, T. et Wyss-Coray, T. (2016) Erratum to: Network-driven plasma proteomics expose molecular changes in the Alzheimer's brain. Molecular neurodegeneration.

Jämsä, A., Hasslund, K., Cowburn, R. F., Bäckström, A. et Vasänge, M. (2004) The retinoic acid and brain-derived neurotrophic factor differentiated SH-SY5Y cell line as a model for Alzheimer's disease-like tau phosphorylation. Biochemical and biophysical research communications, vol. 319, n°3, p. 993-1000.

Jensen, M., Hoerndli, F. J., Brockie, P. J., Wang, R., Johnson, E., Maxfield, D., Francis, M. M., Madsen, D. M. et Maricq, A. V. (2012) Wnt Signaling Regulates Acetylcholine Receptor Translocation and Synaptic Plasticity in the Adult Nervous System. Cell, vol. 149, n°1, p. 173-187.

Ji, R., Meng, L., Jiang, X., Cvm, N. K., Ding, J., Li, Q. et Lu, Q. (2014) TAM Receptors Support Neural Stem Cell Survival, Proliferation and Neuronal Differentiation. PloS one, vol. 9, n°12, p. e115140.

Jiang, S., Li, Y., Zhang, C., Zhao, Y., Bu, G., Xu, H. et Zhang, Y. W. (2014) M1 muscarinic acetylcholine receptor in Alzheimer's disease. Neuroscience bulletin, vol. 30, n°2, p. 295-307.

Jiang, X., Xin, H., Ren, Q., Gu, J., Zhu, L., Du, F., Feng, C., Xie, Y., Sha, X. et Fang, X. (2014) Nanoparticles of 2-deoxy-d-glucose functionalized poly(ethylene glycol)-co-poly(trimethylene carbonate) for dual-targeted drug delivery in glioma treatment. Biomaterials, vol. 35, n°1, p. 518-529.

Johnson, P. H. et Quay, S. C. (2005) Advances in nasal drug delivery through tight junction technology. Expert opinion on drug delivery, vol. 2, n°2, p. 281-298.

Johnson, G. V et Stoothoff, W. H. (2004) Tau phosphorylation in neuronal cell function and dysfunction. Journal of cell science, vol. 117, n°Pt 24, p. 5721-5729.

Jollivet, C., Aubert-Pouessel, A., Clavreul, A., Venier-Julienne, M.-C., Remy, S., Montero-Menei, C. N., Benoit, J.-P. et Menei, P. (2004) Striatal implantation of GDNF releasing biodegradable microspheres promotes recovery of motor function in a partial model of Parkinson's disease. Biomaterials, vol. 25, n°5, p. 933-942.

Jones, C. K., Byun, N. et Bubser, M. (2012) Muscarinic and nicotinic acetylcholine receptor agonists and allosteric modulators for the treatment of schizophrenia. Neuropsychopharmacology : official publication of the American College of Neuropsychopharmacology, vol. 37, n°1, p. 16-42.

Jonsson, T., Stefansson, H., Steinberg, S., Jonsdottir, I., Jonsson, P. V, Snaedal, J., Bjornsson, S., Huttenlocher, J., Levey, A. I., Lah, J. J., Rujescu, D., Hampel, H., Giegling, I., Andreassen, O. A., Engedal, K., Ulstein, I., Djurovic, S., Ibrahim-Verbaas, C., Hofman, A., Ikram, M. A., van Duijn, C. M., Thorsteinsdottir, U., Kong, A. et Stefansson, K. (2013) Variant of TREM2 associated with the risk of Alzheimer's disease. The New England journal of medicine, vol. 368, n°2, p. 107-116.

Joshi, S. A., Chavhan, S. S. et Sawant, K. K. (2010) Rivastigmine-loaded PLGA and PBCA nanoparticles: Preparation, optimization, characterization, in vitro and pharmacodynamic studies. European Journal of Pharmaceutics and Biopharmaceutics, vol. 76, n°2, p. 189-199.

Kaliner, M., Marom, Z., Patow, C. et Shelhamer, J. (1984) Human respiratory mucus. The Journal of allergy and clinical immunology, vol. 73, n°3, p. 318-323.

Kamalinia, G., Khodagholi, F., Atyabi, F., Amini, M., Shaerzadeh, F., Sharifzadeh, M. et Dinarvand, R. (2013) Enhanced brain delivery of deferasirox-lactoferrin conjugates for iron chelation therapy in neurodegenerative disorders: in vitro and in vivo studies. Molecular pharmaceutics, vol. 10, n°12, p. 4418-4431.

Kang, D. E., Pietrzik, C. U., Baum, L., Chevallier, N., Merriam, D. E., Kounnas, M. Z., Wagner, S. L., Troncoso, J. C., Kawas, C. H., Katzman, R. et Koo, E. H. (2000) Modulation of amyloid beta-protein clearance and Alzheimer's disease susceptibility by the LDL receptor-related protein pathway. The Journal of clinical investigation, vol. 106, n°9, p. 1159-1166.

Kang, Q., Sun, M. H., Cheng, H., Peng, Y., Montag, A. G., Deyrup, A. T., Jiang, W., Luu, H. H., Luo, J., Szatkowski, J. P., Vanichakarn, P., Park, J. Y., Li, Y., Haydon, R. C. et He, T. C. (2004) Characterization of the distinct orthotopic bone-forming activity of 14 BMPs using recombinant adenovirus-mediated gene delivery. Gene therapy, vol. 11, n°17, p. 1312-1320.

Kao, P. F., Banigan, M. G., Vanderburg, C. R., McKee, A. C., Polgar, P. R., Seshadri, S. et Delalle, I. (2012) Increased expression of TrkB and Capzb2 accompanies preserved cognitive status in early Alzheimer disease pathology. Journal of neuropathology and experimental neurology, vol. 71, n°7, p. 654-664.

Kawaguchi-Niida, M., Shibata, N. et Furuta, Y. (2017) Smad4 is essential for directional progression from committed neural progenitor cells through neuronal differentiation in the postnatal mouse brain. Molecular and cellular neurosciences, vol. 83, p. 55-64.

Kim, E. K. et Choi, E.-J. (2010) Pathological roles of MAPK signaling pathways in human diseases. Biochimica et Biophysica Acta (BBA) - Molecular Basis of Disease, vol. 1802, n°4, p. 396-405.

Kim, J.-H., Peacock, M. R., George, S. C. et Hughes, C. C. W. (2012) BMP9 induces EphrinB2 expression in endothelial cells through an Alk1-BMPRII/ActRII-ID1/ID3-dependent pathway: implications for hereditary hemorrhagic telangiectasia type II. Angiogenesis, vol. 15, n°3, p. 497-509.

Kim, J. H., Song, P., Lim, H., Lee, J. H., Lee, J. H., Park, S. A. et Initiative, A. D. N. (2014) Gene-based rare allele analysis identified a risk gene of Alzheimer's disease. PloS one, vol. 9, n°10, p. e107983.

Kim, K. K., Adelstein, R. S. et Kawamoto, S. (2009) Identification of neuronal nuclei (NeuN) as Fox-3, a new member of the Fox-1 gene family of splicing factors. The Journal of biological chemistry, vol. 284, n°45, p. 31052-31061.

Kim, N. A., Lim, D. G., Lim, J. Y., Kim, K. H. et Jeong, S. H. (2014) Fundamental analysis of recombinant human epidermal growth factor in solution with biophysical methods. Drug development and industrial pharmacy.

Kim, S. N., Kim, S. G., Park, S. D., Cho-Chung, Y. S. et Hong, S. H. (2000) Participation of type II protein kinase A in the retinoic acid-induced growth inhibition of SH-SY5Y human neuroblastoma cells. Journal of cellular physiology, vol. 182, n°3, p. 421-428.

Kirby, G. T. S., White, L. J., Rahman, C. V., Cox, H. C., Qutachi, O., Rose, F. R. A., Hutmacher, D. W., Shakesheff, K. M. et Woodruff, M. A. (2011) PLGA-based microparticles for the sustained release of BMP-2. Polymers, vol. 3, n°1, p. 571-586.

Kissel, T. et Werner, U. (1998) Nasal delivery of peptides: an in vitro cell culture model for the investigation of transport and metabolism in human nasal epithelium. Journal of Controlled Release, vol. 53, n°1–3, p. 195-203.

Kitagishi, Y., Nakanishi, A., Ogura, Y. et Matsuda, S. (2014) Dietary regulation of PI3K/AKT/GSK-3beta pathway in Alzheimer's disease. Alzheimer's research & therapy, vol. 6, n°3, p. 35.

Kitiyanant, N., Kitiyanant, Y., Svendsen, C. N. et Thangnipon, W. (2012) BDNF-, IGF-1- and GDNF-secreting human neural progenitor cells rescue amyloid beta-induced toxicity in cultured rat septal neurons. Neurochemical research, vol. 37, n°1, p. 143-152.

Kiyota, T., Ingraham, K. L., Jacobsen, M. T., Xiong, H. et Ikezu, T. (2011) FGF2 gene transfer restores hippocampal functions in mouse models of Alzheimer's disease and has therapeutic implications for neurocognitive disorders. Proceedings of the National Academy of Sciences of the United States of America, vol. 108, n°49, p. E1339-48.

Knusel, B., Michel, P. P., Schwaber, J. S. et Hefti, F. (1990) Selective and nonselective stimulation of central cholinergic and dopaminergic development in vitro by nerve growth factor, basic fibroblast growth factor, epidermal growth factor, insulin and the insulin-like growth factors I and II. The Journal of neuroscience : the official journal of the Society for Neuroscience, vol. 10, n°2, p. 558-570.

Kohyama, J., Sanosaka, T., Tokunaga, A., Takatsuka, E., Tsujimura, K., Okano, H. et Nakashima, K. (2010) BMP-induced REST regulates the establishment and maintenance of astrocytic identity. The Journal of cell biology, vol. 189, n°1, p. 159-170.

Konishi, Y., Takahashi, K., Chui, D.-H., Rosenfeld, R. G., Himeno, M. et Tabira, T. (1994) Insulin-like growth factor II promotes in vitro cholinergic development of mouse septal neurons: Comparison with the effects of insulin-like growth factor I. Brain research, vol. 649, n°1-2, p. 53-61.

Konofagou, E. E., Tung, Y. S., Choi, J., Deffieux, T., Baseri, B. et Vlachos, F. (2012) Ultrasound-induced blood-brain barrier opening. Current Pharmaceutical Biotechnology, vol. 13, n°7, p. 1332-1345.

Kopf, S. R., Buchholzer, M. L., Hilgert, M., Löffelholz, K., Klein, J., Loffelholz, K. et Klein, J. (2001) Glucose plus choline improve passive avoidance behaviour and increase hippocampal acetylcholine release in mice. Neuroscience, vol. 103, n°2, p. 365-371.

Koriyama, Y., Furukawa, A., Muramatsu, M., Takino, J. et Takeuchi, M. (2015) Glyceraldehyde caused Alzheimer's disease-like alterations in diagnostic marker levels in SH-SY5Y human neuroblastoma cells. Scientific Reports, vol. 5.

Korsching, S., Auburger, G., Heumann, R., Scott, J. et Thoenen, H. (1985) Levels of nerve growth factor and its mRNA in the central nervous system of the rat correlate with cholinergic innervation. The EMBO journal, vol. 4, n°6, p. 1389-1393.

Korsmeyer, R. W., Gurny, R. et Doelker, E. (1983) Mechanisms of solute release from porous hydrophilic polymers. International journal of pharmaceutics, vol. 15, n°1, p. 25-35.

Kozikowski, A. P., Gaisina, I. N., Petukhov, P. A., Sridhar, J., King, L. T., Blond, S. Y., Duka, T., Rusnak, M. et Sidhu, A. (2006) Highly potent and specific GSK-3beta inhibitors that block tau phosphorylation and decrease alpha-synuclein protein expression in a cellular model of Parkinson's disease. ChemMedChem, vol. 1, n°2, p. 256-266.

Kozlovskaya, L., Abou-Kaoud, M. et Stepensky, D. (2014) Quantitative analysis of drug delivery to the brain via nasal route. Journal of Controlled Release, vol. 189, n°0, p. 133-140.

Kreuter, J. (2001) Nanoparticulate systems for brain delivery of drugs. Nanoparticulate Systems for Improved Drug Delivery, vol. 47, n°1, p. 65-81.

Kreuter, J. (2013) Mechanism of polymeric nanoparticle-based drug transport across the blood-brain barrier (BBB). Journal of microencapsulation, vol. 30, n°1, p. 49-54.

Kreuter, J. (2014) Drug delivery to the central nervous system by polymeric nanoparticles: What do we know? 2014 Editor's Collection, vol. 71, n°0, p. 2-14.

Kreuter, J., Ramge, P., Petrov, V., Hamm, S., Gelperina, S. E., Engelhardt, B., Alyautdin, R., von Briesen, H. et Begley, D. J. (2003) Direct evidence that polysorbate-80-coated poly(butylcyanoacrylate) nanoparticles deliver drugs to the CNS via specific mechanisms requiring prior binding of drug to the nanoparticles. Pharmaceutical research, vol. 20, n°3, p. 409-416.

Krewson, C. E. et Saltzman, W. M. (1996) Transport and elimination of recombinant human NGF during long-term delivery to the brain. Brain research, vol. 727, n°1–2, p. 169-181.

Kumar, M. N. V. R., Muzzarelli, R. A. A., Muzzarelli, C., Sashiwa, H. et Domb, A. J. (2004) Chitosan chemistry and pharmaceutical perspectives. Chemical reviews, vol. 104, n°12, p. 6017-6084.

Kumar, V., Abbas, A. et Fausto, N. (2005) Robbins & Cotran, Pathologic basis of disease. China : Elsevier Sanders.

Kuo, Y.-C. et Liang, C.-T. (2011) Catanionic solid lipid nanoparticles carrying doxorubicin for inhibiting the growth of U87MG cells. Colloids and Surfaces B: Biointerfaces, vol. 85, n°2, p. 131-137.

Kuo, Y.-C. et Rajesh, R. (2017) Targeted delivery of rosmarinic acid across the blood-brain barrier for neuronal rescue using polyacrylamide-chitosan-poly(lactide-co-glycolide) nanoparticles with surface cross-reacting material 197 and apolipoprotein E. International journal of pharmaceutics, vol. 528, n°1-2, p. 228-241.

Kuo, Y. C. et Chou, P. R. (2014) Neuroprotection against degeneration of sk-N-mc cells using neuron growth factor-encapsulated liposomes with surface cereport and transferrin. Journal of pharmaceutical sciences, vol. 103, n°8, p. 2484-2497.

Kuo, Y. C. et Shih-Huang, C. Y. (2013) Solid lipid nanoparticles carrying chemotherapeutic drug across the blood-brain barrier through insulin receptor-mediated pathway. Journal of drug targeting, vol. 21, n°8, p. 730-738.

Kurakhmaeva, K. B., Djindjikhashvili, I. A., Petrov, V. E., Balabanyan, V. U., Voronina, T. A., Trofimov, S. S., Kreuter, J., Gelperina, S., Begley, D. et Alyautdin, R. N. (2009) Brain targeting of nerve growth factor using poly(butyl cyanoacrylate) nanoparticles. Journal of drug targeting, vol. 17, n°8, p. 564-574.

Kurtz, D. B., Zhao, K., Hornung, D. E. et Scherer, P. (2004) Experimental and numerical determination of odorant solubility in nasal and olfactory mucosa. Chemical senses, vol. 29, n°9, p. 763-773.

Lad, S. P., Neet, K. E. et Mufson, E. J. (2003) Nerve growth factor: structure, function and therapeutic implications for Alzheimer's disease. Current drug targets.CNS and neurological disorders, vol. 2, n°5, p. 315-334.

LaFerla, F. M. et Oddo, S. (2005) Alzheimer's disease: Aβ, tau and synaptic dysfunction. Trends in molecular medicine, vol. 11, n°4, p. 170-176.

Lai, R.-F., Li, Z.-J., Zhou, Z.-Y., Feng, Z.-Q. et Zhao, Q.-T. (2013) Effect of rhBMP-2 sustained-release nanocapsules on the ectopic osteogenesis process in Sprague-Dawley rats. Asian Pacific journal of tropical medicine, vol. 6, n°11, p. 884-888.

Lai, S. K., Wang, Y. Y., Wirtz, D. et Hanes, J. (2009) Micro- and macrorheology of mucus. Advanced Drug Delivery Reviews, vol. 61, n°2, p. 86-100.

Latina, V., Caioli, S., Zona, C., Ciotti, M. T., Amadoro, G. et Calissano, P. (2017) Impaired NGF/TrkA Signaling Causes Early AD-Linked Presynaptic Dysfunction in Cholinergic Primary Neurons. Frontiers in cellular neuroscience, vol. 11, p. 68.

Lauzon, M.-A. (2014) Modélisation d'un système de libération d'un peptide dérivé de la BMP-9 et étude mécanistique comparative entre la BMP-9 et la BMP-2. Thèse de doctorat, Université de Sherbrooke, 1-141 p.

Lauzon, M.-A., Bergeron, E., Marcos, B. et Faucheux, N. (2012) Bone repair: new developments in growth factor delivery systems and their mathematical modeling. Journal of controlled release : official journal of the Controlled Release Society, vol. 162, n°3, p. 502-20.

Lauzon, M.-A., Bergeron, É., Marcos, B. et Faucheux, N. (2012) Bone repair: New developments in growth factor delivery systems and their mathematical modeling. Journal of Controlled Release.

Lauzon, M.-A., Daviau, A., Drevelle, O., Marcos, B. et Faucheux, N. (2014) Identification of a Growth Factor Mimicking the Synergistic Effect of Fetal Bovine Serum on BMP-9 Cell Response. Tissue engineering.Part A.

Lauzon, M.-A., Daviau, A., Marcos, B. et Faucheux, N. (2015a) Growth factor treatment to overcome Alzheimer's dysfunctional signaling. Cellular signalling, vol. 27, n°6, p. 1025-1038.

Lauzon, M.-A., Daviau, A., Marcos, B. et Faucheux, N. (2015b) Growth factor delivery systems: A new way to treat Alzheimer's disease. Journal of Controlled Release.

Lauzon, M.-A., Daviau, A., Marcos, B. et Faucheux, N. (2015c) Nanoparticle-mediated growth factor delivery systems: A new way to treat Alzheimer's disease. Journal of controlled release : official journal of the Controlled Release Society, vol. 206, p. 187-205.

Lauzon, M.-A., Drevelle, O. et Faucheux, N. (2017) Peptides derived from the knuckle epitope of BMP-9 induce the cholinergic differentiation and inactivate GSk3beta in human SH-SY5Y neuroblastoma cells. Scientific reports, vol. 7, n°1, p. 4695.

Lauzon, M.-A., Marcos, B. et Faucheux, N. (2014) Effect of initial pBMP-9 loading and collagen concentration on the kinetics of peptide release and a mathematical model of the delivery system. Journal of Controlled Release, vol. 182, n°1, p. 73-82.

Lavenius, E., Parrow, V., Nanberg, E. et Pahlman, S. (1994) Basic FGF and IGF-I promote differentiation of human SH-SY5Y neuroblastoma cells in culture. Growth factors (Chur, Switzerland), vol. 10, n°1, p. 29-39.

Lee, I. S., Jung, K., Kim, I. S. et Park, K. I. (2013) Amyloid-beta oligomers regulate the properties of human neural stem cells through GSK-3beta signaling. Experimental & molecular medicine, vol. 45, p. e60.

Leikas, J. V, Kohtala, S., Theilmann, W., Jalkanen, A. J., Forsberg, M. M. et Rantamaki, T. (2017) Brief isoflurane anesthesia regulates striatal AKT-GSK3beta signaling and ameliorates motor deficits in a rat model of early-stage Parkinson's disease. Journal of neurochemistry, vol. 142, n°3, p. 456-463.

Lemmon, S. K., Riley, M. C., Thomas, K. A., Hoover, G. A., Maciag, T. et Bradshaw, R. A. (1982) Bovine fibroblast growth factor: Comparison of brain and pituitary preparations. Journal of Cell Biology, vol. 95, n°1, p. 162-169.

Leugers, C. J., Koh, J. Y., Hong, W. et Lee, G. (2013) Tau in MAPK activation. Frontiers in neurology, vol. 4, p. 161.

Leventhal, P. S., Randolph, A. E., Vesbit, T. E., Schenone, A., Windebank, A. et Feldman, E. L. (1995) Insulin-like growth factor-II as a paracrine growth factor in human neuroblastoma cells. Experimental cell research, vol. 221, n°1, p. 179-186.

Li, J.-S. et Yao, Z.-X. (2013) Modulation of FGF receptor signaling as an intervention and potential therapy for myelin breakdown in Alzheimer's disease. Medical hypotheses, vol. 80, n°4, p. 341-344.

Li, J., Zhang, C., Li, J., Fan, L., Jiang, X., Chen, J., Pang, Z. et Zhang, Q. (2013) Brain delivery of NAP with PEG-PLGA nanoparticles modified with phage display peptides. Pharmaceutical research, vol. 30, n°7, p. 1813-1823.

Li, P., Dai, Y.-N., Zhang, J.-P., Wang, A.-Q. et Wei, Q. (2008) Chitosan-alginate nanoparticles as a novel drug delivery system for nifedipine. International journal of biomedical science : IJBS, vol. 4, n°3, p. 221-228.

Li, X., Schwarz, E. M., Zuscik, M. J., Rosier, R. N., Ionescu, A. M., Puzas, J. E., Drissi, H., Sheu, T. J. et O'Keefe, R. J. (2003) Retinoic acid stimulates chondrocyte differentiation and enhances bone morphogenetic protein effects through induction of Smad1 and Smad5. Endocrinology, vol. 144, n°6, p. 2514-2523.

Li, Z. G., Zhang, W. et Sima, A. A. (2003) C-peptide enhances insulin-mediated cell growth and protection against high glucose-induced apoptosis in SH-SY5Y cells. Diabetes/metabolism research and reviews, vol. 19, n°5, p. 375-385.

Liu, F., Grundke-Iqbal, I., Iqbal, K. et Gong, C. X. (2005) Contributions of protein phosphatases PP1, PP2A, PP2B and PP5 to the regulation of tau phosphorylation. The European journal of neuroscience, vol. 22, n°8, p. 1942-1950.

Liu, L., Wan, W., Xia, S., Kalionis, B. et Li, Y. (2014) Dysfunctional Wnt/β-catenin signaling contributes to blood–brain barrier breakdown in Alzheimer's disease. Neurochemistry international, vol. 75, n°0, p. 19-25.

Liu, X., Qin, J., Luo, Q., Bi, Y., Zhu, G., Jiang, W., Kim, S. H., Li, M., Su, Y., Nan, G., Cui, J., Zhang, W., Li, R., Chen, X., Kong, Y., Zhang, J., Wang, J., Rogers, M. R., Zhang, H., Shui,

W., Zhao, C., Wang, N., Liang, X., Wu, N., He, Y., Luu, H. H., Haydon, R. C., Shi, L. L., Li, T., He, T.-C. et Li, M. (2013) Cross-talk between EGF and BMP9 signalling pathways regulates the osteogenic differentiation of mesenchymal stem cells. Journal of cellular and molecular medicine, vol. 17, n°9, p. 1160-1172.

Liu, Z., Gao, X., Kang, T., Jiang, M., Miao, D., Gu, G., Hu, Q., Song, Q., Yao, L., Tu, Y., Chen, H., Jiang, X. et Chen, J. (2013) B6 peptide-modified PEG-PLA nanoparticles for enhanced brain delivery of neuroprotective peptide. Bioconjugate chemistry, vol. 24, n°6, p. 997-1007.

Lochhead, J. J. et Thorne, R. G. (2012) Intranasal delivery of biologics to the central nervous system. Advanced Drug Delivery Reviews, vol. 64, n°7, p. 614-628.

Lopes, C., Ribeiro, M., Duarte, A. I., Humbert, S., Saudou, F., Pereira de Almeida, L., Hayden, M. et Rego, A. C. (2014) IGF-1 intranasal administration rescues Huntington's disease phenotypes in YAC128 mice. Molecular neurobiology, vol. 49, n°3, p. 1126-1142.

Lopes, F. M., Schroder, R., da Frota, M. L. C. J., Zanotto-Filho, A., Muller, C. B., Pires, A. S., Meurer, R. T., Colpo, G. D., Gelain, D. P., Kapczinski, F., Moreira, J. C. F., Fernandes, M. da C. et Klamt, F. (2010) Comparison between proliferative and neuron-like SH-SY5Y cells as an in vitro model for Parkinson disease studies. Brain research, vol. 1337, p. 85-94.

Lopez-Coviella, I., Berse, B., Krauss, R., Thies, R. S., Blusztajn, J. K., López-Coviella, I., Berse, B., Krauss, R., Thies, R. S. et Blusztajn, J. K. (2000) Induction and maintenance of the neuronal cholinergic phenotype in the central nervous system by BMP-9. Science, vol. 289, n°5477, p. 313-316.

Lopez-Coviella, I., Berse, B., Thies, R. S., Blusztajn, J. K., López-Coviella, I., Berse, B., Thies, R. S. et Krzysztof Blusztajn, J. (2002) Upregulation of acetylcholine synthesis by bone morphogenetic protein 9 in a murine septal cell line. Journal of physiology, Paris, vol. 96, n°1-2, p. 53-59.

Lopez-Coviella, I., Follettie, M. T., Mellott, T. J., Kovacheva, V. P., Slack, B. E., Diesl, V., Berse, B., Thies, R. S. et Blusztajn, J. K. (2005) Bone morphogenetic protein 9 induces the transcriptome of basal forebrain cholinergic neurons. Proceedings of the National Academy of Sciences of the United States of America, vol. 102, n°19, p. 6984-6989.

Lopez-Coviella, I., Mellott, T. J., Schnitzler, A. C. et Blusztajn, J. K. (2011) BMP9 protects septal

neurons from axotomy-evoked loss of cholinergic phenotype. PloS one, vol. 6, n°6, p. e21166.

Lopez-Coviella, I., Mellott, T. M., Kovacheva, V. P., Berse, B., Slack, B. E., Zemelko, V., Schnitzler, A. et Blusztajn, J. K. (2006) Developmental pattern of expression of BMP receptors and Smads and activation of Smad1 and Smad5 by BMP9 in mouse basal forebrain. Brain research, vol. 1088, n°1, p. 49-56.

Lopez-Leon, T., Carvalho, E. L. S., Seijo, B., Ortega-Vinuesa, J. L., Bastos-Gonzalez, D., López-León, T., Carvalho, E. L. S., Seijo, B., Ortega-Vinuesa, J. L. et Bastos-González, D. (2005) Physicochemical characterization of chitosan nanoparticles: electrokinetic and stability behavior. Journal of colloid and interface science, vol. 283, n°2, p. 344-351.

Luterman, J. D., Haroutunian, V., Yemul, S., Ho, L., Purohit, D., Aisen, P. S., Mohs, R. et Pasinetti, G. M. (2000) Cytokine gene expression as a function of the clinical progression of Alzheimer disease dementia. Archives of Neurology, vol. 57, n°8, p. 1153-1160.

Lv, Q., Lan, W., Sun, W., Ye, R., Fan, X., Ma, M., Yin, Q., Jiang, Y., Xu, G., Dai, J., Guo, R. et Liu, X. (s.d.) Intranasal nerve growth factor attenuates tau phosphorylation in brain after traumatic brain injury in rats. Journal of the neurological sciences, n°0.

Lv, Q., Lan, W., Sun, W., Ye, R., Fan, X., Ma, M., Yin, Q., Jiang, Y., Xu, G., Dai, J., Guo, R. et Liu, X. (2014) Intranasal nerve growth factor attenuates tau phosphorylation in brain after traumatic brain injury in rats. Journal of the neurological sciences, vol. 345, n°1-2, p. 48-55.

Ma, X., Liu, P., Zhang, X., Jiang, W., Jia, M., Wang, C., Dong, Y., Dang, Y. et Gao, C. (2016) Intranasal Delivery of Recombinant AAV Containing BDNF Fused with HA2TAT: a Potential Promising Therapy Strategy for Major Depressive Disorder. Scientific reports, vol. 6, p. 22404.

Mabie, P. C., Mehler, M. F. et Kessler, J. A. (1999) Multiple roles of bone morphogenetic protein signaling in the regulation of cortical cell number and phenotype. The Journal of neuroscience : the official journal of the Society for Neuroscience, vol. 19, n°16, p. 7077-7088.

Madziar, B., Shah, S., Brock, M., Burke, R., Lopez-Coviella, I., Nickel, A. C., Cakal, E. B., Blusztajn, J. K. et Berse, B. (2008) Nerve growth factor regulates the expression of the cholinergic locus and the high-affinity choline transporter via the Akt/PKB signaling pathway. Journal of neurochemistry, vol. 107, n°5, p. 1284-1293.

Maesako, M., Uemura, K., Kuzuya, A., Sasaki, K., Asada, M., Watanabe, K., Ando, K., Kubota,

M., Kihara, T. et Kinoshita, A. (2011) Presenilin Regulates Insulin Signaling via a ?-Secretase-independent Mechanism*. The Journal of Biological Chemistry, vol. 286, n°28, p. 25309-25316.

Maity, S., Mukhopadhyay, P., Kundu, P. P. et Chakraborti, A. S. (2017) Alginate coated chitosan core-shell nanoparticles for efficient oral delivery of naringenin in diabetic animals-An in vitro and in vivo approach. Carbohydrate polymers, vol. 170, p. 124-132.

Manfe, V., Kochoyan, A., Bock, E. et Berezin, V. (2010) Peptides derived from specific interaction sites of the fibroblast growth factor 2-FGF receptor complexes induce receptor activation and signaling. Journal of neurochemistry, vol. 114, n°1, p. 74-86.

Marangos, P. J., Goodwin, F. K., Parma, A., Lauter, C. et Trams, E. (1978) Neuron specific protein (NSP) in neuroblastoma cells: relation to differentiation. Brain research, vol. 145, n°1, p. 49-58.

Marei, H. E. S., Farag, A., Althani, A., Afifi, N., Abd-Elmaksoud, A., Lashen, S., Rezk, S., Pallini, R., Casalbore, P. et Cenciarelli, C. (2015) Human olfactory bulb neural stem cells expressing hNGF restore cognitive deficit in Alzheimer's disease rat model. Journal of cellular physiology, vol. 230, n°1, p. 116-130.

Marques, F., Sousa, J. C., Sousa, N. et Palha, J. A. (2013) Blood-brain-barriers in aging and in Alzheimer's disease. Molecular neurodegeneration, vol. 8, p. 38.

Massague, J. et Gomis, R. R. (2006) The logic of TGFbeta signaling. FEBS letters, vol. 580, n°12, p. 2811-2820.

Masuda, A., Kobayashi, Y., Kogo, N., Saito, T., Saido, T. C. et Itohara, S. (2016) Cognitive deficits in single App knock-in mouse models. Neurobiology of learning and memory, vol. 135, p. 73-82.

Matrone, C., Ciotti, M. T., Mercanti, D., Marolda, R. et Calissano, P. (2008) NGF and BDNF signaling control amyloidogenic route and Abeta production in hippocampal neurons. Proceedings of the National Academy of Sciences of the United States of America, vol. 105, n°35, p. 13139-13144.

Matrone, C., Di Luzio, A., Meli, G., D'Aguanno, S., Severini, C., Ciotti, M.-T., Cattaneo, A. et Calissano, P. (2008) Activation of the amyloidogenic route by NGF deprivation induces

apoptotic death in PC12 cells. Journal of Alzheimer's disease : JAD, vol. 13, n°1, p. 81-96.

Mattsson, M. E., Enberg, G., Ruusala, A. I., Hall, K. et Pahlman, S. (1986) Mitogenic response of human SH-SY5Y neuroblastoma cells to insulin-like growth factor I and II is dependent on the stage of differentiation. The Journal of cell biology, vol. 102, n°5, p. 1949-1954.

McGinley, L. M., Sims, E., Lunn, J. S., Kashlan, O. N., Chen, K. S., Bruno, E. S., Pacut, C. M., Hazel, T., Johe, K., Sakowski, S. A. et Feldman, E. L. (2016) Human Cortical Neural Stem Cells Expressing Insulin-Like Growth Factor-I: A Novel Cellular Therapy for Alzheimer's Disease. Stem cells translational medicine, vol. 5, n°3, p. 379-391.

McShea, A., Lee, H., Petersen, R. B., Casadesus, G., Vincent, I., Linford, N. J., Funk, J.-O., Shapiro, R. A. et Smith, M. A. (2007) Neuronal cell cycle re-entry mediates Alzheimer disease-type changes. Cell Cycle Dysregulation and Neurodegenerative Diseases, vol. 1772, n°4, p. 467-472.

Mehdipour, A. R. et Hamidi, M. (2009) Brain drug targeting: a computational approach for overcoming blood-brain barrier. Drug discovery today, vol. 14, n°21-22, p. 1030-1036.

Mehler, M. F., Mabie, P. C., Zhang, D. et Kessler, J. A. (1997) Bone morphogenetic proteins in the nervous system. Trends in neurosciences, vol. 20, n°7, p. 309-317.

Mehler, M. F., Marmur, R., Gross, R., Mabie, P. C., Zang, Z., Papavasiliou, A. et Kessler, J. A. (1995) Cytokines regulate the cellular phenotype of developing neural lineage species. International journal of developmental neuroscience : the official journal of the International Society for Developmental Neuroscience, vol. 13, n°3-4, p. 213-240.

Melancon, B. J., Tarr, J. C., Panarese, J. D., Wood, M. R. et Lindsley, C. W. (2013) Allosteric modulation of the M1 muscarinic acetylcholine receptor: improving cognition and a potential treatment for schizophrenia and Alzheimer's disease. Drug discovery today, vol. 18, n°23–24, p. 1185-1199.

Mellott, T. J., Pender, S. M., Burke, R. M., Langley, E. A. et Blusztajn, J. K. (2014) IGF2 Ameliorates Amyloidosis, Increases Cholinergic Marker Expression and Raises BMP9 and Neurotrophin Levels in the Hippocampus of the APPswePS1dE9 Alzheimer's Disease Model Mice. PLoS ONE, vol. 9, n°4, p. . doi:10.1371/journal.pone.0094287.

Mellott, T., Lopez-Coviella, I., Blusztajn, J. K. et Berse, B. (2002) Mitogen-activated protein kinase

kinase negatively modulates ciliary neurotrophic factor-activated choline acetyltransferase gene expression. European journal of biochemistry / FEBS, vol. 269, n°3, p. 850-858.

Mercado-Gomez, O., Hernandez-Fonseca, K., Villavicencio-Queijeiro, A., Massieu, L., Chimal-Monroy, J. et Arias, C. (2008) Inhibition of Wnt and PI3K signaling modulates GSK-3beta activity and induces morphological changes in cortical neurons: role of tau phosphorylation. Neurochemical research, vol. 33, n°8, p. 1599-1609.

Mercier, F. et Douet, V. (2014) Bone morphogenetic protein-4 inhibits adult neurogenesis and is regulated by fractone-associated heparan sulfates in the subventricular zone. Journal of chemical neuroanatomy, vol. 57–58, n°0, p. 54-61.

Meyers, E. A., Gobeske, K. T., Bond, A. M., Jarrett, J. C., Peng, C.-Y. et Kessler, J. A. (2016) Increased bone morphogenetic protein signaling contributes to age-related declines in neurogenesis and cognition. Neurobiology of aging, vol. 38, p. 164-175.

Mi, F.-L., Sung, H.-W. et Shyu, S.-S. (2002) Drug release from chitosan-alginate complex beads reinforced by a naturally occuring cross-linking agent. Carbohydrates Polymers, vol. 48, p. 61-72.

Mie, M., Sasaki, S. et Kobatake, E. (2014) Construction of a bFGF-tethered multi-functional extracellular matrix protein through coiled-coil structures for neurite outgrowth induction. Biomedical materials (Bristol, England), vol. 9, n°1, p. 15004.

Migliore, M. M., Ortiz, R., Dye, S., Campbell, R. B., Amiji, M. M. et Waszczak, B. L. (2014) Neurotrophic and neuroprotective efficacy of intranasal GDNF in a rat model of Parkinson's disease. Neuroscience, vol. 274, n°0, p. 11-23.

Mira, H., Andreu, Z., Suh, H., Lie, D. C., Jessberger, S., Consiglio, A., San Emeterio, J., Hortiguela, R., Marques-Torrejon, M. A., Nakashima, K., Colak, D., Gotz, M., Farinas, I. et Gage, F. H. (2010) Signaling through BMPR-IA regulates quiescence and long-term activity of neural stem cells in the adult hippocampus. Cell stem cell, vol. 7, n°1, p. 78-89.

Misra, A., Ganesh, S., Shahiwala, A. et Shah, S. P. (2003) Drug delivery to the central nervous system: a review. Journal of pharmacy & pharmaceutical sciences : a publication of the Canadian Society for Pharmaceutical Sciences, Societe canadienne des sciences pharmaceutiques, vol. 6, n°2, p. 252-273.

Mistry, A., Glud, S. Z., Kjems, J., Randel, J., Howard, K. A., Stolnik, S. et Illum, L. (2009a) Effect of physicochemical properties on intranasal nanoparticle transit into murine olfactory epithelium. Journal of drug targeting, vol. 17, n°7, p. 543-552.

Mistry, A., Stolnik, S. et Illum, L. (2009b) Nanoparticles for direct nose-to-brain delivery of drugs. International journal of pharmaceutics, vol. 379, n°1, p. 146-157.

Molino, I., Colucci, L., Fasanaro, A. M., Traini, E. et Amenta, F. (2013) Efficacy of Memantine, Donepezil, or Their Association in Moderate-Severe Alzheimer's Disease: A Review of Clinical Trials. The Scientific World Journal, vol. 2013, p. 10.1155/2013/925702.

Mookherjee, P. et Johnson, G. V. W. (2001) Tau phosphorylation during apoptosis of human SH-SY5Y neuroblastoma cells. Brain research, vol. 921, n°1–2, p. 31-43.

Moretti, R., Caruso, P., Dal Ben, M., Conti, C., Gazzin, S. et Tiribelli, C. (2017) Vitamin D, Homocysteine, and Folate in Subcortical Vascular Dementia and Alzheimer Dementia. Frontiers in aging neuroscience, vol. 9, p. 169.

Mota, S. I., Ferreira, I. L. et Rego, A. C. (2014) Dysfunctional synapse in Alzheimer's disease - A focus on NMDA receptors. Neuropharmacology, vol. 76, n°PART A, p. 16-26.

Motion, J. P., Huynh, G. H., Szoka Jr, F. C. et Siegel, R. A. (2011) Convection and retro-convection enhanced delivery: some theoretical considerations related to drug targeting. Pharmaceutical research, vol. 28, n°3, p. 472-479.

Mufson, E. J., Counts, S. E., Perez, S. E. et Ginsberg, S. D. (2008) Cholinergic system during the progression of Alzheimer's disease: therapeutic implications. Expert review of neurotherapeutics, vol. 8, n°11, p. 1703-1718.

Mukhopadhyay, P., Chakraborty, S., Bhattacharya, S., Mishra, R. et Kundu, P. P. (2015) pH-sensitive chitosan/alginate core-shell nanoparticles for efficient and safe oral insulin delivery. International journal of biological macromolecules, vol. 72, p. 640-648.

Munoz, L. et Ammit, A. J. (2010) Targeting p38 MAPK pathway for the treatment of Alzheimer's disease. Neuropharmacology, vol. 58, n°3, p. 561-568.

Murphy, M. P. et LeVine 3rd, H. (2010) Alzheimer's disease and the amyloid-beta peptide. Journal of Alzheimer's disease : JAD, vol. 19, n°1, p. 311-323.

Nagpal, K., Singh, S. K. et Mishra, D. N. (2010) Chitosan nanoparticles: a promising system in novel drug delivery. Chemical & pharmaceutical bulletin, vol. 58, n°11, p. 1423-1430.

Nagpal, K., Singh, S. K. et Mishra, D. N. (2013) Optimization of brain targeted chitosan nanoparticles of Rivastigmine for improved efficacy and safety. International journal of biological macromolecules, vol. 59, n°0, p. 72-83.

Naslund, J., Haroutunian, V., Mohs, R., Davis, K. L., Davies, P., Greengard, P. et Buxbaum, J. D. (2000) Correlation between elevated levels of amyloid beta-peptide in the brain and cognitive decline. JAMA : the journal of the American Medical Association, vol. 283, n°12, p. 1571-1577.

Neiiendam, J. L., Kohler, L. B., Christensen, C., Li, S., Pedersen, M. V, Ditlevsen, D. K., Kornum, M. K., Kiselyov, V. V, Berezin, V. et Bock, E. (2004) An NCAM-derived FGF-receptor agonist, the FGL-peptide, induces neurite outgrowth and neuronal survival in primary rat neurons. Journal of neurochemistry, vol. 91, n°4, p. 920-935.

Neves, A. R., Queiroz, J. F., Lima, S. A. C. et Reis, S. (2017) Apo E-Functionalization of Solid Lipid Nanoparticles Enhances Brain Drug Delivery: Uptake Mechanism and Transport Pathways. Bioconjugate chemistry, vol. 28, n°4, p. 995-1004.

Nicholson, C. (1995) Interaction between diffusion and Michaelis-Menten uptake of dopamine after iontophoresis in striatum. Biophysical journal, vol. 68, n°5, p. 1699-1715.

Nicholson, C. et Phillips, J. M. (1981) Ion diffusion modified by tortuosity and volume fraction in the extracellular microenvironment of the rat cerebellum. Journal of Physiology. Affiliation: Dept. Physiol. Biophys., New York Univ. Med. Cent., New York, NY 10016, United States.

Nicholson, C., Phillips, J. M. et Gardner-Medwin, A. R. (1979) Diffusion from an iontophoretic point source in the brain: role of tortuosity and volume fraction. Brain research, vol. 169, n°3, p. 580-584.

Nicholson, C. et Tao, L. (1993) Hindered Diffusion of high molecular weight compounds in brain extracellular microenvironment measured with integrative optical imaging. Biophysical journal, vol. 65, n°6, p. 2277-2290.

Nigam, S. M., Xu, S., Kritikou, J. S., Marosi, K., Brodin, L. et Mattson, M. P. (2017) Exercise and BDNF reduce Abeta production by enhancing alpha-secretase processing of APP. Journal of

neurochemistry, vol. 142, n°2, p. 286-296.

Nilbratt, M., Porras, O., Marutle, A., Hovatta, O. et Nordberg, A. (2010) Neurotrophic factors promote cholinergic differentiation in human embryonic stem cell-derived neurons. Journal of Cellular and Molecular Medicine, vol. 14, n°6B, p. 1476-1484.

Ninawe, P. R. et Parulekar, S. J. (2012) Drug delivery using stimuli-responsive polymer gel spheres. Industrial and Engineering Chemistry Research, vol. 51, n°4, p. 1741-1755.

Noda, M., Takii, K., Parajuli, B., Kawanokuchi, J., Sonobe, Y., Takeuchi, H., Mizuno, T. et Suzumura, A. (2014) FGF-2 released from degenerating neurons exerts microglial-induced neuroprotection via FGFR3-ERK signaling pathway. Journal of neuroinflammation, vol. 11, p. 76.

Noh, M. Y., Koh, S. H., Kim, S. M., Maurice, T., Ku, S. K. et Kim, S. H. (2013) Neuroprotective effects of donepezil against Abeta42-induced neuronal toxicity are mediated through not only enhancing PP2A activity but also regulating GSK-3beta and nAChRs activity. Journal of neurochemistry, vol. 127, n°4, p. 562-574.

Noshita, T., Murayama, N., Oka, T., Ogino, R., Nakamura, S. et Inoue, T. (2012) Effect of bFGF on neuronal damage induced by sequential treatment of amyloid β and excitatory amino acid in vitro and in vivo. European journal of pharmacology, vol. 695, n°1–3, p. 76-82.

O'Kusky, J. R., Ye, P. et D'Ercole, A. J. (2000) Insulin-like growth factor-I promotes neurogenesis and synaptogenesis in the hippocampal dentate gyrus during postnatal development. The Journal of neuroscience : the official journal of the Society for Neuroscience, vol. 20, n°22, p. 8435-8442.

O'Kusky, J. et Ye, P. (2012) Neurodevelopmental effects of insulin-like growth factor signaling. Frontiers in neuroendocrinology, vol. 33, n°3, p. 230-251.

O'Neill, C. (2013) PI3-kinase/Akt/mTOR signaling: impaired on/off switches in aging, cognitive decline and Alzheimer's disease. Experimental gerontology, vol. 48, n°7, p. 647-653.

Oberstein, T. J., Spitzer, P., Klafki, H.-W., Linning, P., Neff, F., Knölker, H.-J., Lewczuk, P., Wiltfang, J., Kornhuber, J. et Maler, J. M. (2015) Astrocytes and microglia but not neurons preferentially generate N-terminally truncated Aβ peptides. Neurobiology of disease, vol. 65, n°0, p. 24-35.

Oddo, S., Billings, L., Kesslak, J. P., Cribbs, D. H. et LaFerla, F. M. (2004) Aβ Immunotherapy Leads to Clearance of Early, but Not Late, Hyperphosphorylated Tau Aggregates via the Proteasome. Neuron, vol. 43, n°3, p. 321-332.

Oddo, S., Caccamo, A., Kitazawa, M., Tseng, B. P. et LaFerla, F. M. (2003) Amyloid deposition precedes tangle formation in a triple transgenic model of Alzheimer's disease. Molecular and Cellular Basis of Synaptic Loss and Dysfunction in Alzheimer's Disease, vol. 24, n°8, p. 1063-1070.

Odelstad, L., Pahlman, S., Nilsson, K., Larsson, E., Lackgren, G., Johansson, K. E., Hjerten, S. et Grotte, G. (1981) Neuron-specific enolase in relation to differentiation in human neuroblastoma. Brain research, vol. 224, n°1, p. 69-82.

Okano-Uchida, T., Naruse, M., Ikezawa, T., Shibasaki, K. et Ishizaki, Y. (2013) Cerebellar neural stem cells differentiate into two distinct types of astrocytes in response to CNTF and BMP2. Neuroscience letters, vol. 552, p. 15-20.

Olajide, O. J., Yawson, E. O., Gbadamosi, I. T., Arogundade, T. T., Lambe, E., Obasi, K., Lawal, I. T., Ibrahim, A. et Ogunrinola, K. Y. (2017) Ascorbic acid ameliorates behavioural deficits and neuropathological alterations in rat model of Alzheimer's disease. Environmental toxicology and pharmacology, vol. 50, p. 200-211.

Olivero, G., Grilli, M., Chen, J., Preda, S., Mura, E., Govoni, S. et Marchi, M. (2014) Effects of soluble beta-amyloid on the release of neurotransmitters from rat brain synaptosomes. Frontiers in aging neuroscience, vol. 6, p. 166.

Olivier, J. C. (2005) Drug transport to brain with targeted nanoparticles. NeuroRx : the journal of the American Society for Experimental NeuroTherapeutics, vol. 2, n°1, p. 108-119.

Onishi, H. et Machida, Y. (1999) Biodegradation and distribution of water-soluble chitosan in mice. Biomaterials, vol. 20, n°2, p. 175-182.

Orejana, L., Barros-Miñones, L., Aguirre, N. et Puerta, E. (2013) Implication of JNK pathway on tau pathology and cognitive decline in a senescence-accelerated mouse model. Experimental Gerontology, vol. 48, n°6, p. 565-571.

Pang, Z., Gao, H., Yu, Y., Chen, J., Guo, L., Ren, J., Wen, Z., Su, J. et Jiang, X. (2011) Brain delivery and cellular internalization mechanisms for transferrin conjugated biodegradable

polymersomes. International journal of pharmaceutics, vol. 415, n°1–2, p. 284-292.

Paques, J. P., van der Linden, E., van Rijn, C. J. M. et Sagis, L. M. C. (2014) Preparation methods of alginate nanoparticles. Advances in colloid and interface science, vol. 209, p. 163-171.

Pardeshi, C. V et Belgamwar, V. S. (2013) Direct nose to brain drug delivery via integrated nerve pathways bypassing the blood-brain barrier: an excellent platform for brain targeting. Expert opinion on drug delivery, vol. 10, n°7, p. 957-972.

Pardridge, W. M. (2007) Blood-brain barrier delivery. Drug discovery today, vol. 12, n°1-2, p. 54-61.

Parent, M. J., Bedard, M. A., Aliaga, A., Minuzzi, L., Mechawar, N., Soucy, J. P., Schirrmacher, E., Kostikov, A., Gauthier, S. G. et Rosa-Neto, P. (2013) Cholinergic Depletion in Alzheimer's Disease Shown by [(18) F]FEOBV Autoradiography. International journal of molecular imaging, vol. 2013, p. 205045.

Pascual-Lucas, M., Viana da Silva, S., Di Scala, M., Garcia-Barroso, C., Gonzalez-Aseguinolaza, G., Mulle, C., Alberini, C. M., Cuadrado-Tejedor, M. et Garcia-Osta, A. (2014) Insulin-like growth factor 2 reverses memory and synaptic deficits in APP transgenic mice. EMBO molecular medicine.

Patthey, C., Gunhaga, L. et Edlund, T. (2008) Early development of the central and peripheral nervous systems is coordinated by Wnt and BMP signals. PLoS ONE, vol. 3, n°2.

Pei, Y., Brun, S. N., Markant, S. L., Lento, W., Gibson, P., Taketo, M. M., Giovannini, M., Gilbertson, R. J. et Wechsler-Reya, R. J. (2012) WNT signaling increases proliferation and impairs differentiation of stem cells in the developing cerebellum. Development (Cambridge, England), vol. 139, n°10, p. 1724-1733.

Peng, Y. S., Lai, P. L., Peng, S., Wu, H. C., Yu, S., Tseng, T. Y., Wang, L. F. et Chu, I. M. (2014) Glial cell line-derived neurotrophic factor gene delivery via a polyethylene imine grafted chitosan carrier. International journal of nanomedicine, vol. 9, p. 3163-3174.

Perale, G., Arosio, P., Moscatelli, D., Barri, V., Muller, M., Maccagnan, S. et Masi, M. (2009) A new model of resorbable device degradation and drug release: transient 1-dimension diffusional model. Journal of controlled release : official journal of the Controlled Release Society, vol. 136, n°3, p. 196-205.

Pieri, A., Liguri, G., Cecchi, C., Degl'Innocenti, D., Nassi, P. et Ramponi, G. (1997) Alteration of intracellular free calcium and acylphosphatase levels in differentiating SH-SY5Y neuroblastoma cells. Biochemistry and molecular biology international, vol. 43, n°3, p. 633-641.

Pilakka-Kanthikeel, S., Atluri, V. S., Sagar, V., Saxena, S. K. et Nair, M. (2013) Targeted brain derived neurotropic factors (BDNF) delivery across the blood-brain barrier for neuro-protection using magnetic nano carriers: an in-vitro study. PloS one, vol. 8, n°4, p. e62241.

Pinzon-Daza, M., Garzon, R., Couraud, P., Romero, I., Weksler, B., Ghigo, D., Bosia, A. et Riganti, C. (2012) The association of statins plus LDL receptor-targeted liposome-encapsulated doxorubicin increases in vitro drug delivery across blood-brain barrier cells. British journal of pharmacology, vol. 167, n°7, p. 1431-1447.

Pinzon-Daza, M. L., Salaroglio, I. C., Kopecka, J., Garzon, R., Couraud, P. O., Ghigo, D. et Riganti, C. (2014) The cross-talk between canonical and non-canonical Wnt-dependent pathways regulates P-glycoprotein expression in human blood-brain barrier cells. Journal of cerebral blood flow and metabolism : official journal of the International Society of Cerebral Blood Flow and Metabolism, vol. 34, n°8, p. 1258-1269.

Placido, A. I., Pereira, C. M. F., Duarte, A. I., Candeias, E., Correia, S. C., Santos, R. X., Carvalho, C., Cardoso, S., Oliveira, C. R., Moreira, P. I., Plácido, A. I., Pereira, C. M. F., Duarte, A. I., Candeias, E., Correia, S. C., Santos, R. X., Carvalho, C., Cardoso, S., Oliveira, C. R. et Moreira, P. I. (2014) The role of endoplasmic reticulum in amyloid precursor protein processing and trafficking: implications for Alzheimer's disease. Biochimica et biophysica acta, vol. 1842, n°9, p. 1444-1453.

Poon, W. W., Blurton-Jones, M., Tu, C. H., Feinberg, L. M., Chabrier, M. A., Harris, J. W., Jeon, N. L. et Cotman, C. W. (2011) beta-Amyloid impairs axonal BDNF retrograde trafficking. Neurobiology of aging, vol. 32, n°5, p. 821-833.

Povellato, G., Tuxworth, R. I., Hanger, D. P. et Tear, G. (2014) Modification of the Drosophila model of in vivo Tau toxicity reveals protective phosphorylation by GSK3beta. Biology open, vol. 3, n°1, p. 1-11.

Poynton, A. R. et Lane, J. M. (2002) Safety profile for the clinical use of bone morphogenetic proteins in the spine. Spine, vol. 27, n°16 Suppl 1, p. S40-8.

Prades, R., Guerrero, S., Araya, E., Molina, C., Salas, E., Zurita, E., Selva, J., Egea, G., López-Iglesias, C., Teixidó, M., Kogan, M. J. et Giralt, E. (2012) Delivery of gold nanoparticles to the brain by conjugation with a peptide that recognizes the transferrin receptor. Biomaterials, vol. 33, n°29, p. 7194-7205.

Prakash, N., Cohen-Cory, S., Penschuck, S. et Frostig, R. D. (2004) Basal forebrain cholinergic system is involved in rapid nerve growth factor (NGF)-induced plasticity in the barrel cortex of adult rats. Journal of neurophysiology, vol. 91, n°1, p. 424-437.

Purro, S. A., Galli, S. et Salinas, P. C. (2014) Dysfunction of Wnt signaling and synaptic disassembly in neurodegenerative diseases. Journal of molecular cell biology, vol. 6, n°1, p. 75-80.

Rahaiee, S., Hashemi, M., Shojaosadati, S. A., Moini, S. et Razavi, S. H. (2017) Nanoparticles based on crocin loaded chitosan-alginate biopolymers: Antioxidant activities, bioavailability and anticancer properties. International journal of biological macromolecules, vol. 99, p. 401-408.

Rahaiee, S., Shojaosadati, S. A., Hashemi, M., Moini, S. et Razavi, S. H. (2015) Improvement of crocin stability by biodegradeble nanoparticles of chitosan-alginate. International journal of biological macromolecules, vol. 79, p. 423-432.

Ramkrishna, D. (2000) Population balances ,theory and applications to particulate systems in engineering. Elsevier.

Reimold, I., Domke, D., Bender, J., Seyfried, C. A., Radunz, H.-E. et Fricker, G. (2008) Delivery of nanoparticles to the brain detected by fluorescence microscopy. European Journal of Pharmaceutics and Biopharmaceutics, vol. 70, n°2, p. 627-632.

Rempe, R., Cramer, S., Hüwel, S. et Galla, H.-J. (2011) Transport of Poly(n-butylcyano-acrylate) nanoparticles across the blood–brain barrier in vitro and their influence on barrier integrity. Biochemical and biophysical research communications, vol. 406, n°1, p. 64-69.

Rempe, R., Cramer, S., Qiao, R. et Galla, H. J. (2014) Strategies to overcome the barrier: use of nanoparticles as carriers and modulators of barrier properties. Cell and tissue research, vol. 355, n°3, p. 717-726.

Ren, R. F. et Flanders, K. C. (1996) Transforming growth factors-β protect primary rat hippocampal neuronal cultures from degeneration induced by β-amyloid peptide. Brain research, vol. 732, n°1–2, p. 16-24.

Revilla, S., Ursulet, S., Alvarez-Lopez, M. J., Castro-Freire, M., Perpina, U., Garcia-Mesa, Y., Bortolozzi, A., Gimenez-Llort, L., Kaliman, P., Cristofol, R., Sarkis, C. et Sanfeliu, C. (2014) Lenti-GDNF Gene Therapy Protects Against Alzheimer's Disease-Like Neuropathology in 3xTg-AD Mice and MC65 Cells. CNS neuroscience & therapeutics.

Rivera, E. J., Goldin, A., Fulmer, N., Tavares, R., Wands, J. R. et de la Monte, S. M. (2005) Insulin and insulin-like growth factor expression and function deteriorate with progression of Alzheimer's disease: link to brain reductions in acetylcholine. Journal of Alzheimer's disease : JAD, vol. 8, n°3, p. 247-268.

Roberson, E. D., Scearce-Levie, K., Palop, J. J., Yan, F., Cheng, I. H., Wu, T., Gerstein, H., Yu, G. Q. et Mucke, L. (2007) Reducing endogenous tau ameliorates amyloid beta-induced deficits in an Alzheimer's disease mouse model. Science (New York, N.Y.), vol. 316, n°5825, p. 750-754.

Roney, C., Kulkarni, P., Arora, V., Antich, P., Bonte, F., Wu, A., Mallikarjuana, N. N., Manohar, S., Liang, H.-F., Kulkarni, A. R., Sung, H.-W., Sairam, M. et Aminabhavi, T. M. (2005) Targeted nanoparticles for drug delivery through the blood-brain barrier for Alzheimer's disease. Journal of Controlled Release, vol. 108, n°2-3, p. 193-214.

Ronn, L. C. B., Dissing, S., Holm, A., Berezin, V. et Bock, E. (2002) Increased intracellular calcium is required for neurite outgrowth induced by a synthetic peptide ligand of NCAM. FEBS letters, vol. 518, n°1-3, p. 60-66.

Rourke, A. M., Cha, Y. et Collins, D. (1996) Stabilization of granulocyte colony-stimulating factor and structurally analogous growth factors by anionic phospholipids. Biochemistry, vol. 35, n°36, p. 11913-11917.

Saito, A., Suzuki, Y., Ogata, S., Ohtsuki, C. et Tanihara, M. (2003) Activation of osteo-progenitor cells by a novel synthetic peptide derived from the bone morphogenetic protein-2 knuckle epitope. Biochimica et biophysica acta, vol. 1651, n°1-2, p. 60-67.

Saito, A., Suzuki, Y., Ogata, S., Ohtsuki, C. et Tanihara, M. (2005) Accelerated bone repair with the use of a synthetic BMP-2-derived peptide and bone-marrow stromal cells. Journal of biomedical materials research.Part A, vol. 72, n°1, p. 77-82.

Saito, T., Matsuba, Y., Mihira, N., Takano, J., Nilsson, P., Itohara, S., Iwata, N. et Saido, T. C. (2014) Single App knock-in mouse models of Alzheimer's disease. Nature neuroscience, vol.

17, n°5, p. 661-663.

Salegio, E. A., Streeter, H., Dube, N., Hadaczek, P., Samaranch, L., Kells, A. P., San Sebastian, W., Zhai, Y., Bringas, J., Xu, T., Forsayeth, J. et Bankiewicz, K. S. (2014) Distribution of nanoparticles throughout the cerebral cortex of rodents and non-human primates: Implications for gene and drug therapy. Frontiers in neuroanatomy, vol. 8, p. 9.

Saraiva, C., Praca, C., Ferreira, R., Santos, T., Ferreira, L. et Bernardino, L. (2016) Nanoparticle-mediated brain drug delivery: Overcoming blood-brain barrier to treat neurodegenerative diseases. Journal of controlled release : official journal of the Controlled Release Society, vol. 235, p. 34-47.

Sarvaiya, J. et Agrawal, Y. K. (2015) Chitosan as a suitable nanocarrier material for anti-Alzheimer drug delivery. International journal of biological macromolecules, vol. 72, n°0, p. 454-465.

Saunders, N. R., Habgood, M. D. et Dziegielewska, K. M. (1999) Barrier mechanisms in the brain, I. Adult brain. Clinical and experimental pharmacology & physiology, vol. 26, n°1, p. 11-19.

Sayas, C. L., Moreno-Flores, M. T., Avila, J. et Wandosell, F. (1999) The neurite retraction induced by lysophosphatidic acid increases Alzheimer's disease-like Tau phosphorylation. The Journal of biological chemistry, vol. 274, n°52, p. 37046-37052.

Scali, C., Caraci, F., Gianfriddo, M., Diodato, E., Roncarati, R., Pollio, G., Gaviraghi, G., Copani, A., Nicoletti, F., Terstappen, G. C. et Caricasole, A. (2006) Inhibition of Wnt signaling, modulation of Tau phosphorylation and induction of neuronal cell death by DKK1. Neurobiology of disease, vol. 24, n°2, p. 254-265.

Schindowski, K., Belarbi, K. et Buee, L. (2008) Neurotrophic factors in Alzheimer's disease: role of axonal transport. Genes, brain, and behavior, vol. 7 Suppl 1, p. 43-56.

Schmeisser, M. J., Baumann, B., Johannsen, S., Vindedal, G. F., Jensen, V., Hvalby, O. C., Sprengel, R., Seither, J., Maqbool, A., Magnutzki, A., Lattke, M., Oswald, F., Boeckers, T. M. et Wirth, T. (2012) IkappaB kinase/nuclear factor kappaB-dependent insulin-like growth factor 2 (Igf2) expression regulates synapse formation and spine maturation via Igf2 receptor signaling. The Journal of neuroscience : the official journal of the Society for Neuroscience, vol. 32, n°16, p. 5688-5703.

Schmetsdorf, S., Arnold, E., Holzer, M., Arendt, T. et Gartner, U. (2009) A putative role for cell

cycle-related proteins in microtubule-based neuroplasticity. The European journal of neuroscience, vol. 29, n°6, p. 1096-1107.

Schnitzler, A. C., Mellott, T. J., Lopez-Coviella, I., Tallini, Y. N., Kotlikoff, M. I., Follettie, M. T. et Blusztajn, J. K. (2010) BMP9 (bone morphogenetic protein 9) induces NGF as an autocrine/paracrine cholinergic trophic factor in developing basal forebrain neurons. The Journal of neuroscience : the official journal of the Society for Neuroscience, vol. 30, n°24, p. 8221-8228.

Segklia, A., Seuntjens, E., Elkouris, M., Tsalavos, S., Stappers, E., Mitsiadis, T. A., Huylebroeck, D., Remboutsika, E. et Graf, D. (2012) Bmp7 regulates the survival, proliferation, and neurogenic properties of neural progenitor cells during corticogenesis in the mouse. PloS one, vol. 7, n°3, p. e34088.

Seira, O. et Del Río, J. A. (2014) Glycogen synthase kinase 3 beta (GSK3ß) at the tip of neuronal development and regeneration. Molecular neurobiology, vol. 49, n°2, p. 931-944.

Selkoe, D. J. et Podlisny, M. B. (2002) Deciphering the genetic basis of Alzheimer's disease. Annual review of genomics and human genetics, vol. 3, p. 67-99.

Sensenbrenner, M. (1993) The neurotrophic activity of fibroblast growth factors. Progress in neurobiology, vol. 41, n°6, p. 683-704.

Senta, H., Park, H., Bergeron, E., Drevelle, O., Fong, D., Leblanc, E., Cabana, F., Roux, S., Grenier, G. et Faucheux, N. (2009) Cell responses to bone morphogenetic proteins and peptides derived from them: biomedical applications and limitations. Cytokine & growth factor reviews, vol. 20, n°3, p. 213-222.

Sepulveda, F. J., Fierro, H., Fernandez, E., Castillo, C., Peoples, R. W., Opazo, C. et Aguayo, L. G. (2014) Nature of the neurotoxic membrane actions of amyloid-beta on hippocampal neurons in Alzheimer's disease. Neurobiology of aging, vol. 35, n°3, p. 472-481.

Shevtsov, M. A., Nikolaev, B. P., Yakovleva, L. Y., Marchenko, Y. Y., Dobrodumov, A. V, Mikhrina, A. L., Martynova, M. G., Bystrova, O. A., Yakovenko, I. V et Ischenko, A. M. (2014) Superparamagnetic iron oxide nanoparticles conjugated with epidermal growth factor (SPION-EGF) for targeting brain tumors. International journal of nanomedicine, vol. 9, p. 273-287.

Shi, J., Alves, N. M. et Mano, J. F. (2008) Chitosan coated alginate beads containing poly(N-isopropylacrylamide) for dual-stimuli-responsive drug release. Journal of biomedical materials research. Part B, Applied biomaterials, vol. 84, n°2, p. 595-603.

Shimizu, F., Sano, Y., Saito, K., Abe, M. A., Maeda, T., Haruki, H. et Kanda, T. (2012) Pericyte-derived glial cell line-derived neurotrophic factor increase the expression of claudin-5 in the blood-brain barrier and the blood-nerve barrier. Neurochemical research, vol. 37, n°2, p. 401-409.

Shou, J., Murray, R. C., Rim, P. C. et Calof, A. L. (2000) Opposing effects of bone morphogenetic proteins on neuron production and survival in the olfactory receptor neuron lineage. Development (Cambridge, England), vol. 127, n°24, p. 5403-5413.

Sidell, N., Lucas, C. A. et Kreutzberg, G. W. (1984) Regulation of acetylcholinesterase activity by retinoic acid in a human neuroblastoma cell line. Experimental cell research, vol. 155, n°1, p. 305-309.

Siepmann, J., Elkharraz, K., Siepmann, F. et Klose, D. (2005) How autocatalysis accelerates drug release from PLGA-based microparticles: a quantitative treatment. Biomacromolecules, vol. 6, n°4, p. 2312-2319.

Siepmann, J., Faisant, N. et Benoit, J. P. (2002) A new mathematical model quantifying drug release from bioerodible microparticles using Monte Carlo simulations. Pharmaceutical research, vol. 19, n°12, p. 1885-1893.

Siepmann, J., Kranz, H., Bodmeier, R. et Peppas, N. A. (1999c) HPMC-matrices for controlled drug delivery: a new model combining diffusion, swelling, and dissolution mechanisms and predicting the release kinetics. Pharmaceutical research, vol. 16, n°11, p. 1748-1756.

Siepmann, J., Lecomte, F. et Bodmeier, R. (1999b) Diffusion-controlled drug delivery systems: calculation of the required composition to achieve desired release profiles. Journal of controlled release : official journal of the Controlled Release Society, vol. 60, n°2-3, p. 379-389.

Siepmann, J. et Peppas, N. A. (2000) Hydrophilic matrices for controlled drug delivery: an improved mathematical model to predict the resulting drug release kinetics (the « sequential layer » model). Pharmaceutical research, vol. 17, n°10, p. 1290-1298.

Siepmann, J. et Peppas, N. A. (2001) Modeling of drug release from delivery systems based on hydroxypropyl methylcellulose (HPMC). Advanced Drug Delivery Reviews, vol. 48, n°2-3, p. 139-157.

Siepmann, J., Podual, K., Sriwongjanya, M., Peppas, N. A. et Bodmeier, R. (1999a) A new model describing the swelling and drug release kinetics from hydroxypropyl methylcellulose tablets. Journal of pharmaceutical sciences, vol. 88, n°1, p. 65-72.

Siepmann, J. et Siepmann, F. (2011) Mathematical modeling of drug release from lipid dosage forms. Mathematical modeling of drug delivery systems: Fifty years after Takeru Higuchi's models, vol. 418, n°1, p. 42-53.

Siepmann, J., Siepmann, F. et Florence, A. T. (2006) Local controlled drug delivery to the brain: Mathematical modeling of the underlying mass transport mechanisms. Local Controlled Drug Delivery to the Brain, vol. 314, n°2, p. 101-119.

Simpson, P. B., Bacha, J. I., Palfreyman, E. L., Woollacott, A. J., McKernan, R. M. et Kerby, J. (2001) Retinoic acid evoked-differentiation of neuroblastoma cells predominates over growth factor stimulation: an automated image capture and quantitation approach to neuritogenesis. Analytical biochemistry, vol. 298, n°2, p. 163-169.

Sinha, S. et Lieberburg, I. (1999) Cellular mechanisms of beta-amyloid production and secretion. Proceedings of the National Academy of Sciences of the United States of America, vol. 96, n°20, p. 11049-11053.

Sodhi, R. K. et Singh, N. (2014) Retinoids as potential targets for Alzheimer's disease. Pharmacology, biochemistry, and behavior, vol. 120, p. 117-123.

Soliman, G. M., Zhang, Y. L., Merle, G., Cerruti, M. et Barralet, J. (2014) Hydrocaffeic acid–chitosan nanoparticles with enhanced stability, mucoadhesion and permeation properties. European Journal of Pharmaceutics and Biopharmaceutics, vol. 88, n°0, p. 1026-1037.

Song, Y., Du, D., Li, L., Xu, J., Dutta, P. et Lin, Y. (2017) In Vitro Study of Receptor-Mediated Silica Nanoparticles Delivery across Blood-Brain Barrier. ACS applied materials & interfaces, vol. 9, n°24, p. 20410-20416.

Sontag, J. M. et Sontag, E. (2014) Protein phosphatase 2A dysfunction in Alzheimer's disease. Frontiers in molecular neuroscience, vol. 7, p. 16.

Soumen, R., Johnston, A. H., Moin, S. T., Dudas, J., Newman, T. A., Hausott, B., Schrott-Fischer, A. et Glueckert, R. (2012) Activation of TrkB receptors by NGFbeta mimetic peptide conjugated polymersome nanoparticles. Nanomedicine : nanotechnology, biology, and medicine, vol. 8, n°3, p. 271-274.

Spencer, B., Verma, I., Desplats, P., Morvinski, D., Rockenstein, E., Adame, A. et Masliah, E. (2014) A neuroprotective brain-penetrating endopeptidase fusion protein ameliorates Alzheimer disease pathology and restores neurogenesis. The Journal of biological chemistry, vol. 289, n°25, p. 17917-17931.

Spillantini, M. G., Iovino, M. et Vuono, R. (2011) Release of growth factors by neuronal precursor cells as a treatment for diseases with tau pathology. Archives Italiennes de Biologie, vol. 149, n°2, p. 215-223.

Steen, E., Terry, B. M., Rivera, E. J., Cannon, J. L., Neely, T. R., Tavares, R., Xu, X. J., Wands, J. R. et de la Monte, S. M. (2005) Impaired insulin and insulin-like growth factor expression and signaling mechanisms in Alzheimer's disease--is this type 3 diabetes? Journal of Alzheimer's disease : JAD, vol. 7, n°1, p. 63-80.

Stevens, H. E., Jiang, G. Y., Schwartz, M. L. et Vaccarino, F. M. (2012) Learning and Memory Depend on Fibroblast Growth Factor Receptor 2 Functioning in Hippocampus. Optogenetics and the Translational Neuroscience of Psychiatry, vol. 71, n°12, p. 1090-1098.

Stockwell, J., Abdi, N., Lu, X., Maheshwari, O. et Taghibiglou, C. (2014) Novel central nervous system drug delivery systems. Chemical biology & drug design, vol. 83, n°5, p. 507-520.

Streit, A. et Stern, C. D. (1999) Establishment and maintenance of the border of the neural plate in the chick: involvement of FGF and BMP activity. Mechanisms of development, vol. 82, n°1-2, p. 51-66.

Sullivan, A. M., Opacka-Juffry, J., Pohl, J. et Blunt, S. B. (1999) Neuroprotective effects of growth/differentiation factor 5 depend on the site of administration. Brain research, vol. 818, n°1, p. 176-179.

Sun, L., Liu, S. Y., Zhou, X. W., Wang, X. C., Liu, R., Wang, Q. et Wang, J. Z. (2003) Inhibition of protein phosphatase 2A- and protein phosphatase 1-induced tau hyperphosphorylation and impairment of spatial memory retention in rats. Neuroscience, vol. 118, n°4, p. 1175-1182.

Suzuki, Y., Ohga, N., Morishita, Y., Hida, K., Miyazono, K. et Watabe, T. (2010) BMP-9 induces proliferation of multiple types of endothelial cells in vitro and in vivo. Journal of cell science, vol. 123, n°Pt 10, p. 1684-1692.

Suzuki, Y., Tanihara, M., Suzuki, K., Saitou, A., Sufan, W. et Nishimura, Y. (2000) Alginate hydrogel linked with synthetic oligopeptide derived from BMP-2 allows ectopic osteoinduction in vivo. Journal of Biomedical Materials Research, vol. 50, n°3, p. 405-409.

Szutowicz, A., Bielarczyk, H., Jankowska-Kulawy, A., Pawelczyk, T. et Ronowska, A. (2013) Acetyl-CoA the Key Factor for Survival or Death of Cholinergic Neurons in Course of Neurodegenerative Diseases. Neurochemical research, vol. 38, n°8, p. 1523-1542.

Tah, B., Pal, P., Mishra, S. et Talapatra, G. B. (2014) Interaction of insulin with anionic phospholipid (DPPG) vesicles. Physical chemistry chemical physics : PCCP, vol. 16, n°39, p. 21657-21663.

Takahashi, K., Piao, S., Yamatani, H., Du, B., Yin, L., Ohta, T., Kawagoe, J., Takata, K., Tsutsumi, S. et Kurachi, H. (2011) Estrogen induces neurite outgrowth via Rho family GTPases in neuroblastoma cells. Molecular and cellular neurosciences, vol. 48, n°3, p. 217-224.

Takamura, R., Watamura, N., Nikkuni, M. et Ohshima, T. (2017) All-trans retinoic acid improved impaired proliferation of neural stem cells and suppressed microglial activation in the hippocampus in an Alzheimer's mouse model. Journal of neuroscience research, vol. 95, n°3, p. 897-906.

Takashima, A., Noguchi, K., Michel, G., Mercken, M., Hoshi, M., Ishiguro, K. et Imahori, K. (1996) Exposure of rat hippocampal neurons to amyloid β peptide (25–35) induces the inactivation of phosphatidyl inositol-3 kinase and the activation of tau protein kinase I/glycogen synthase kinase-3β. Neuroscience letters, vol. 203, n°1, p. 33-36.

Takashina, K., Bessho, T., Mori, R., Kawai, K., Eguchi, J. et Saito, K. (2008) MKC-231, a choline uptake enhancer: (3) Mode of action of MKC-231 in the enhancement of high-affinity choline uptake. Journal of neural transmission (Vienna, Austria : 1996), vol. 115, n°7, p. 1037-1046.

Tam, R. Y., Fuehrmann, T., Mitrousis, N. et Shoichet, M. S. (2014) Regenerative therapies for central nervous system diseases: A biomaterials approach. Neuropsychopharmacology, vol. 39, n°1, p. 169-188.

Tan, J., Wang, Y., Yip, X., Glynn, F., Shepherd, R. K. et Caruso, F. (2012) Nanoporous peptide

particles for encapsulating and releasing neurotrophic factors in an animal model of neurodegeneration. Advanced materials (Deerfield Beach, Fla.), vol. 24, n°25, p. 3362-3366.

Tanabe, K., Matsushima-Nishiwaki, R., Iida, M., Kozawa, O. et Iida, H. (2012) Involvement of phosphatidylinositol 3-kinase/Akt on basic fibroblast growth factor-induced glial cell line-derived neurotrophic factor release from rat glioma cells. Brain research, vol. 1463, n°0, p. 21-29.

Tang, D.-W., Yu, S.-H., Ho, Y.-C., Mi, F.-L., Kuo, P.-L. et Sung, H.-W. (2010) Heparinized chitosan/poly(γ-glutamic acid) nanoparticles for multi-functional delivery of fibroblast growth factor and heparin. Biomaterials, vol. 31, n°35, p. 9320-9332.

Tang, M., Shi, S., Guo, Y., Xu, W., Wang, L., Chen, Y., Wang, Z. et Qiao, Z. (2014) GSK-3/CREB pathway involved in the gx-50's effect on Alzheimer's disease. Neuropharmacology, vol. 81, n°0, p. 256-266.

Tapia-Arancibia, L., Aliaga, E., Silhol, M. et Arancibia, S. (2008) New insights into brain BDNF function in normal aging and Alzheimer disease. Brain Research Reviews, vol. 59, n°1, p. 201-220.

Teipel, S. J., Meindl, T., Grinberg, L., Grothe, M., Cantero, J. L., Reiser, M. F., Moller, H. J., Heinsen, H. et Hampel, H. (2011) The cholinergic system in mild cognitive impairment and Alzheimer's disease: an in vivo MRI and DTI study. Human brain mapping, vol. 32, n°9, p. 1349-1362.

Teppola, H., Sarkanen, J.-R., Jalonen, T. O. et Linne, M.-L. (2016) Morphological Differentiation Towards Neuronal Phenotype of SH-SY5Y Neuroblastoma Cells by Estradiol, Retinoic Acid and Cholesterol. Neurochemical research, vol. 41, n°4, p. 731-747.

Thomas, R., Morris, A. W. J. et Tai, L. M. (2017) Epidermal growth factor prevents APOE4-induced cognitive and cerebrovascular deficits in female mice. Heliyon, vol. 3, n°6, p. e00319.

Thomas, R., Zuchowska, P., Morris, A. W. J., Marottoli, F. M., Sunny, S., Deaton, R., Gann, P. H. et Tai, L. M. (2016) Epidermal growth factor prevents APOE4 and amyloid-beta-induced cognitive and cerebrovascular deficits in female mice. Acta neuropathologica communications, vol. 4, n°1, p. 111.

Thorne, R. G., Emory, C. R., Ala, T. A. et Frey II, W. H. (1995) Quantitative analysis of the olfactory

pathway for drug delivery to the brain. Brain research, vol. 692, n°1–2, p. 278-282.

Thorne, R. G. et Nicholson, C. (2006) In vivo diffusion analysis with quantum dots and dextrans predicts the width of brain extracellular space. Proceedings of the National Academy of Sciences of the United States of America, vol. 103, n°14, p. 5567-5572.

Thorne, R. G., Pronk, G. J., Padmanabhan, V. et Frey II, W. H. (2004) Delivery of insulin-like growth factor-I to the rat brain and spinal cord along olfactory and trigeminal pathways following intranasal administration. Neuroscience, vol. 127, n°2, p. 481-496.

Tian, L., Guo, R., Yue, X., Lv, Q., Ye, X., Wang, Z., Chen, Z., Wu, B., Xu, G. et Liu, X. (2012) Intranasal administration of nerve growth factor ameliorate β-amyloid deposition after traumatic brain injury in rats. Brain research, vol. 1440, n°0, p. 47-55.

Tong, L., Balazs, R., Thornton, P. L. et Cotman, C. W. (2004) Beta-amyloid peptide at sublethal concentrations downregulates brain-derived neurotrophic factor functions in cultured cortical neurons. The Journal of neuroscience : the official journal of the Society for Neuroscience, vol. 24, n°30, p. 6799-6809.

Toulouse, A., Collins, G. C. et Sullivan, A. M. (2012) Neurotrophic effects of growth/differentiation factor 5 in a neuronal cell line. Neurotoxicity research, vol. 21, n°3, p. 256-265.

Triaca, V., Sposato, V., Bolasco, G., Ciotti, M. T., Pelicci, P., Bruni, A. C., Cupidi, C., Maletta, R., Feligioni, M., Nistico, R., Canu, N. et Calissano, P. (2016) NGF controls APP cleavage by downregulating APP phosphorylation at Thr668: relevance for Alzheimer's disease. Aging cell, vol. 15, n°4, p. 661-672.

Tricco, A. C., Soobiah, C., Berliner, S., Ho, J. M., Ng, C. H., Ashoor, H. M., Chen, M. H., Hemmelgarn, B. et Straus, S. E. (2013) Efficacy and safety of cognitive enhancers for patients with mild cognitive impairment: a systematic review and meta-analysis. CMAJ : Canadian Medical Association Journal, vol. 185, n°16, p. 1393-1401.

Tusi, S. K., Khalaj, L., Ashabi, G., Kiaei, M. et Khodagholi, F. (2011) Alginate oligosaccharide protects against endoplasmic reticulum- and mitochondrial-mediated apoptotic cell death and oxidative stress. Biomaterials, vol. 32, n°23, p. 5438-5458.

Uberti, D., Rizzini, C., Spano, P. et Memo, M. (1997) Characterization of tau proteins in human neuroblastoma SH-SY5Y cell line. Neuroscience letters, vol. 235, n°3, p. 149-153.

Ueberham, U. et Arendt, T. (2013) The Role of Smad Proteins for Development, Differentiation and Dedifferentiation of Neurons, Uwe Ueberham and Thomas Arendt (2013). The Role of Smad Proteins for Development, Differentiation and Dedifferentiation of Neurons, Trends in Cell Signaling Pathw. (S. D. Wislet-Gendebien, Dir.) (InTech.).

Ueberham, U., Hilbrich, I., Ueberham, E., Rohn, S., Glöckner, P., Dietrich, K., Brückner, M. K. et Arendt, T. (2012) Transcriptional control of cell cycle-dependent kinase 4 by Smad proteins—implications for Alzheimer's disease. Neurobiology of aging, vol. 33, n°12, p. 2827-2840.

Ueberham, U., Ueberham, E., Gruschka, H. et Arendt, T. (2003) Connective tissue growth factor in Alzheimer's disease. Neuroscience, vol. 116, n°1, p. 1-6.

Ueberham, U., Ueberham, E., Gruschka, H. et Arendt, T. (2006) Altered subcellular location of phosphorylated Smads in Alzheimer's disease. The European journal of neuroscience, vol. 24, n°8, p. 2327-2334.

United Nation (2015) World population aging. New York : 164 p.

Urist, M. R. et Strates, B. S. (1971) Bone morphogenetic protein. Journal of dental research, vol. 50, n°6, p. 1392-1406.

Utsumi, H., Chiba, H., Kamimura, Y., Osanai, M., Igarashi, Y., Tobioka, H., Mori, M. et Sawada, N. (2000) Expression of GFRalpha-1, receptor for GDNF, in rat brain capillary during postnatal development of the BBB. American journal of physiology.Cell physiology, vol. 279, n°2, p. C361-8.

Vaka, S. R., Murthy, S. N., Balaji, A. et Repka, M. A. (2012) Delivery of brain-derived neurotrophic factor via nose-to-brain pathway. Pharmaceutical research, vol. 29, n°2, p. 441-447.

Vargas, J. Y., Fuenzalida, M. et Inestrosa, N. C. (2014) In vivo activation of Wnt signaling pathway enhances cognitive function of adult mice and reverses cognitive deficits in an Alzheimer's disease model. The Journal of neuroscience : the official journal of the Society for Neuroscience, vol. 34, n°6, p. 2191-2202.

Vazquez de la Torre, A., Junyent, F., Folch, J., Pelegri, C., Vilaplana, J., Auladell, C., Beas-Zarate, C., Pallas, M., Verdaguer, E. et Camins, A. (2013) PI3 k/akt inhibition induces apoptosis through p38 activation in neurons. Pharmacological research : the official journal of the Italian Pharmacological Society, vol. 70, n°1, p. 116-125.

Vesey, R., Birrell, J. M., Bolton, C., Chipperfield, R. S., Blackwell, A. D., Dening, T. R. et Sahakian, B. J. (2002) Cholinergic nicotinic systems in Alzheimer's disease: Prospects for pharmacological intervention. CNS Drugs, vol. 16, n°7, p. 485-500.

Vila, A., Sánchez, A., Janes, K., Behrens, I., Kissel, T., Jato, J. L. V. et Alonso, M. J. (2004) Low molecular weight chitosan nanoparticles as new carriers for nasal vaccine delivery in mice. Chitosan, vol. 57, n°1, p. 123-131.

Vinores, S. A., Marangos, P. J., Parma, A. M. et Guroff, G. (1981) Increased levels of neuron-specific enolase in PC12 pheochromocytoma cells as a result of nerve growth factor treatment. Journal of neurochemistry, vol. 37, n°3, p. 597-600.

Voigt, N., Henrich-Noack, P., Kockentiedt, S., Hintz, W., Tomas, J. et Sabel, B. A. (2014) Surfactants, not size or zeta-potential influence blood–brain barrier passage of polymeric nanoparticles. Theme Issue: Nanomedicine, vol. 87, n°1, p. 19-29.

Wagner, D. O., Sieber, C., Bhushan, R., Börgermann, J. H., Graf, D. et Knaus, P. (2010) BMPs: From bone to body morphogenetic proteins. Science Signaling, vol. 3, n°107.

Wan, W., Xia, S., Kalionis, B., Liu, L. et Li, Y. (2014) The role of Wnt signaling in the development of Alzheimer's disease: a potential therapeutic target? BioMed research international, vol. 2014, p. 301575.

Wang, J.-Z. et Liu, F. (2008) Microtubule-associated protein tau in development, degeneration and protection of neurons. Progress in neurobiology, vol. 85, n°2, p. 148-175.

Wang, Y., Cooke, M. J., Sachewsky, N., Morshead, C. M. et Shoichet, M. S. (2013) Bioengineered sequential growth factor delivery stimulates brain tissue regeneration after stroke. Journal of Controlled Release, vol. 172, n°1, p. 1-11.

Wang, Z. F., Li, H. L., Li, X. C., Zhang, Q., Tian, Q., Wang, Q., Xu, H. et Wang, J. Z. (2006) Effects of endogenous beta-amyloid overproduction on tau phosphorylation in cell culture. Journal of neurochemistry, vol. 98, n°4, p. 1167-1175.

Wang, Z., Han, N., Wang, J., Zheng, H., Peng, J., Kou, Y., Xu, C., An, S., Yin, X., Zhang, P. et Jiang, B. (2014) Improved peripheral nerve regeneration with sustained release nerve growth factor microspheres in small gap tubulization. American journal of translational research, vol. 6, n°4, p. 413-421.

Wang, Z., Xiong, L., Wan, W., Duan, L., Bai, X. et Zu, H. (2017) Intranasal BMP9 Ameliorates Alzheimer Disease-Like Pathology and Cognitive Deficits in APP/PS1 Transgenic Mice. Frontiers in molecular neuroscience, vol. 10, p. 32.

Weiser, J. R. et Saltzman, W. M. (2014) Controlled release for local delivery of drugs: barriers and models. 30th Anniversary Special Issue, vol. 190, n°0, p. 664-673.

Westwood, A. J., Beiser, A., Decarli, C., Harris, T. B., Chen, T. C., He, X. M., Roubenoff, R., Pikula, A., Au, R., Braverman, L. E., Wolf, P. A., Vasan, R. S. et Seshadri, S. (2014) Insulin-like growth factor-1 and risk of Alzheimer dementia and brain atrophy. Neurology, vol. 82, n°18, p. 1613-1619.

Williams, B. J., Bimonte-Nelson, H. A. et Granholm-Bentley, A. C. (2006) ERK-mediated NGF signaling in the rat septo-hippocampal pathway diminishes with age. Psychopharmacology, vol. 188, n°4, p. 605-618.

Wilson, B., Samanta, M. K., Santhi, K., Kumar, K. P., Paramakrishnan, N. et Suresh, B. (2008) Targeted delivery of tacrine into the brain with polysorbate 80-coated poly(n-butylcyanoacrylate) nanoparticles. European journal of pharmaceutics and biopharmaceutics : official journal of Arbeitsgemeinschaft fur Pharmazeutische Verfahrenstechnik e.V, vol. 70, n°1, p. 75-84.

Wilson, B., Samanta, M. K., Santhi, K., Kumar, K. P., Ramasamy, M. et Suresh, B. (2010) Chitosan nanoparticles as a new delivery system for the anti-Alzheimer drug tacrine. Nanomedicine : nanotechnology, biology, and medicine, vol. 6, n°1, p. 144-152.

Wilson, B., Samanta, M. K., Santhi, K., Kumar, K. P. S., Paramakrishnan, N. et Suresh, B. (2008) Poly(n-butylcyanoacrylate) nanoparticles coated with polysorbate 80 for the targeted delivery of rivastigmine into the brain to treat Alzheimer's disease. Brain research, vol. 1200, p. 159-168.

Winbanks, C. E., Chen, J. L., Qian, H., Liu, Y., Bernardo, B. C., Beyer, C., Watt, K. I., Thomson, R. E., Connor, T., Turner, B. J., McMullen, J. R., Larsson, L., McGee, S. L., Harrison, C. A. et Gregorevic, P. (2013) The bone morphogenetic protein axis is a positive regulator of skeletal muscle mass. The Journal of cell biology, vol. 203, n°2, p. 345-357.

Wohlfart, S., Gelperina, S. et Kreuter, J. (2012) Transport of drugs across the blood-brain barrier by

nanoparticles. Journal of Controlled Release, vol. 161, n°2, p. 264-273.

Wohlfart, S., Khalansky, A. S., Gelperina, S., Begley, D. et Kreuter, J. (2011) Kinetics of transport of doxorubicin bound to nanoparticles across the blood–brain barrier. Journal of Controlled Release, vol. 154, n°1, p. 103-107.

Wolak, D. J. et Thorne, R. G. (2013) Diffusion of macromolecules in the brain: implications for drug delivery. Molecular pharmaceutics, vol. 10, n°5, p. 1492-1504.

Wolfe, M. S. (2009) Tau mutations in neurodegenerative diseases. The Journal of biological chemistry, vol. 284, n°10, p. 6021-6025.

Woodbury, M. E. et Ikezu, T. (2014) Fibroblast growth factor-2 signaling in neurogenesis and neurodegeneration. Journal of neuroimmune pharmacology : the official journal of the Society on NeuroImmune Pharmacology, vol. 9, n°2, p. 92-101.

World Health Organization (2012) Dementia, A public health priority. United Kingdom : WHO press : 1-102 p.

World Health Organization (2017) Dementia, Fact sheet.

Wyss-Coray, T., Lin, C., Yan, F., Yu, G. Q., Rohde, M., McConlogue, L., Masliah, E. et Mucke, L. (2001) TGF-beta1 promotes microglial amyloid-beta clearance and reduces plaque burden in transgenic mice. Nature medicine, vol. 7, n°5, p. 612-618.

Xu, C.-J., Wang, J.-L. et Jin, W.-L. (2016) The Emerging Therapeutic Role of NGF in Alzheimer's Disease. Neurochemical research, vol. 41, n°6, p. 1211-1218.

Xu, H., Huang, W., Wang, Y., Sun, W., Tang, J., Li, D., Xu, P., Guo, L., Yin, Z. Q. et Fan, X. (2013) The function of BMP4 during neurogenesis in the adult hippocampus in Alzheimer's disease. Ageing research reviews, vol. 12, n°1, p. 157-164.

Xu, Y., Asghar, S., Yang, L., Li, H., Wang, Z., Ping, Q. et Xiao, Y. (2017) Lactoferrin-coated polysaccharide nanoparticles based on chitosan hydrochloride/hyaluronic acid/PEG for treating brain glioma. Carbohydrate polymers, vol. 157, p. 419-428.

Xu, Y. et Du, Y. (2003) Effect of molecular structure of chitosan on protein delivery properties of chitosan nanoparticles. International journal of pharmaceutics, vol. 250, n°1, p. 215-226.

Xu, Y., Jia, Y., Wang, Z. et Wang, Z. (2013) Mathematical modeling and finite element simulation

of slow release of drugs using hydrogels as carriers with various drug concentration distributions. Journal of pharmaceutical sciences, vol. 102, n°5, p. 1532-1543.

Yan, Y.-H., Li, S.-H., Gao, Z., Zou, S.-F., Li, H.-Y., Tao, Z.-Y., Song, J. et Yang, J.-X. (2016) Neurotrophin-3 promotes proliferation and cholinergic neuronal differentiation of bone marrow- derived neural stem cells via notch signaling pathway. Life sciences, vol. 166, p. 131-138.

Yanagisawa, D., Taguchi, H., Yamamoto, A., Shirai, N., Hirao, K. et Tooyama, I. (2011) Curcuminoid binds to amyloid-ß 1-42 oligomer and fibril. Journal of Alzheimer's Disease, vol. 24, n°SUPPL. 2, p. 33-42.

Yanagisawa, M., Takizawa, T., Ochiai, W., Uemura, A., Nakashima, K. et Taga, T. (2001) Fate alteration of neuroepithelial cells from neurogenesis to astrocytogenesis by bone morphogenetic proteins. Neuroscience research, vol. 41, n°4, p. 391-396.

Yang, C., Liu, Y., Ni, X., Li, N., Zhang, B. et Fang, X. (2014) Enhancement of the nonamyloidogenic pathway by exogenous NGF in an Alzheimer transgenic mouse model. Neuropeptides, vol. 48, n°4, p. 233-238.

Yang, G. C., Scherer, P. W., Zhao, K. et Mozell, M. M. (2007) Numerical modeling of odorant uptake in the rat nasal cavity. Chemical senses, vol. 32, n°3, p. 273-284.

Yang, H., Wang, J., Wang, F., Liu, X., Chen, H., Duan, W. et Qu, T. (2016) Dopaminergic Neuronal Differentiation from the Forebrain-Derived Human Neural Stem Cells Induced in Cultures by Using a Combination of BMP-7 and Pramipexole with Growth Factors. Frontiers in neural circuits, vol. 10, p. 29.

Yang, Y., Corona III, A. et Henson, M. A. (2012) Experimental investigation and population balance equation modeling of solid lipid nanoparticle aggregation dynamics. Journal of colloid and interface science, vol. 374, n°1, p. 297-307.

Yang, Y. et Herrup, K. (2007) Cell division in the CNS: Protective response or lethal event in post-mitotic neurons? Cell Cycle Dysregulation and Neurodegenerative Diseases, vol. 1772, n°4, p. 457-466.

Ye, J., Lin, H., Mu, J., Cui, X., Ying, H., Lin, M., Wu, L., Weng, J. et Lin, X. (2010) Effect of basic fibroblast growth factor on hippocampal cholinergic neurons in a rodent model of ischaemic

encephalopathy. Basic & clinical pharmacology & toxicology, vol. 107, n°6, p. 931-939.

Yemisci, M., Caban, S., Gursoy-Ozdemir, Y., Lule, S., Novoa-Carballal, R., Riguera, R., Fernandez-Megia, E., Andrieux, K., Couvreur, P., Capan, Y. et Dalkara, T. (2015) Systemically administered brain-targeted nanoparticles transport peptides across the blood-brain barrier and provide neuroprotection. Journal of cerebral blood flow and metabolism : official journal of the International Society of Cerebral Blood Flow and Metabolism, vol. 35, n°3, p. 469-475.

Yi, X., Manickam, D. S., Brynskikh, A. et Kabanov, A. V (2014) Agile Delivery of Protein Therapeutics to CNS. Journal of Controlled Release, vol. 190, n°0, p. 637-663.

Yin, R. H., Yu, J. T. et Tan, L. (2014) The Role of SORL1 in Alzheimer's Disease. Molecular neurobiology.

Yu, J. T., Tan, L. et Hardy, J. (2014) Apolipoprotein E in Alzheimer's disease: an update. Annual Review of Neuroscience, vol. 37, p. 79-100.

Yu, Y. J. et Watts, R. J. (2013) Developing therapeutic antibodies for neurodegenerative disease. Neurotherapeutics : the journal of the American Society for Experimental NeuroTherapeutics, vol. 10, n°3, p. 459-472.

Zatkova, M., Reichova, A., Bacova, Z., Strbak, V., Kiss, A. et Bakos, J. (2017) Neurite Outgrowth Stimulated by Oxytocin Is Modulated by Inhibition of the Calcium Voltage-Gated Channels. Cellular and molecular neurobiology.

Zeng, J., Li, T., Gong, M., Jiang, W., Yang, T., Chen, J., Liu, Y. et Chen, L. (2017) Marginal Vitamin A Deficiency Exacerbates Memory Deficits Following Abeta1-42 Injection in Rats. Current Alzheimer research, vol. 14, n°5, p. 562-570.

Zhang, B., Sun, X., Mei, H., Wang, Y., Liao, Z., Chen, J., Zhang, Q., Hu, Y., Pang, Z. et Jiang, X. (2013) LDLR-mediated peptide-22-conjugated nanoparticles for dual-targeting therapy of brain glioma. Biomaterials, vol. 34, n°36, p. 9171-9182.

Zhang, C., Browne, A., Child, D. et Tanzi, R. E. (2010) Curcumin decreases amyloid-ß peptide levels by attenuating the maturation of amyloid-ß precursor protein. Journal of Biological Chemistry, vol. 285, n°37, p. 28472-28480.

Zhang, C., Chen, J., Feng, C., Shao, X., Liu, Q., Zhang, Q., Pang, Z. et Jiang, X. (2014) Intranasal nanoparticles of basic fibroblast growth factor for brain delivery to treat Alzheimer's disease.

International journal of pharmaceutics, vol. 461, n°1-2, p. 192-202.

Zhang, C., Wu, B., Beglopoulos, V., Wines-Samuelson, M., Zhang, D., Dragatsis, I., Sudhof, T. C. et Shen, J. (2009) Presenilins are Essential for Regulating Neurotransmitter Release. Nature, vol. 460, n°7255, p. 632-636.

Zhang, J., Moats-Staats, B. M., Ye, P. et D'Ercole, A. J. (2007) Expression of insulin-like growth factor system genes during the early postnatal neurogenesis in the mouse hippocampus. Journal of neuroscience research, vol. 85, n°8, p. 1618-1627.

Zhang, S., Wang, Z., Cai, F., Zhang, M., Wu, Y., Zhang, J. et Song, W. (2017) BACE1 cleavage site selection critical for amyloidogenesis and Alzheimer's pathogenesis. The Journal of neuroscience : the official journal of the Society for Neuroscience.

Zhang, W., Deng, Z. L., Chen, L., Zuo, G. W., Luo, Q., Shi, Q., Zhang, B. Q., Wagner, E. R., Rastegar, F., Kim, S. H., Jiang, W., Shen, J., Huang, E., Gao, Y., Gao, J. L., Zhou, J. Z., Luo, J., Huang, J., Luo, X., Bi, Y., Su, Y., Yang, K., Liu, H., Luu, H. H., Haydon, R. C., He, T. C. et He, B. C. (2010) Retinoic acids potentiate BMP9-induced osteogenic differentiation of mesenchymal progenitor cells. PloS one, vol. 5, n°7, p. e11917.

Zhang, Y., Ma, R. H., Li, X. C., Zhang, J. Y., Shi, H. R., Wei, W., Luo, D. J., Wang, Q., Wang, J. Z. et Liu, G. P. (2014) Silencing [Formula: see text] Rescues Tau Pathologies and Memory Deficits through Rescuing PP2A and Inhibiting GSK-3beta Signaling in Human Tau Transgenic Mice. Frontiers in aging neuroscience, vol. 6, p. 123.

Zhang, Y. W., Chen, Y., Liu, Y., Zhao, Y., Liao, F. F. et Xu, H. (2013) APP regulates NGF receptor trafficking and NGF-mediated neuronal differentiation and survival. PloS one, vol. 8, n°11, p. e80571.

Zhao, L., Seth, A., Wibowo, N., Zhao, C.-X., Mitter, N., Yu, C. et Middelberg, A. P. J. (2014) Nanoparticle vaccines. Vaccine, vol. 32, n°3, p. 327-337.

Zhao, Y.-Z., Lin, M., Lin, Q., Yang, W., Yu, X.-C., Tian, F.-R., Mao, K.-L., Yang, J.-J., Lu, C.-T. et Wong, H. L. (2016) Intranasal delivery of bFGF with nanoliposomes enhances in vivo neuroprotection and neural injury recovery in a rodent stroke model. Journal of controlled release : official journal of the Controlled Release Society, vol. 224, p. 165-175.

Zhao, Y. Z., Li, X., Lu, C. T., Lin, M., Chen, L. J., Xiang, Q., Zhang, M., Jin, R. R., Jiang, X., Shen,

X. T., Li, X. K. et Cai, J. (2014) Gelatin nanostructured lipid carriers-mediated intranasal delivery of basic fibroblast growth factor enhances functional recovery in hemiparkinsonian rats. Nanomedicine : nanotechnology, biology, and medicine, vol. 10, n°4, p. 755-764.

Zheng, W.-H., Bastianetto, S., Mennicken, F., Ma, W. et Kar, S. (2002) Amyloid β peptide induces tau phosphorylation and loss of cholinergic neurons in rat primary septal cultures. Neuroscience, vol. 115, n°1, p. 201-211.

Zheng, W. H. et Quirion, R. (2004) Comparative signaling pathways of insulin-like growth factor-1 and brain-derived neurotrophic factor in hippocampal neurons and the role of the PI3 kinase pathway in cell survival. Journal of neurochemistry, vol. 89, n°4, p. 844-852.

Zhou, Q. H., Boado, R. J. et Pardridge, W. M. (2012) Selective plasma pharmacokinetics and brain uptake in the mouse of enzyme fusion proteins derived from species-specific receptor-targeted antibodies. Journal of drug targeting, vol. 20, n°8, p. 715-719.

Zhou, Q. H., Lu, J. Z., Hui, E. K., Boado, R. J. et Pardridge, W. M. (2011) Delivery of a peptide radiopharmaceutical to brain with an IgG-avidin fusion protein. Bioconjugate chemistry, vol. 22, n°8, p. 1611-1618.

Zhu, X., Mei, M., Lee, H. G., Wang, Y., Han, J., Perry, G. et Smith, M. A. (2005) P38 activation mediates amyloid-beta cytotoxicity. Neurochemical research, vol. 30, n°6-7, p. 791-796.

Zhu, X., Raina, A. K., Rottkamp, C. A., Aliev, G., Perry, G., Boux, H. et Smith, M. A. (2001) Activation and redistribution of c-jun N-terminal kinase/stress activated protein kinase in degenerating neurons in Alzheimer's disease. Journal of neurochemistry, vol. 76, n°2, p. 435-441.

Zhu, Y., Yang, G. Y., Ahlemeyer, B., Pang, L., Che, X. M., Culmsee, C., Klumpp, S. et Krieglstein, J. (2002) Transforming growth factor-beta 1 increases bad phosphorylation and protects neurons against damage. The Journal of neuroscience : the official journal of the Society for Neuroscience, vol. 22, n°10, p. 3898-3909.